



Norwegian University of
Science and Technology

Development of a Energy Efficient Powertrain

For a Shell Eco-Marathon Vechile

Sivert Rød Hatletveit

Master of Science in Mechanical Engineering

Submission date: August 2018

Supervisor: Knut Einar Aasland, MTP

Norwegian University of Science and Technology
Department of Mechanical and Industrial Engineering

Abstract

This Master's thesis is a continuation of author's work in the pre-master thesis where an inertia motor/generator test bench were designed as a support for development of a new powertrain for a "Urban-Concept" battery-electric vehicle competing in Shell Eco-Marathon.

This test bench makes it possible to mount one of two symmetric powertrains where energy is transferred through a roller. By simulating the forces acting on a car the test bench supports powertrain development in the test phases in the following ways:

- Provide a more controlled test environment for development the power electronics and the mechanical sub systems of a powertrain
- Reduce risk of failure on track by providing an easy way to stress test and drive simulated laps
- Measure performance with a built-in torque transducer and Realtime tracking system

The team also set a goal to reduce 5 kilograms of weight while keeping the monocoque made by the DNV GL Fuel Fighter 2017 team. To reach this goal, the development of carbon fiber rims was included as a part of a new geared powertrain design with the support of regeneration of energy. This powertrain has a clutch system that synchronizes the gears speed and connects/disconnects the motor from the system to remove powertrain losses while rolling. The gearing happens with a 1-stage custom-made gear system with a custom-made internal spur ring gear with 375 teeth providing a possible reduction ratio of more than 20:1.

Some findings done on the new test bench by measurements done on the test rig was:

- Efficient acceleration and braking
- The effect of tare losses by having motor always connected at different speeds
- Efficiency plot for different speeds and motor torques for the powertrain as a whole

Other findings in the thesis includes the theoretical effect of having two different gearing ratios or overvolting the DC motors used in the car.

The tare losses measured gives reason to believe that a geared powertrain is more efficient as well as supporting efficient regeneration of energy. In addition, the new powertrain and carbon fiber rims were responsible for a weight reduction of over 7.2 kilograms where 4.7 kilograms of the savings were due the lightweight carbon fiber rims at 1.4 kilograms each.

The car's performance was proven on track in Shell Eco-Marathon with a respectable 2nd place in the race and about 10% of recovery of energy through regeneration of power. In addition, the team took 2nd place in the communication off-track award.

Sammendrag

Denne masteroppgaven er en videre arbeid av forfatters prosjektoppgave hvor en motor-/generator testbenk som også simulerer treghet ble utformet som en støtte for utvikling av en ny drivlinje til en "Urban-Concept" elbil laget for konkurransen Shell Eco- Marathon.

En av to symmetriske drivlinje-enheter er montert til denne testbenken og overfører krefter via en rulle. Ved å simulere kreftene som virker på bilen støtter testbenken utvikling av drivlinjen i teststadiet på følgende måter:

- Gi et mer kontrollert testmiljø for utvikling av kraftelektronikk og mekaniske delsystemer
- Redusere risikoen for feil under løpet ved å forenkle stresstesting og simulering av løpskjøring
- Måle ytelse med en innebygd momentmåler og datatolkning i sanntid

Teamet satte også et mål om å redusere 5 kilo av bilens vekt uten å endre chassiset laget av DNV GL Fuel Fighter 2017-teamet. For å nå dette målet ble utviklingen av karbonfiberfelger inkludert som en del av en ny drivlinjekonstruksjon, med støtte for regenerering av energi. Den endelige drivlinjen har et clutchsystem som synkroniserer girets hastighet og kobler/frikobler motoren til og fra ringgiret for å fjerne unødige tap under rulling. Giringen skjer via en ett-trinns spesiallaget girsystem med et tilpasset internt ringgir med 375 tenner som gir et reduksjonsforhold på over 20:1.

Noen funn som er gjort på den nye testbenken ved målinger er:

- Hva som er effektiv akselerasjon og bremsing
- Effekten av «tare»-tap ved å ha motor koblet til men uten å overføre moment. Dette er målt i forskjellige hastigheter
- Effektivitetsmålinger for forskjellige hastigheter og motormoment for drivlinjen som helhet

Andre funn i avhandlingen inneholder teoretisk gevinst av å ha to forskjellige giringsforhold og av å overvolte likestrømsmotorene brukt i bilen.

«Tare»-tapene målt gir grunn til å tro at ett giret drivverk er mer effektivt enn belteoverføringen i det gamle drivverket, samt at støtte for effektiv regenerering av strøm er en fordel. Totalt var de nye drivlinjene og karbonfiberfeltene ansvarlige for en vektreduksjon på 7,2 kilo, hvorav 4,7 kilo av besparelsene skyldes karbonfiberfelgene med egenvekt på kun 1,4 kilo per felg.

Bilens ytelse ble målt som svært god i løpet med en respektabel andreplass og ca. 10% innhentet energi via regenerativ bremsing. I tillegg tok teamet andreplass i offtrack communication award.

Preface

Being part of the DNV GL Fuel Fighter-team for two years and seeing the ideas transform into a ultra-efficient 85 kilogram vehicle have been truly amazing. I will therefore like to thank all who have contributed the project these two years (more than 60 persons!)

I'm especially thankful to have these members who continued staying in the team from last year: Håvard Vestad, Anne-Mare Karlstad, Renate Molvik and Jørgen Jackowitz. This made the job as a project manager a breeze.

And to Johannes Nadler, Tanguy Simons and Niklas Kaack for working as a team on the powertrain/rim development. The achievements presented in this master wouldn't been possible without the common goal of making an efficient powertrain and lightweight rims.

I would also like to thank the main driving forces behind this project: My supervisor Knut Aasland who has been responsible teacher for the project in more than 10 years and to Kristina Dahlberg and the rest of DNV GL for making economically possible and for sharing DNV GLs knowledge with the team in the 10.th year in a row.

Also, thanks to the following employees at MTP for helping out with the project: Børge Holen, Roar Munkebye, Cecilia Haskins, Natalia Trotsenko, Aud Mork and Nils Petter Vedvik

Lastly thanks to my girlfriend Kamilla supporting me through a hectic, but truly amazing year.

Table of Contents

Abstract	i
Sammendrag	iii
Preface.....	v
Table of Contents	vii
1 Introduction.....	1
1.1 Shell Eco Marathon (SEM).....	1
1.2 Team Goals for SEM 2018	1
1.3 The Team	2
1.4 Previous work.....	3
1.5 Readers Guide	5
2 Method.....	7
2.1 Vee Model and Risk Management	7
3 The Motors	10
3.1 Motor Model and Efficiency of The Motors.....	12
3.2 The Effect of Two Different Gear Ratios.....	14
3.3 Overvolting the Motors.....	16
3.4 Verification of The Motor Model	17
3.5 Strategy for Acceleration and Braking.....	20
4 The Rim.....	22
4.1 Requirements	22
4.2 Carbon Fiber as Material	23
4.3 The Solution.....	26
4.4 Strength Calculations.....	28
4.5 Production	29
4.6 The Result	35
5 The Powertrain	36
5.1 The Old Powertrain	37
5.2 Requirements for the New Powertrain.....	38
5.3 Designing the Gears.....	42
5.4 Load Cases	45
5.5 A Few Concepts	48
5.6 The Optimal Shape	53
5.7 Sliding Motor Mount	57
5.8 Finite Element Analyze of The Final Design.....	58
5.9 Production	60

5.10	The Result	66
6	Physical Testing on the Powertrain Test Bench	67
6.1	Tare Losses	68
6.2	Efficiency of the New Powertrain.....	70
6.3	Driving strategy verification	70
7	Full Scale Testing	72
8	The race	76
8.1	Day 1 – Unpacking.....	76
8.2	Day 2 – Technical Inspection	77
8.3	Day 3 – First Track Test.....	77
8.4	Day 4 – Last Day of Testing.....	78
8.5	Analyzing Shells Telemetry Data	80
9	Discussion	84
10	Recommended Further Work.....	85
11	Conclusion	86
	Sources	87
Appendix A:	Race Results.....	88
Appendix B:	Articles.....	89
Appendix C:	Rim Calculations	92
Appendix D:	Rotary vs stationary axle	99
Appendix E:	FEA of The Carbon Fiber Rim.....	103
Appendix F:	FEA of the Powertrain Design.....	110
Appendix G:	Gears.....	116
Appendix H:	Old Rims Calculations	120
Appendix I:	Maxon RE50/65, Datasheet.....	122
Appendix J:	Analyze of SEM Telemetry Data	124
Appendix K:	Modeling and Simulation of the Car on the Track	125
Appendix L:	Behavior of DC Machines	132
Appendix M:	Motor Efficiency Maxon RE50/RE65	136
Appendix N:	Topology optimized design vs square tubes	138
Appendix O:	Datasheet for Actuonix P16.....	142
Appendix P:	Datasheet for Divinycell H	145
Appendix Q:	Datasheet for Michelin Urban Concept Tires.....	146
Appendix R:	Risk Assessment	147
Appendix S:	Pre-Master Thesis.....	157

List of Figures

- Figure 1.1 The team celebrating 2nd place at SEM 2018 2
- Figure 1.2 Render of the powertrain test bench and a picture of the final build. 4
- Figure 1.3 The internal components of the powertrain test bench..... 4
- Figure 1.4 The concept of two gears visualized. 5
- Figure 2.1 Risk level depends on both likelihood 8
- Figure 2.2 The Vee Model 9
- Figure 3.1 The Maxon RE50..... 10
- Figure 3.2 The four quadrants of DC Motor Drive 11
- Figure 3.3 The final motor controller design for this year’s car..... 11
- Figure 3.4 Efficiency of the Maxon RE50 48V..... 13
- Figure 3.5 The effect of two gears vs one gear 14
- Figure 3.6 Simulation of the amount of energy lost trying to accelerate the car 15
- Figure 3.7 Investigation of when the simulation wants to change gears 16
- Figure 3.8 The effect of two gears vs one gear 16
- Figure 3.9 Regeneration Efficiency at different motor voltages 17
- Figure 3.10 CAD model of the motor to motor configuration 18
- Figure 3.11 Two Maxon motors mounted in our test configuration 18
- Figure 3.12 Data points measured for the RE50 48V 19
- Figure 3.13 Interpolation of the data points gathered 19
- Figure 3.14 Tests done on the RE50..... 20
- Figure 3.15 Speed profiles from some of the simulated steps 21
- Figure 4.4 Some of the geometrical constraints 23
- Figure 4.5 Michelins dimensional requirements for the rim profile..... 23
- Figure 4.1 Specific stiffness and specific strength of different materials. 24
- Figure 4.2 Example from Solid Metal Versus Sandwich Panels..... 25
- Figure 4.3 Common core materials: Aluminum honeycomb and PVC foam..... 25
- Figure 4.6 CAD of the rim 26
- Figure 4.7 Different concepts for the center plate 26
- Figure 4.8 A commercial carbon fiber rim for Michelin Solar Race Tires..... 27
- Figure 4.9 Easycomposites XPREG XC110 28
- Figure 4.10 The FEA model of the outer ring 29
- Figure 4.11 The 50mm block mounted 30
- Figure 4.12 CNC milling of the rim contour right before finishing cut 30
- Figure 4.13 The mould during layup of carbon fiber..... 31
- Figure 4.14 The finished center plate mould 32
- Figure 4.15 Lower layer and foam laid in the mould. 32
- Figure 4.16 The Aluminum Center 33
- Figure 4.17 The Centering tool..... 33
- Figure 4.18 The centering tool fastened to the mould 34
- Figure 4.19 Demoulding 34
- Figure 4.20 The Rim..... 35
- Figure 5.1 The old Powertrain Mounted on the Powertrain Test Bench 37
- Figure 5.2 Production of the bulkhead/firewall in 2017. 38
- Figure 5.3 CAD of the 3D printed gears for rapid prototyping..... 40
- Figure 5.4 3D printed functional prototype of the two-gear solution 42
- Figure 5.5 The drawings for the gears designed in NX..... 45

Figure 5.6 Geometry for hitting a bump.	47
Figure 5.7 Hitting a bump with height of 10cm at 10m/s speed	48
Figure 5.8 Stationary axle with a hub (I) vs. rotating axle (II) mounted with bearings.....	49
Figure 5.9 Back To back Preloaded Angular Contact bearing (SKF, 2018)	49
Figure 5.10 The final solution.....	50
Figure 5.11 Motors minimum travel distance based on the gears center lines meeting.	51
Figure 5.12 Forces Acting on a spur gear mesh.....	51
Figure 5.13 Actuonix P16 with 100 mm stroke length Source: actuonix.com	52
Figure 5.14 DT Swiss X313s displacement curves	52
Figure 5.15 Three different mountings for the powertrains.....	53
Figure 5.16 The design spaces for topology optimization.....	54
Figure 5.17 Settings used for shape optimization of the mid-motor design.	55
Figure 5.18 Concept A after topology optimization	55
Figure 5.19 Concept B after topology optimization	56
Figure 5.20 Generative design inspired arm vs tubed solution	57
Figure 5.21 The final design for the motor mount with spring walls.....	58
Figure 5.22 The powertrain assembly	59
Figure 5.23 FEA results for the “Bump force” load case	60
Figure 5.24 Welding jig for the frame	61
Figure 5.25 The prototype frame	62
Figure 5.26 The first produced gear.	62
Figure 5.27 Removing rust from the gears with vinegar, salt and electric toothbrush	64
Figure 5.28 Epoxy mixed with micro balloons added the rim.....	64
Figure 5.29 Track cut out for gear with tight tolerance	64
Figure 5.30 Milling track to the gear	65
Figure 5.31 A square steel tube was used for mounting.....	65
Figure 5.32 Final version of the powertrain mounted in the car	66
Figure 6.1 Losses in spur gears at different speeds and torque transfers	68
Figure 6.2 Measured tare losses for the powertrains.	69
Figure 6.3 Efficiency at different currents and speeds.....	70
Figure 6.4 One of the most efficient driven laps on the test bench	71
Figure 7.1 Stripped down version of the car at the first testing	72
Figure 7.2 The car with the new carbon fiber rims	74
Figure 7.3 The car with new powertrains mounted.....	74
Figure 7.4 The end stops for the motors.....	75
Figure 8.1 Part of the track in London including the sharpest corner at the lower left	76
Figure 8.2 Fractured old ball joint vs. new Heim joints.....	77
Figure 8.3 The fractured part in the suspension system.....	78
Figure 8.4 Toe misalignments effect on fuel consumption.....	79
Figure 8.5 Energy consumption per lap.	81
Figure 8.6 Lap 10 of 15 in our best attempt in London.....	81
Figure 8.7 GPS points from Shells telemetry system	82
Figure 8.8 Comparison of DNV GL Fuel Fighters laps and the winning TIM07 car’s lap.	83
Figure 9.1 A alternative driving strategy	85

List of abbreviations Saker

BLDC: Brushless DC	5
CAD: Computer Aided Design	17
CNC: Computer Numerical Control	17
FEA: Finite Element Analysis	28
FF: DNV GL Fuel Fighter.....	83
PLA: polylactide.....	57
PU: Polyurethane	17
RPM: Rotations per Minute	40
SEM: Shell Eco-Marathon.....	1
SiT: Studentsamskipnaden i Trondheim.....	72
UART: Universal asynchronous receiver-transmitter.....	41
V&V: Verification and Validation	9

1 Introduction

1.1 Shell Eco Marathon (SEM)

Shell Eco Marathon is a student competition held by Shell where the goal is to drive using the least amount of energy. The competition was first held in 1939 by scientists in Shell that we're competing in driving the longest distance on a certain amount of fuel. From 1985 the current became a student competition in France for students to make the most efficient cars.

The competition is divided into two different classes: The Prototype class and the Urban-Concept (UC) class. In the prototype class the cars are built for maximum efficiency where the vehicles have three wheels and usually the driver lying inside the car. In urban concept the cars have size constraints and constraints like the need of lights, window wiper and luggage compartment. The goal in this class is both to design an ultra-efficient car and to make a concept car that could potentially inspire the industry. Both the both classes are again divided into three sources of energy: Internal combustion engines, battery-electric and hydrogen.

NTNU first competed in SEM in 2008 and have competed in the race each year since then. The team has mostly built UC cars, but one Prototype vehicle have also been made. This year the team has been working on improving the DNV GL Fuel Fighter 4 which first competed in the 2017, but unfortunately without results.

1.2 Team Goals for SEM 2018

The team have had a few years with problems in the race leading to no valid result. For this reason, a working car by far had the highest priority this year. To maximize the chances of a working vehicle the decision to keep the monocoque (load bearing carbon fiber chassis) and rather focus on physical testing with the goal to develop a reliable and efficient car.

With keeping the old monocoque some overall goals for the team were set to improve the car both in terms of efficiency, reliability and esthetics. These focus areas became:

- Focus on verification and validation of the vehicle's performance
- Design of new motor controller with ability to regenerate braking energy
- Powertrain that supports regenerative braking
- Get the car rolling early (February as goal)
- Carbon fiber rims
- Changing badly formed windows to new windows for improved visibility
- Weight: Under 90 kilograms by changing structural parts
- More stable door mechanism

With these focus areas the team hoped to get satisfactory results on-track. The hope was to be top three. In addition, the team could compete in two off-track awards out of five in SEM. With a marketing team that opted for one more year the Communication Award became a logical choice. The other award the team wanted to go for was the vehicle design award.

1.3 The Team



Figure 1.1 The team celebrating 2nd place at SEM 2018

In the beginning of the year author and four other members from the old team decided to continue working on the project. In addition to this one of the team members of the French team TIM contacted us during SEM17 and decided to join the 2018 team as well as he was going to be an exchange student at NTNU.

Among the members that joined from start the author took the position as Project Manager(PM) as the only team member that were going to write his master thesis on the project.

The position responsibility as electrical leader was taken by the French exchange student Tanguy Simons where he had help from the former electrical leader as a team member. To get enough members to the group various positions were announced. Among these were data logging, dashboard electronics, telemetry, clutch system and power distribution.

With a car built the need for a huge mechanical team wasn't that huge as the years where a new monocoque is built. However, there still were a goal to get some members joining. Therefore, positions for new door hinge, carbon fiber rim, window production and mechanical team leader among others were announced.

A group for Research and Development were made with Eirik Furuholmen who was going to write his pre-master for the project the 2018 season and his master thesis the following year. By the rules of SEM 2019 two doors is mandatory for the 2019 car. With the existing car unable to be rebuilt due to the asymmetrical monocoque the goal for this group was to explore new tools for vehicle design like generative design and to give a head start for the 2019 team with some knowledge transfer and continuity.

After the last recruitment to this project the team were counting 31 members with different educational backgrounds and five nationalities. The team had the following distribution of members on each sub-group:

Mechanical Team	6
Electrical Team	9
Research and Development	8
Design Team	2
Marketing team	5

1.4 Previous work

As a lot of parameters like motor performance, gear performance and reliability can't be purely calculated analytically. The author's pre-master thesis was development of a testbench that acted as a support for the development of the powertrain both as a verification of mechanical reliability, verification of the electric systems functionality, to check if the system performs as wanted and to validate that the efficiency of the car was as needed.

The main driving factors for making such a device was that experience from the 2017 team the following things led to a slower development of the car:

- For motor controller development there was a need for a test bench simulating the driving conditions by mimicking forces acting on the car. The team made one in the 2017 year, but that one wasn't easy controllable, had the motor and belt directly connected to a Prony brake and didn't mimic the car's speed and acceleration depending forces. Driving and working on this test bench didn't cause the same problems as on track. Especially important here was that the components tended to brake during acceleration on track but never failed on the test bench.
- Due to the need of transporting the car to do physical testing it was a time-consuming task. In addition, it was hard to measure what went wrong on the motor controller with full scale testing as one ideally should be able to scope electrical circuits with oscilloscope and use debugging tools to find potential problems.
- By reading reports from 2015 and 2016 it was noted that they also had problems with the powertrains that weren't solved in a good way. These years the vehicle had problems with the belts reducing motor speed to the wheel slipping and getting enough startup torque among others. With the knowledge that propulsion is one of the statistically most failing parts as well as the knowledge that almost every report on the car project states that the physical testing didn't start early enough due to unknown problems delaying testing the wish to decouple the powertrain testing from car was wanted.
- It's easy to read how manufacturers of belts, motors, bearings, gears etc. promises high peak efficiency. However, the actual efficiency is depending on too many factors like how it's implemented, speeds and torque transmitted. For the 2017 powertrain the belts are promised to be up to 97% efficient. This however doesn't say if we're able to reach these numbers during driving or if it's losing a lot of energy while not connected.

To best support the development of a testbench for an ultra-efficient car, some knowledge about the powertrains in the car was needed. By rules SEM-vehicles can't have more than two driven axles. Most teams tackle this rule by either having two symmetrical powertrain units or one- wheel drive. For the "DNV GL Fuel Fighter 4"-vehicle the powertrain units are mounted to the firewall and which separates drivers' compartment. The powertrain units have certain similarities with the swing arms on a motorbike where brakes, motor gears, suspension etc. are connected. This made the design quite modular where the entire units could either be replaced or taken out of the car for testing as long as it had a test bench to be mounted on.

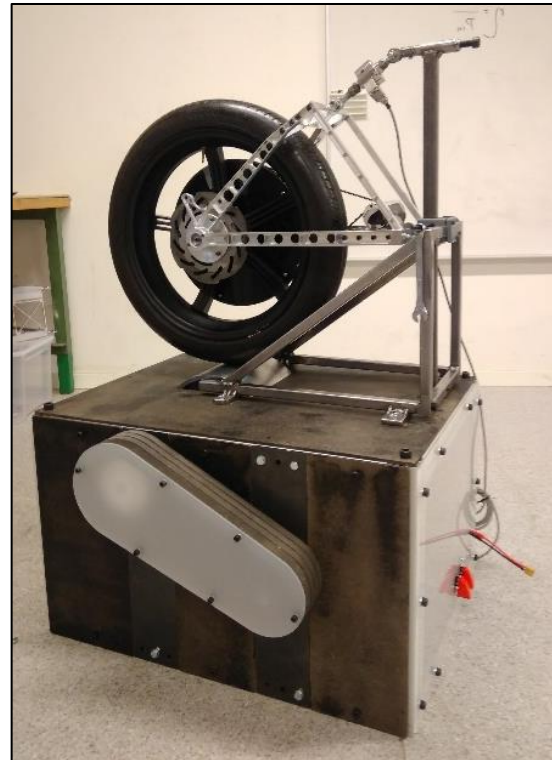
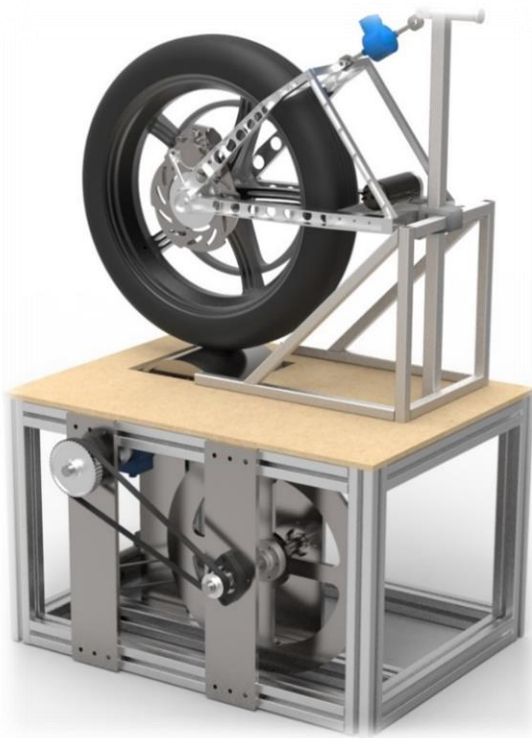


Figure 1.2 Render of the powertrain test bench and a picture of the final build.
Source: Pre-Master work

To utilize the fact that the powertrains were modular and symmetrical the decision to make a inertia motor/generator test bench were one of two powertrains were mounted. By simulating (half of) the theoretical forces the powertrain was exposed the goal was to mimic real conditions. To explain how this powertrain test bench works an explanation of the rotational parts is needed.

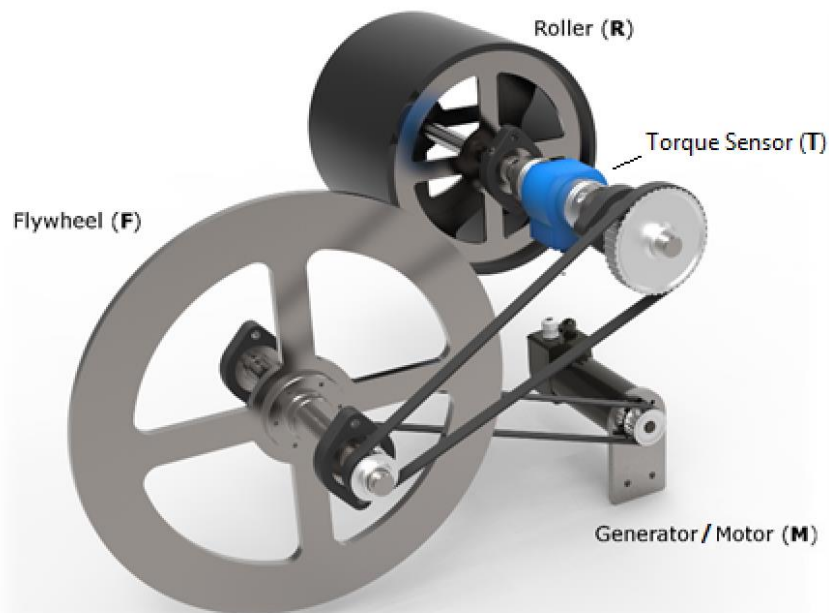


Figure 1.3 The internal components of the powertrain test bench

Figure 1.3 shows the internal rotational parts of the test bench and the roller is the part where the wheel traction force goes into. On the shaft that connects this further a 0.5% efficient torque transducer reads torque transmitted from/to the powertrain to the rest of the design. The roller contributes a tiny bit to simulating the inertia of the car, but most of the inertia is simulated by a flywheel that is tuned to the same inertia as the car. This flywheel relates to a gearing of ca 3:1 as an increase in the rotational speed means that a smaller flywheel can be used to save the same amount of kinetic energy. Lastly a Brushless DC (BLDC) motor can apply positive or negative torque to the system to simulate the forces acting on the vehicle. The motors are controlled by a VESC motor controller. This motor controller has control loops for constant torque and constant speed which are both useful for stress testing. Simulink by MATLAB is then again used to gather sensor info as speed and torque and used to control the test bench and read sensor outputs real-time.

A further explanation on how this testbench works as well as a description on which forces that are acting on the car, theory of efficient driving and works is also written in this the pre-master that could be considered as the foundation of this master thesis and therefore highly recommended reading.

1.5 Readers Guide

For this master thesis the goal was to continue the work started in the pre-master. In this report it was stated that future work would be planned to be:

1. Mimic real driving on the test bench
2. Measure efficiency
3. Use the test rig as support for further work developing a new powertrain with regenerative braking with an overall better design

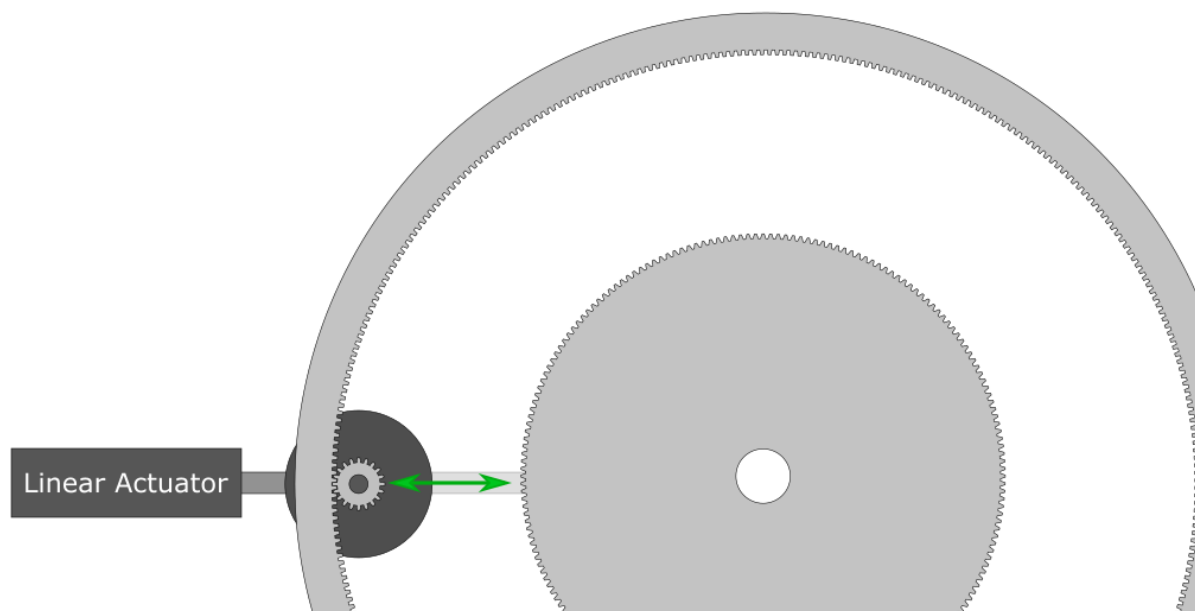


Figure 1.4 The concept of two gears visualized.

With only one transmission losses should be kept at a minimum as well as utilizing the power of two gears

For the development of a new powertrain it was also a goal to investigate how two gears controlled by sliding mechanism could increase efficiency, as it was hard to find literature mentioning the synchronization of gears. Figure 1.4 shows a drawing of this concept.

To develop the final powertrain and get it light enough, development of a new carbon fiber rim that were more suited for the task and made it possible to keep the old powertrains as is were also developed with focus on producibility, so it could be made cost effective by the team utilizing NTNUs facilities. The works and product development to reach the goal of an ultra-efficient powertrain is therefore a huge part of what will be discussed in this master thesis as well as physical testing, documenting of the process and a analyze of the race.

It's also important to notice that the work on all aspects of the car is team work with the common goal to engineer the best possible car. For this reason, I want to present the sub-teams and their area of responsibility as well as author's role. Some of their work is included in the Appendixes as well as in some of the figures.

The Powertrains

- Tanguy Simons: Responsible for motor controller development and communication and the logic behind the clutch control.
- Johannes Nadler: Responsible for the clutch board and execution of the test bench measurements. Main responsible for the motor model and the car model. In addition; welding and helping with machining.
- Author's role: Leader of the development process with the idea behind the clutch system CAD design and FEA simulations, production, gear calculations, 3D printing and calculations on gear efficiency, overvolting and analyze of the track results.

The Carbon Fiber Rim

- Nicklas Kaack: Guru of carbon fiber, manufacturing of the rims.
- Author's role: Simulations, CAD design, Milling and design of the moulds. As well as setting the requirements for the rim and some production. Noted here is that author haven't taken any composite courses, so the help from professor Nils Petter Vedvik to setup carbon fiber as a FEM material was done as well as Nicklas Kaack to join analyzing the results.

With the author responsible for the PM role as well a lot of work that haven't been related to the powertrain development has also been done. However, including too much of that would have done this master very long as well as the work presented here is what author have enjoyed the most and thinks are of greatest value to document for future teams.

2 Method

In the pursuit of building the most efficient and suitable vehicle for Shell Eco-Marathon the development process becomes quite unilinear by nature. The development of the powertrain and rim have therefore naturally been quite iterative where knowledge sometimes only gets available after testing or investigating various options. Many of the alternatives presented in this master have therefore been tested, either full scale or by simulations and prototyping in the search of a solution that could be validated as efficient but not as the one answer on how to do it.

This product development process could sometimes be described as set-based which according to Lean Enterprise Institutes have the following characteristics(Lean Enterprise Institutes, 2018):

1. Use trade-off curves and design guidelines to characterize (or describe) known feasible design sets, and thus focus the search for designs.
2. Identify and develop multiple alternatives and eliminate alternatives only when proven inferior or infeasible.
3. Start with design targets and allow the actual specifications and tolerances to emerge through analysis and testing.

Delay selecting the final design or establishing the final specifications until the team knows enough to make a good decision.

In addition to using set-based design there is a need to understand bigger picture of the car to reduce risk. To give a short explanation to methods used to reduce there some theory used theory from systems engineering as the Vee model and methods to reduce the risk by will be described in the following subchapter.

2.1 Vee Model and Risk Management

Most projects have a certain uncertainty which leads to a risk of something going wrong or things not working as planned. Especially for a project like building a one-of-a-kind car, these uncertainties become inevitable. By trying to push the limits of what's possible mechanical safety factors are kept low and components that are designed to be efficient, meaning that the risk of less reliable and too fragile parts. To deal with this the understanding of risk and how to reduce it is crucial.

To estimate the probability of a risk happening, two components should be measured: the undesirable consequence if the event if it occurs and the likelihood that the event occurs. (Walden et al., 2015) In such a way the level of risk could be estimated as in Figure 2.1. There's no other way to eliminate almost all risk other than to set the technical goals very low by using only failsafe parts. However, this isn't a good way to design a vehicle meant to push boundaries to be among the most efficient cars in its competition. It could also be argued if there is anything such of failsafe parts even with tons of safety factors and simplicity in the design when there still is the possibility of assumptions being wrong in every choice taken. Therefore, to reduce the probability of something happening by making a good risk management plan is needed.

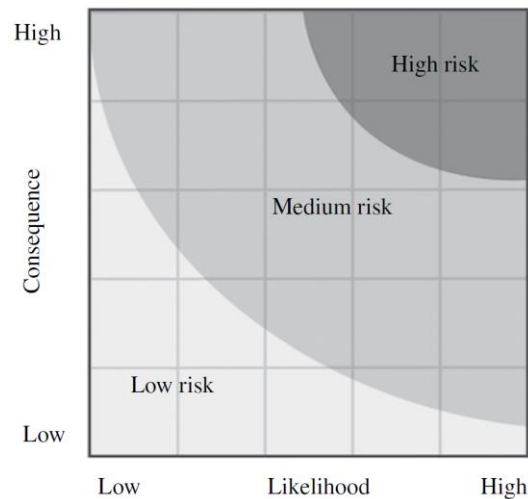


Figure 2.1 Risk level depends on both likelihood and consequence (Walden et al., 2015)

One way to reduce the consequence for our car to fail at the race is to design the car in such a way that it could be fixed during competition. This could be done by for example bringing spare parts, tools like lathes, glue and 3D printers for making better rapid or better dimensioned parts and avoid risks that could potentially have horrible outcomes, like for example to small safety factors on the brakes or parts that break. Or by making new designs interchangeable with designs that for various reasons gets changed in the development of an efficient car.

Likelihood could be expressed as a probability for an undesirable event happening. Therefore, mapping out and reducing the probability of an event could be an effective way to allow risks with high consequences without having to have a high probability. It's not always easy to map out the likelihood for components to fail before using them.

Therefore, testing as a strategy in the product development to reduce likelihood before accepting a solution could clearly give results. For illustrating this problem looking at the Vee model. Commonly used as in systems engineering (Walden et al., 2015) could be done. The Verification, integration and validation phases must be done to verify that the needs of the product are met.

According to the PMBOK(Institute, 2015) validation and verification (V&V) could be defined in the following ways:

"Validation: The assurance that a product, service, or system meets the needs of the customer and other identified stakeholders. It often involves acceptance and suitability with external customers. Contrast with verification."

"Verification: The evaluation of if a product, service, or system complies with a regulation, requirement, specification, or imposed condition. It is often an internal process. Contrast with validation."

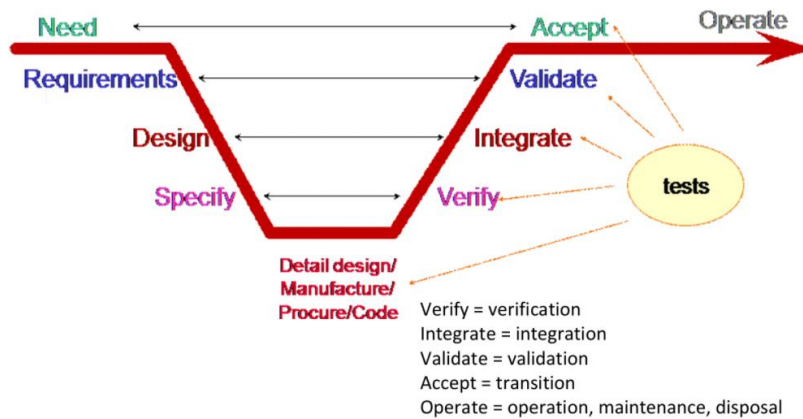


Figure 2.2 The Vee Model

Focusing on testing through V&V to make sure that the physical parts gets verified to be designed and manufactured as planned and validated to meet the requirements greatly improves the probability of the car performing according to it needs which ultimately are to drive results that gets accepted as valid in the race.

This work to reduce risk as well as not being afraid to change requirements if component tends to not satisfy the needs usually leads to an incremental and iterative development where problems are fixed by going back and forth as shown with the horizontal arrows and potentially changing design, subcomponents and requirements, design and specifications to meet the needs and the goals of having an ultra-efficient vehicle.

3 The Motors



Figure 3.1 The Maxon RE50

By switching from the hydrogen class to battery electric class the rules for motor controller also changed, where the team needed to have a self-developed motor controller. The self-developed motor controller in the 2017 car were one of the biggest issues of that year's team. It never worked as intended and stopped working quite often. One of the biggest focus areas in the beginning of this year was to get a stable motor controller. As the team member that worked on our motor control had been developing DC motor controller for another SEM team before with the same motor type as us and seeing several of the best teams in the competition using these over several years made the choice to keep using DC motors preferable.

In theory DC motors should be one of the easiest electric motors to control. However, some of the biggest difficulties with control of the Maxon DC motors is the low resistance and inductance that means that while they're efficient they could also be terrifying combined with bad motor control. As a worst-case scenario being controlled such that they get they're directly connected to the batteries nominal voltage without any can give quite a lot of torque and draw a lot of current— which they aren't rated for. The stall torque of the RE50 48V used in 2017 are 7.37Nm and 17 times higher than the long term 0.42Nm nominal max torque) which translates into a potential torque that could accelerate the car at 210Nm with one motor per powertrain with gearing set to 1:15 reduction. This will potentially overheat the motor in no time if no mechanical parts break first due to the torque. Assuming stall torque and 15:1 in gearing the car have 220Nm of torque, in comparison the electric sport car i3 with 250Nm of torque. This amount of power is neither wanted or needed for our car, that likes it best where the motors performs as efficient as possible.

The 2017 motor controller was controlling the motors with a single mosfet meaning that only one quadrant operation was possible. In theory this solution should have very low losses in the mosfet and be an appropriate solution for control of the car with one-way bearings. However, with a fly-back diode over the motor it also means that the car can't be moved backwards, as the diode would then burn the energy from being in the quadrant two where energy is going into the diode. Another huge drawback is that a one quadrant controller can't regenerate power (QIV, Figure 3.2) and drive that car forward (Q1, Figure 3.2).

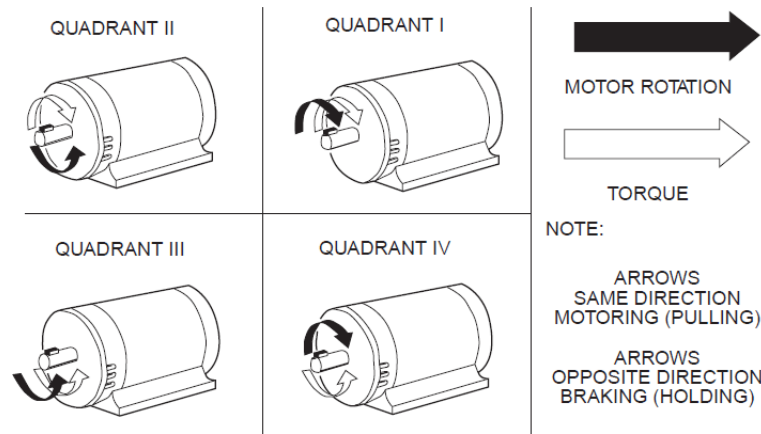


Figure 3.2 The four quadrants of DC Motor Drive
 ("What's the difference between a non-regenerative DC drive and a regenerative DC drive? | Quantum Controls' Energy Saving Blog," n.d.)

With the pressure from 2017 on getting a working motor controller of the biggest priorities early in the project this year. And, by not having a good enough solution in spare the risks of going for an unknown motor type like brushless dc wasn't acceptable. Some pros on keeping the same motors as last year, the 200watt Maxon RE50 DC motor were as following:

- Being DC motors, they don't need any accurate control based on the motor magnets position.
- They also have the highest efficiencies of all commercial motors we have found in the power range for the car (<1kW) on the market so far with 94% efficiency according to Maxon.
- They are lightweight with 1.1kg per motor
- They are well documented with learning materials available

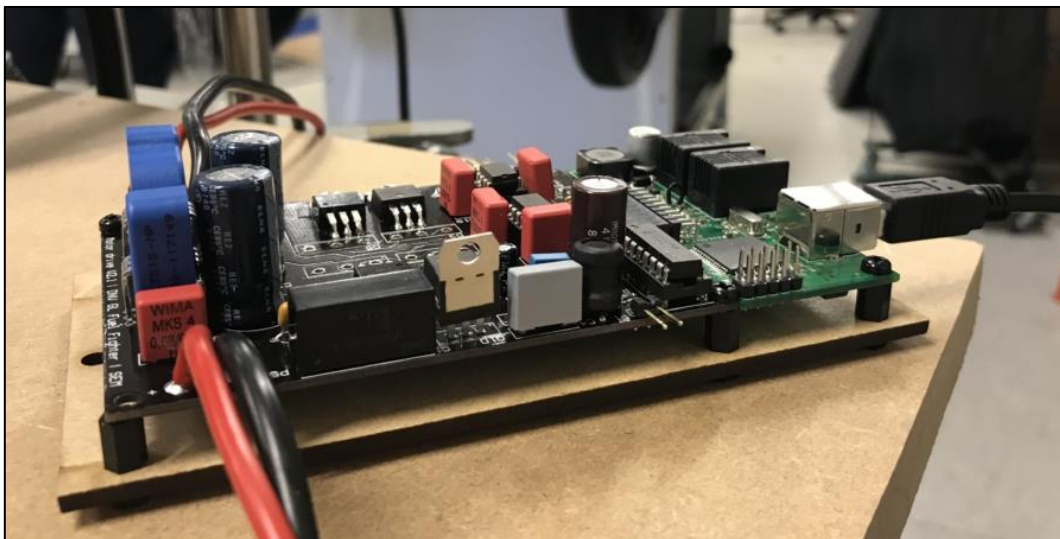


Figure 3.3 The final motor controller design for this year's car.
 The controller made by the team uses a universal module for its logic (module made by FF09 and much used for electronic control since). H bridge for support of all quadrants as well as a current control loop for accurate control of the motor torque.

3.1 Motor Model and Efficiency of The Motors

Most electric DC motors have iron between their windings to strengthen the magnetic field and thereby their torque output. The Maxon Motors are however ironless motors, meaning that they don't have the eddy current losses as most other DC motors have due to steel rotating in a variable magnetic field. This among others make the Maxon motor perhaps the most efficient motors in their size with up to 94% efficiency according to their datasheet.

According to Maxon motor there's still two factors to the losses: electrical losses from the windings and mechanical losses from the bearings. By using the formulas from 0 the losses could be described mathematically:

The electrical power required to give a certain torque (T) at a certain rotational speed (ω) could be written as:

$$P_{el} = R \cdot k_{\omega}^2 (T + T_f)^2 + \omega \cdot (T + T_f)$$

Where R is the motor resistance, k_{ω} is the no load friction, ω is rotational speed and T_f is the motors internal friction, mostly caused by the bearings but also brush friction. If the frictional torque from Maxons datasheets are assumed constant, a closer investigation of the maximum no load speed and current draw gives the value for the frictional torque. Since the only work done by the generated electrical torque is to overcome internal losses the following formula could be used:

$$T_f = I_0 \cdot k_t$$

Where the values no load current (I_0) and torque constant (k_t) could be found in Maxons datasheets.

To say something about the efficiency (η) of the motors at different speeds and torques the mechanical work ($P_{mech} = T \cdot \omega$) versus electrical work must be investigated.

The efficiency of positive accelerating with the car (η_M) (Quadrant I / III operation) could be described as following:

$$\eta_M = \frac{P_{mech}}{P_{el}} = \frac{T \cdot \omega}{R \cdot k_{\omega}^2 (T + T_f)^2 + \omega \cdot (T + T_f)}$$

While regeneration efficiency which is torque given in the opposite direction of the forward speed (quadrant II / IV) could be described as following:

$$\eta_G = \frac{P_{el}}{P_{mech}} = \frac{R \cdot k_{\omega}^2 (T + T_f)^2 + \omega \cdot (T + T_f)}{T \cdot \omega}$$

By plotting these efficiencies, one gets the following graph:

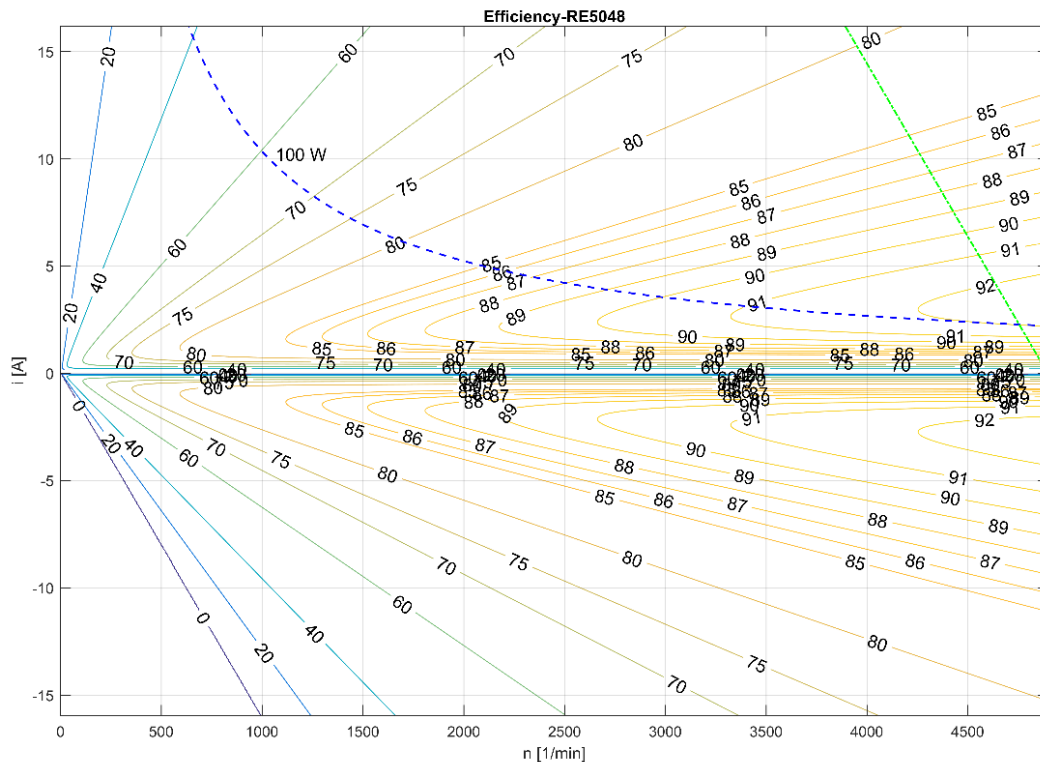


Figure 3.4 Efficiency of the Maxon RE50 48V
 Y axis is electric current and x axis rotational speed of the motor. Green line is where the back emf is bigger than the voltage to drive the motors and hence max speed at supply voltage, blue line is where electrical power equals 100w.

In the graph the green line is the limiting speed of the motors caused by the back emf canceling out the rated voltage of 48V of the motors.

$$I = \frac{V_{in} - V_{emf}}{R}$$

The motors can spin faster than rated and only have the mechanical bearing rating and a thermal current limit heat to consider according to Maxon. However, in the SEM rules it says that maximum voltage is 48V which means that can't get the 48V RE50 used in the 2017 car to spin faster than this. Luckily Maxon produces their motor with different windings, meaning that one could change the speed characteristics by changing winding configuration.

Interesting observations from the theoretical efficiency calculations of the motors are as following:

- Higher rotational speed means higher efficiency
- Higher current draws at given speed means more efficiency till a certain point
- Regeneration have close to similar performance as forward motion with one main exception: Braking at very low speed means that work must be done while braking at higher speed means that energy is gained. This is also caused by the back-emf and the fact that the V_{emf} meets the regenerated $-V_{in}$
- Maximum efficiency is at ca 3-4 Amps in the simulation

3.2 The Effect of Two Different Gear Ratios

With the knowledge of where the motors perform best it could easily be seen that there are areas where you get some more efficiency out of the motors. And that keeping close to the speed where the maximum speed is good.

With much of our assumed power consumption to happen in acceleration and deceleration in the beginning and end of each lap a want to accelerate efficient but fast the idea of two gears were investigated. The pros of having two gears where one has a higher gearing ratio is that your closer to having an efficient rotational speed for the motors at lower speeds as well. In addition higher motor speed combined with higher gearing ratio means higher torque outputs to the wheel with the same amount of control current. The concept is illustrated in Figure 3.5.

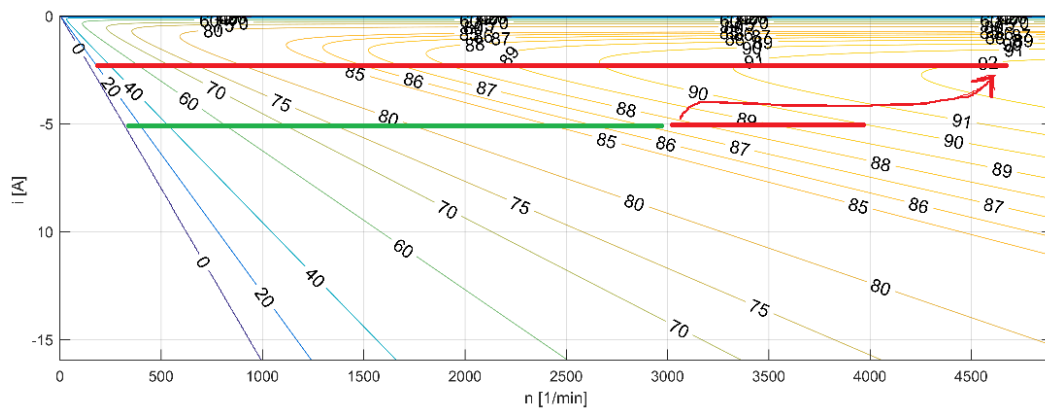


Figure 3.5 The effect of two gears vs one gear

To investigate whether two gears had enough influence the assumption of constant torque acceleration and a model only considering the available kinetical energy worked in each speed step and the motor efficiency was made.

One more criterion in the simulation was that gearing from first to second gear should change unless it more efficient to change and possible due to maximum speed of the motors. In the simulation the motor data selected was the RE50 48V as used by the 2017 team. It was assumed that the higher gear was 15:1 and that the lower was changed in increments. On the graph results could be seen for different accelerations (Nm) at different assumption of how the second gear should be in gearing ratio.

The results for different amounts of constant acceleration (torque on wheel) to the wheel with different gearings are shown in the following graphs:

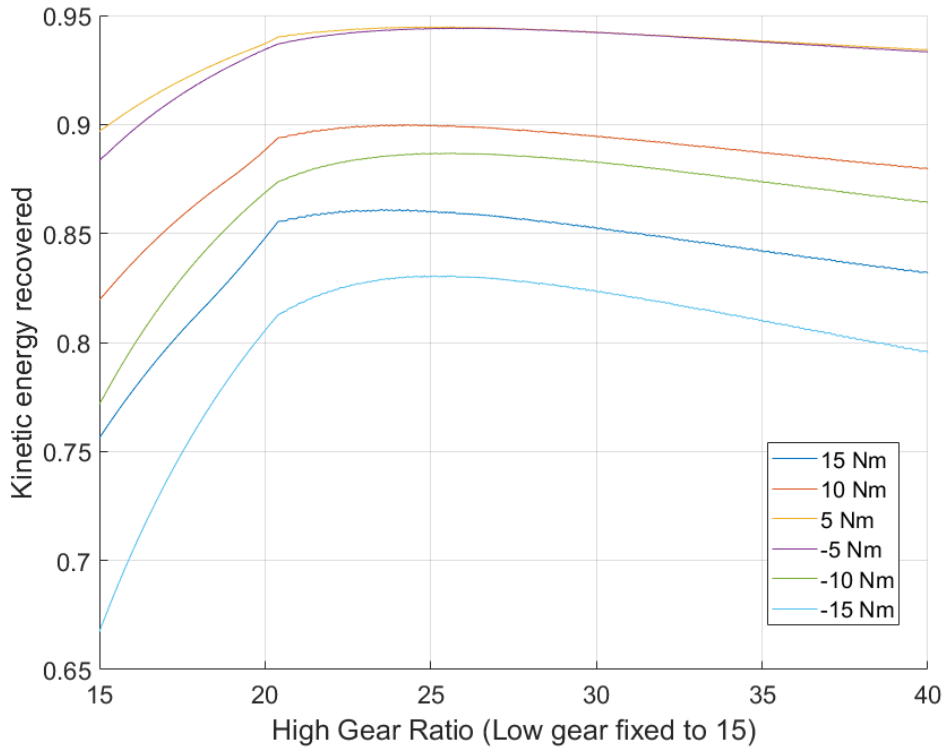


Figure 3.6 Simulation of the amount of energy lost trying to accelerate the car to 8m/s at constant wheel torque and with different gearing ratios for the second gear. Note that 15 in gearing ratio for both high and low gear means one gear.

To better illustrate what the graph is showing a time for constant speed needs to be made. By assuming that inertia forces from accelerating the car is dominating this means that the car with two powertrains will accelerate with a force being:

$$a = \frac{2 * T}{r_{wheel} m_{car}}$$

This gives the following time to go to/from 8 m/s to stand still a car with a car mass at $m_{car} = 160 \text{ kg}$:

+/- 5 Nm	35.5 seconds
+/- 10 Nm	17.75 seconds
+/- 15Nm	11.83 seconds

A closer investigation of what happens in one of the more efficient braking torques (-7.5Nm constant braking) in the simulation with a realistic gearing of 25:1 and 15:1 a plot of the speed and RPM I the motor was made. In Figure 3.7 the state of the motor is shown. The motor switches gear as fast as it's able to, where the motor can go up to speed. Figure 3.8 illustrates the motor efficiency changes when the motor switches gear and spins faster and with less motor current.

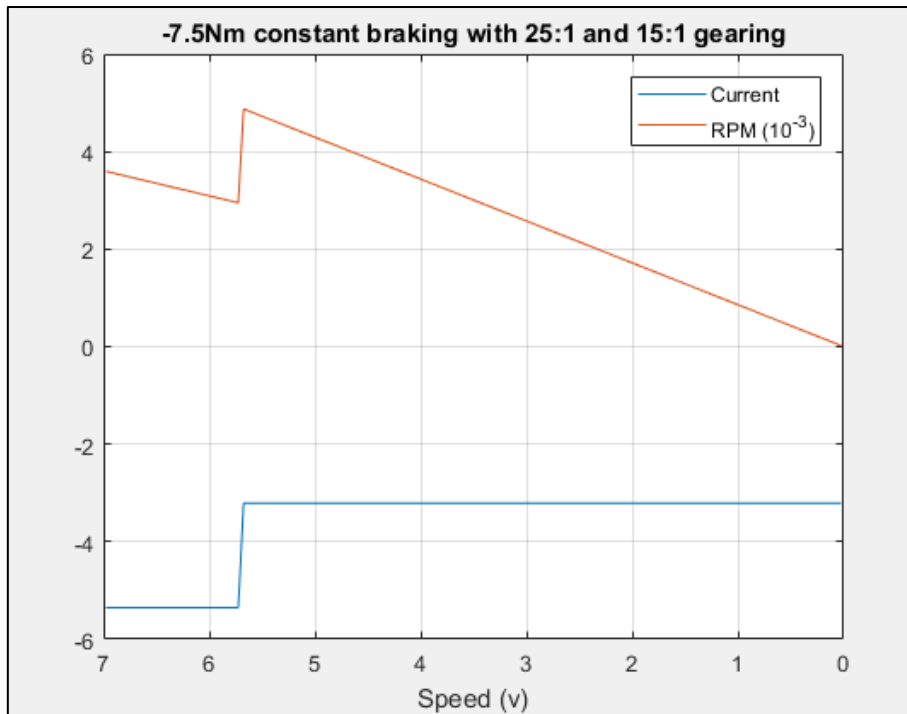


Figure 3.7 Investigation of when the simulation wants to change gears at a one of the more ideal gearing ratios at 25:1 and 15:1 while regen at -7.5Nm

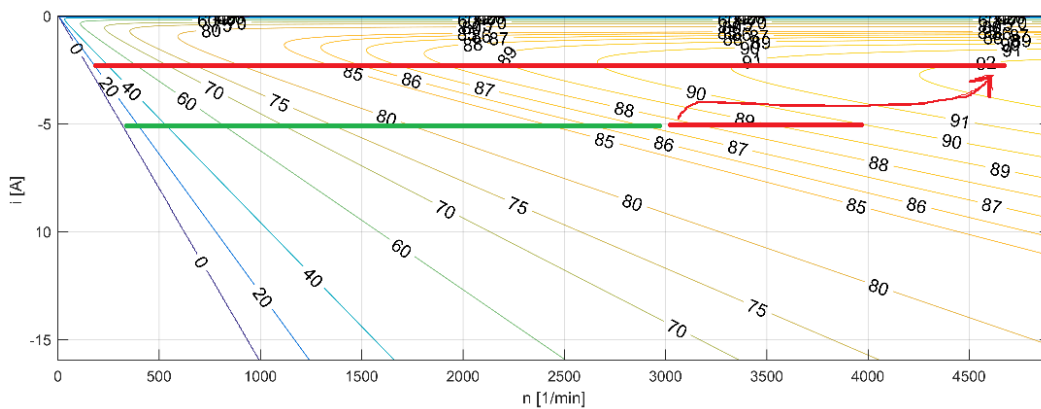


Figure 3.8 The effect of two gears vs one gear

3.3 Overvolting the Motors

As earlier mentioned the only limit for how fast the motors could spin is when the back emf are equal to the voltage applied. Therefore, alternative to the two gears was to change the RE50 motor to one with a lower speed constant. By doing so one could get the motor to spin faster than the nominal speed they have. For this investigation we looked at how efficient the motors would be at negative torque during the deceleration phase. The assumption was that each motor should be able to bring the car to the same speed of about 25km/h and that the voltage applied was maximum 44V, as SEM rules says 48V nominal voltage is max and the batteries in the car are at 44V nominal.

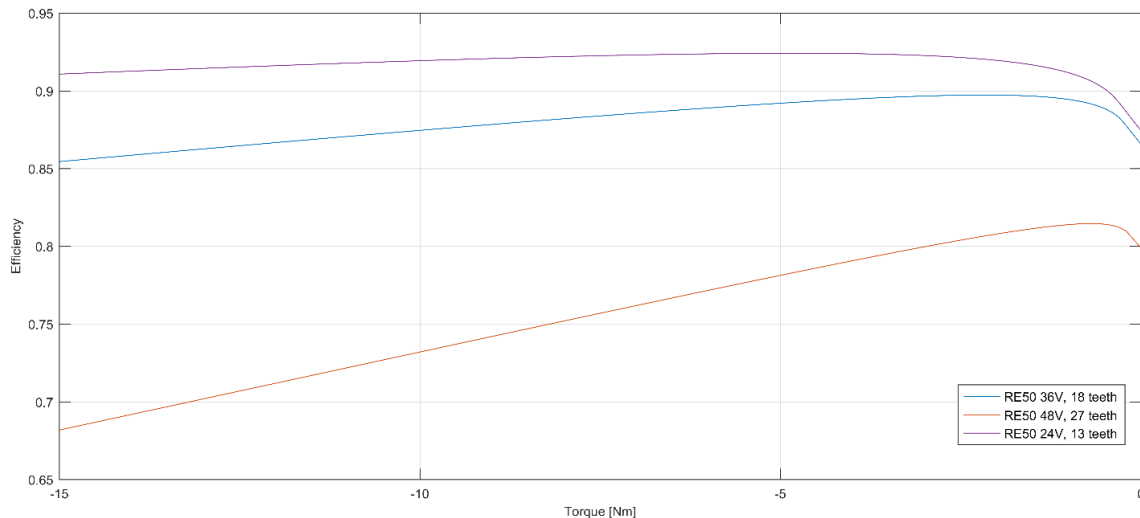


Figure 3.9 Regeneration Efficiency at different motor voltages

The results for this simulation showed that with the Maxon RE50 the higher the rotational speed is the better efficiency theoretically. Also, for the RE50 24V the gearing used for the simulations means that bearings will go faster than 9000rpm which they aren't rated for and 13 teeth for the gear means that the assumption of a ring gear with 375 teeth at module 1 and 20-degree attack angle as the driven gear isn't possible without gear addendum modifications

However, some verification for that the motors performs as expected at higher loads is needed. Is for example the bearings as good as expected at high rotational speeds?

3.4 Verification of The Motor Model

As theoretical values don't always reflect reality as much one would like and uncertainties the team had in whether we were able to control the motors as efficient as we thought a test rig for testing only motor efficiency was wanted. With the learnings from the powertrain test bench much of the same electronics were used to measure the efficiency of the motors with the use of the following:

- Motor to motor setup with a Maxon Motor for the load/acceleration These motors are ideal for the application as load motor due to low torque ripple
- A VESC Motor controller (Four quadrant control) for the load motor with possibility for constant speed loop meaning that the test could be quasi static with constant rotational speed and thereby constant torque to measure
- Lorenz Messtechnik GmbH DR-2477 2Nm Torque torque transducer for torque readings
- One of the UM-boards with an ADC reading chip sending data about torque measurements
- Purpose-built motor controller for the car to drive the measured side.
- Simulink gathering all sensor data for torque, speed and electrical current / power use
- CNC milled motor block made of PU-foam to hold the motors together with reuse of the motor mounts of the 2017 powertrain

The final CAD of the mounting bracket could be seen in Figure 3.10 with a few features to highlight: The old powertrains aluminum motor mounts were made to fit in the PU-block. To get the correct positioning of the motors a "T" shape was added on one side of the motor mounts. This is done to get rid of the trouble that a three-axis milling machine can't make sharp corners in the horizontal direction given the tools round geometry. Eventually rounded corners wouldn't allowed as accurate mounting of the aluminum holders. These tracks were cut a tenth of a millimeter too small by purpose and iterations of the final cut gave us a snug fit after removing enough material that there was 0.02mm

less clearance on the walls than the aluminum holders. Semi-flexible couplings for connecting motors to the sensor were used to take up small errors in the placements of the parts. Lastly screws through the holding block were used to mount the aluminum mounts and the torque sensor to the block.

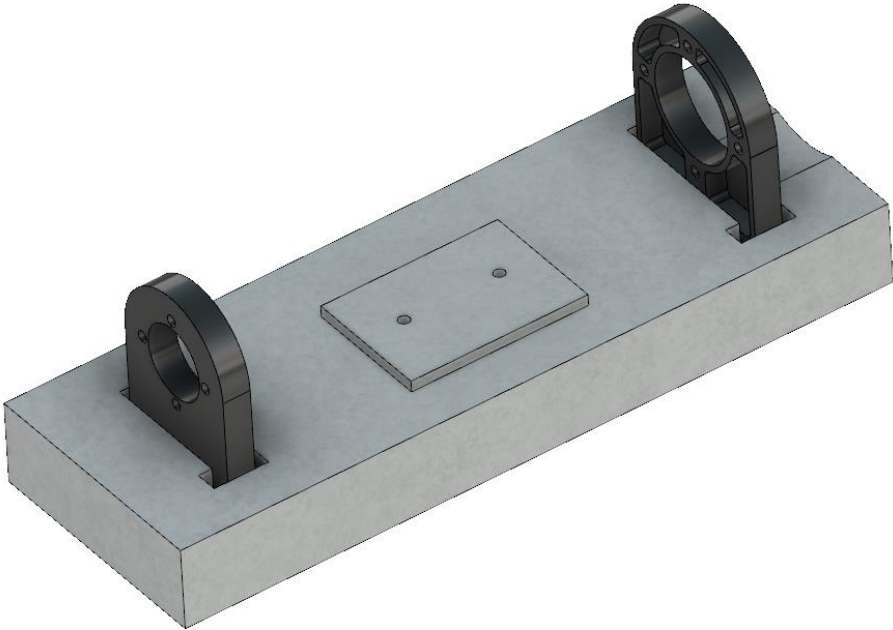


Figure 3.10 CAD model of the motor to motor configuration

A picture of the test bench in use is Figure 3.11 with motor to motor configuration with the torque transducer connected in between the motor with flexible shaft connectors. The Lorenz Messtechnik GmBK DR-2477 2Nm Torque transducer were chosen for its combination of low cost and decent accuracy class of 0.25%.



Figure 3.11 Two Maxon motors mounted in our test configuration

This setup was used to collect various data points with a Simulink through Serial Communication via USB. Tests were done at different torques incrementally, while “locking” the load motor/generator to constant speed with the built-in constant speed loop of the Vesc. The results for the measurements done on the both regen, and acceleration is shown in the graph underneath and the efficiency measured was including losses from the motor controller as this was easier to read than after the controller and gave additional info on how efficient the combined system was.

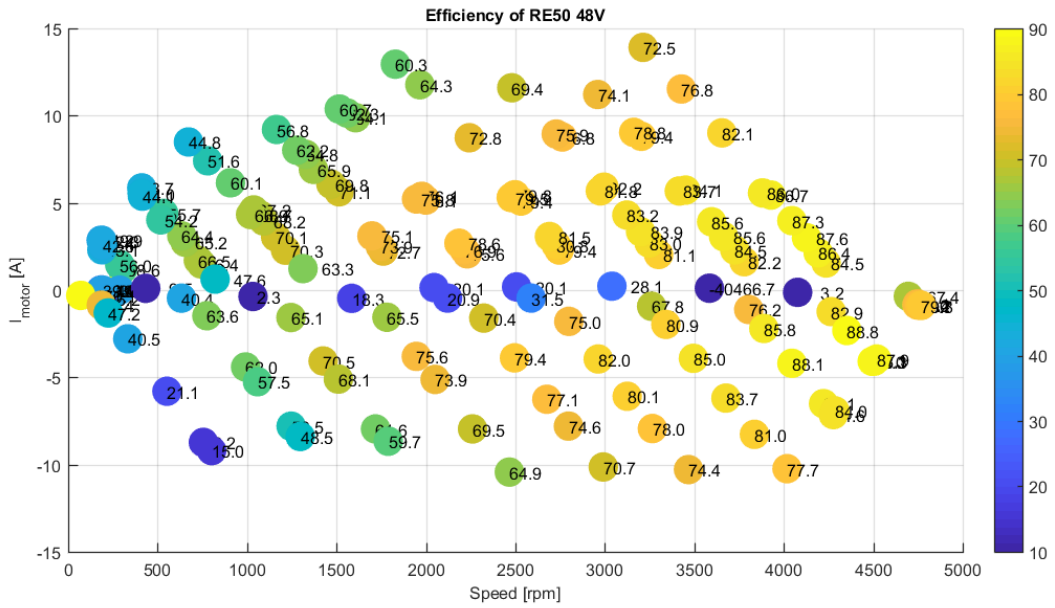


Figure 3.12 Data points measured for the RE50 48V

By using interpolation of the data plots in MATLAB the following beach plots for the Maxon RE50 48V:

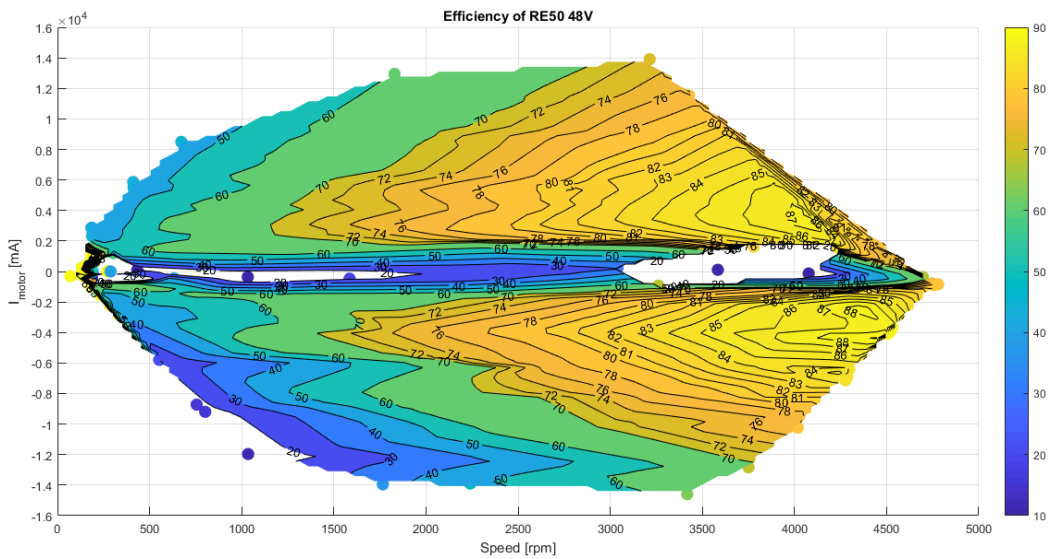


Figure 3.13 Interpolation of the data points gathered

In addition to the RE50 48V the RE50 36V motor was tested, but only in one for acceleration due to a partly broken torque transducer that could only read one way.

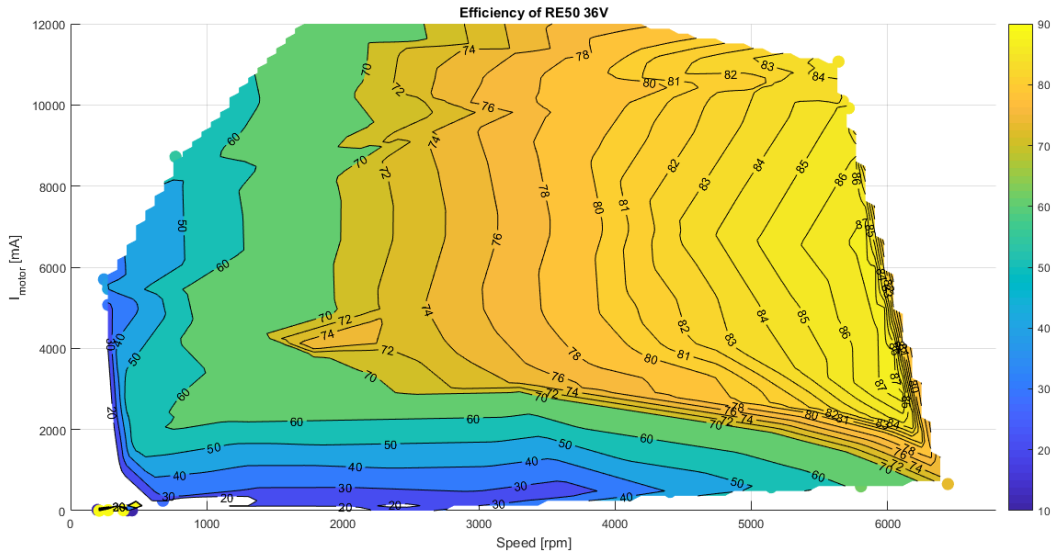


Figure 3.14 Tests done on the RE50

The results showed that the motors efficiency plots were comparable to the motor model. In addition, the team got a confirmation on that regenerative braking are efficient sending energy back to the battery.

A few potential error sources which makes it hard to trust that the results were consistent were as following:

- The motor temperature has influence on efficiency as its mainly caused by coppers resistance. Copper windings in a motor at 100 degrees Celsius versus 20 degrees will for example have about 2% less conductivity / more resistance
- Bearings are the other loss. The viscosity of the lubrication of these also change the efficiency
- The test system was vibrating a bit, meaning that some energy could have been lost here and lost at different rates
- The systems for reading mechanical and electrical power are team developed, not approved commercial systems (but designed according to datasheets)

Still the reading confirms that the motor model and the team's control of the motors aren't too different.

3.5 Strategy for Acceleration and Braking

Higher torque on the motors means that the transmission must be strengthened which usually indirectly reduces the efficiency of belts / gears etc. by for example needing a wider contact area for the belts or gears or a higher rated belt. To keep the losses to a minimum as well as to make a strong enough transfer of the motor power an understanding of which acceleration being necessary are important. To find out which motor currents are most efficient with our motors a simulation model was made by the team. This model is using the car model presented in author's pre-master (Appendix S:).

The car simulation accelerates and deaccelerate the simulated vehicle at constant torque and calculates the forces working on the car at each time step. The forces in the simple model was explained as:

$$\Sigma F = F_{Traction} - F_{Aerodynamic Drag} - F_{Rolling Resistance} - F_{Inertia}$$

As an output it gives how much energy theoretically used per lap and serves as a tool to find the ideal motor currents.

The model is described in Appendix K: and one of the most important findings here was that accelerating with about 6 Amps for the Maxon RE50 48V were proven the most efficient. This meant that that 10 Amps as maximum motor current were assumed as a good value for maximum driving current needed.

According to the motor model and measurements for this motor 3-4 Amps is the current where the most efficient conversion of energy happens. However, the trade of between having to high speed and fighting more aerodynamics and not getting everything back in the end shows that it's a tradeoff. This is illustrated in Figure 3.15 where it's clear that with 4 Amps of acceleration the maximum speed needs to be high.

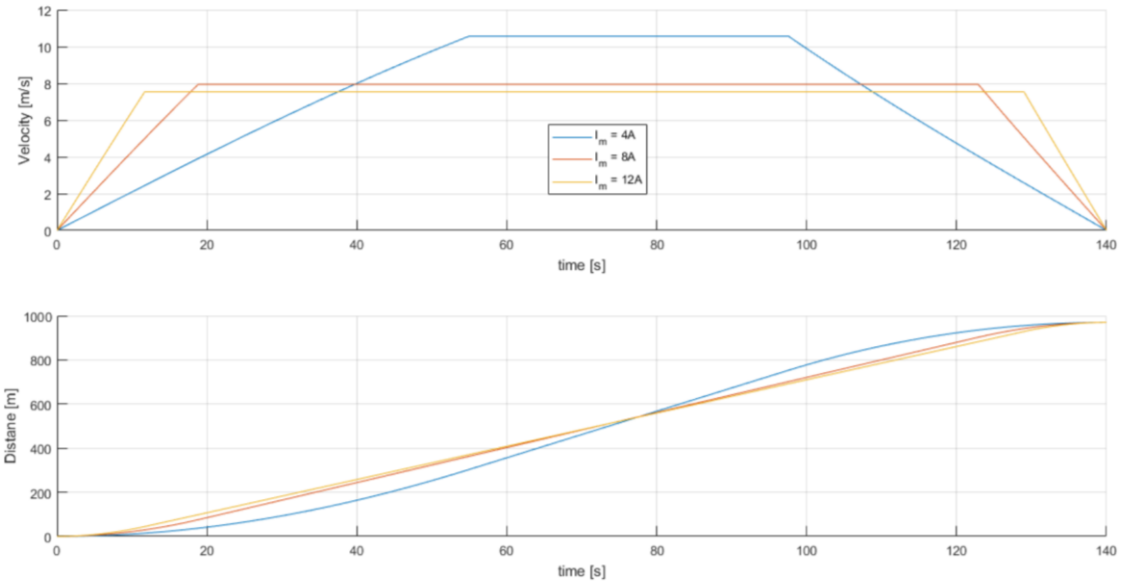


Figure 3.15 Speed profiles from some of the simulated steps

4 The Rim

With the goal to keep the same monocoque as last year but still cut at least 5 kilograms of the weight of the car it's was natural to focus on big structural parts. The rims with tires accounts for the for the second biggest weight of the structural parts according to the master thesis written on the project in 2017 (Carlsen and Oma, 2017). In this report it's advised that the 2018 team to investigate how to save weight by making new rims in carbon fiber.

Another reason to cut weight in the rims of a car is that it's needed to add energy to accelerate wheels both due to the weight and the contribution of rotational inertia. This means that added energy is lost during the acceleration and deceleration of the car where this energy is inputted and partly taken back by the efficiency of the propulsion as the loss. The loss of accelerating and decelerating this inertia could be seen by analyzing the formula for kinetic energy:

$$E_k = \frac{1}{2} I \omega^2$$

By substituting with $\omega = \frac{v}{r}$ and setting rotational kinetic energy equal as the kinetic energy of a linearly moving object ($E_k = \frac{1}{2} m v^2$) the rotational inertia could be compared to the mass of the car as following:

$$m_{\text{equivalent}} = \frac{I}{r_{\text{wheel}}^2}$$

In the DNV GL Fuel Fighter 4 as presented in 2017 the rims used were made in aluminum. These rims were specifically made for the DNV GL Fuel Fighter car in 2014 and had the following specs:

Weight per wheel	2.57kg
Rotational inertia per wheel	I=0.069 kg/m ² => m _{equivalent} = 1.05kg

4.1 Requirements

To make new rims a requirement list was made. The requirements were as following:

Lightweight	< 1.5kg (Should)
Rim profile	Michelin UC R95/80 R16 (Must)
Dimensional Constraints	Need to fit in existing geometry (Must)
Mounting	Five M6 screws, fitting the existing design (Must)
Compatible with new powertrain concept	Must be possible to mount ring gear
Air pressure	Hold 5 bars without leaking too much
Lateral force	500N bending (minimum)

Making carbon fiber rims isn't straight forward and the risks of making rims that aren't good enough by design is always there. Because of this risk on of the most important things with the rims was that they should be backwards compatible - meaning that they should be possible to mount to the car's existing suspension system and the other way around if they were to fail.

For the dimensional constraints to the center of the rim the front suspension has the least amount of clearance between the existing rim and the suspension assembly. The geometrical limits for this were inspected closely as shown in Figure 4.1.

The rules of SEM also say that the tire itself should be minimum 8 cm wide. For the urban concept class there's a purpose-made tire that almost all top team uses, the Michelin UC95/80 R16. It has a much

lower rolling resistance than any other tire on the market with a rolling coefficient of 0.013. This tire has the constraints for the rim profile as showed in Figure 4.2 and with SEM rules stating that it's mandatory to follow the manufacturer of the tires rim profile the dimensions of the rim also becomes a requirement.

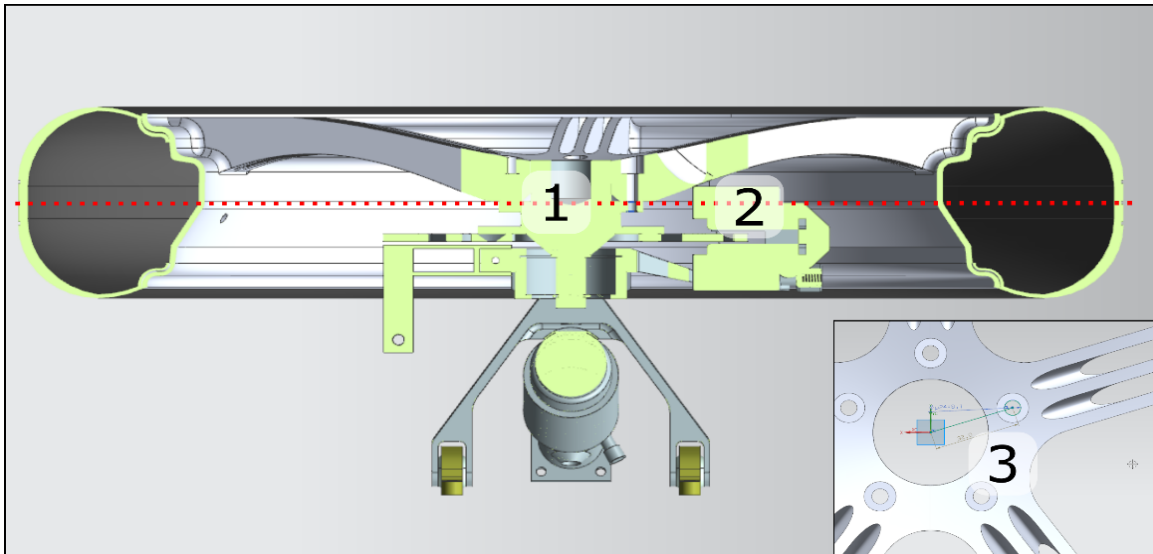


Figure 4.1 Some of the geometrical constraints

- 1: The rim needs to be mounted on a flat area in the axial center of the tire
- 2: The brake caliper is pointing out meaning that it needs additional clearance not to touch it
- 3: 5 M6 screws are holding the wheel at a distance 32mm together with a cylindrical center with a clearance fit

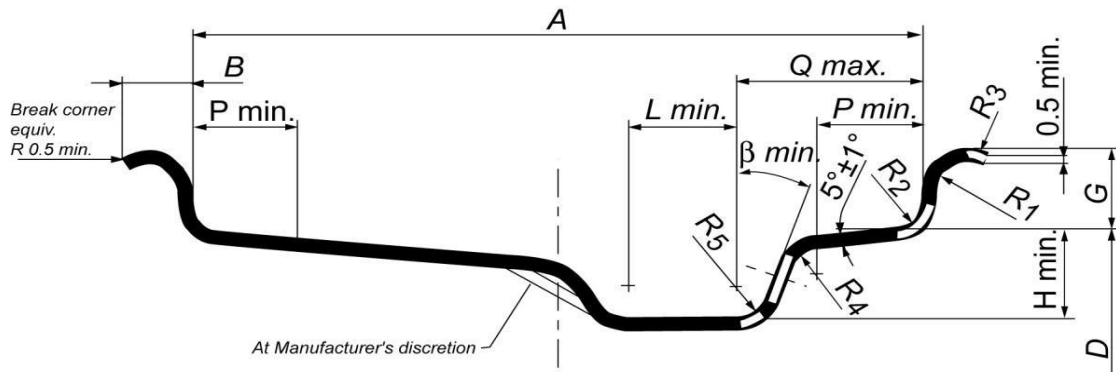


Figure 4.2 Michelins dimensional requirements for the rim profile.

4.2 Carbon Fiber as Material

The current rims are made in high strength aluminum and designed specifically to the DNV Fuel Fighter 2 in 2013. The expectations of cutting much weight on an improved design for rims wasn't too big with continuing using aluminum. By looking at what other teams were doing the two usual materials for lightweight rims was either carbon fiber or aluminum. Since the outer ring of the rim was already quite thin-walled the choice of making it in steel or other denser metals than aluminum, with the need of a certain thickness for successful milling wasn't looked at. Carbon fiber however were a good option and as Figure 4.3 shows carbon fiber can outperform aluminum when it comes to specific stiffness and specific strength.

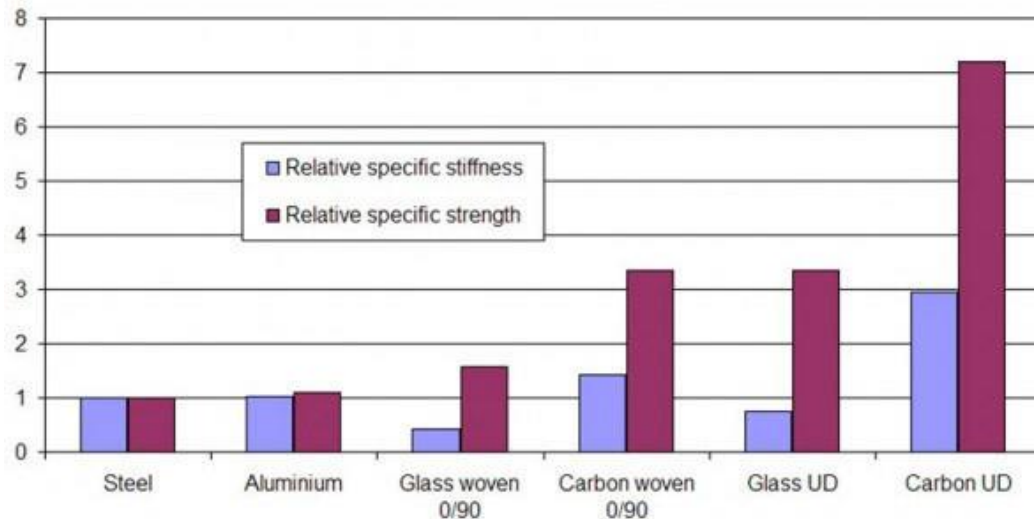


Figure 4.3 Specific stiffness and specific strength of different materials.
Source: carbonovus.com (2018)

4.2.1 Wet vs. Dry Carbon Fiber

When it comes to carbon fiber lay-up there is two common ways to do it: Wet fiber layup and dry fiber (prepreg).

With wet fiber layup dry carbon fiber sheets are added epoxy before the final production. This is usually done either by adding epoxy to the mould, then fiber, then more epoxy and fibers if needed and vacuum bagging it while it cures or by adding dry fiber sheets into the mould and sucking epoxy resin through the dry fibers (vacuum infusion).

Dry carbon fibers, also known as pre-impregnated carbon fiber is carbon fiber that have been added slow curing epoxy during production of the fiber. This means that no epoxy needs to be added during final production. The epoxy used for this application is usually fine having out for days /weeks in room temperature and much longer when stored in a freezer. At elevated temperatures the epoxy cures much faster and is therefore usually cured with an autoclave (pressurized oven).

Some characteristics of the different production methods are:

Wet fiber layup	Prepreg
<ul style="list-style-type: none"> • Cheaper than prepreg • Easier to add core material in one operation • Doesn't need heat to cure • Less need of expansive equipment 	<ul style="list-style-type: none"> • Easier to add into moulds • Ideal ratio between fiber and epoxy , meaning one could expect up to 70% lighter parts (Espel, 2018) • Most prepreg fibers need an autoclave to cure • Less defects and bubbles mean stronger parts • Elevated temperatures set limits to which core and mould materials could be used • Moulds tend to deform during heating

4.2.2 Sandwich Structures

Sandwich structures utilize spacing of the material with lightweight materials to increase the second moment of inertia(I) in a similar way as I-beams. With carbon fiber the common way to do it is by gluing a lightweight core material in-between carbon fiber walls.

By assuming that the carbon fiber plates are orthogonal the stiffness could be written as:

$$\text{Stiffness without sandwich structure} = EI = Ebt^3/12 \tag{4.1}$$

$$\text{Stiffness of Sandwich Structure} = EI = E * \frac{t/2 * h^2 * b}{2} \tag{4.2}$$

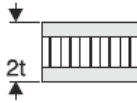
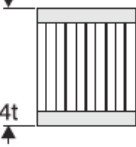
	Solid Material	Core Thickness t	Core Thickness 3t
			
Stiffness	1.0	7.0	37.0
Flexural Strength	1.0	3.5	9.2
Weight	1.0	1.03	1.06

Figure 4.4 Example from Solid Metal Versus Sandwich Panels (stressebook.com, 2015)

Increasing the thickness of a material increases the second area moment without increasing the weight too much, as Figure 4.4 which utilizes equation (4.1) and (4.2) shows.

In practice the core material can be made of a range of different materials. Figure 4.5 shows PVC and honeycomb which both are popular choices and relevant the rim center plate.

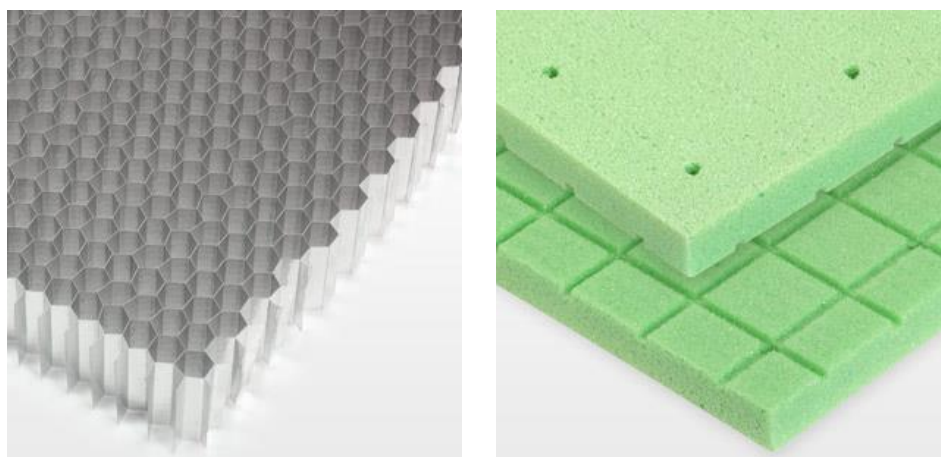


Figure 4.5 Common core materials: Aluminum honeycomb and PVC foam

The key is that it needs to be light enough, compatible with the process used. In addition, it needs to be checked if the composite will be under a lot of crushing forces which especially foam is weak against or shear forces which can be quite high. Two common core materials are shown in Figure 4.5.

4.3 The Solution

As the outside of the rim are also a part of the visual part from the outside, the wish to make it as aerodynamic as possible was wanted. With spokes potentially destroying the aerodynamics of the wheel the choice to go for fully covered center plates were taken.

The Final CAD for the design could be seen in Figure 4.6 and an explanation of the how its designed will follow.

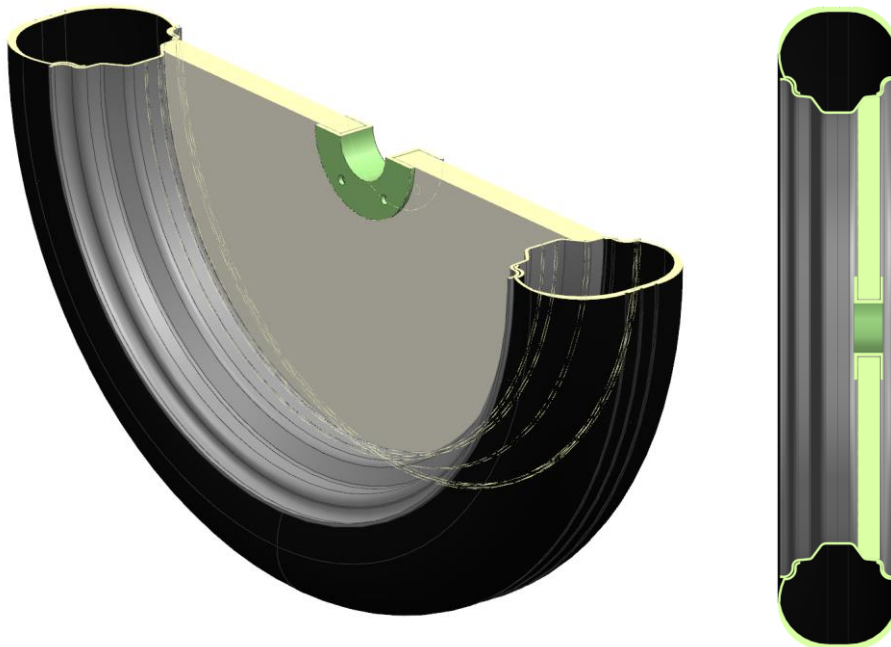


Figure 4.6 CAD of the rim

4.3.1 The Center Plate

To make the rims central plate and to get the rims stiff enough the two different geometrical solutions to hold the outer ring of the rim to the rotational center were considered, as shown in Figure 4.7.

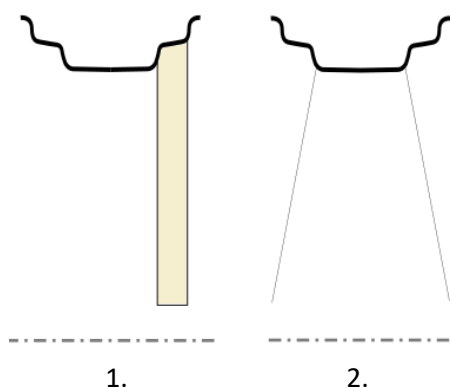


Figure 4.7 Different concepts for the center plate

The main reason to only consider fully covering plates and not a regular spoked center was that the principle of having plates would mess up the air less than a regular spoke design as well as plates being easy to make out of carbon fiber. Solution 1 would use a sandwich wall to hold the rim together while

solution 2 would utilize the strength of two sidewalls at an angle proven to be quite stiff according to the PAC-Car book (Santin, 2007).

However, as the geometrical constraints presented in Figure 4.1 made the solution to make the central part of one single flat plate made of sandwich structure the easiest. Other pros with this design were as following:

- The team did a similar design in 2011, main difference was placing the center in the middle.
- Cost. The team had a lot of core material from previous years in the thickness of 20mm with various strengths.

In Figure 4.8 a commercial solution like our choice of center plate is shown, but with aluminum honeycomb.

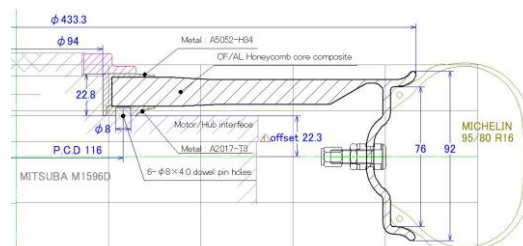


Figure 4.8 A commercial carbon fiber rim for Michelin Solar Race Tires

4.3.2 The Outer Ring

With the dimensional constraint for the rim profile of the Michelin tires as the main constraint the rim design proved to be a quite hard design to lay fiber on. For this reason, producibility became the main concern and goal to master to make the outer ring of the rims.

With the knowledge that pre-impregnated carbon fiber usually is considered easier working with on complex shapes as well as assumed to give more consistent, lightweight results as the epoxy ratio is predetermined the decision to make the choice was somehow obvious. However, cost was part of the picture as well, making it harder to support the choice of prepreg as it usually needs an autoclave to cure, where the closest the team could get access to was placed south in Norway.

With the wish of not having to travel far due to increased cost an alternative to conventional prepreg was wanted. Therefore “Out-of-Autoclave” prepreg which is specially made to cure at lower temperatures and only under without the need of an autoclave were investigated.

With easycomposites.co.uk being one of few distributors focusing on the DIY market and thereby making instructional videos as well as having the “XPREG XC 110”-system which only needed vacuum and an industrial oven to get good results.

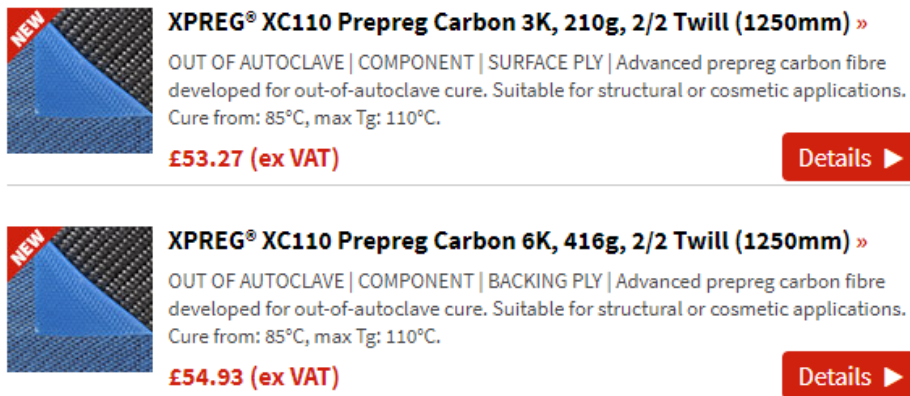


Figure 4.9 Easycomposites XPREG XC110

This product series is consisting of two different sheet-thicknesses (Figure 4.9) where the thinnest at 210 gram/m² being surface plies with extra epoxy on the surface side to get a good surface finish. The 416 gram/m² is for the backing plies.

4.4 Strength Calculations

Carbon fiber is known to fail quite instantly without any warnings. Combining this with the high pressure to inflate the tires makes the most frightening failure mode that the rim could explode. With this knowledge a way to verify if the rim is strong enough to withstand the forces applied is critical. Its therefore critical to understand the forces involved and especially the pressure forces. A strategy to make the rim in a safe way was therefore:

- Estimate needed layers of carbon fiber and study different layups by FEA
- Make the outer ring and pressure test it
- Evaluate how the ring performs and repeat until wanted results
- Pressure test every rim produced with the final layup and center plate mounted

The design criteria for the rims became that they should handle the following

- 8 bar pressure (5 bar maximum rating of the tires)
- 2x the forces calculated for the rear powertrain (Chapter 5.4)

FEA Simulations were used as a starting point where the assumption that the outer ring was more or equally prone to explode without the center ring. With the knowledge that smaller radiuses would increase the stresses Michelines rim profile with maximum permissible radiuses and aa asymmetrical design with less radiuses on the side it was allowed were used. The mesh were made from with 2 mm cquad4 elements and every node were set to have the same 2D normal orientation and shell element direction. The results were analyzed with the commonly used unitless Tsai-Wu failure criteria where results less than or equal 1 mean it's able to hold the load.

First the rim was simulated to be right under 1 with the following layup from bottom up:

1x XC110 Surface Layer (210 gram/m²)

6x XC110 Surface Layer (416 gram/m²)

This rim was produced in the composite lab at the realization lab at NTNU according to easy composites recommended curing times for the oven. The production didn't go entirely to plan with a "pinned"

surface finish that were suspected to be due to a leak in the vacuum bag. Still, during pressure testing it handled the 8 bar of pressure.

With the knowledge that the rim with 6+1 layers were strong enough one more layer of carbon fiber was added for safety. All layers were simulated to have the 0/90 degrees weave in the in the same directions that the mesh. This were done since the bending force from the pressure would then try to bend along the fibers.

The FEA-model was updated with one more layer, and results can be seen in Figure 4.10. The forces applied was a pressure force of 10 bar where the rim will be covered by the tire (blue arrows) and calculated wall forces of 105kN pointing outwards in each direction (red arrows) simulating the tire wall pressure forces.

The core material of type Diab Divinycell H100 were simulated strong enough in compression and shear to be used and the other the load cases were almost neglectable on the outer ring as Appendix E: shows.

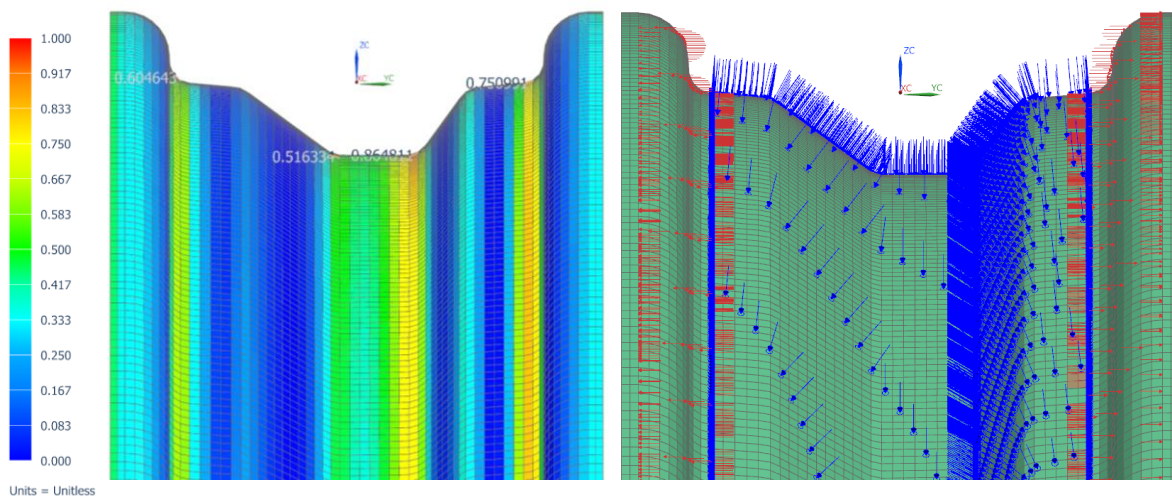


Figure 4.10 The FEA model of the outer ring

4.5 Production

The prerequisite to start production of the rims were the moulds. With the workshop having big enough CNC milling machines but not big enough CNC lathes (that gives better accuracy for round parts) the option became to make the moulds in aluminum for the rim center and epoxy tooling board for the center plate.

For the outer ring a two-split mould with surrounding the outsides of the rim were decided to be used. With this there was a possibility of the rims being hard to get out due to the mould geometry. However, as it would save time and material and reading that the 2011 team were doing something similar it was chosen as the final solution.



Figure 4.11 The 50mm block mounted

The aluminum blocks the team had was 50mm thick which was half the thickness needed. The choice became to screw the mould together making each part of the moulds consist of a two-piece aluminum block bolted together. The moulds were designed in such a way that the holes used to mount the pieces were also the holes used for bolting the aluminum pieces to the CNC machine where as shown in Figure 4.12.

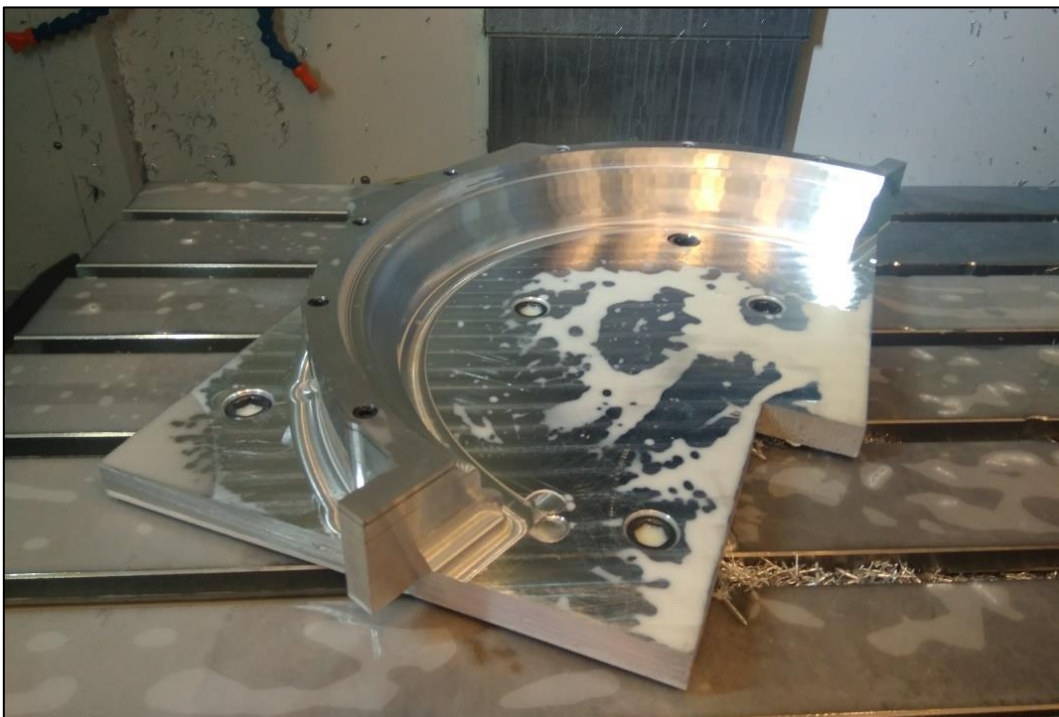


Figure 4.12 CNC milling of the rim contour right before finishing cut

With the limiting factor to the layup of the rim being the geometrical shape square prepreg patches which possible to lay were used with an overlap of about 1 cm. In Figure 4.13 layup of four patches is done.



Figure 4.13 The mould during layup of carbon fiber

When all layers were added an industrial oven combined with a hose from the vacuum pump into vacuum bag were used and the curing cycles recommended by Easy Composites were followed.

Next in the process was to produce the center plate. For this a wet layup with a CNC cut 20mm thick Divinycell H100 foam carbon combined with fiber on each side was opted for. The mould made it possible to “seal” the fiber layers on each side of the foam reducing risk of delamination between core and fiber. “Pizza slices” cut in shape were used on each side with two layers as simulated. In this case there was no overlapping in between the layers but rather an offset of the layers making the corners of the slices cover the center of the previous layers slice. Finally, vacuum, release film and breather material were used during curing to remove excess resin and compress the fibers. This curing happened at room temperature as the core material wasn’t suitable for heat.

Pictures of the process are shown in Figure 4.14 and Figure 4.15



Figure 4.14 The finished center plate mould



Figure 4.15 Lower layer and foam laid in the mould.

With center and the outer ring produced bonding them together as well as gluing the aluminum center (Figure 4.16) was left to do. Epoxy glue of the type Araldite 2031 were used for all glued connections. To get the center aligned with the wheel a jig tool made with the CNC-mill that had a snug fit to the sides of the outer ring mould and an 8mm hole in the middle were used. In-between the holes a circular tool made with the lathe to tight tolerances was added. This made it possible to glue the parts in place while holding the aluminum center centered. After gluing of these pieces demoulding and sanding of the edges were completed. Pictures of the alignment-process is shown on the following pages:



Figure 4.16 The Aluminum Center



Figure 4.17 The Centering tool



Figure 4.18 The centering tool fastened to the mould

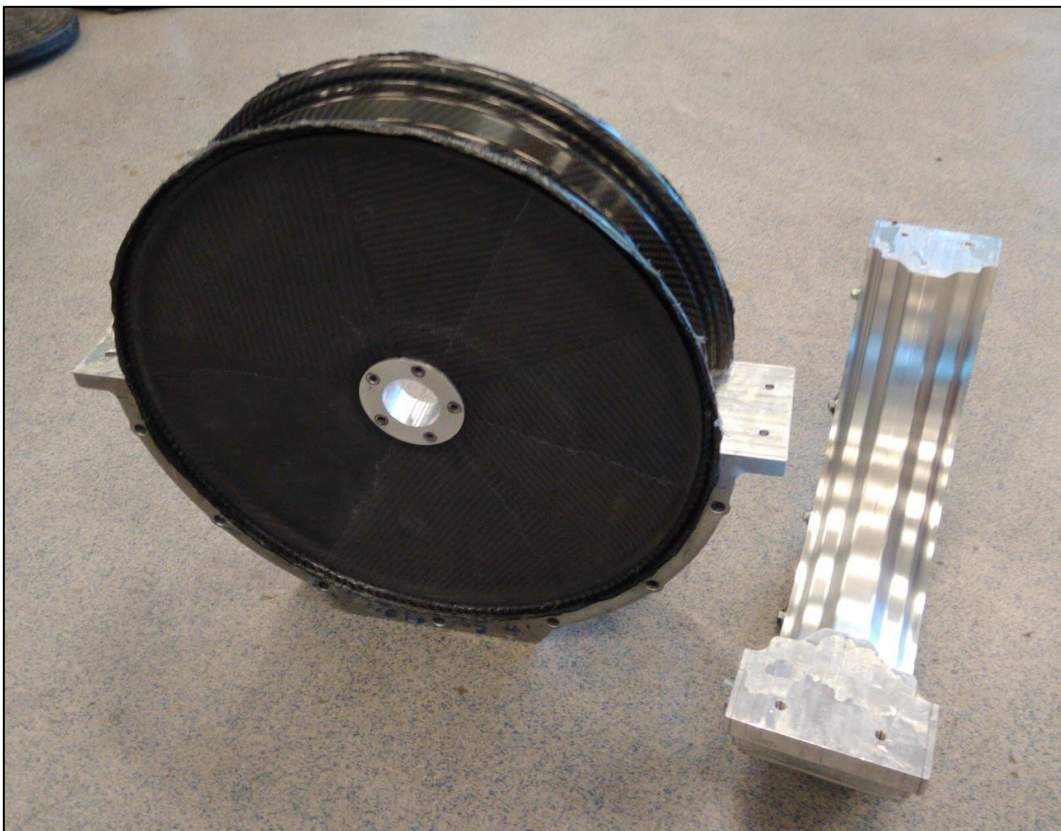


Figure 4.19 Demoulding

4.6 The Result

The final rim ended up at a measured weight of 1.40 kg and thereby reaching the goal of being less than 1.5 kg. The previous rim was 2.57 kg which meant that production of rim made a huge contribution in the pursuit of a 5 kg weight saving with 4.7kg overall reduction of weight. Unfortunately, one of the wheels had to be used with a tube as it were leaking a bit and were used with a tube that added a few 100 grams in weight.



Figure 4.20 The Rim

The centering tool also did a fairly good job at centering, but for one of the rims the mistake of placing the aluminum center wrong were done and it resulted in some misalignment of the rim. It was also noticeable that the rim wasn't totally round when it rotated. This is expected to be partially due to heat deformation and partially due to the use of a CNC mill to make the mould. However, with the Michelin tires being hand made with a radius change of one millimeter the imperfections of the rim weren't that noticeable and at a lower scale.

5 The Powertrain

The powertrain can be defined as the main components giving propulsion to a vehicle. For an electric car this means that everything transmitting energy from the battery to the driven wheel could be considered parts of the powertrain. ("Powertrain," 2018). Over the years in Fuel Fighter many different concepts have been utilized. On the energy side the car has either been running on Fuel Cells or with battery electric. As a black box these two technologies are quite equal where hydrogen fuel cell that have enough hydrogen could be having quite the same behavior as a charged battery in terms of how voltage is nearly constant with a voltage drop happens if too much current is drawn. However, the LIPOs are also able to receive charge quite efficiently.

For the race and understanding of how they measure energy consumption is also important. In the hydrogen-class the energy is measured by measuring the amount of hydrogen used before the chemical reactions inside the fuel cell occurs. This means that to achieve a good result an understanding of how the fuel cells are behaving most efficiently is required. Some parameters often investigated are at which current draw the energy conversion efficiency is the most efficient. Other parameters often investigated are how the time between purging's of the cell and cooling of the fuel cell increases efficiency.

For the battery class the actual efficiency measurements is easier and only measured off the energy used after the battery and battery management system. The formula for efficiency therefore becomes.

$$P_{\text{battery}} = \frac{dE_{\text{battery}}}{dt} = U_{\text{battery}} * I_{\text{battery}}$$

This means that voltage drops due to internal resistance losses of the battery isn't measured. In the 2017 and 2018 version of the vehicle two high power batteries for radio controlled(RC) devices of the Type Tattu 7000mAh 6S LiPo is used in series ("Tattu 7000mAh 6S 22.2V Lipo Battery, DJI S800 Lipo battery - Gens Ace," n.d.).

These have a discharge rate of 25C continuously and a 3C charge rate. The specs give the following energy and power limits:

Nominal voltage	$U = 3.7V * 12 = 44.1V$
Available energy	$E = 3.7V * 6S * 2 * 7000mAh = 310.8Wh$
Continuously power out	$P_{\text{out}} = 44.1V * 7000mAh * 25C = 7.77kW$
Continuously Power in	$P_{\text{in}} = 310.8Wh * 3C = 932W$

The reason for why these RC batteries is chosen are that they have quite high charge- and discharge rates (C rates) and a high density relatively to most other lithium batteries.

5.1 The Old Powertrain

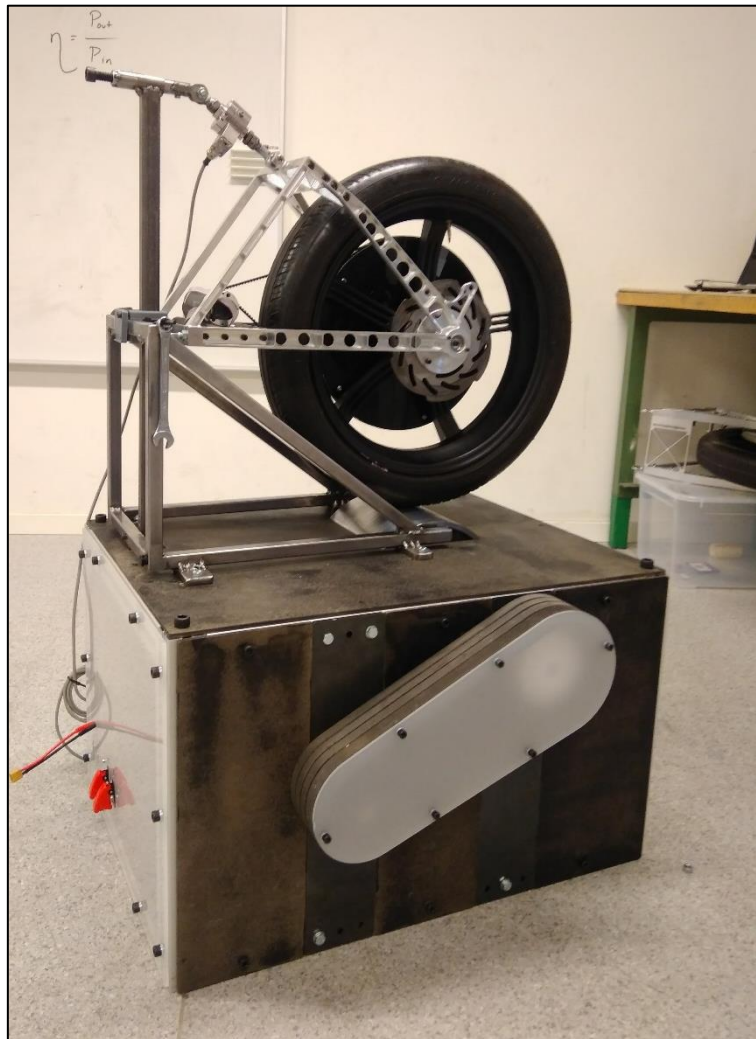


Figure 5.1 The old Powertrain Mounted on the Powertrain Test Bench

Author was one of the main contributors to the powertrain design last year. The final design ended up as two symmetrical swing arms units mounted to the firewall. In addition to transmitting the motors power to the wheel the system worked as a rear suspension. A 15:1 gearing ratio with a custom-made water jetted belt gear was used in combination with a Maxon RE50 48V motor. Synchronous belts were used since the 2016 team recommended it and had solutions on how to improve reliability

The goal with this powertrain was a reliable, adjustable powertrain where motor- and powertrain axle would be easily connected by belts in different lengths depending on which motor to be used. This made it possible to select which motor to use by need. CAD software with FEA optimizations were heavily used to achieve the wanted stiffness and geometrical shape. This also made the production complex as the machining time for milling it was assumed to be about 25 hours according to the CNC-machinist at the university.

Being complex in the shape with almost no clearance between the belt wheel and powertrain frame gave quite little room for improvements as adding controllable clutch system to the belt wheel or changing from belt drive to something else. The frame design also made the adjustment of it and changing of wheels very time demanding due to many screws and the need to fully dismantle to change settings as wheel position or belt position.

The fact that it was hard to iterate on the design to reach the goal of a more efficient energy transfer made the decision to make a new powertrain.

The strategy where learning from the old powertrain with verification of performance and stability was important. To verify that both the 2017 powertrain and a new design was meeting expectations the test bench were going to be used in the testing phases. A crucial part of the process was to gain insight in how the powertrain performed from battery to ground and make sure that motor controllers worked. It also made it safer to take risks in the development as the overall risk was reduced by having a backup system.

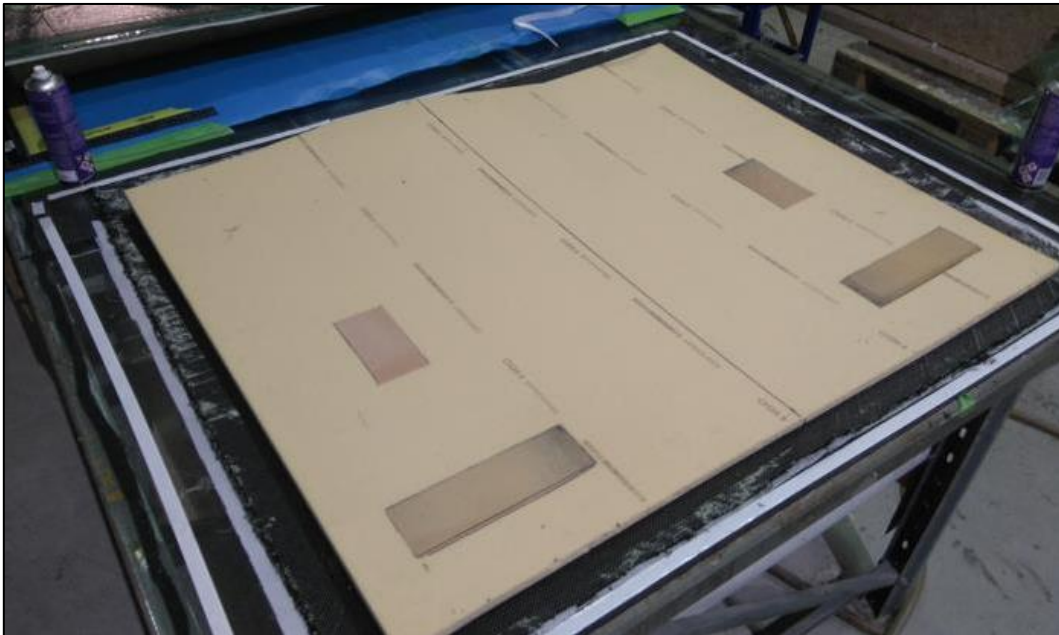


Figure 5.2 Production of the bulkhead/firewall in 2017.

The powertrains insert as shown as the darker denser core material. These gives one of the biggest geometrical limits of a new powertrain mounting. (Carlsen and Oma, 2017)

After use of the old design in both the powertrain test bench and from real driving some notes were taken: wanted were wanted for a new powertrain:

- Belt drive causes wheels to stop fast if belts are connected – meaning huge power losses?
- New powertrain needs to be stiffer – belt wheel is moving a lot and brakes are touching during cornering on the old design
- Suspension way to stiff – the forces on the shock isn't big enough with the current geometry – even at lowest compression ratio of the air shock
- Current design is expensive and time demanding to reproduce – simpler design wanted where the production of a spare isn't too expensive

5.2 Requirements for the New Powertrain

To improve the powertrain based on learnings from the powertrain that were already in the car a few requirements were set:

- Stiffer overall
- Stiffer bearings (lot of play causes the frame to behave worse than simulated)
- Mounting to the wall, where there is inserts in the carbon fiber fire wall

- Support for regenerative braking
- Low weight to reach the 90kg goal
- High efficiency (>98%)
- Mounting for Hydraulic Disc Brake (By SEM-rules, bicycle brakes not allowed)

5.2.1 Geared vs Direct Drive

A crucial aspect for the powertrain was how the car gets its energy transferred from the motor to the ground. To convert the electrical energy in the motor to energy a common way is to do it by reduction of gears. For these three different efficient reduction methods are commonly used: Gears, Chain and synchronous belts. In addition to gear reductions direct drive (DD) could also be considered. However, a DD-motor is usually heavier due to the need for more torque meaning more magnets due to lower rotational speed. To make the choice a pros/con list were made early in the project:

Tabell 5-A Energy transfer from motor to wheel.

	Efficiency*	Pros	Cons
Synchronous Belts	99%	<ul style="list-style-type: none"> • Easy to change gearing ratio • Silent • “Known technology”, used in the team the three last years • High tolerances not needed -> could be water jetted • Only one source of loss: teeth to teeth 	<ul style="list-style-type: none"> • One gear only • Used in the previous powertrain. The assembly stops fast • Usually need belt tensioner for good operation which means more losses
Gears	99.9%	<ul style="list-style-type: none"> • Most efficient solution 	<ul style="list-style-type: none"> • Complex to add more than one gear → more losses • Needs high tolerances in the production of the gear tooth shape • Noisy (spur gear)
Chain	98.5%	<ul style="list-style-type: none"> • Not used by the team previously • High tolerances not needed -> could be water jetted 	<ul style="list-style-type: none"> • Many links bending → losses happen in the chain

Direct drive	No gearing losses, but electric motors tend to be heavier when running at low RPM with the same torque levels	<ul style="list-style-type: none"> • No gearing losses • Silent • Used by the team earlier 	<ul style="list-style-type: none"> • Eddy current losses (losses due to magnets passing metal) • Mostly undocumented china motors on the market • Mostly brushless DC motors commercially available • Complex to make self-made motors • Heavier by design (needs more magnets to get higher torque due to no gearing)
---------------------	---	---	---

The choice to work on a two geared spur gears with one involute and one regular gear where the motor is engaged in the gear by synchronization of motor speed and a linear actuator that pushes the motors in gear was (almost) decided in December in the author's project thesis. The fact that it's possible to implement two gears without losing efficiency for this concept together with the possibility to use the teams previously used Maxon motors were key reasons to the choice. So were the fact that transmission only have one source of loss: the gear meshing

5.2.2 Prototyping Two 1-Stage Gear Ratios

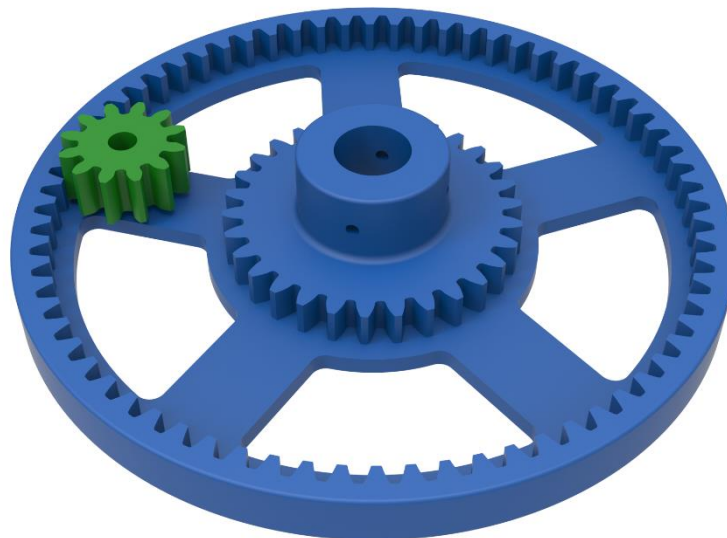


Figure 5.3 CAD of the 3D printed gears for rapid prototyping

Multiple speed reductions are quite common for both bikes, cars etc. However, since the electrical motor can transmit a lot of torque at low speeds and handles the entire speed range well it's not needed to have gears for electrical vehicles as electric cars and e-bikes. However, as the motor plots and efficiency tests presented in Chapter 3. there's still a benefit of gearing a vehicle to be closer to the most efficient operational range of the motor and to extend lower limit where regeneration can't happen due to back-EMF.

With gear being the most promising reduction technology in terms of efficiency and one speed reduction giving the least possible losses in theory it were wanted to utilize this by shifting a motor directly between a low and a high gear. As author couldn't find literature about engaging by doing

synchronization of gear speeds and physically forcing it in place connecting the motor the need to validate that synchronization works was needed. From a theoretical perspective it should be possible to engage two gears if they are synced, but we had to make an experiment to test and verify it. Some of the main concerns was if the gears would engage or just crash gear teeth top to gear teeth top.

The powertrain test rig had by purpose been built with the rollers axle a bit longer than necessary in case one more roller was to be connected or that other devices were connected. With the possibility to accelerate the roller to more than double angular speed as the car's wheel this meant that we didn't have to go full-scale with a prototype gear to get the correct pitch velocity in the gear mesh. To easily test that the transmission worked 3D printing combined with Fusion 360s gear modeler was utilized to make a rapid prototype of a gear assembly with an internal and one external ring gear that could be fitted to the powertrain test bench roller axle. The CAD for the of this could be seen in Figure 5.3.

The tests on the powertrain test bench were conducted by using two of the Vesc motor controllers that both measures speed where one of them was to control the testbench as previously explained. The other was controlling the Maxon RE50. In addition, a prototype board for actuator control was made which were able to talk to through UART and set the position of the linear actuator accurately. To get the synchronization working the following were implemented in Simulink:

1. Measure rotational speed of the driven gear
2. Calculate wanted rotational speed for motor, depending on selected gear
3. Check if the motor can spin fast enough
4. Voltage control (duty cycle) to the DC motor to get the correct speed
($RPM = C_{electric\ speed\ constant} * V$)
5. Engage clutch if step 3 is true and motor have gotten correct speed
6. Change to Current control for the motor
7. Regular motor control
8. Disengage when motor isn't in use anymore.

The tests for gearing were successful and could be seen in Figure 5.4. The plastic gears were even able to transfer high torque for the motors. With these tests successful the risks of making the full-scale version of the concept was smaller as the concept of synchronization and engagement were proven to work. Some findings were however noted:

1. Motor controller needs to be four quadrants for two gears to work as synchronization to the outer and inner gear requires the motor to spin in different direction
2. Synchronization works better while the system is in movement.

For the first learning the need of two directional motor control is logical. It however sets an additional requirement for the motor controller over how it have been used for the 2017 powertrain where only one quadrant control. The second learning was that the motors work better for synchronization at high speed. In our experiment this meant that the motors would have some problems engaging at almost stand still and stand still since the teeth tops sometimes were crashing meaning that synchronization had to be done once more. To avoid this problem two different solutions were thought of and tested:

1. Spin the DC motor a bit faster than the calculated synchronization speed at low speed
2. Have the motors always engaged.

Both strategies worked and made the low speed problem a non-issue.

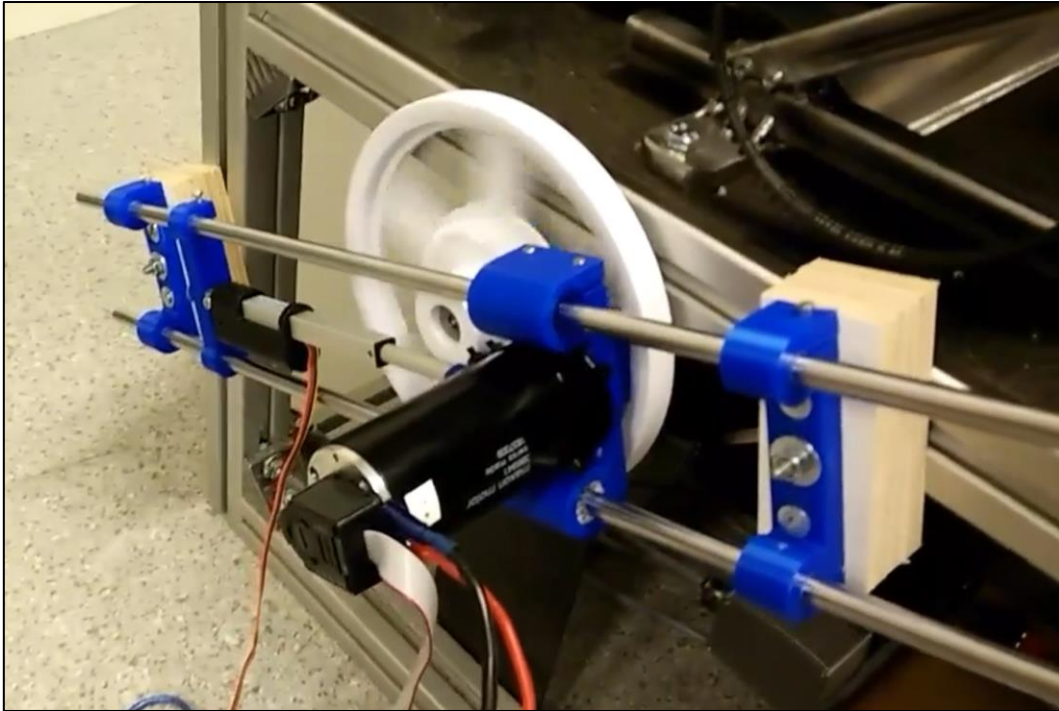


Figure 5.4 3D printed functional prototype of the two-gear solution

5.3 Designing the Gears

With the goal to still only have one gearing transmission (1-Stage) to reduce the losses to the minimum, a full-scale version of the prototyped gearing solution had to be designed with the following taken into consideration:

- Type of gear to produce
- Strength calculations for the gear
- Wanted gearing ratios archived
- Production and material

To design the gears a choice of which kind of gears to use had to be made. For this straight cut spur and helical gears were considered as following:

	Spur (straight cut gears)	Helical (angular teeth)
Pros	<ul style="list-style-type: none"> • More efficient • Easy to make • Easy to assemble 	<ul style="list-style-type: none"> • Strong • Quiet operation
Cons	<ul style="list-style-type: none"> • Noisy 	<ul style="list-style-type: none"> • More friction losses → lower efficiency than spur gears. • They produce radial loads

The fact that the spur gears were considered more efficient benefits our car. It's also shown in motorsport where drag racers for usually have straight cut gears. They are however also known to be quite noisy in operation at high speeds. With the helical also having some pros like better load distribution and silent drive both options were considered as good alternatives.

With no commercial gears in the wanted diameter with a small enough diameter the Plan A was to contact a manufacturer of gears to get the custom gears made. As gear making is quite complicated and the possibilities to do mistakes in the design are huge the help from one of several custom gear makers in Europe would be to great help. However only one out of five companies answered our request, and they had months of lead time meaning that the gears wouldn't be ready in time.

With no luck finding local gear makers the choice to produce the gears in some of the local machine shops in Trondheim was taken. This meant that machines like wire-EDM or water jetting had to be used which made it beneficial to make the gears straight cut to simplify production.

$$\sigma = W_t * P / FY \tag{5.1}$$

To find correct size and calculate that the gears handled to transmit enough torque the Lewis Stress equation(5.1) were used. This formula calculates the bending stress in gears with the assumptions that only one gear is load bearing at once and that the transmitted force attacks the top of the tooth. In this formula W_t is the transmitted force tangential to the rotation circle of the gear, P is the diametral pitch, F is tooth width and Y is the Lewis form factor that compensates for the teeth shape.

There are other more accurate ways to calculate the stresses of gears like the AGMAs method that adds a lot of factors to compensate for temperature, surface, fatigue, operational speed, motor torque ripple etc. to the basic Lewis strength equation or a FEA approach. However, as the goal was to create a prototype gear the choice of a safety factor these formulas were investigated, but with uncertainties of which constants to use when the gears are produced, made it easier just to set a safety factor of about 2 for the custom gear as well as the requirement to add a small radius in the tooth bottom of the design to prevent stress concentrations.

For materials to use both plastic and steel were considered (Table 5-A). Other materials like aluminum to make a more lightweight gear was also looked at, but due to high friction coefficient of aluminum it wasn't considered a good alternative for the gears. For strength a higher yield strength means that it could be made with a smaller module. According to the book about PAC car II (Santin, 2007) smaller module makes gears more efficient, which makes up for steels higher friction coefficient .

Table 5-A Plastic vs steel as material for gears

	Plastic	Steel
Friction coefficient	<ul style="list-style-type: none"> Plastic to metal, dry: 0.1 – 0.3 (dynamic)* Plastic to metal, lubricated: 0.04-0.1 (dynamic) 	<ul style="list-style-type: none"> steel to steel, dry: 0.5-0.6 (dynamic)* steel to steel, lubricated: 0.15 (dynamic)* steel to steel with Diamond like coating (DLC), dry: 0.1 - 0.2 (static)
Strength	Typical 90Mpa*** Weak – needs bigger teeth / wider tooth area	Typical 660Mpa*** Strongest commonly used material for gear production
Producibility	<ul style="list-style-type: none"> casting (most common for mass production) water jetting (small scale production) Milling (small scale production) 	<ul style="list-style-type: none"> Gear hobbing (only for external) Gear shaping (internal and external) Wire – edm (small scale production) Milling (small scale production)

* *Source: Coefficient of friction, Rolling resistance, Air resistance, Aerodynamics (tribology-abc.com, 2018)*

** *Source: Surface Coatings for Superior Gears (gearsolutions.com, 2018)*

*** *Source: Plastic Gears Are the Future (machinedesign.com, 2017)*

For finding good design parameters, the maximum assumed current from the RE50 48V was assumed 10A. Certain different sizes was calculated, and the following found:

- To make a gear that is both strong enough and transmits enough torque is hard with the constraint of a high gearing ratio. Plastic as used by the team previously wasn't considered a good alternative when higher gearing ratios were wanted.
- With steel to steel the driving(motor) gear is more fragile to tooth bending with a smaller cross section at its root. However, it's also much cheaper to replace/make spares if it brakes
- Less than 17 teeth were needed to get 25:1 ratio. With standard gears this means that the gears either have to be modified using a addendum modification factor in order to not mesh badly or less than 25:1 have to be accepted as biggest gearing ratio

By looking at all choices(Appendix G:) and wanting the highest gearing ratio, the final choice was to produce the gears with module $m=1\text{mm}$ that were glued onto the carbon fiber rim and either accept lower than 25:1 or to custom made the smaller gear. For production Wire-EDM were considered the only precise enough method available in Trondheim to make the gears.

With wire-EDM to remove material instead of cutting pre-hardened 10mm steel plates of the type Hardox 450 with a yield strength of 1250MPa and Brinell Hardness of 450HB were selected (SSAB, 2018). This is one of the most abrasion resistant steel types available and are commonly used in demanding conditions. The main reasons for going with this material is that it gave a quite high safety factor.

Even though the plan was to synchronize the motors not to have crashing of the motors there was the need to make the software run on our rule approved motor controller with all sensors working full scale. This meant physical testing and the likelihood of several crashes due to bad meshing. By selecting a type of steel that are used for things like digging machines the hope was to destroy the smaller replaceable gear before the large one.

As an iterative plan to make the gears the following configurations were planned:

1. Manufacture the bigger gear and run it with the Maxon RE50 48V with more teeth (lower speed) than necessary for the race
2. Test the Maxon RE50 36V with 18 teeth on the outer gear
3. Manufacture the smaller external ring gear and 15 teeth gear from the remaining cutouts

The we're two main reasons for this approach:

1. Getting one gear to work can be hard enough – especially when electronics and code for control needs to be developed. By focusing on the first gear the car had a good solution if the RE50 36V we're used with overvoltage according to theory
2. The university have a wire-EDM machine that the team can use. However, the internal ring gear planned we're bigger than this machines dimensions. By planning to use the leftover materials from making the outer ring gear for a inner gear and addendum modified driving gear the total cost of producing the gears would be lower

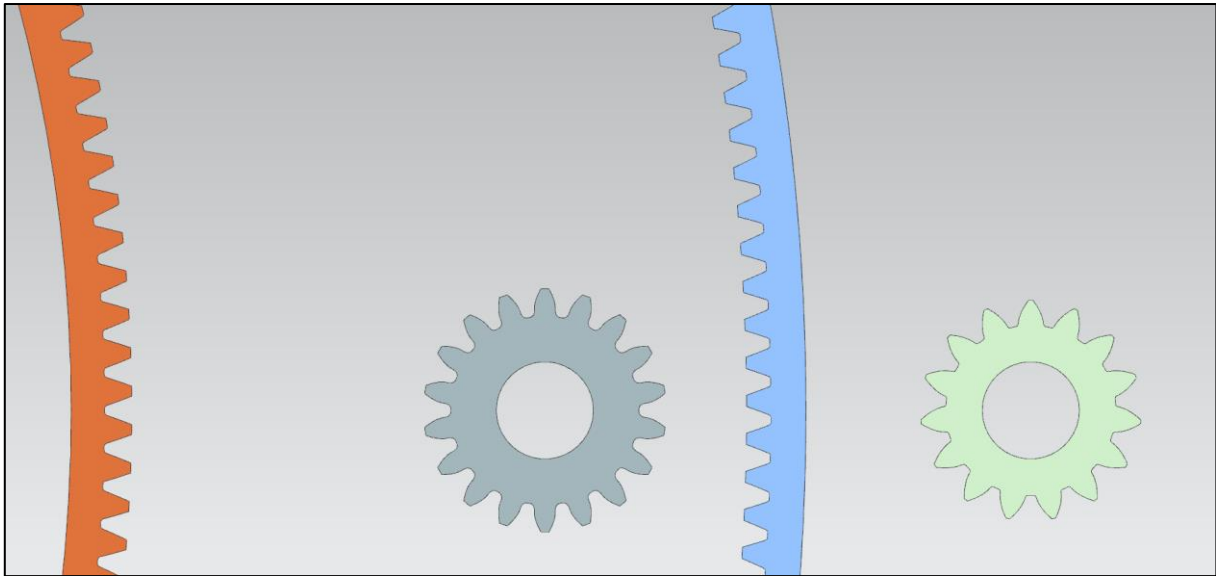


Figure 5.5 The drawings for the gears designed in NX.

Due to one failed production the blue gear was the only one made used with the an overvolted RE50 36V. Blue Internal gear: 375teeth with outer diameter of 383mm, thickness of 10mm and a measured weight of 377 grams

Unfortunately, the production of the external ring gear was delayed by months due to material not coming in time and the workshop produced bad gears at first try. Therefore, the team made one gear and chose to rather use the overvolting of the RE50 36V as described in chapter 3.3. The design process of the powertrains should however still be good for mounting one more gear to in the future.

5.4 Load Cases

With a working concept the development of a full-scale frame working both as a swing arm with suspension built in and as a gear connector was needed. To begin this process the assumed most important load cases for the FEA simulations were investigated.

5.4.1 Mass of the Car with Driver

To understand how the weight of the car was distributed a simple experiment was done. The driver sat inside the car while weighing the mass contribution on left side of the front wheel and left side wheel of the wheel in the back of the car with human body weights and adding spacers in the same height as the weights on the other side of the car. The results were as following:

	With driver (measured before new powertrain unit was added, but with carbon fiber rims in the front)
One front wheel	46.5kg
One rear wheel	25.3kg

Assuming symmetry in weight and this weight distribution for the entire car is dangerous as there were some potential error sources:

- The two cheap weights showed about 0.5kg different weight on the driver measuring 65kg
- Most components were inside the car, but not the following
 - Weights that are needed to get the driver as close to the 70kg weight target as possible wasn't mounted. This will add a few kgs towards the rear
- Assumption of the car having a center of gravity in the plane between the wheels

In addition, the weight of the wheel is held up by itself reducing the total weight distributed through the powertrains suspension to the bulkhead by ca 4-5kg and the powertrains own weight also decreases this value a bit.

In total the mass held up by the powertrain were assumed to be 30 kg, giving a bit of safety factor to the measurements potentially being bad and the added weight of unforeseen parts.

5.4.2 Cornering Forces

To According to SEMs rules the following must be true:

The turning radius must be 8 m or less. The turning radius is the distance between the center of the circle and the external wheel of the vehicle. The external wheel of the vehicle must be able to follow a 90° arc of 8 m radius in both directions. The steering system must be designed to prevent any contact between tire and body or chassis.

-- Article 42b from the Shell Eco Marathon Rules 2018, Chapter 1

By assuming that no understeer or oversteer is taking place the cornering forces could be described as following by calculating the centripetal acceleration and using Newtons Second Law:

$$F_{\text{cornering}} = m * a = m * v^2 / r$$

Table 5-B Assumptions for calculations of cornering forces

Cornering speed	$v = 8\text{m/s}^2$
Mass of the car in the rear per wheel	$m = 30\text{kg}$
Safety factor	2

As there is a lot of other factors also playing a role like the fact that the center of gravity of the car will give more forces to the wheels in the outer edge of the corner a safety factor of two is added to the calculations. By using the formula for cornering forces the result becomes:

$$F_{\text{cornering}} = 492\text{N}$$

5.4.3 Bump Forces

The powertrain units' own weight was $m_{\text{powertrain}} = 7\text{kg}$ when the car was weighted. By assuming that when the car hits a bump one wheel could lose ground contact the weight held up by the powertrains could be described as following:

$$F_{\text{bump}} = 2 * (m_c - m_p) * a * s$$

To take into consideration the fact that hitting a bump is a quite dynamical event where the car will take the hit of the bump a safety factor of $s=3$ was introduced. The fact that the car is driving

$$F_{\text{bump}} = 2 * (30\text{kg} - 7\text{kg}) * 9.81\text{m/s}^2 * 3 = 1354\text{N}$$

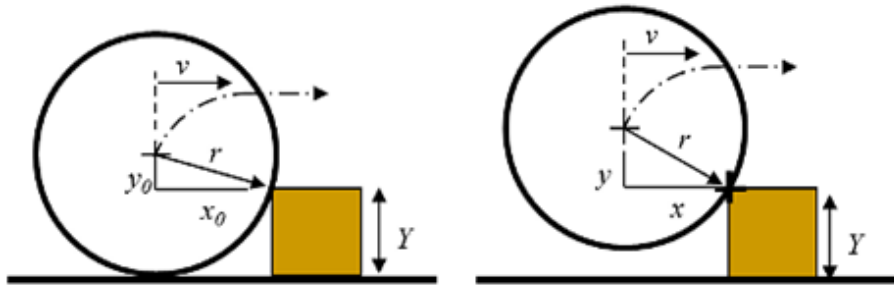


Figure 5.6 Geometry for hitting a bump.
Source: ShimReStackor.com, 2018

To verify that this safety factor is good an assumption an investigation of the car driving over a bump at full speed with no suspension were made:

For the model it's assumed that the initial position is where the wheel just hits the bump of height Y , meaning that the initial positions x and y could be described as:

$$y_0 = r - Y$$

And:

$$x_0 = \sqrt{r^2 - y_0^2}$$

Then the assumption that hitting the bump doesn't change the car's speed is made meaning that the car speed position for $x(t)$ is:

$$x(t) = x_0 - v * t$$

And $y(t)$ is:

$$y(t) = \sqrt{r^2 - x^2} = \sqrt{r^2 - (x_0 - v * t)^2}$$

Derivation of the wheels speed gives the following force due to change in speed:

$$a(t) = \frac{dy}{dt} = \frac{(v * t - x_0) * v}{\sqrt{r^2 - (x_0 - v * t)^2}}$$

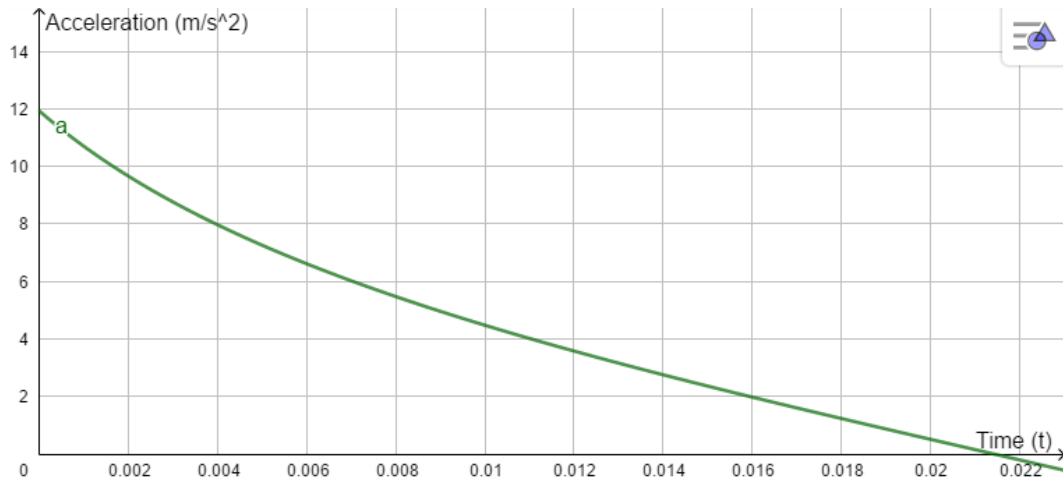


Figure 5.7 Hitting a bump with height of 10cm at 10m/s speed

This worst-case scenario would be if our car is capable of driving at the speed of $v = 10\text{m/s}$ which is more than we need during the race and that the bump is as big as the car's ground clearance ($Y=0.1\text{m}$). This would give a maximum acceleration of 12m/s^2 as Figure 5.7 shows. This means that the actual acceleration becomes:

$$a_{total} = g + a_{bump} = 21.8\text{m/s}^2 = 2.22 * g$$

Which is less than the chosen safety factor of 3. Also, the suspension would take some of the forces from the bump meaning less change in the car's position the forces from hitting a bump further decrease.

5.4.4 Braking Forces

For braking the limit on where the brakes stop braking is when the friction force becomes so big that the wheel will lose traction and start to glide. Another contributing factor is that the center of gravity will try to lift the car forwards if the front brake is also applied. This means less downforce on the rear wheel than the front wheel. Based on a friction coefficient of 0.72 for car tire to asphalt (engineeringtoolbox.com, 2018) with a safety factor of 1.5 the maximal braking forces where the wheel meets the ground will become:

$$F_{braking}' = s * \mu_{\text{tire to asphalt}} * m_{\text{rear}} * g = 1.5 * 0.72 * 30\text{kg} * 9.81\text{m/s}^2 = 317.8\text{N}$$

Then, by assuming that the brakes force is being applied the brake rotor meets the brake calipers pads at a distance from the rotational center of $r_b = 84.8\text{ mm}$ This gives the following brake force:

$$F_{braking} = F_{braking}' * r_{\text{wheel}}/r_{\text{brakepad}} = 1042\text{N}$$

5.5 A Few Concepts

With the goal to make a powertrain with two gears, motor mounting and brakes as the most important parts connected a few considerations regarding design choices were made to make the system work as intended.

5.5.1 Wheel Hub vs. Rotating Axle

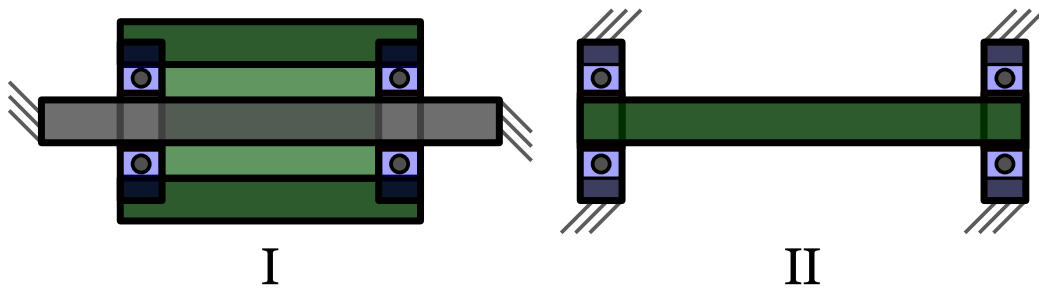


Figure 5.8 Stationary axle with a hub (I) vs. rotating axle (II) mounted with bearings

With the requirements to fit two gears and the brake system it wasn't enough space on one side of the rim to put everything there. Therefore, the decision to mount the powertrain in a swingarm-like assembly like done on many motor bikes were selected. The previous powertrain had a rotating axle where the axle is mounted to the powertrain with bearings in-between (solution I, Figure 5.8). The bearings used for this solution was highly efficient single row ceramic ball bearings. The assumption done in the FEA of the previous powertrain was made was that this kind of bearings are stiff in rotation. However, this isn't the case, where the bearings had noticeable play making the axle only locked for translation and not for rotation. This made the powertrain less stiff than planned both in the frame and in the axle that wasn't hold back by momentum from the fixation points. A different solution with a rotating hub outside the axle was therefore investigated.

It was found that for one of the initial designs of the powertrain frame the deformations of the cornering forces increased 2.8 times (Appendix D:) with the powertrain with stationary axle. If this numbers are representable for the old powertrain which had about 15mm of deformations according to CAD isn't sure but suspected since applying small forces deformed the wheel noticeably more than expected.

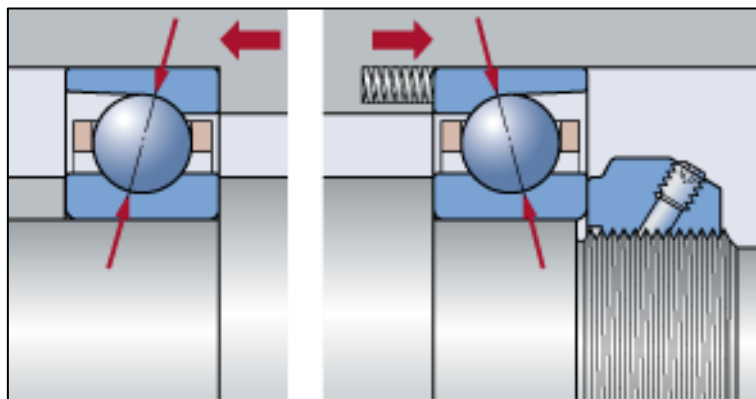


Figure 5.9 Back To back Preloaded Angular Contact bearing (SKF, 2018)

Another pro with the bearings in the hub is that it makes it possible to pretension by tensioning the hubs bearings to the axle. With this it's possible to use angular row bearings which are more efficient according to the book about PAC CAR II (Santin, 2007). Pretensioned angular row bearings are also used in many high precisions because pretension removes the play from regular ball bearings. These two factors make these kinds of bearings commonly used in demanding machinery like high speed/high precision CNC spindles.

The final hub design made it possible to mount the carbon fiber rim to and the brake disc to the hub with threaded connections. The system was made less stiff with a spring to reduce the effects of bad machining. For this Bonneville springs were placed before the nut going on the threaded area on the axle. Since the axle was made manually on a lathe as well as we didn't have the official measurements of the brake caliper some extra clearance were placed on the right side by purpose so circular shims could be placed to get the correct position of brake rotor relative to the brake caliper. As for the strength calculations for the hub a simple statically fem analysis was made. This showed that the hub was way too strong, but as it was wanted to get it produced at a workshop at NTNU further optimization were considered risky as it would be too time demanding for NTNU to make.

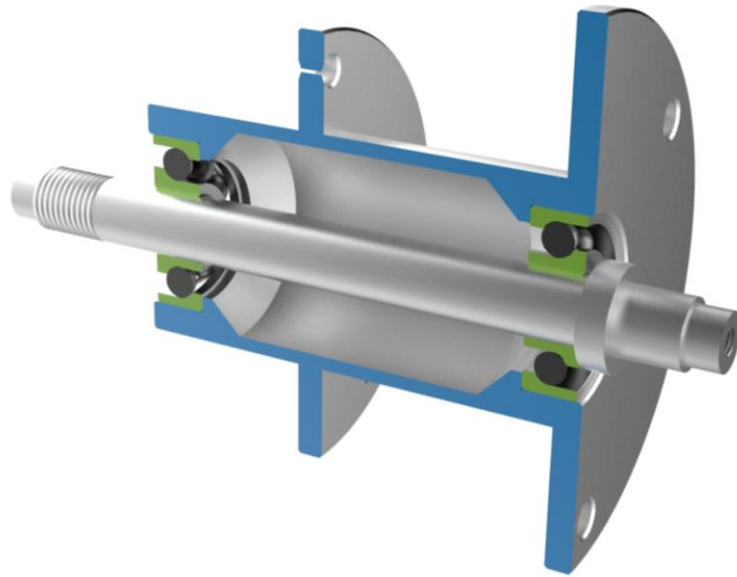


Figure 5.10 The final solution

5.5.2 Motor Movement

To find the needed travel of the motor few assumptions were done: From the simulations of which gearing ratios proved to be the best the 15:1 and 25:1 gear was assumed. The biggest gear was assumed to be the 375mm. To estimate the distance the motor, a drawing was created with two scenarios: motor mounted on the same height as the wheel axle and motors mounted 50mm over the wheel axle while moving horizontal. The wish to have the motors close to where the frame was going had several advantages like the want to have small deformations between the gear and frame due to cornering and supporting a compact frame design.

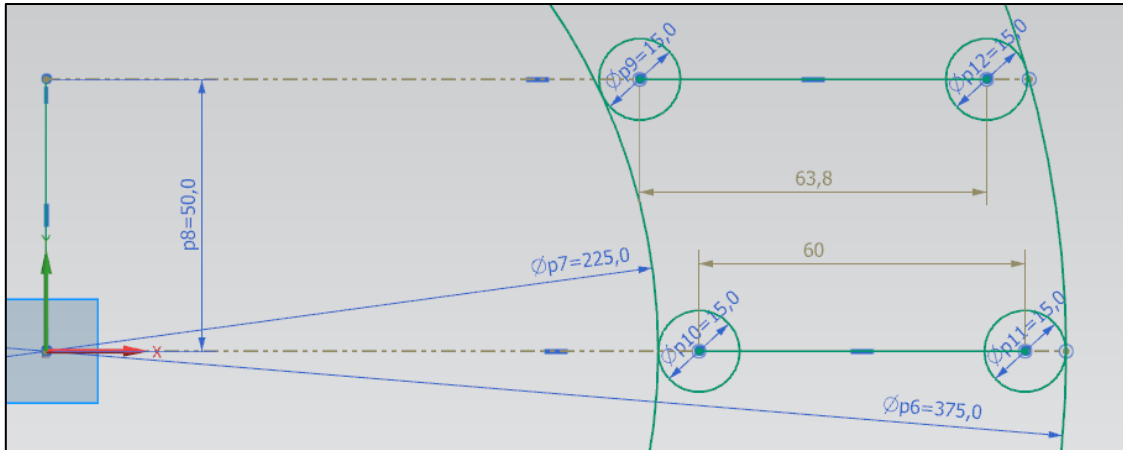


Figure 5.11 Motors minimum travel distance based on the gears center lines meeting. Assuming the biggest gear of 25:1 for the outer and 15:1 gearing for the inner gear means that the motor need to travel 64mm.

With the knowledge that gears meet each other in the center line the diameters for the smaller gear became $d_{Inner\ gear} = \frac{15}{25} * d_{Outer\ gear} = 225\text{mm}$ and $d_{Driving\ gear} = \frac{1}{25} * d_{Outer\ gear} = 15\text{mm}$ with this the distance needed for travel became 60mm if motor was placed in the center and 64mm for a offset motor placement.

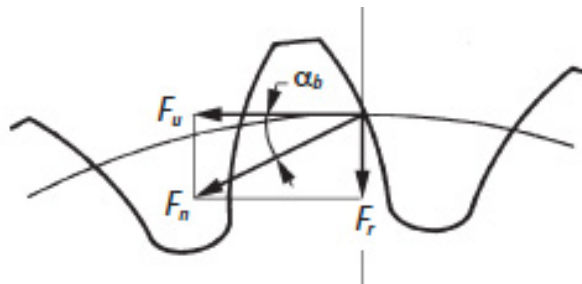


Figure 5.12 Forces Acting on a spur gear mesh
Source: sdp-si.com

In addition, the moving solution had to hold the motor in place while driving – preferably without any power consumption. For this the RE50 with the assumption of a torque of a motor torque of $T = k_t * 10A = 93.4\text{mNm/A} * 10A = 0.934\text{Nm}$ and the formula for calculating the radial force on a gear mesh transferring torque (SDP/SI, 2018) were used to find required holding force:

$$F_r = \tan(\alpha) * F_u = \tan(\alpha) * T/r_{driving} = \tan(20) * 0.934\text{Nm}/7.5\text{mm} = 45.3\text{N}$$

Lastly gear changes shouldn't be a too slow process or add to much weight. Therefore, the final requirements were that gearing should happen in less than three seconds and preferably have a weight of less than 200 grams.

With these requirements an electric motor solution was searched for and linear actuators was locked on as a preferred solution because of the following characteristics:

1. Linear movement with consistent speed over the stroke
2. Stroke distance feedback with pot meter is common
3. By design have a certain force that needs to be overcome to move the actuator

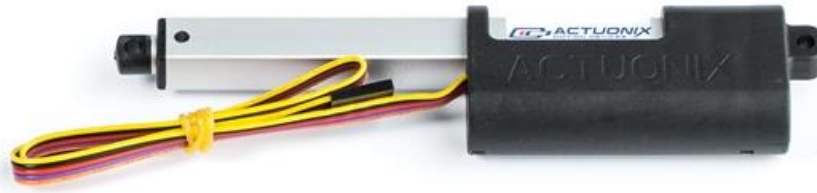


Figure 5.13 Actuonix P16 with 100 mm stroke length Source: actuonix.com

Few actuator companies were making linear actuators for our needs, especially regarding weight. There was however one suitable actuator found, the Actuonix P16. The actuator could be ordered in many different lengths and with different gearings for the internal actuator screw.

The 100mm 22:1 geared version was chosen since this was the fastest available actuator of the type and that it had a back-drive force of 75N meaning that's the force required to push it backwards unpowered. In addition, it was able to do 46mm/s without load. The datasheet for the linear actuator could be found in Appendix O:.

5.5.3 Suspension

A Shell Eco-Marathon vehicle is racing on relatively good asphalt meaning that some of the roughest use will occur in the event of driving over a bump or a sudden change in the asphalt. Some teams in SEM are therefore skipping suspension systems in their cars. However, some good reasons to have suspension are:

1. There's a rule in SEM stating that all wheels must be in constant contact to the road, meaning that if one-wheel lifts during racing it's not rule compliant
2. Suspension systems absorb some of the initial shock from driving over a bump
3. Driver's comfort improves with a suspension system

To get light enough suspension systems with the wanted travel there's only one commercial choice: to use shocks made for mountain bikes. Among these there are two different types: spring loaded and air loaded shocks.

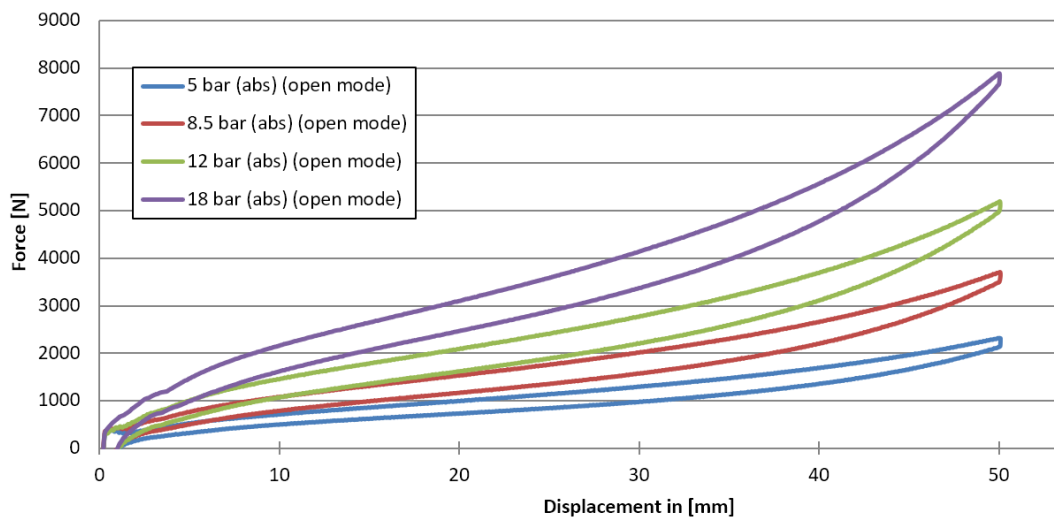


Figure 5.14 DT Swiss X313s displacement curves

Some of the main benefits with air shocks over regular spring suspensions is that it's inflatable and therefore easier to change the behavior by adding or reducing the air pressure. They're also lighter and the preferred choice for light weight bikes. The main disadvantages are that the shocks aren't

linear in its behavior and that they don't go back to the old displacement after being pushed in. These effects are illustrated in Figure 5.14 which shows the displacement curves for the lightest commercially available bicycle shock, DT Swiss X313.

The 2017 powertrain was mounted to the wall as shown in alternative I Figure 5.15. One of the main problems with that design was that the Fox Float R shock used in the assembly was too stiff to work properly, even on the lowest configuration. This meant that the wheels didn't stay on the ground while hitting bumps and that the driver's' comfort and the ability to reduce huge impacts forces wasn't as good as wanted. To fix this problem a few two different solutions were thought of.

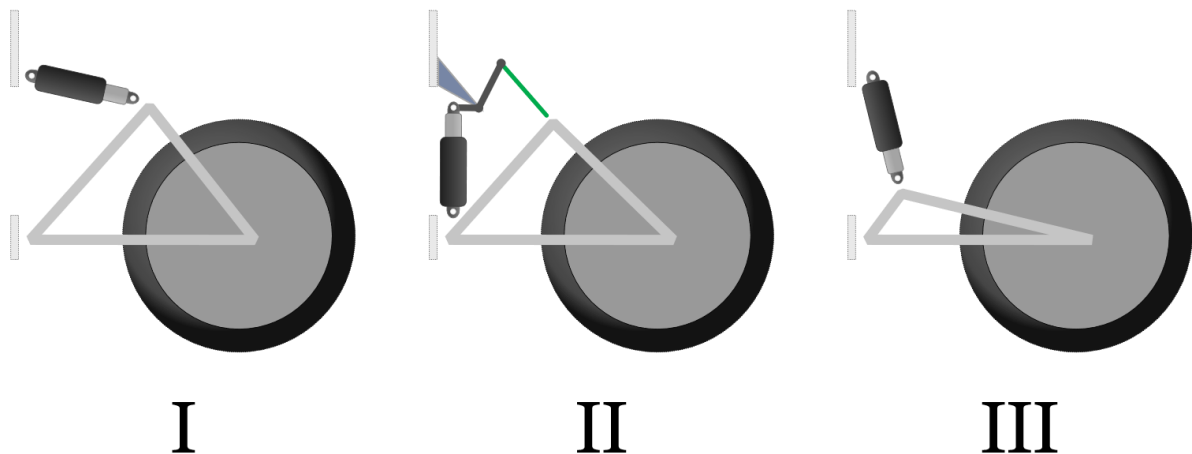


Figure 5.15 Three different mountings for the powertrains

One of them were to have the design and replace the shock with a less stiff one. However, the eye to eye length of the shock and the mountings geometry made it hard to find suitable shocks on the market -meaning that a custom design had to be made.

Therefore, changing the geometry of how the suspension were mounted was investigated. One way to do it without having to change the suspensions mounting point were to make a leveler arm that increased the amount of force that goes into the shock (alternative II, Figure 5.15) while the other potential solution was to move the entire mounting point closer to the wall (alternative III), which also makes the forces transferred from ground to shock bigger.

All three options were considered to do the job, however due to the simplicity of using a premade shock and not having to make a leveler system III were chosen as the preferred solution for the further development of a new powertrain.

5.6 The Optimal Shape

With the entire open space in the rear of the vehicle as the design space for the powertrains and the inserts in the firewall of the car as main constraints the search for an optimal mechanical shape started.

For this process a topology optimization analysis was done in Fusion 360. Shortly explained this works by reducing the parts of the FEA mesh least contributing to carry load at a mutation rate and doing it over and over so that less and less material is present. The result you get is supposed to be the optimal structure. And in Fusion this optimization is based on stiffness vs weight.

To decide how the powertrain should look like two design spaces was analyzed. One with the constraints of what a tubed solution would look like and one where much of the physical area available can be used. For both solutions a sliding motor and brakes had space to be mounted in the design. However, in the smaller design space (Concept A) the assumption is that motor is possible to mount

with a sliding mechanism at an offset to the center line, while in the larger design space (Concept B) motor and brakes are placed in the center so that the frame could utilize the distance over and under the motors and brakes for stiffness. Both concepts design spaces could be seen in Figure 5.16.

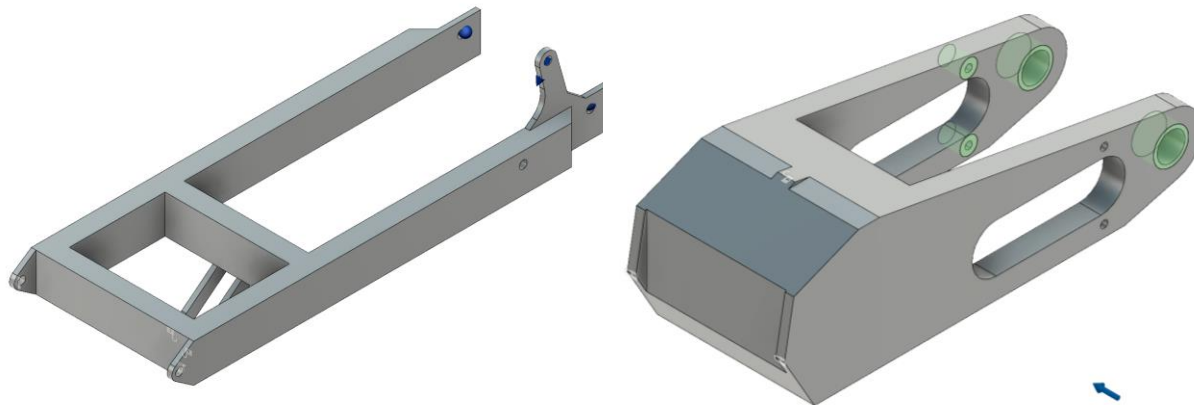


*Figure 5.16 The design spaces for topology optimization
Concept A (left) and Concept B (right)*

For the simulation both concepts were constrained two places to the firewall with translational locking only (free to rotate). This gives it freedom to movement only in one rotation. For simulating the suspension, a “simple support”. By doing so it simulates a normal suspension mount which also just locks in one direction. A spring could be implemented in the simulation, but as this makes the simulation unnecessary complicated for a static simulated given the assumption of very small changes in loads directions due to a potential spring movement

For the forces the values previously defined was used. For the forces applied to the wheel it was assumed that these worked directly into the two places where the axle would have been mounted to the frame. Braking forces were for simplicity assumed to work directly where the screwing connections would have met the frame. Areas that was needed in the design like the brake holes were constrained as unremovable material. For Concept B the brake force was added on both sides with a symmetry plane in between to force a symmetrical design and equal material removal on both sides.

Concept A had 217 082 parabolic tetraether elements (TET10) with the mesh element size set to 3mm in while concept B had TET10 elements with mesh size set to 1% of the model size giving 227 226 elements. The reason for not choosing more elements was that simulation already took hours to solve with Fusion 360s cloud being the only solving option. Less elements were also tried but didn’t give meaningful results. For both designs the target mass were set to $\leq 25\%$ as shape optimization criteria meaning that only 25% of the elements should be left after the simulation (Figure 5.17).

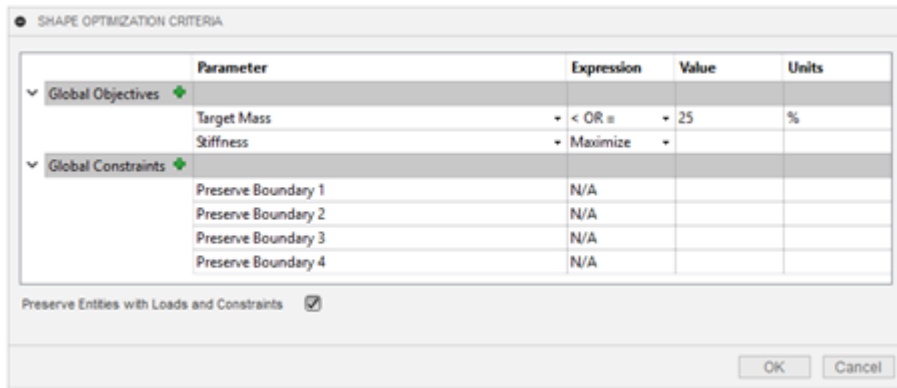


Figure 5.17 Settings used for shape optimization of the mid-motor design.

The results for the simulations were as following:

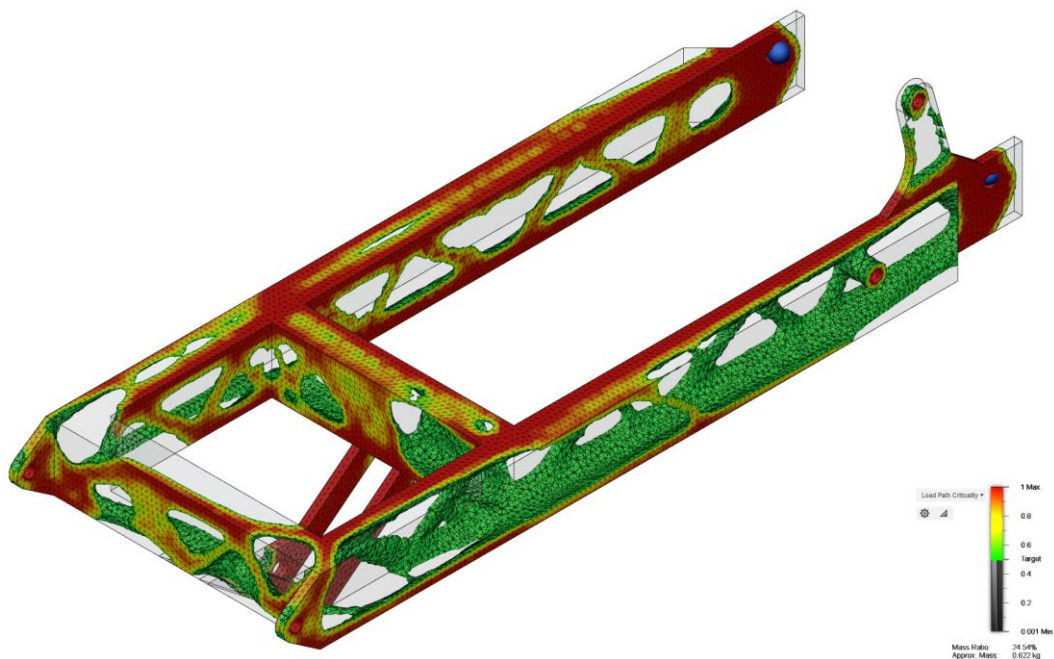


Figure 5.18 Concept A after topology optimization

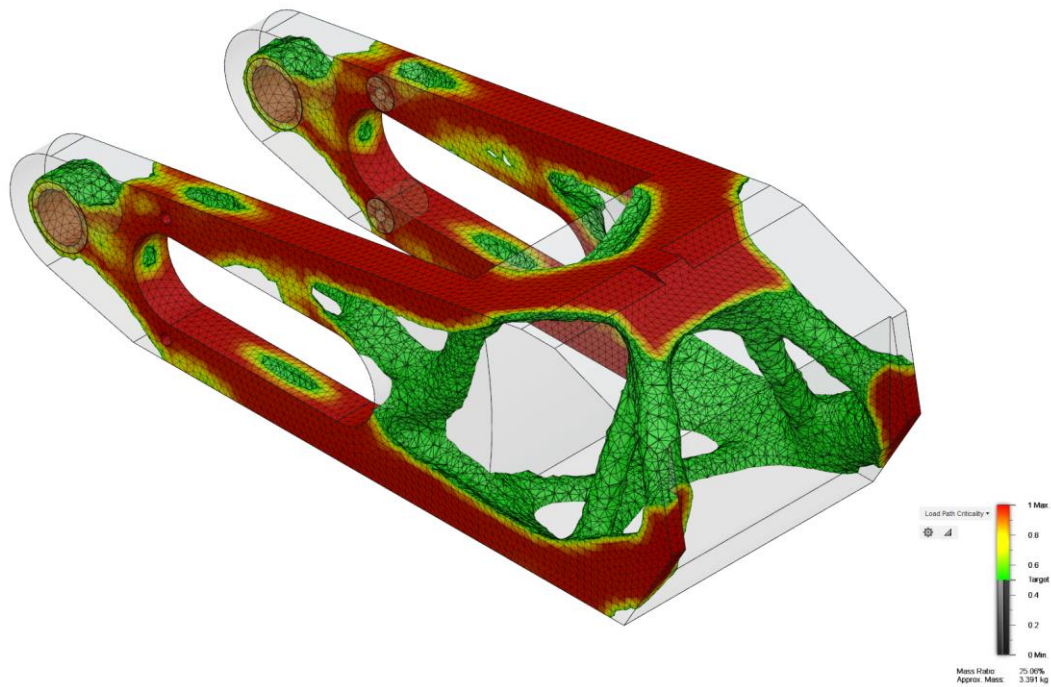


Figure 5.19 Concept B after topology optimization

As concept B looked much more complicated to make with conventional methods and were too big to 3D print in metal it was discarded as a solution.

Concept A however didn't need too many modifications to make it possible to be CNC milled. With a three axis CNC mill being available at the workshop the goal became to make a design where the powertrain was millable from 30mm thick high strength 7075-T6 aluminum plates with the goal to mimic the generative designed arms.

This design was then to be compared against a design with commercially available square tubes. To better compare the triangular shape to square tubes the parts where the suspension goes in to the arms remained unchanged and these square tubes were assumed 2mm thick. After a few iterations on the generative inspired design in NX the result looked like part I in Figure 5.20.

The square tubed solution with 2mm walls were made. With square tubes having all its material far from the center lines the stiffness should be quite good in such a design. Both parts had the same geometry for the "ear" mounting the brake and the same mounting points to the car.

Ideally the mounting points to the wall for the generative should have been positioned so that it could have been milled in one operation, but for the comparisons sake the only thing that changed were the arms structural design.

The forces applied in the comparison was all load cases found previously at once. The reason for this is that it would both show if the designs were strong enough (handling all load cases) and and more important stiff enough in the corners. The cornering forces were also found to be dominating.

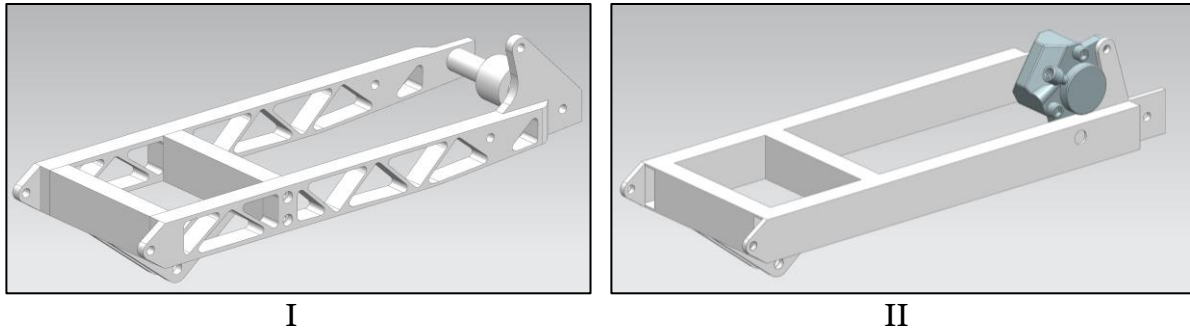


Figure 5.20 Generative design inspired arm vs tubed solution

The FEA results could be seen in Appendix N: and the main findings are shown in Table 5-C

Table 5-C Results from the FEA simulations

	Design I (generative)	Design II (tubed)
Weight of arm with brake	484grams	362grams
Stiffness assembly	13.3mm	9.3mm sideways
Plastic deformation	No	No

Overall the results showed that design II was preferable as being both stiffer and 0.25 kg lighter per powertrain. The fact that the square tubed design was also much easier to make made the choice easy.

5.7 Sliding Motor Mount

To make the motor slide two different solutions were looked at: Using low profile linear guide system or making a custom-made sliding mechanism to slide along the square tubes. With limited space, and wish of low weight rail of the Drylin® N guide rail with a width of 40mm were ordered.

With the Drylin N rail having too much play the development of a custom holder began. The holder was first printed in PLA and was proven to work. However, a few potential issues were noted:

- The aluminum part was too weak and were redesigned and milled
- PLA could have trouble with heat
- Accurate sanding of the pads had to be done to get it to slide with low friction. Too much sanding meant that the motors would be a bit loose

A few iterations later the part looked as in Figure 5.21. Some of the tweaks done to fix the initial problems was to include internal springs to the 3D print. The plastic type was also changed to Iglidur I150 specifically made by Iigus for sliding 3D printed parts. This was promised to much more wear resistant than PLA and handled high temperatures quite well.

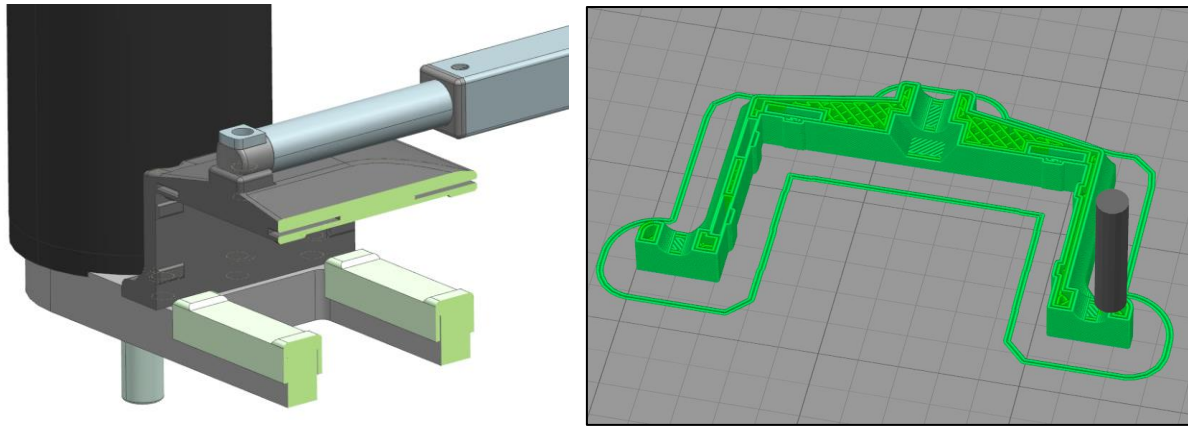


Figure 5.21 The final design for the motor mount with spring walls

5.8 Finite Element Analyze of The Final Design

To verify that the design theoretically was able to handle the loads a FEA of the final design were done. The load cases calculated in the load case section was used. The goal with this one wasn't absolute precision as there were many uncertainties in how the welds as welded by a team member would perform. Some physical testing of the car was still needed and done by adding weight/ forces to simulate the bump forces and forces from cornering were planned. As the car is only made for a single race where it's safe to assume that loads near the yield limit wouldn't occur more than a few times. Fatigue was therefore not considered.

For the axle the diameters with threads added was treated according to the effective area as in ("NS-EN ISO 898-1:2013," 2013) meaning that the pretension screw for the bearings being M12 had a diameter of 10.36mm and the M5 holes that were used to screw it to the swing arms inserts were simulated with a diameter of 4.25mm. For the M5 connections it was also assumed that the forces from tensioning of the screw wasn't important and strong enough to make a close to solid connection between the mounting points.

The mounts used to the carbon fiber fire wall was also added in the simulation as fixed to the wall. The lower mounts were made of 3D printed steel and made by a team member for the application.

The rim was assumed mounted to the hub where the screws forces it in with a RBE2 spider element (stiff elements) going down to where the wheel meets the ground. The new brake mount made in last minute to fix brake issues were also added in the final calculations.

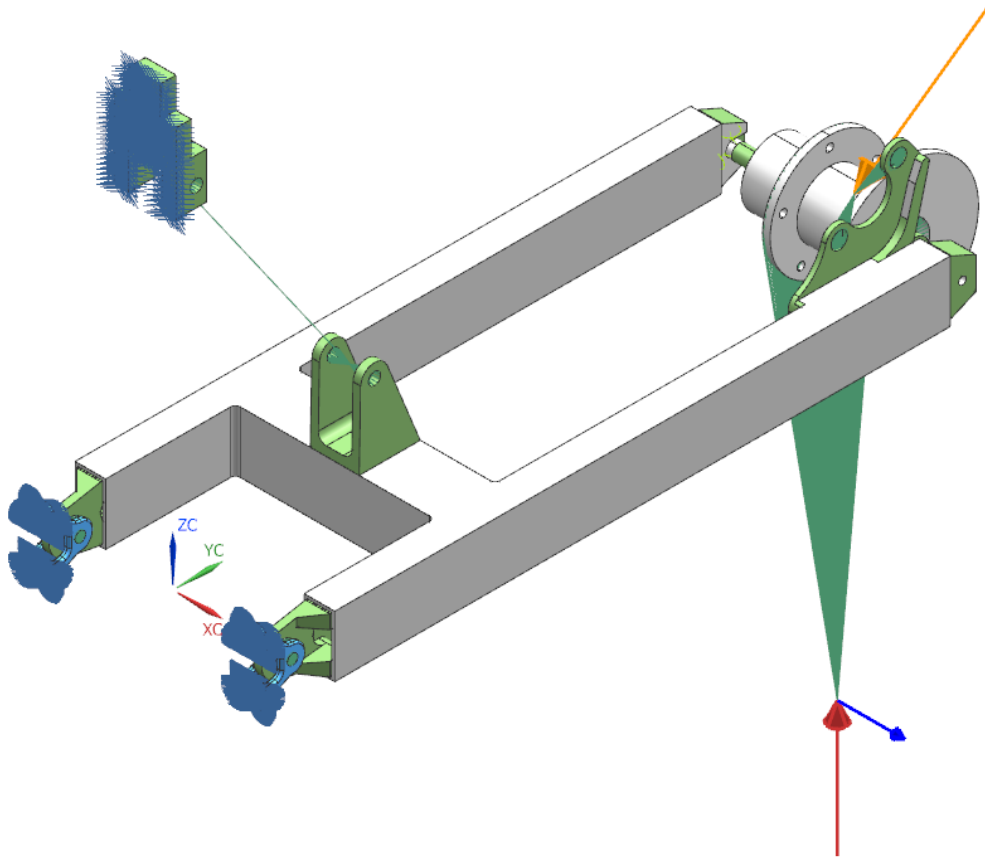


Figure 5.22 The powertrain assembly

Figure 5.22 shows the powertrain arms which is made of 2mm thick 40mmx20mm square tubes of 6060-T6 aluminum welded together with a 40mmx40mm 3mm thick aluminum tube, the lower wall mounts are made from 3D printed steel and designed by a team member. The other parts are high strength 70xx series alloys.

5.8.1 Results

The FEA results is presented in Appendix F: and they showed that cornering force is the dominating one both in terms of stresses and strains. The inserts were all made of high strength aluminum of the type 7075-T651 with a yield of about 500MPa. As they were also designed to be easy to mill rather than to be as lightweight as possible they are all far away from reaching the yield stresses in the simulations.

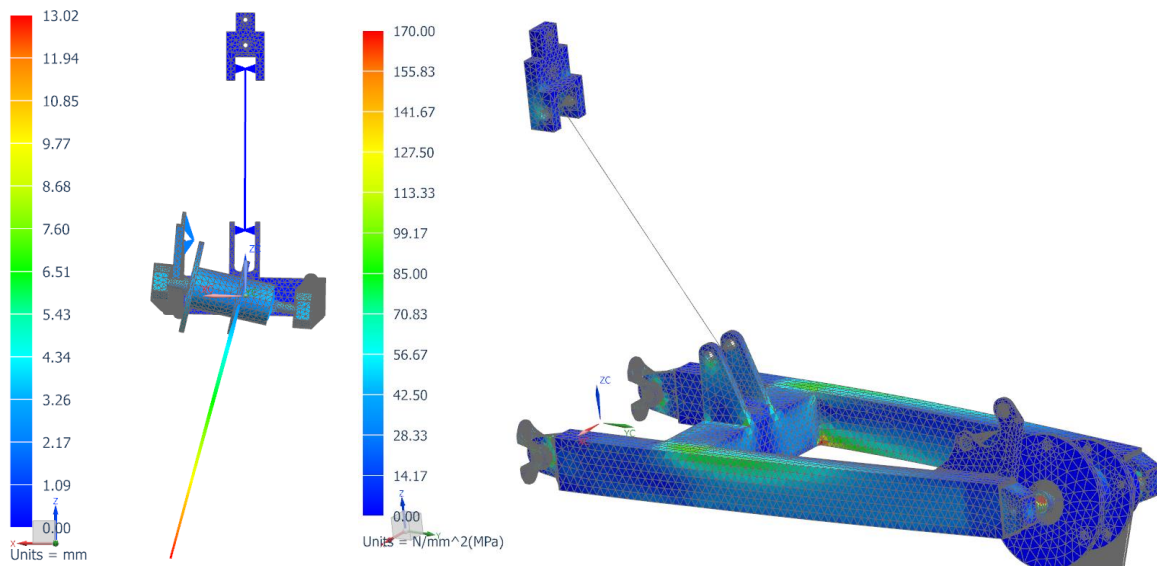


Figure 5.23 FEA results for the “Bump force” load case

The part with the highest stresses were the axle with a von mises stress of 375MPa max. As this was made with the “super alloy” Alumec 89 with a yield of 630Mpa it was assumed more than strong enough.

This left the square tube frame that was originally supposed to be made in 6061-t6 alloy the weakest part. As this was made with 6060-t6 alloy the yield strength were only 170 MPa. The simulations showed a maximum von mises stress of about 100 MPa where the welds were planned.

With plans that one of our members who were a hobby welder was going to weld the frame the main goal to became to have nice welds that looked nice. After talking to a professor with expertise on welds he suggested that a criterion of 60% of the yield strength

6060-T6 aluminum have for the heat affected area. This meant that the maximum permissible load became 102MPa around the welds which was about the expected loads in this area.

With an assumption that the aluminum was quite ductile the potential failure mode would be bending which wasn’t assumed to critical. This was later tested and verified by bending one of the test pieces from the welding process.

5.9 Production

To produce the main frame a strategy to test a risky design with lightweight laser cut aluminum inserts were planned. This design was risky for several reasons:

1. The axle would be held up only by screwing force and not have supporting walls to secure it
2. The aluminum used was laser cutter with low tolerances
3. Thin plates having cutouts for weight savings were assumed hard to weld

The reasons for testing aluminum inserts were the wish to produce all insert in one cutting job. Trondheim Steel sponsored this cutting which meant that it was time saving, cost efficient and more lightweight than most other solutions.

Despite the fact the inserts were hard to weld it was doable. However, a few things were noted:

- The tolerance specified for a press fit of the spherical rod end wasn’t done properly and was optimistic by design

- The aluminum inserts were prone to damage from the axle in harder aluminum

For these reasons the goal to cut as much weight as possible by welding inserts were discarded and inserts CNC milled at NTNU with screw connections to mount them were used instead. In addition the suspension mount were milled as there was a change in the plans for suspension mechanism to use after the prototype were designed.

The prototype frame with laser cut inserts therefore served as a spare frame and the frame that were used on the test bench. Pictures of it and a jig milled to hold it in place while welding are shown in the images below:



Figure 5.24 Welding jig for the frame



Figure 5.25 The prototype frame

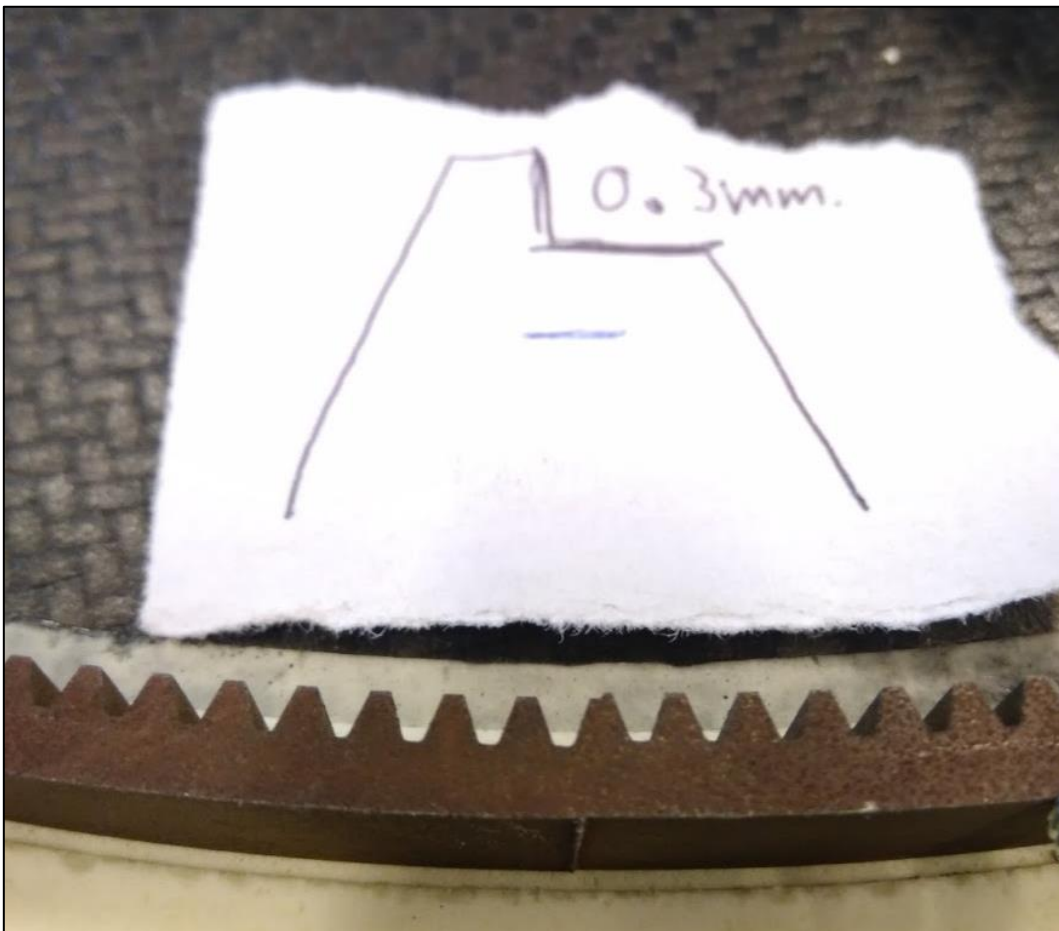


Figure 5.26 The first produced gear.

The gear was the by far most complex part to produce and as NTNU didn't have a big enough wire-EDM the company Nomek in Trondheim were given the job. The production was planned to be done

in the beginning of April. Unfortunately, the delivery of materials got more than two weeks delayed. In addition to this the first try to produce it wasn't a success and as shown in Figure 5.26. The agreement with the workshop therefore became that we could test it and get new produced if they didn't satisfy our needs.

The result after being mounted on a rim that were made with too weak core material was mainly made it suited for the test bench was that it kind of worked but made horrible noises each time it passed the 0.3mm tall bump. With this new gear were machined and the badly produced used in the development of the control software and for testing.

Pictures on the process of mounting the gears are shown in the following figures. As Figure 5.28 shows epoxy mixed with micro-balloons which are hollow lightweight glass balls used to make a lightweight epoxy paste were added. This was then milled away with the rim mounted in the powertrain frame and manually rotated and removing radially removing 0.1mm until the gear just fitted in the groove as shown in Figure 5.29 and Figure 5.30.

The gear was lastly glued to the rim and measured to be almost perfectly aligned with a maximum error of 0.05mm.



Figure 5.27 Removing rust from the gears with vinegar, salt and electric toothbrush



Figure 5.28 Epoxy mixed with micro balloons added the rim with a lasercutted disc to hold micro balloons in place



Figure 5.29 Track cut out for gear with tight tolerance



Figure 5.30 Milling track to the gear

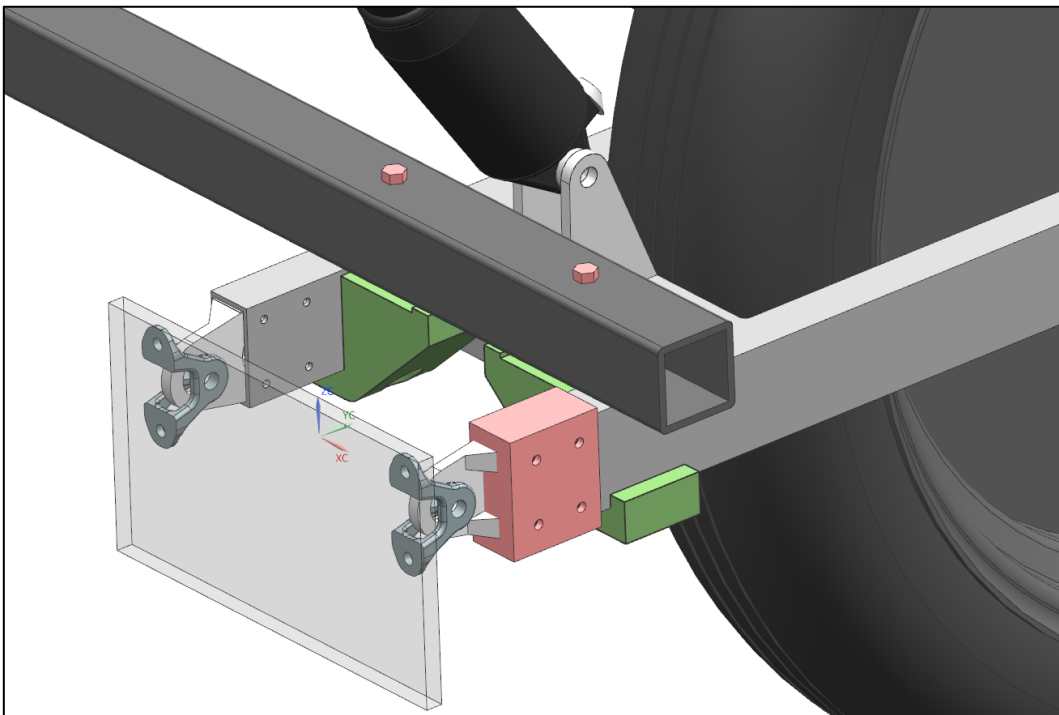


Figure 5.31 A square steel tube was used for mounting.
The red and green pieces are 3D-printed where green is for clamping and red are drill guide for drilling holes in the inserts

Lastly the powertrains were mounted in the vehicle with the tool shown in Figure 5.31 as a guide.

5.10 The Result

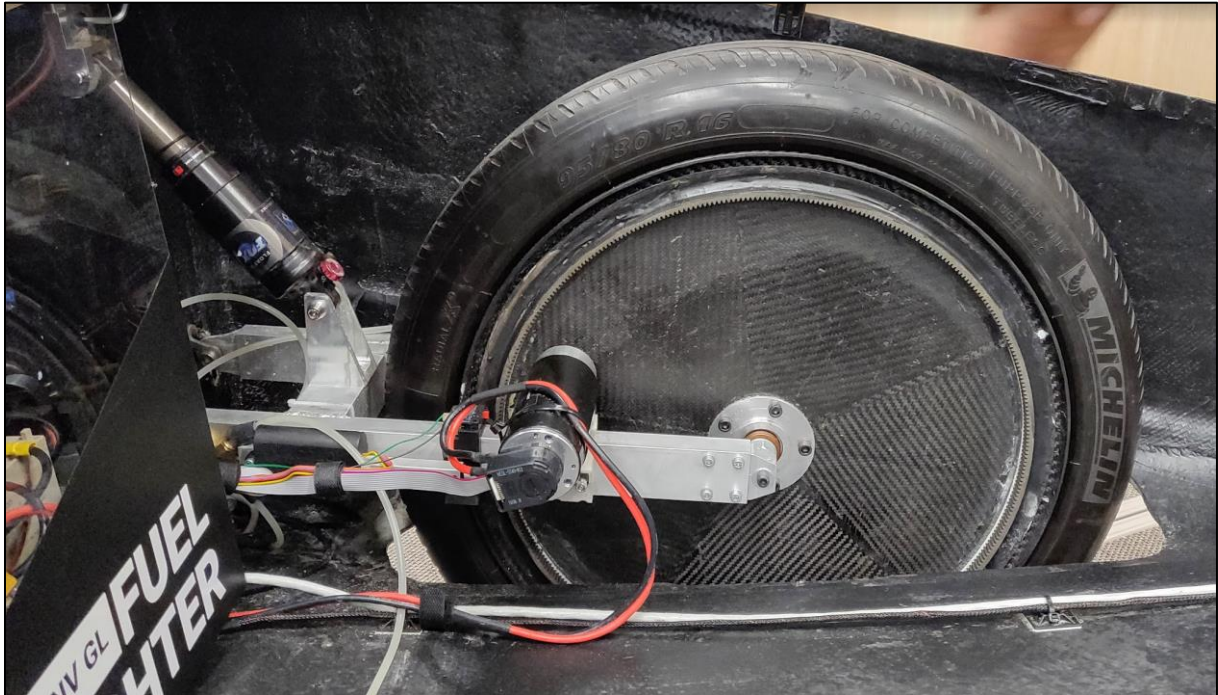


Figure 5.32 Final version of the powertrain mounted in the car

The final CAD file showed a weight of 1.25 kg in NX for all aluminum parts in the frame. With utilizing the same mounts as the old powertrain, the total weight save was measured by measuring the powertrains as complete units with motors and wheels connected. The result showed in a difference of 2.4kg compared to the old one weighting 9.3kg. The new powertrain weighted 6.9 kg.

Half of this reduction were due to the change of the rim and the other due to a more lightweight powertrain design with less parts. Mechanically it also worked much better with suspension that could be tuned as wanted both stiff and hard. The choice of angular bearings in the wheel hub combined with a stiffer frame increased the overall stiffness as well.

6 Physical Testing on the Powertrain Test Bench

As a lot of parameters like motor performance, gear performance and reliability can't be purely calculated analytically the strategy to use the testbench intensely for the development were taken. This was done to verify mechanical reliability, verify of the electric system, to check if the system performs as designed and to say something about the ability to reach wanted efficiency.

Arguably, the most important use of the powertrain test bench has been done without the need of any of the advanced functions. As this isn't needed to develop sub-components of the powertrain as the motor controller, synchronization of motors (actuator control) and iterate towards a good mechanical design for energy transfer. A cite by electrical leader and developer of the motor controller is as following:

“Designing the motor controller has been a progressive work, starting from the basic functions and improving the design each time. Siverts testbench was one of the most important modules I used for testing and validating each function, and it was absolutely essential to my design process. The test bench enabled me to test my module and the whole driving system in real conditions, under varying load, to execute a burn-in test and to establish driving strategies for the competition. It was also useful to measure the precision, reliability and the efficiency of the motor controller.”

– Tanguy Simons

With a torque sensor and speed readings efficiency can also be measured. However, this efficiency is measured with the potential losses of the transmission between wheel to roller. As this transfer is of the type friction drive which is known to be inefficient the overall losses are expected to big high.

One trick to get better readings given this loss is to measure the torque with only wheel and subtracting this value. It's also to be noted that wheel to asphalt is sort of friction drive.

There is also caused an opposing torque from the inertia (I) of the roller to the wheel which are making the raw readings wrong in acceleration. This can however be described by knowing the inertia of the roller and is dependent on rotational acceleration of the roller $\dot{\omega}$ in the following way:

$$T = I\dot{\omega}$$

6.1 Tare Losses

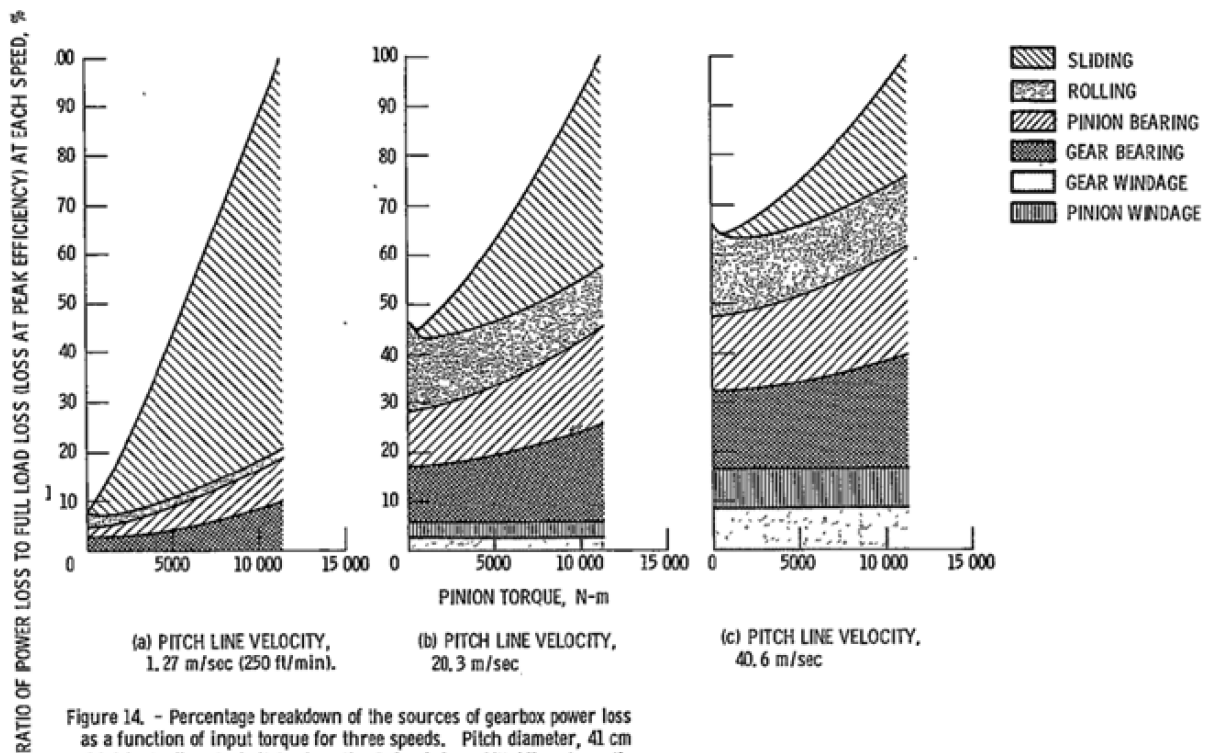


Figure 6.1 Losses in spur gears at different speeds and torque transfers (Anderson and Loewenthal, 1981)

Losses in gearing conversions with spur gears could have many different causes and are usually nonlinear in its behavior and depending on many factors like gear quality, precision of mounting of the gears, lubrication, surface finish. Figure 6.1 shows which different factors causes losses in a spur gear at different speeds and that so-called tare losses where the gears aren't transferring any torque are also caused by different sources of losses. According to the article "Spur-Gear-System Efficiency at Part and Full Load" (Anderson and Loewenthal, 1981) these losses can represent up to 65% of the losses at maximum load. These measurements were done with much higher loads and a bigger module so to simulated. What could however be assumed is that these tare losses don't go away in high torques leaving always present.

Losses from the synchronous belts are neither as easy to predict as wanted. The manufacturer of the HTD5 belts only state that it's highly efficient and up to 97% efficient. This however doesn't say anything about how the efficiency is at no-load and neither for our exact setup. It's however stated that the belts width is linear in losses and load capacity, meaning that the belts shouldn't be wider than necessary. One thing that however was assumed to have an influence was the tightness of the belt. Therefore, the belts were set up with a though minimum tightness for belts not to skip teeth and a quite tightened belt to make sure no losses happen.

In addition, internal friction losses in the Maxon motor needs to be considered. As the motors are ironless the torque losses could be estimated in the following way according to Maxon:

$$T_f \simeq I_0 \cdot k_T = 8.256 \text{ mNm}$$

With a gearing of about $n \simeq 15$ for both powertrains the theoretical power losses can be estimated with the following formula:

$$P_{bearing\ loss} = \omega_{motor} * T_f = \frac{n * v}{r_{wheel}} T_f = 58.6 * v * T_f$$

Giving the following losses: from the bearing at different speeds:

Speed [m/s]	1	2	3	4	5	6	7	8
P _{bearing loss} [W]	0.5	1.0	1.5	1.9	2.4	2.9	3.4	3.9

To get a better understanding of the powertrains, tare losses for both powertrains were measured. To eliminate potential losses before the torque sensor as described above the tests were “tared” at the different speeds right before connecting the motors. The measurements were done quasi-static by setting the powertrains controller to run at constant locked speed. In this way it was ensured that potential losses were kept to a minimum and only the effect of the tare losses were measured

The results from the measurements done were as following:

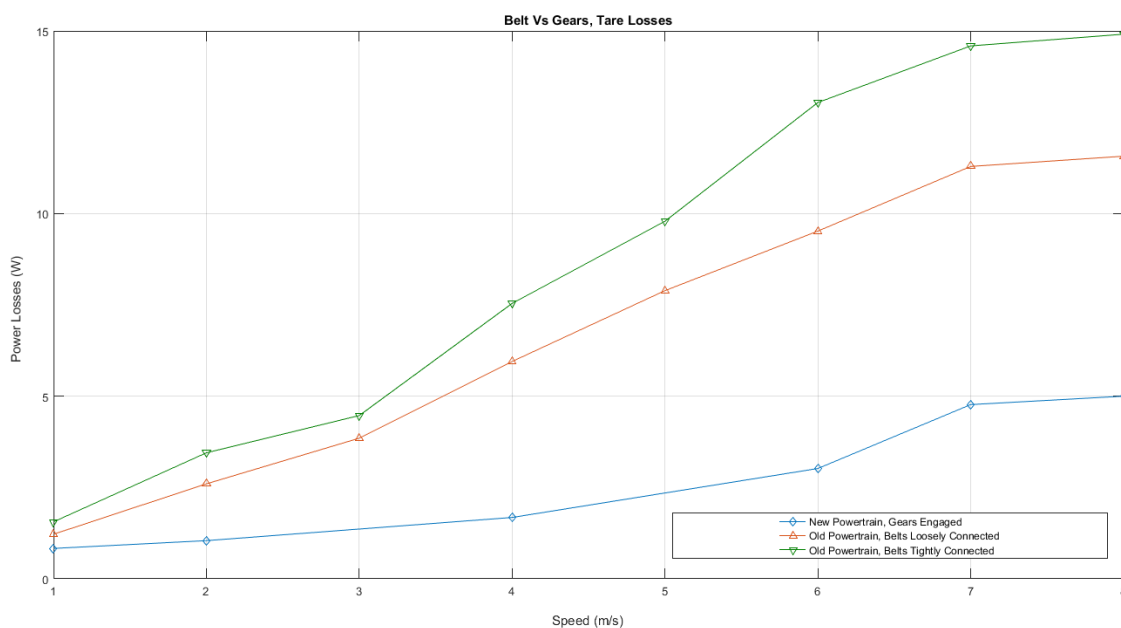


Figure 6.2 Measured tare losses for the powertrains.

Rolling losses (with motor disengaged) have been subtracted, giving the power losses of the gearing reduction + motor engaged

With a lot of error sources with a self made measuring system and some noise in the readings it's dangerous to draw conclusions purely based on the readings. In addition the tests on the geared powertrain was done on the prototype gear without the dry lube used in the final gears. Purely based on the noise levels produced on the good vs the bad gears there's a reason to believe that the good gears would have gotten better results.

By subtracting the teoretical internal losses from the motor and keeping the assumption that tare losses are the minimum loss possible during torque transfer this gives the maximum efficiency of gearing transfer if energy converison is assmed. At 8m/s with assumption that nominal mechanical motor transfer happens at 200 watts the following maximum potential efficieny are gained is:

$$\text{Loose belt: } \eta_{max} = \frac{E_{out}}{E_{in}} * \frac{200 - (12 - 3.9)}{200} = 0.960$$

$$\text{Tight belt: } \eta_{max} = \frac{E_{out}}{E_{in}} * \frac{200 - (15 - 3.9)}{200} = 0.945$$

Spur gear: $\eta_{\max} = \frac{E_{out}}{E_{in}} * \frac{200-(5-3.9)}{200} = 0.995$

6.2 Efficiency of the New Powertrain

To measure the efficiency plots of the powertrain the roller was assumed to having close to the same acceleration depending losses as the wheel to asphalt's acceleration depending losses. The same procedure of “taring” at different speeds to remove effect of rolling resistance from the roller was done. One drawback for this test were that the motor of the test bench had trouble handling more than 6 Amps of current drawn from the motors and less than -3 Amps while keeping constant speed.

Dynamic tests could potentially be used as an alternative here, but with the added complexity and potential errors due to wrong inertia calculations it was decided not to do that. Changing the motor of the test bench could also have been done, but due to time constraint and economics this option was also abandoned.

The measured data points can be seen in Figure 6.3. For regeneration of power it doesn't give enough data to say anything else than the total efficiency at -3Amps for the setup. For speed however with the assumption that there is only one peak point which at least is true for the theoretical motor model a rule of thumb that about 6 amps is the ideal power transfer at flat driving with RE50 48V. Meaning that for a pulse drive strategy aiming for 6 amps and then disengaging to remove the tare losses would be the most efficient.

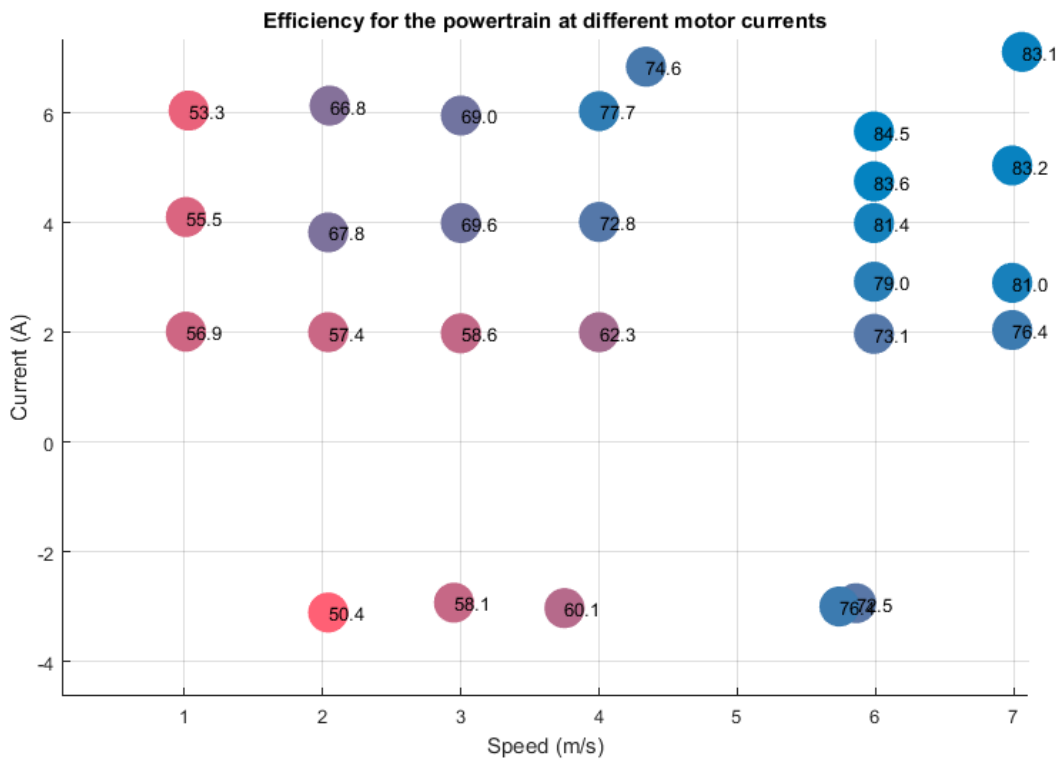


Figure 6.3 Efficiency at different currents and speeds.
Maxon RE50 48V with 24 teeth used in the actual testing

6.3 Driving strategy verification

With the assumption that the test rig 1 Amp of motor/generator use was tuned quite similar as the car model presented in author's pre-master testing of different driving strategies on the testbench were done. After some attempts with different strategies of how much current used in the beginning, at

steady state with the goal to drive close to the 140 second lap several good laps were measured like the one in Figure 6.4.

The powertrain used was the “prototype” of the final with the gears that wasn’t manufactured after the requirements of precision. The motor used was the RE50 36V with at 375:18 gearing and the best simulated lap driven was as following:

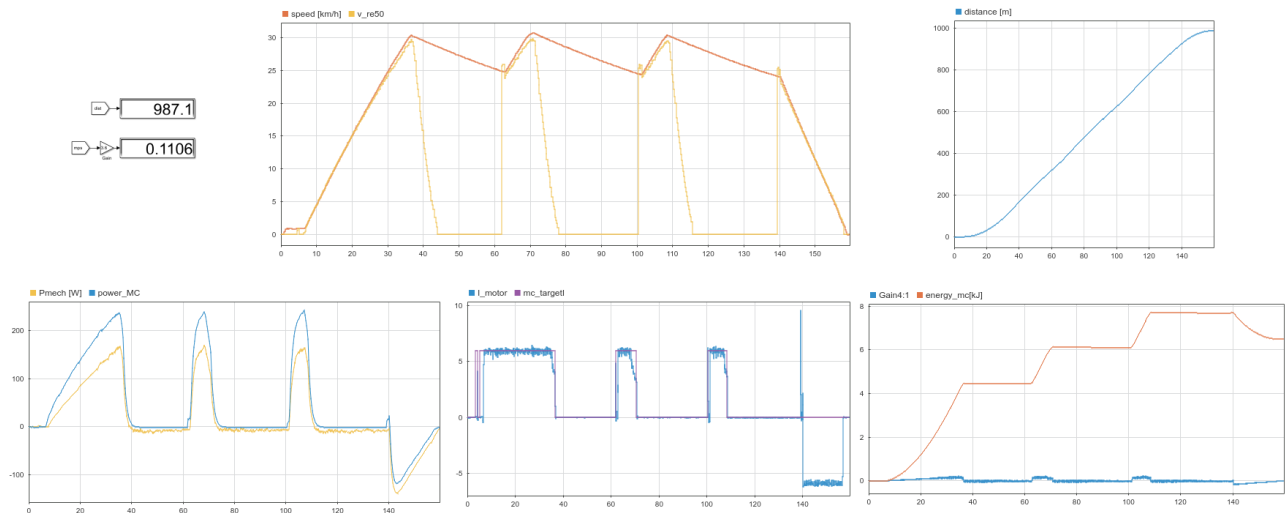


Figure 6.4 One of the most efficient driven laps on the test bench

It was hard to drive exactly on the target time and distance to get comparable results. However, some tendencies from the testing on the test bench was as following:

- Pulse drive – disengaging of the motor with short bursts gave the most efficient tracks times overall
- Regeneration of gave quite a lot of energy back ($\approx \frac{7.5-6.5}{7.5} = 13\%$ in Figure 6.4)
- The clutch in used almost no energy. By zooming in on the graph a **small** increase in energy use before regen can be seen

Arguably, even more important the following were that problems with the powertrain were easy to spot while driving the track: and made it possible to work on problems that would be hard to debug with components in the car, like:

- The 3D printed sliding mechanism was hard to get right
- Electric noise made wrong readings for speed, motor engagement etc.
- Motor engagement sometimes didn’t synchronize, much because of the sensors
- The radial forces produced from the gearing units were handled well
- The motor mounts aluminum part was delicate, and while it didn’t bend during driving it was bent on a few occasions while remounting / moving the powertrain. (new was designed)
- Various bugs in the steering wheels micro controller code causing clutching to go in randomly among others

In the end it was verified that the powertrain configuration as a system on the test bench were able to do the following:

- Get up to speed of 30 km/h (but not much faster) with 375:18 gearing
- Accelerate faster than the peak of efficient driving

- Regeneration of energy

7 Full Scale Testing

In addition to testing performance of the powertrain actual driving is also crucial to reduce the risk of a sub-systems not working together. With many sub-systems the potential failure modes are endless and by driving the car one gets closer to a validation of the different systems function. For the testing overall, the goal was as following:

- Start early, preferably when snow is gone from the track and before indoor
- Test as much as possible
- Verify that the aluminum rims and old powertrain works so backup systems were available
- Try to mimic race situations in terms driving with a timer and doing cornering

March 12.th - Indoor Testing

With snow covering Trondheim in the middle of march the first testing happened indoor. Many gyms and owners of big indoor areas was skeptical to let us drive or didn't have a entrance big enough for the car. However, in the end we got permission to drive at SiT Dragvoll Idrettssenter. With a quite small area to drive on there was no possibility to simulate lap times. The car at this state were a quite stripped stripped-down version of the 2017 car in the middle of being prepared for the reveal planned 17. April. This meant that the old powertrains, aluminum rims and the old steering wheel was mounted.



Figure 7.1 Stripped down version of the car at the first testing

The testing was successful as the car worked and the following weak spots were found that needed to be worked on:

- Front brakes we're subbing (rear brakes disc brakes disconnected)
- The motors got hot
- The electronics of the car was working for the entire session (ca. one hour)

For the motors getting hot the reason was a newly designed version of the circuit board installed. This read 1/3 of the actual current due to a wiring error and therefore sent too much power to the motors. In addition, the H-bridge control was afterwards changed from bipolar to unipolar switching which is supposed to be more efficient.

April 30.th – First Outdoor Testing

After a month with focus on the reveal of the car and Easter holidays there was time for more testing. A local track (Øya løpebane) running at 400 meters were used for this testing. The old powertrain was still in use as the new ones wasn't ready yet. The same was the case for the carbon fiber rim.

With this testing the motors weren't as hot as the previous time. However, the brakes that wasn't working as expected. They were constantly subbing and not retracting after use. This had such a huge effect that the car wouldn't get up to more than 20km/h with max motor force and the brakes were assumed to be the biggest issue for this as the car performed better after manually pushing the brake pads out. In addition, the fact that the track driven on were a running track wasn't ideal as the ground surface was rubber and expected to give some additional rolling resistance losses.

May 31.th – Second Outdoor Testing

The second outdoor testing happened one month after the first one and new brake calipers were changed to spring-loaded version (MCP-650). New brake rotors to support this system was mounted. New carbon fiber rims were also mounted in the front to be physically tested on the car.

This test was a great success and the fact that the car had been driving longer than it needed in the race during this test without overheated motors or subbing brakes. A few things remained though:

- The new powertrains
- Rear carbon fiber rims

In addition, there were some concerns with the following things:

- Brake lights were unstable and blinking
- The displays in the car had unstable communication
- The horn caused weird behavior on the car by falsely pressing buttons in the steering wheel

This was later found to be fixed by updating the steering wheel to do multiple readings to filter out noise.



Figure 7.2 The car with the new carbon fiber rims

June 10.th - First Outdoor Testing with the New Powertrain

With a full-scale prototype with badly produced gears of the new powertrain working on the test bench for three weeks with regenerative braking and synchronization the hopes were high when the testing in the car was going to take place. The car was tested at the parking lot at NTNU Dragvoll to test it on asphalt. However, luck was short.

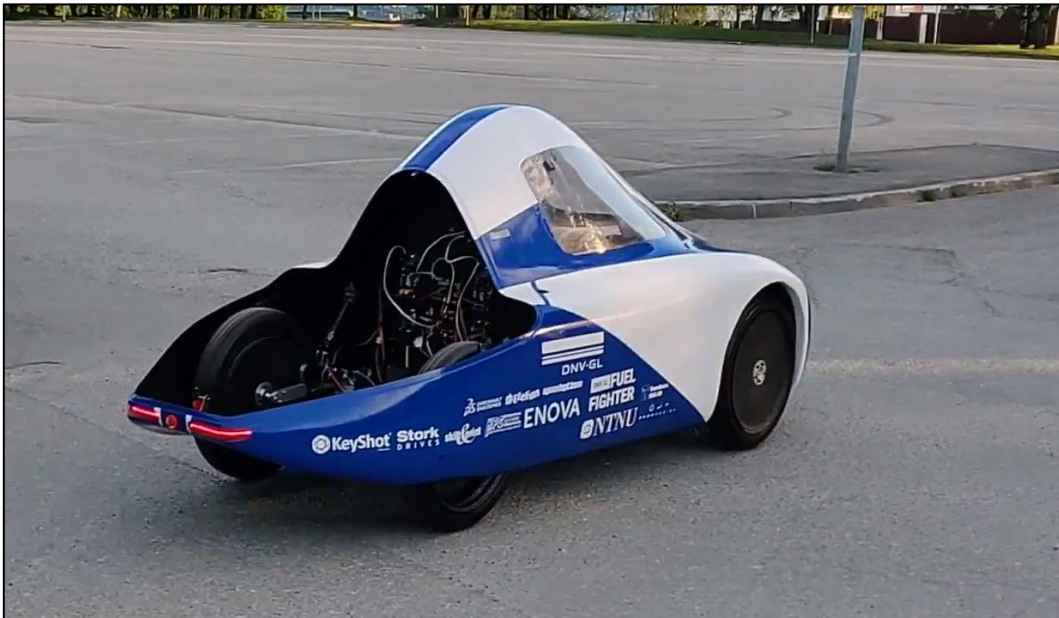


Figure 7.3 The car with new powertrains mounted

The communication between the electronic boards behaved weirdly. The clutch sometimes went in and out uncontrollably. And other times it looked like the controllers never got any response or didn't understand that it had done a synchronization. In addition, the 3D printed motor mounts made travel for the plastic harder in the cold. A quick fix for this was to loosen the screws a bit.

With this one side work as planned while the other failed it's communication. After a few hours of debugging at the field and code changes by the one responsible for motor control a solution in-between was made. As the geared powertrain was measured to have quite low tare losses (chapter 6.1) one of two motor mounts were forced to always be engaged. By this locking of the motors, a valuable function was made in case similar problems were happening during the race. In addition, the system was coded in such a way that if no actuator boards were present on the CAN-network the motor controllers would automatically assume that motors were always connected.

On the positive side the new powertrain behaved like they were designed for in regards of the suspension working and making the drive more comfortable. The last-minute fix to support the new brakes also worked as planned. In addition, the roads on Dragvoll was quite bad and the corners somewhat sharp so the assumed maximum sharpness of corners and assumed worse that road conditions at SEM18 were tested.

June 16.th 2018

The problems with the new gearing system was continuing, and the board controlling the actuator was after two burned linear actuators found to misread the position of the actuators. With two out of three linear actuators were burnt up, only one powertrain had synchronization (new actuators were ordered). After inspecting the analog to digital reader of the linear actuators it was also found that the readings became notably worse in the car than on the test bench. Electromagnetic noise was once again assumed one of the reasons to the problems. To solve the noise problem a 3D-printed end switch which previously had been one of the alternative solutions for reading position of the actuators. The way these functioned was to clamp tight enough around the square tubes of the powertrains and doing two things: To make sure that the linear actuator lined up at the same each time by resting on the mount and to report that it was in gear. The same clamping mount were placed on the other side of the powertrain without a working linear actuator to always lock it in gear.

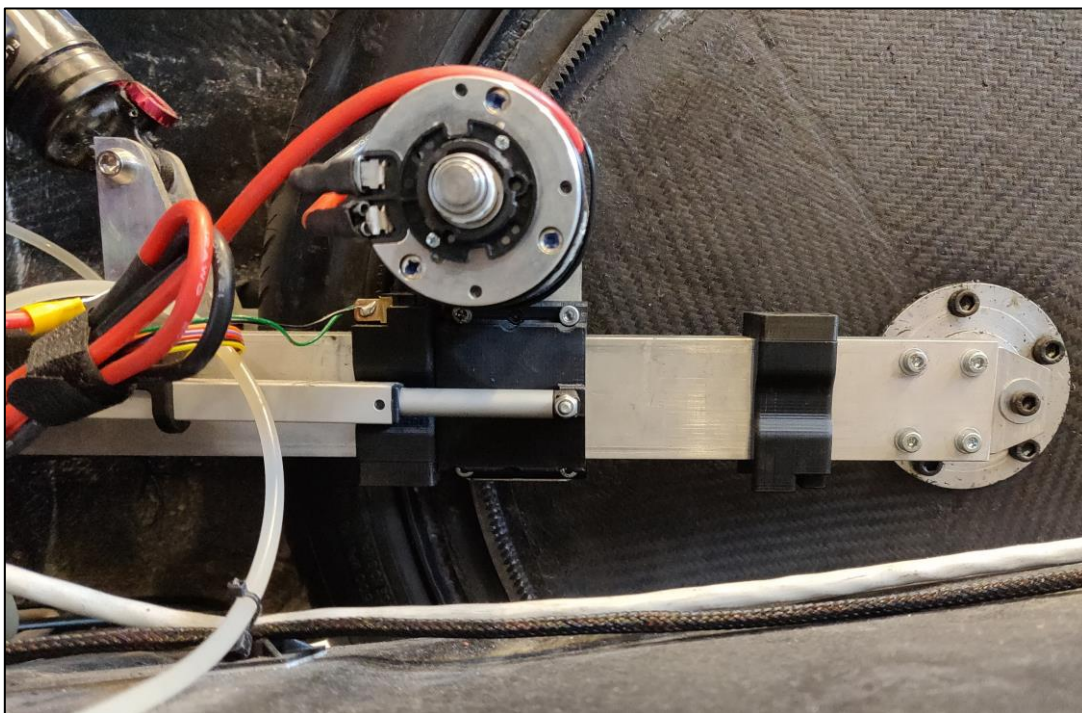


Figure 7.4 The end stops for the motors

At this testing the powertrain behaved mostly as they should where one went in and out and the other were locked. However, one problem was spotted: The motor controller struggled with giving 10A, 9A

was fine. But at 10A it sometimes gave a harsh sound from the motors and went in error mode. As the error made the motors became pushed back made us assume that too much current through the motors making too much. However, the testing was promising as both the clutching and non-clutching powertrain would have finished a race in the condition it was in.

19.th June - Final Test, in Hell

As a final test before the race the car was driven at “NAF Øvingsbane Lånke” in Hell. With huge open areas the goal was to get as close to real conditions with driving to max speed and cornering. In addition

- Everything works
- One powertrain with actuator, one always engaged
- A lowering in the PI current control loops P value were found as a solution for the over current problem at 10A

With the successful testing the team looked forward to London knowing that the car had been driving at each test – if not always in the best condition.

8 The race



Figure 8.1 Part of the track in London including the sharpest corner at the lower left

At arrival in London the final details of the race track were given to us. Length were 945 meters instead of the estimated 960 meters announced before the race. The rules were still to finish 15 laps with a complete stop between each lap and finish at a maximum time at 35 minutes. The event started July 2nd with 18 of our members on-site.

8.1 Day 1 – Unpacking

The first day were used to prepare the car for technical inspection and two issues were found:

- The heat in London. With one week with the 30 degrees forecasted and a sun heating more than in Norway the fear for of similar issues as the year before where one mirror fell of due to a melted glue connection

- The motor synchronization showed the same signs of instability as earlier in the project without the electrical team knowing why. Sometimes one of them wouldn't respond, others they synchronized with the wrong speed

8.2 Day 2 – Technical Inspection

Day 2 were dedicated to technical inspection of the car which opened in the middle of the day. With the same heat as the day before the decision to test if the car handled the heat were done. It was therefore on purpose left out in the sun with one goal: Parts to fall off/fail due to heat. This resulted in the following finding: A bad glue connection at the door locking mechanism where hot glue most likely had been used. It was fixed by using epoxy glue.

The car was allowed in at technical inspection at about 12:00 and passed in only three hours without any major hiccups.

With three days before the team could validate runs on the testing track and still not having found the reason for unstable engagement of the motors the decision to drive the car with motors always engaged were taken. However, troubleshooting this issue became second priority after track testing.

8.3 Day 3 – First Track Test

With the race starting first at Day 5 two days where teams could do practicing on the track were scheduled. The first lap of the first testing was driven with success. However, from driver's(author's) point of view the track were in a considerably worse shaped than the last year with some minor bumps in the track, a speed bump and corners that were much sharper than the corners the year before.



Figure 8.2 Fractured old ball joint vs. new Heim joints

In the second lap of the first test the worst thinkable happened. The front wheel fell off driving at 30 km/h over the speed bump causing the car to a sudden stop. Luckily, the wheel had rested in the wheel bow of the care. The cause of the failure was that the ball joint that connected the lower A arm to the upright dislocated due to the locking pin piercing through the steel. It was also found that this joint were the only broken part in the suspension system.



Figure 8.3 The fractured part in the suspension system

With the assumption that the front system worked with a lot of stress testing on worse quality roads than the good asphalt of SEM17 the fact that a part fractured were a surprise. The fracture could have been due to fatigue, however looking at other cars driving over the same bump and taking quite a hit made us fear that the ball joints just couldn't handle it. After a quite extensive search on these kinds of ball joints no good datasheets with ratings could be found. However, the steel was found quite mild and easy to make dents in.

The combination of no knowledge of the parts strength, no good reason for selecting the ball joints described in the teams reports from the last year and that it was made us look at alternatives.

After talking to other teams, they were usually using either ball made for automotive use and therefore quite different from ours or ball joints. After some searching we got to borrow Heim joints from another team. This however only had the rating of about 1.5kN, in the upward direction. And by design being the part that transfer the forces from ground to the A arm this left a safety factor of only three from the static forces from driver and car's weight while the back were designed to handle at least 6 times the forces from gravity (Chapter 5.4). For this reason, the front suspension was tuned to be as soft as possible.

8.4 Day 4 – Last Day of Testing

The fixed suspension was proven to work much better the second day of testing. Driving was still done carefully, but more than 40 laps were driven by driver and second driver meaning more than two valid attempts if it had been in the race day. The strategy for driving also became quite clear at this testing. The strategy was close to the strategy presented on the test bench in Chapter 6.3 and due to the tracks geometry acceleration were done at start line and after every corner as seen in Figure 8.8. This strategy made it easy to maintain a relatively steady speed as well as to drive as utilizing the minimum speed in the corners.

Day 5 – First Race Day

At the first day of racing the synchronization of gears with the linear actuator were more reliable. Since it was considered an increased risk to drive with synchronization enabled the car were driven in safest possible configuration with gears always engaged and suspension tuned to be soft. This precaution gave results by finally validating a run at 104.7km/kWh after years without valid results and were placing us in top three at that time.

With a valid result the time for increased risk in the search of a more efficient vehicle began. First out was testing if the clutch system were reliable enough to validate an attempt. In the race a few bad synchronizations, especially in the start/stop area where the car had to be restarted two times to function were noticed. The result was an improvement from the first result giving us 113 km/kWh.

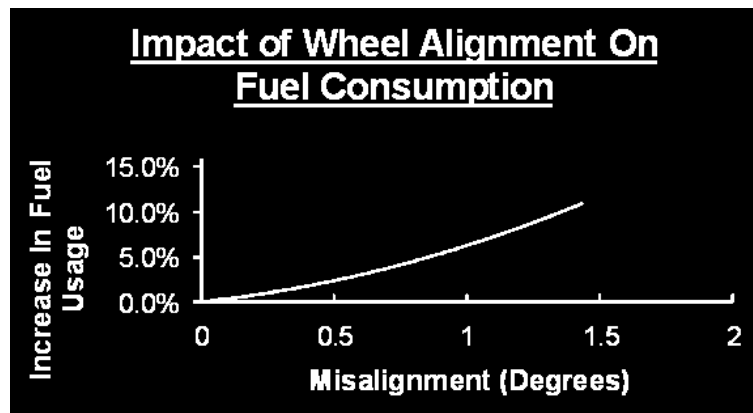


Figure 8.4 Toe misalignments effect on fuel consumption
For a regular car with 30% of its energy losses from rolling resistance (bathwicktyres.co.uk, 2018)

With this the search for the next improvement began and the following things were improved:

Front Suspensions Effect on the Front Wheels Toe Misalignment

The suspensions stroke in / stroke out play (sub-chapter 5.5.3) with driver inside the car was measured to have an effect in the front wheels alignment at about 2 degree (measured by a Track Ace Laser Alignment tool). Toe in / toe out is one of the biggest contributors to increased rolling resistance and Figure 8.4 shows how it affects a “regular” car. Several effects on our car could have an influence on this effect as the team’s car having narrower tires, 50% of its losses while the “regular car have” 30% of its losses from rolling resistance. The graph therefore wasn’t directly comparable to our car. In addition, the fact that a source of the graph is a tire-alignment shop in UK makes the graph risky to trust.

As this misalignment were caused the shocks play that wasn’t removable without changing the behavior of the shock, the decision to increase shock pressure to make it close to stiff were taken. The Track ace Laser Alignment were then used to remove any misalignment again and the change were proven a success by the new measurements.

Left Brake Caliper Misaligned During Racing

After each of the first two race attempts the left wheel were braking so bad that when trying to spin the wheel by hand it stopped in a matter of seconds. Realignment of this front brake caliper was done to fix this before attempt one and two, however the problem kept coming back and in attempt two the following were noticed: In the sharpest corner there’re were a noise coming from the front suspension which sounded like something touching the brake rotors holes for cooling/ ventilation. By closer inspection the heim joints crashed into the suspension which most likely bent the calipers mount at the same time. For this reason, the heim joints were filed down a bit and an additional spacer was added in the brake caliper to reduce the risk of the same happening again.

False Speed Readings at Synchronization

One of the root causes for bad synchronization was finally found. During synchronization there was a voltage peak induced from EMI measured by scoping the speed signal with an oscilloscope. While this

noise from synchronization didn't influence the car at regular operation the use of open loop control by sending constant voltage to get speed for synchronization caused a short burst of current rushing through the motor powerful enough to measure wrong speed and therefore the motors were trying to match the new speed while crashing.

With this knowledge a change in the code made the synchronization trust the last reading before the engagement started. As synchronization worked well but was assumed to increase the risk it was decided that the first out of two remaining attempts were still going to be driven with no synchronization.

Day 6 – Last Race Day

On the last race day everything went as planned. The third crushed the result from the day before with 171 km/kWh and the last result at 176.4 km/kWh. With this the team managed to get close to the winning team TIM07 that with a new world record got a 7% better result at 188.3km/kWh.

The fact that we got top three also meant that we qualified to something called Drivers World Championship (DWC). In this race the main goal is to drive ten laps the fastest with a limited amount of energy that are calculated as a percentage of the main result the team gets. The winner of each category gets 120% of its used energy per lap, second place 110% and third 100%.

The car wasn't designed with this show race in mind, being geared for a low maximum speed for performance. Before the technical inspection one of the master cylinders loosened causing air in the brake system that disqualified us from this race.

As the team had already proven its performance it's arguably to the better that it wasn't allowed to race. 2nd place out of cars in our category was still a huge victory for the team.

8.5 Analyzing Shells Telemetry Data

The team had its own telemetry system in the car as well, but as this wasn't as accurate as the one delivered by Shell, used ca 5 watts and didn't do good power readings this was disconnected during racing. The mandatory system Shell provided have therefore been used for analyze of data.

This data was given out after each attempt as a .csv-file and provided the following data at 10 samples per second:

- GPS speed and position
- Joulemeter current / voltage / total energy use
- Lap count

With the following annoyances:

- GPS speed wrong (lower than real) two places on the track due to a bridge interrupting the signals
- The lap counter didn't count every lap and the mandatory stop was placed before this sensor. This meant that the data had to be manually modified

8.5.1 Energy Use Per Lap

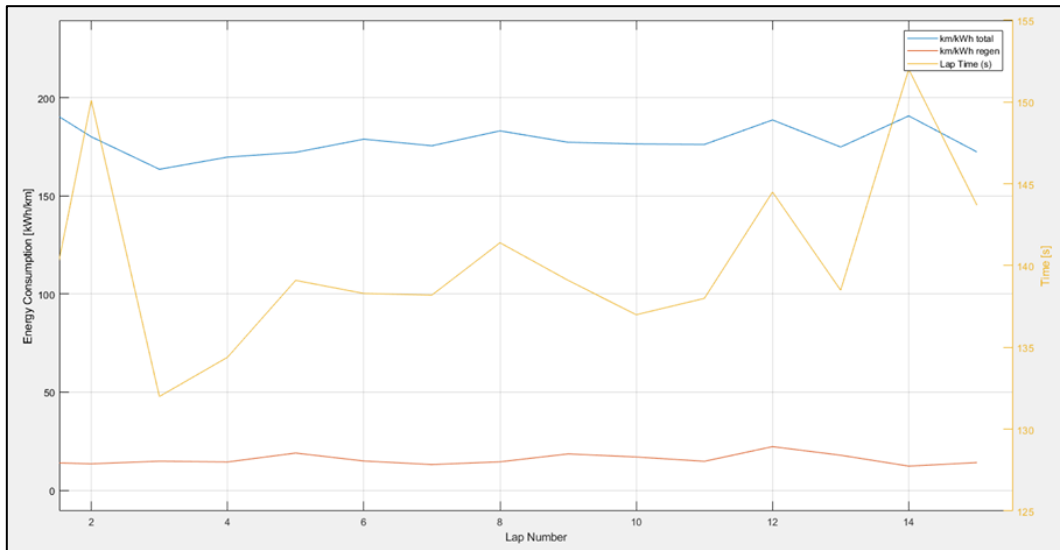


Figure 8.5 Energy consumption per lap.

To analyze how the amount of regenerative and total energy use changed per lap MATLAB were used as shown in Figure 8.5. With Shell using km/kWh for the results this was used for the energy in the comparison as well. The following could be noted:

- 10 out of 15 laps was +/- 5 seconds from 140 seconds
- All laps had similar energy use with a correlation to the time used to do the lap
- Regen was also quite consistent. Hard to see any tendencies other than the fact that energy was recovered after each lap

8.5.2 Data from one lap

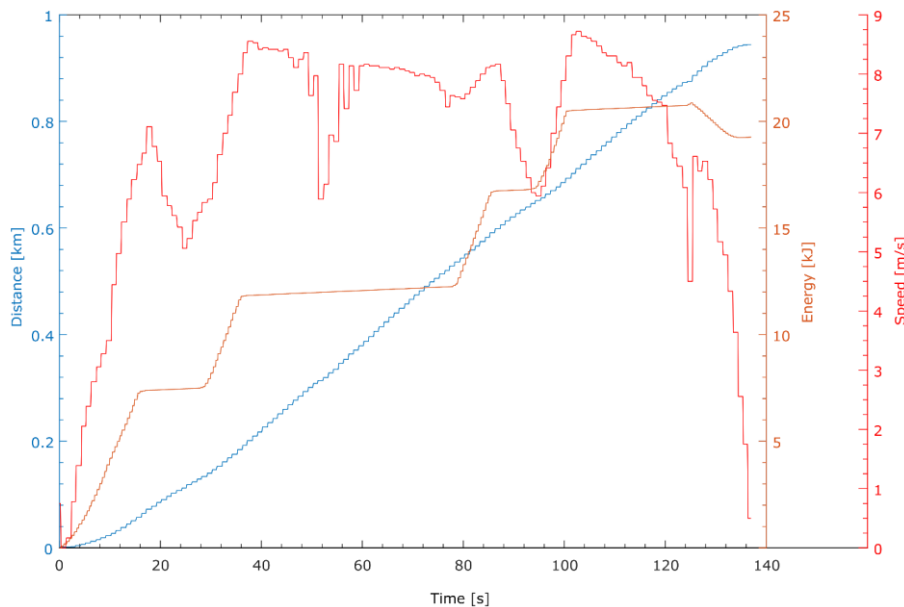


Figure 8.6 Lap 10 of 15 in our best attempt in London.

With all laps from the final attempt being quite similar lap 10 out of 15 were analyzed. The GPS data to relate distance to track is shown in Figure 8.7. The findings from this data (Figure 8.6) are as following:

- About 10% of the energy used were recovered each lap with regenerative braking

- The electric system draws a lot of energy when the powertrains were disconnected
- Powertrains were in use ca. 50 seconds out of 140 seconds
- The pulse drive strategy looks like what we're planned used on the test bench
- Regeneration of energy started after coasting down to ca. 6.5 m/s.
- Driver (author) started to brake mechanically at ca. 4 m/s

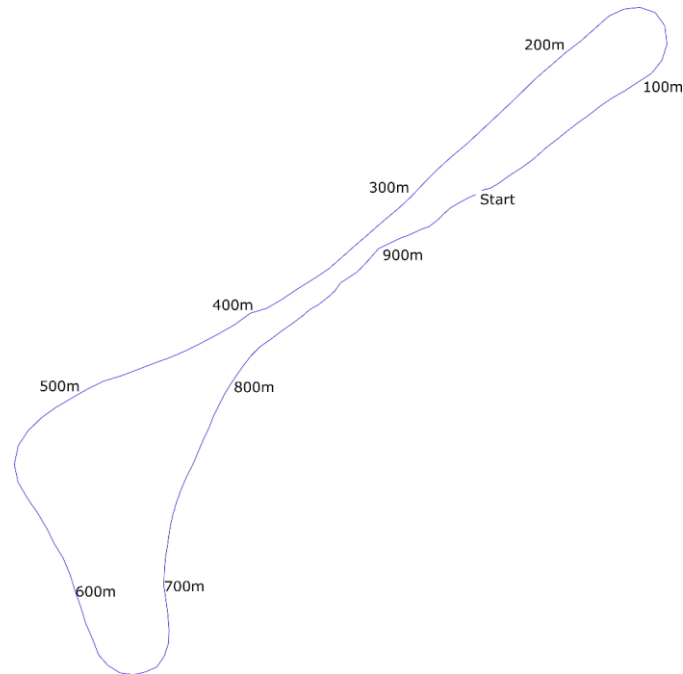


Figure 8.7 GPS points from Shells telemetry system

8.5.3 Comparing with the Results of the Winning Team

The winning team from INSA Toulouse with the car TIM07 were kind enough to share their data. To compare the data, distance were used as the x-axis rather than time. Both laps compared were close to the average lap for the teams with about the same lap time. As the graph shows the TIM07 were coasting and accelerating mostly at the same places as us with. However they didn't have regen and therefore opted for a strategy to coast down to speed and drive faster in the beginning. This could have both positive consequences as regeneration are having some losses to heat while fighting aerodynamic drag at a uneven speed also is inefficient. One thing could however be noted: At 650 meters the energy consumed were about the same with TIM07 having a higher maximum speed as well as using less time to get to this point(higher speed). This gives reason to believe that if this driving strategy is more efficient it isn't much more efficient.

One other improvement would potentially have been if the driver were holding higher speeds in corner one (at 150meter) and two (at 530 meter). However this was risky given the circumstances of the front

brakes. Especially in the 2nd corner where the driver (author) still heard the brake rotor touching while taking the corner as smooth as possible at speeds higher than ca. 28km/h.

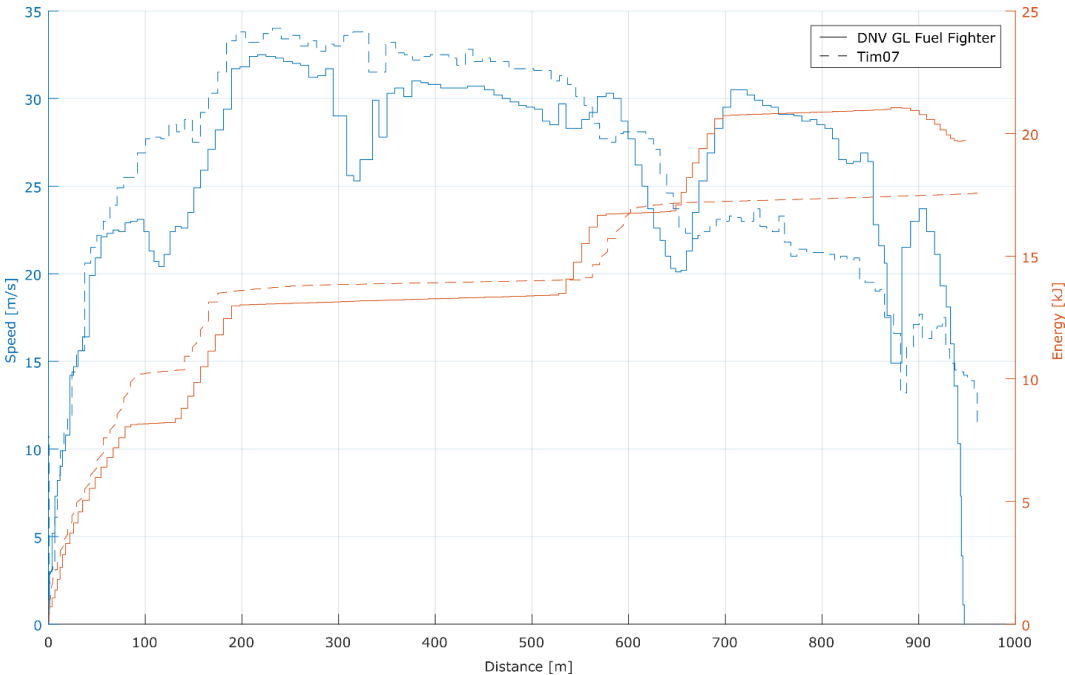


Figure 8.8 Comparison of DNV GL Fuel Fighters laps and the winning TIM07 car’s lap. Shared by permission from team Tim Ups from the INSA Toulouse.

8.5.4 Energy Use by the Electrical System

As the electrical system looked like it was used quite a lot of energy by having a noticeable energy increase even during the motors disengagement the consumption measured at disengagement was analyzed.

To get some context to it the 174.6 km/kWh result were converted into average watts used as 139 watts. In addition, TIM07 and TUfast were both coasting on their telemetry data and are therefore also included in the calculation where $P=UI$ were calculated for an average of measurements where no acceleration was taken place (only electrical system on). The results were as following:

TUfast	3.9 watt
FF	8.7watt
TIM07	7.1 watt

The numbers show that 6.3% of our total energy use was due to the electric system consuming power. It also shows that we were the team with the highest energy use out of the three compared.

9 Discussion

With the development process being an iterative process where the more one gets close to a understanding of how the car works the less sure one is that one has tried the best solution. With this an acknowledgment of the hard work with a 2nd place in the race an only being beaten 7% by the car that have the World Record both in the battery-electric class(2018), ICE class(2017) and are known to be the lightest urban concept car made being with 22kg lighter than our car shows that something must have been done right in the development of the car and improvement of it this year. In addition to this the team managed to get 2nd place in the off-track award for communication.

The last time DNV GL Fuel Fighter got a 2nd place in the main race were back in 2011 the first car built. And with no valid results the three last years of the race all four of four attempts are a proof of the team managing to build a reliable car and mitigating risk by having back up plans in case something was to go wrong. Examples where there was a plan B was if the rims should brake or if the new powertrain broke.

With the test bench as a tool to test under close to real conditions it was also possible to verify that parts like the new motor controller worked early in the process by using the old powertrain. The same process was done with the new powertrain where a 3D-printed prototype of the two geared solution showed that the concept of synchronization worked and was later confirmed working full-scale.

However, both the race and testing showed that small changes like moving the powertrain from test bench to the car could have unwanted consequences. In retrospect electromagnetic noise were especially problematic and the reason for most of the problems we had. For this reason, some of the electronic boards like the steering wheel should be considered remade for the next year's team.

In addition, the last year driver's(author's) assumption that the track wouldn't have sharper corners than tested in Trondheim were painfully wrong causing bad results as well as the fact that the car wasn't able to handle the bump during the first test track shows that one could never be prepared enough.

Trying to understand the car model wasn't easy. Below is the estimated energy use per lap from the car model described in chapter 3.5, the lap driving on the test bench in chapter 6.3 where the test bench motors wasn't used to get the results close to the car model and the real results from the race:

Best attempt:	19.5kJ/lap
Test Bench, unpowered:	$6.5\text{kJ} * 2 = 13\text{kJ/lap}$
The car model:	Ca. 10kJ/lap

This means that some numbers are wrong. To speculate: The one responsible for the 0.138 drag calculation was very skeptical about this number being true. One team in SEM were also saying that they had found the rolling resistance data from Maxon to be too low with a factor of 2. In addition, the fact that the brakes were still touching a bit in the corners could have been an potential loss.

To try to understand the savings with the clutch system tare losses were measured. With race results from the car with mechanical brake issues the first two times but clutch only one of them with clutch and the same for the car after the mechanical issues were fixed a look for some patterns could be done. To calculate estimated loss in kJ/lap for clutch engaged the knowledge that the clutch was disengaged for 90 seconds while coasting at an average speed at about 8m/s this gives a estimated loss of :

$$W_{tare\ losses} = 90\ s * 5\ watt/powertrain * 2powertrains = 0.9kJ/lap$$

Always engaged	104.7km/kwh	232.1watt _{avg}		32.5kJ/lap
Clutch	113km/kwh	215.0watt _{avg}	-	30.1kJ/lap
Difference with mechanical issues			=	2.4kJ/lap
Always engaged	171km/kwh	141.8watt _{avg}		19.9kJ/lap
Clutch	176.4km/kwh	137.8watt _{avg}	-	19.3kJ/lap
Difference without mechanical issues			=	0.6kJ/lap

While it's highly speculative to draw conclusions from the track data with many potential error sources there was a positive effect from the attempts driven with clutch in that could have been caused by the clutch being disengaged. The fact that Maxon and the tare measurements indicate that there is a loss when the motor is engaged should be taken as an indication that clutching makes the car more efficient by a estimated effect of ca. 3%.

Both motor model, powertrain testing and motor to motor testing proved that we could expect high efficiency from regeneration of power. Regeneration were also proven to give energy back by 10% with our driving strategy. What should however have been tested investigated more was the effect of coasting vs regeneration as TIM07's driving strategy was as they didn't have regenerative braking.

Next year team should expand the search for the best speed profile by at least considering the effect of the following (Figure 9.1 to illustrate the points):

1. How long to coast
2. how much and when to regenerate energy (with two gears to increase efficiency and wheel torque?)
3. When to stop the car completely so not that much time on trying to regenerate when there isn't that much more kinetic energy

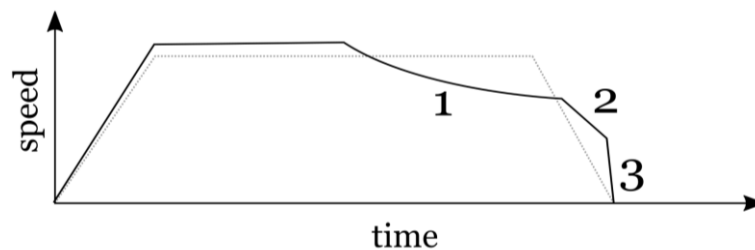


Figure 9.1 A alternative driving strategy

This could be done both analytically but more importantly but is also suggested to be tested during the competition as this is the only way to truly get the numbers were judged on and making sure the strategy fits the track.

The powertrains with synchronization worked well in the end with the 3D-printed part as the trickiest part to get right. For next year's team this solution should be reconsidered or improved to a better solution. In addition, moving the speed sensor to the other side of the powertrain is advisable for easier reach.

10 Recommended Further Work

As the next year's team needs to make a new chassis with two doors focus should be on this part. As the monocoque used this year was responsible for half of car's at about 42 kg while being simulated to being much less production gets important. Read the report from the 2017 team (Carlsen and Oma,

2017) and aim for around 20kg as a required weight. This has been doable for both TIM and the first car SEM car made at NTNU. Also talk to Revolve as they're also making carbon fiber monocoques.

Make sure that the old powertrains fit in the new design, either as a backups solution or as the main system in use. Use both the old car until the new are ready and the test bench to make sure the powertrains work. This is by far the easiest way for new members to learn the powertrains.

Remember that every part on the could break. Stress test the suspension and cornering abilities of the car. And, don't over engineer. More complexity increases the chance of delays and makes it more time consuming to debug and fix systems if something goes wrong.

11 Conclusion

The work presented in this master thesis were critical of top three in the competition. With the 2nd place and four out of four validated runs in London in terms of developing a reliable new powertrain with the old powertrain as a backup. Measurements and theory also suggest that the developments of the new geared powertrain could be expected to transfer energy more efficient from motor to wheel and were proven to regenerate 10% in the race.

The mechanical aspects of the new powertrain improved the stiffness and made the suspensions ability to absorb bump forces and compensate for uneven ground level better by a utilizing an increased load on the shock.

Weight wise the new carbon fiber rims alone made a reduction in 4.7kg of the weight. The new powertrain was also responsible for a weight saving of 2.5 kilogram. This and other changes like new windows and door hinge (not described in this thesis) made the team reach the 90-kilogram goal they set in the beginning of the year with a good margin and the car was weighted to 85 kilogram.

A goal that wasn't realized was the two geared transmission due to time constraints. However, theory shows it could be more efficient and the car as a proof that synchronization of gears work makes it likely that a such powertrain should work. Otherwise using the RE50 36V is also considered better than the 48V version of the same motor.

Sources

- Anderson, N.E., Loewenthal, S.H., 1981. Effect of Geometry and Operating Conditions on Spur Gear System Power Loss. *J. Mech. Des.* 103, 151–159. <https://doi.org/10.1115/1.3254854>
- bathwicktyres.co.uk, 2018. Wheel-alignment [WWW Document]. Bathwick Tyres - Tyres South Engl. Wales. URL <https://www.bathwicktyres.co.uk/wheel-alignment> (accessed 8.8.18).
- Carlsen, B.D., Oma, O.J., 2017. Development, Building and Competing with a New Car in Shell Eco-marathon.
- engineeringtoolbox.com, 2018. Friction and Friction Coefficients [WWW Document]. URL https://www.engineeringtoolbox.com/friction-coefficients-d_778.html (accessed 6.11.18).
- Espel, V., 2018. The Difference Between Wet and Dry Carbon Fiber, Revisited.
- gearsolutions.com, 2018. Surface Coatings for Superior Gears | Gear Solutions Magazine Your Resource to the Gear Industry.
- Institute, P.M., 2015. Business Analysis for Practitioners: A Practice Guide. Project Management Institute.
- Lean Enterprise Institutes, 2018. Set-Based Concurrent Engineering in the Lean [WWW Document]. URL <https://www.lean.org/lexicon/set-based-concurrent-engineering> (accessed 8.7.18).
- machinedesign.com, 2017. Plastic Gears Are the Future [WWW Document]. *Mach. Des.* URL <https://www.machinedesign.com/materials/plastic-gears-are-future> (accessed 8.3.18).
- NS-EN ISO 898-1:2013 [WWW Document], 2013. URL <https://www.standard.no/no/Nettbutikk/produktkatalogen/Produktpresentasjon/?ProductID=630501> (accessed 6.11.18).
- Powertrain, 2018. . Wikipedia.
- Quantum Controls, 2018. What's the difference between a non-regenerative DC drive and a regenerative DC drive? [WWW Document]. URL <http://www.quantum-controls.co.uk/faq/drives/whats-the-difference-between-a-non-regenerative-dc-drive-and-a-regenerative-dc-drive/> (accessed 6.17.18).
- Santin, J.J., 2007. The World's Most Fuel Efficient Vehicle: Design and Development of Pac Car II. vdf Hochschulverlag AG.
- SDP/SI, 2018. Elements of Metric Gear Technology - Measuring accuracy in bevel gears - Page 8 [WWW Document]. URL <http://www.sdp-si.com/resources/elements-of-metric-gear-technology/page8.php> (accessed 8.2.18).
- ShimReStackor.com, 2018. Suspension Bump Velocity [WWW Document]. URL http://www.shimrestackor.com/Code/User_Manual/Sections/Suspension_Velocity/suspension-velocity.htm (accessed 8.1.18).
- SKF, 2018. Angular contact ball bearings [WWW Document]. URL http://www.skf.com/us/products/bearings-units-housings/super-precision-bearings/principles/design-considerations/bearing_preload/actbb/index.html (accessed 8.1.18).
- SSAB, 2018. The most popular abrasion-resistant steel with excellent structural properties. [WWW Document]. SSAB. URL <https://www.ssab.com/products/brands/hardox/products/hardox-450> (accessed 8.3.18).
- stressebook.com, 2015. Solid Metal Versus Sandwich Panels. Stress Ebook LLC.
- Tattu 7000mAh 6S 22.2V Lipo Battery, DJI S800 Lipo battery - Gens Ace [WWW Document], n.d. URL <http://www.gensace.de/tattu-7000mah-22-2v-25c-6s1p-lipo-battery.html> (accessed 6.16.18).
- tribology-abc.com, 2018. Coefficient of friction, Rolling resistance, Air resistance, Aerodynamics [WWW Document]. URL <http://www.tribology-abc.com/abc/cof.htm> (accessed 8.3.18).
- Walden, D., Roedler, G., Forseberg, K.J., Hamelin, R.D., Shortell, T.M., 2015. INCOSE Systems Engineering Handbook: A Guide for System Life Cycle Processes and Activities, 4.th Edition. ed. John Wiley & Sons, Inc., San Diego, CA.

Appendix A: Race Results

Valid attempts and result for the UC-category:



**Shell
Eco-marathon**

Shell Eco-marathon Europe 2018
Final results: UrbanConcept Battery-electric

11/07/2018

Rank	Team n°	Team name	Country	Organization	Institution type	Competition category	Energy type	Best attempt (km/kWh)	Attempt 1 (km/kWh)	Attempt 2 (km/kWh)	Attempt 3 (km/kWh)	Attempt 4 (km/kWh)
1	716	Toulouse Ingénierie Multidisciplinaire	France	INSA de Toulouse	University	UrbanConcept	Battery-electric	188.3	187.4		188.3	
2	721	DNV GL Fuel Fighter	Norway	Norwegian University Of Science And Technology	University	UrbanConcept	Battery-electric	176.4	104.7	113	171	176.4
3	703	Evi Neuruppin	Germany	Evangelische Schule Neuruppin	School	UrbanConcept	Battery-electric	150.6		105.8	134.2	150.6
4	714	Ulg Eco Team	Belgium	Université De Liege	University	UrbanConcept	Battery-electric	140.8		127.4	138	140.8
5	719	mecc -E	Italy	Politecnico Di Milano	University	UrbanConcept	Battery-electric	129.6				129.6
6	704	SZEnergy Team	Hungary	Szechenyi Istvan University	University	UrbanConcept	Battery-electric	124.7	112.2	115.3	121.8	124.7
7	723	CUKUROVA ELECTROMOBILE TEAM	Turkey	Cukurova University	University	UrbanConcept	Battery-electric	119	118.7		119	117.5
8	702	TUfast Eco Team	Germany	Technische Universität Muenchen	University	UrbanConcept	Battery-electric	112.8	112.8	112.3		
NC*	901	St Thomas Academy Experimental Vehicle Te	United States	Saint Thomas Academy	School	UrbanConcept	Battery-electric	96.1	92.2	96.1		
9	706	ENSL Team	France	ENSL Limoges	University	UrbanConcept	Battery-electric	63.9		63.9		
10	717	The Phoenixer	France	IUT Alençon	University	UrbanConcept	Battery-electric	62.8	57	62.8		60.1
11	722	Solar-GT	Spain	C.I.P.F.P. Benicarló	School	UrbanConcept	Battery-electric	57.1				57.1
12	720	Blue Racing Windesheim	Netherlands	Windesheim University of Applied Sciences	University	UrbanConcept	Battery-electric	40.8	33.4	37.6	40.1	40.8

Source: shell.com

2nd place communication, with judges' comment:

Communications

2nd place:

DNV GL Fuel Fighter

Norwegian University Of Science And Technology, Norway

The team set ambitious goals for their communications program, and while they didn't always meet them, they recognized where they fell short and endeavored to improve through the course of the campaign and shifted tactics when necessary. They succeeded in showcasing their diversity and reaching their target audiences by featuring team members and securing coverage in their school newspaper and other media and tried innovative techniques like a campus Easter Egg Hunt that engaged students and educated them on the team's effort and broader energy issues.

Source: shell.com

Appendix B: Articles

BilNorge.no, (8.7.18):



To norske slo de norske

Laget fra NTNU ble nummer to i sin klasse i årets Shell Eco Marathon. Vinneren ble et fransk lag med to nordmenn om bord.

Jon Winding-Sørensen

// Miljø og bil // BilNorge.no // 08-07-2018 // 19:15

Liker 0

Tweet

– Får vi den ned i 90 kg, skal vi vinne, sa Sivert Hatletveit til meg tidligere i år. Han leder **NTNU-gjengen som bygget årets DNV GL Fuel Fighter**, den norske deltakeren i Shell Eco Maraton – løpet der du helst bør produsere energi mens du kjører bortover, for å vinne.

Jeg var i Trondheim og så på forberedelsene, veldig imponert over selvbygde karbonfelger (vektreduksjon fra 2,5 til 1,5 kg på hver) og egenprodusert rigg der de målte rullemotstand og et dashbord som like godt kunnet få plass på et kunstindustrimuseum.

Jeg vet ikke hva som gikk galt. Kanskje nådde de ikke sine 90 kg, eller kanskje hadde vinneren funnet enda noen fordeler – de ble i hvert fall nummer to. Særdeles hederlig – det deltok nesten 150 lag til sammen.

Et problem var imidlertid åpenbart. Banen, som ligger i Olympiaparken i London, var i år kortet ned fra 1,6 km til bare 970 meter.

– Det som skapte mest problemer for bilen vår var den skarpeste svingen etterfulgt av helling, forteller Håvard Vestad – en av de cirka 30 på laget i år.

– På det første forsøket fikk vi litt problemer med hjulopphenget, i tillegg til at dekkene og fjæringa var i mykeste laget. Etter at vi utbedret dette og tok noen grep for å optimalisere motorkontrollene, gikk det bare bedre og bedre».

Bedre og bedre kan han trygt påstå. Lagene hadde til sammen fire forsøk, og DNV GL Fuel Fighter fikk stadig bedre resultater for hvert forsøk.

De startet med å bruke 1 kWh på 105 kilometer, men sluttresultatet ble utrolige 176 km/kWh. Det var bare 6-7 % unna vinnerens resultat.

Ikke at de kan sammenlignes, men for å gi deg en idé: en Nissan Leaf gjør ca. 15 km på 1 kWh.

Hvis vinneren hadde fortsatt som i fjor hadde NTNU blitt det beste laget. For i fjor var bilen fra INSA Toulouse drevet av en forbrenningsmotor. Da vant de den klassen, de kjørte tilsvarende 685 kilometer på én liter bensin!

Men i år hadde de byttet ut bensinmotoren med en 250 kW sterk elmotor og avansert motorstyreprogram. Og akkurat som i fjor hadde de med to norske studenter på laget. Torkel Genet fra Sandnes var årets lagleder og Simen Sandtorv Hansen fra Bergen var fører.

Simen gir oss et godt spor i jakten på hvorfor de, og ikke Trondheim, vant.

– Bilen veide like mye som føreren, med utstyr, avslørte han og kunne fortelle at vektnålen stoppet på 67 kg. Det er med andre ord en del ekstra kilo som skal fjernes før neste års konkurranse.

Det er Eirik Evjan Furuholmen fra Oslo helt klar over. Har ledet lagets R&D-gruppe i år, og skal være prosjektleder for neste års bil.

– Neste år er reglene endret igjen, for eksempel skal bilene i denne klassen da ha to dører. Det betyr at vi må utvikle et nytt og lettere chassis. En krevende jobb, men en vi gleder oss til, sier han.

Han forteller videre at i tillegg til å videreutvikle den elektriske konseptbilen, skal teamet også starte på et prosjekt for å utvikle en autonom bil.

– Vi skal også bygge videre på den data-loggeren vi har i dag for å lage en digital tvilling av bilen. Denne skal vi bruke Live for optimalisering. I tillegg skal vi jobbe for å sikre at våre elektriske systemer blir enda mer pålitelig – og så kommer altså den store oppgaven: et nytt chassis.

Med andre ord: Nok å se frem til.

Selv gleder jeg meg mest til å se neste års bil ferdig. De første skissene jeg ble vist for noen måneder siden tider så veldig bra ut.

Det er ikke lett å gjøre noe originalt innenfor regelverkets trange rammer, men det så virkelig ut som om 2019-bilen også vil bli kandidat til designprisen.

Hvilket minner meg om: Det er en rekke andre priser som skal deles ut i forbindelse med dette arrangementet. Men det skjer først under festen i kveld, lenge etter at dette er skrevet.

Følg med på facebook-siden deres for å se hva som skjer videre.



NUMMER TO: Sivert Rød Hatletveit med bilen DNV GL Fuel Fighter, som tok andreplassen i klassen Urban Concept i Shell Eco-marathon. **FOTO: PRIVAT**

Molde-student nesten helt til topps i «VM» for effektive biler

Sivert Rød Hatletveit tok andreplass i Shell Eco-marathon sammen med andre NTNU-studenter.

NTNU har i et tiår deltatt i konkurransen Shell Eco-marathon i London, «verdensmesterskap» for energieffektive biler. I helga gikk de nesten helt til topps, ledet av Sivert Rød Hatletveit fra Molde.

Bilen oppnådde et energiforbruk tilsvarende 176,4 kilometer per kilowatt time i konkurransen.

– Dersom bilen hadde hatt samme energimengde som en fulladet Tesla Model S100 D, ville den kunne ha tilbakelagt en avstand på 17.640 kilometer! Studentene kunne altså ha kjørt avstanden Trondheim – Cape Town, via London uten ladning. Batteriet hadde først trengt påfyll etter å ha kjørt yt-

terligere et par tusen kilometer til, skriver selskapet DNV GL, som er hovedsponsor for prosjektet, i en pressemelding.

Det holdt til andreplass i klassen Urban Concept, kun slått av ett fransk lag. Studentene fra NTNU består av 30 personer, hovedsakelig studenter fra Norge, men også studenter fra Tyskland, Frankrike, Mexico og Australia. Som sagt ledet av Sivert Rød Hatletveit fra Molde, som jublet høgt etter at resultatet var sikret.

– Det er et komplett lag, bestående av studenter med solid kunnskap innen en rekke fagområder som står bak. Alle 30 har like stor del i dette, jeg er bare en brikke i et fantastisk lag, sier han i pressemeldingen.

Studentene ved NTNU har gjennom flere år utviklet DNV GL Fuel Fighter, en 3 meter lang og 1,2 meter høy bil med aerodynamisk utforming og to elmotorer (200 W). Som veier

85 kilo tilsammen.

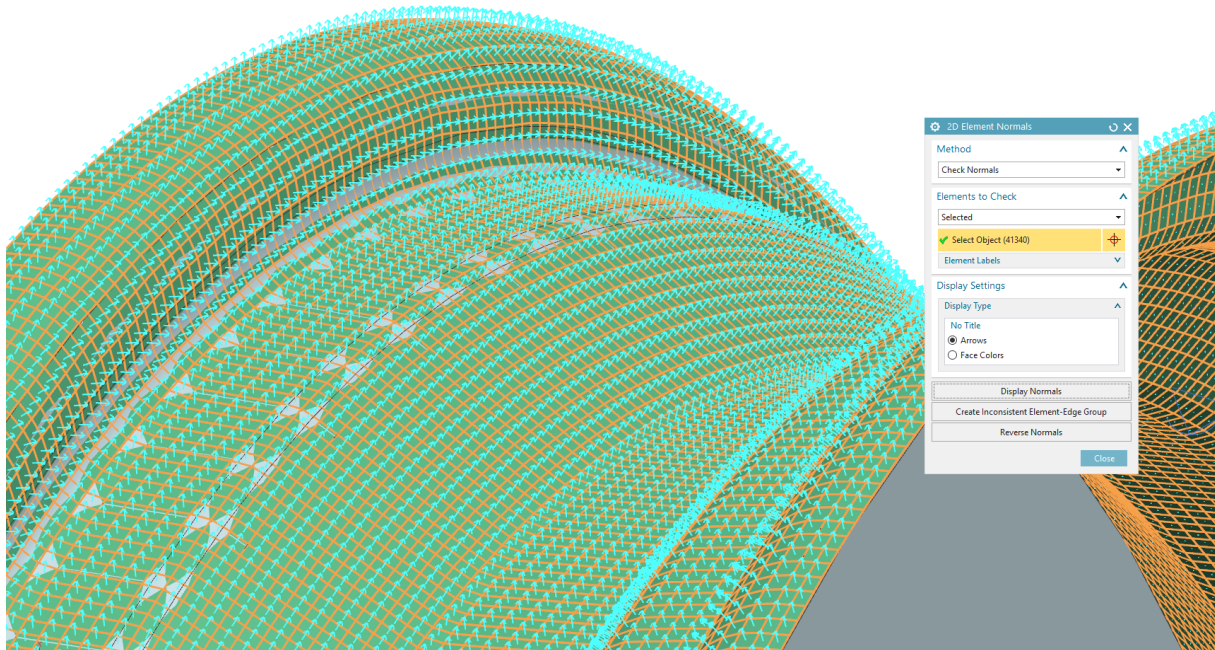
– NTNU har deltatt i denne konkurransen 10 ganger tidligere. Vi bygger videre på erfaringer og løsninger fra tidligere år. Vekt, rullemotstand og aerodynamikk er viktige faktorer. Vi pusher oss selv til å forsøke nye løsninger, søke nye muligheter – hele tiden, sier Rød Hatletveit.

140 lag fra 24 land deltok i årets konkurranse. Klassen NTNU-laget deltok i var for biler designet for å kunne kjøre i ordinær bytrafikk.

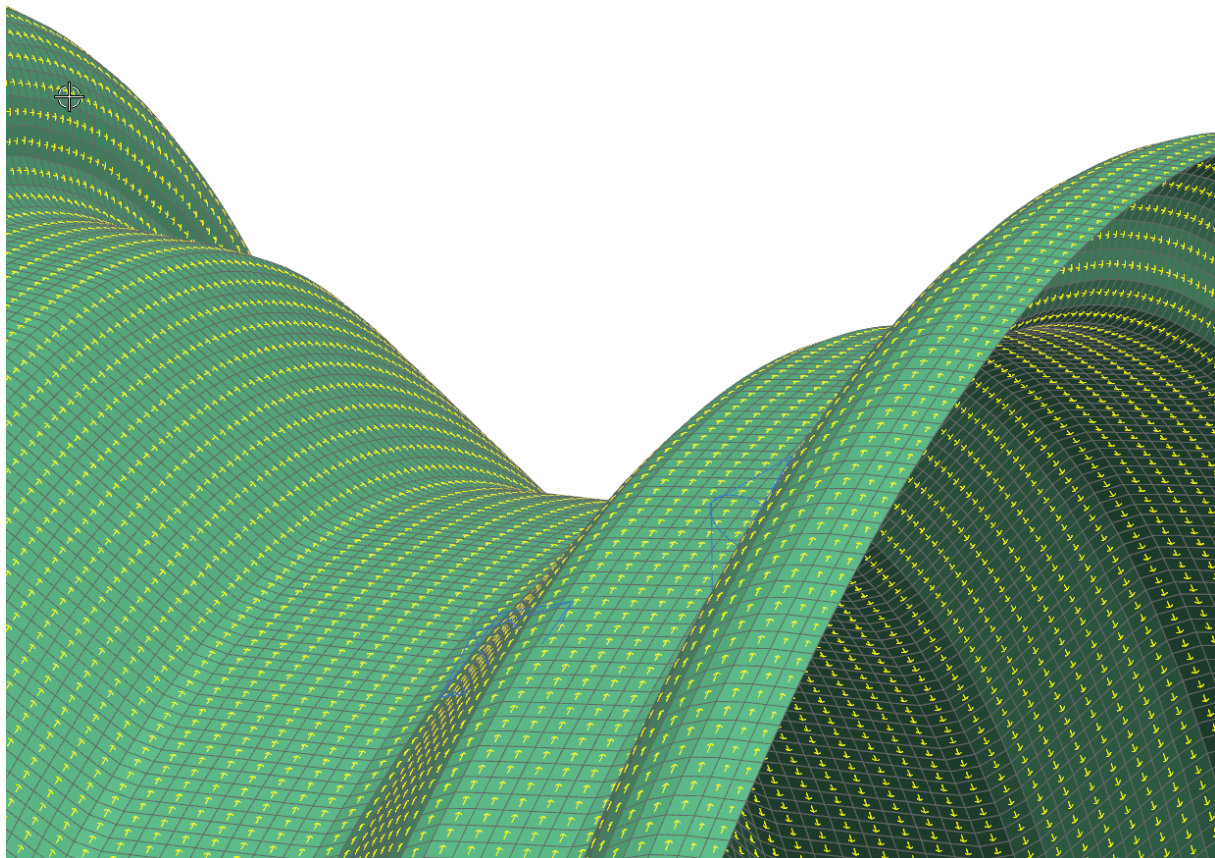
LASSE TOMREN
lasse.tomren@r-b.no

Appendix C: Rim Calculations (Setup with help from Nils Petter Vedvik at MTP)

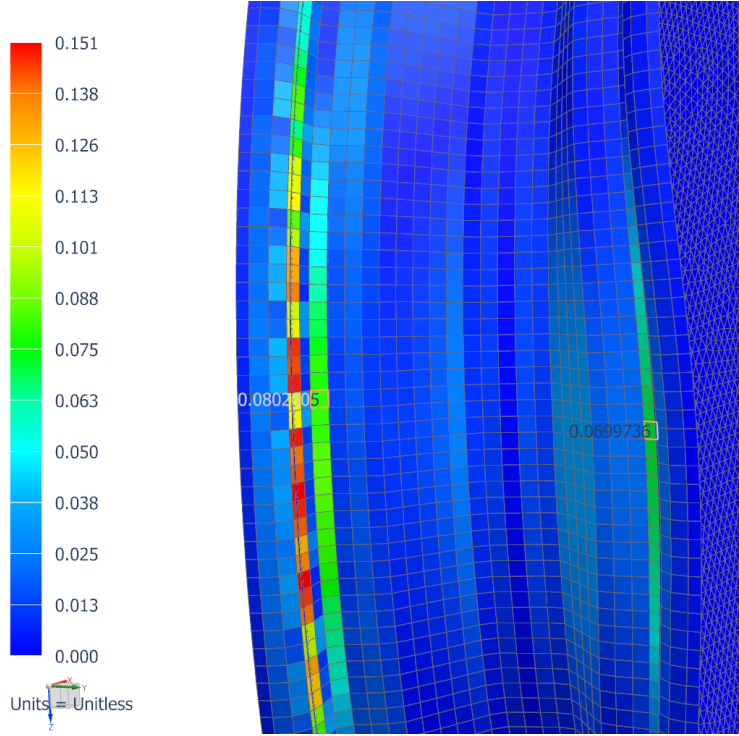
Outer ring 2D Element Normals:



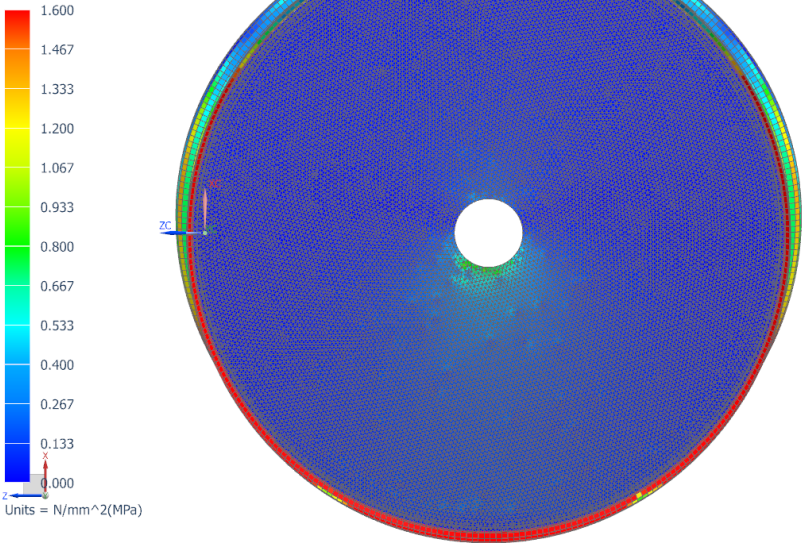
Shell element direction:



Results for simulation of all forces other than the pressure forces:

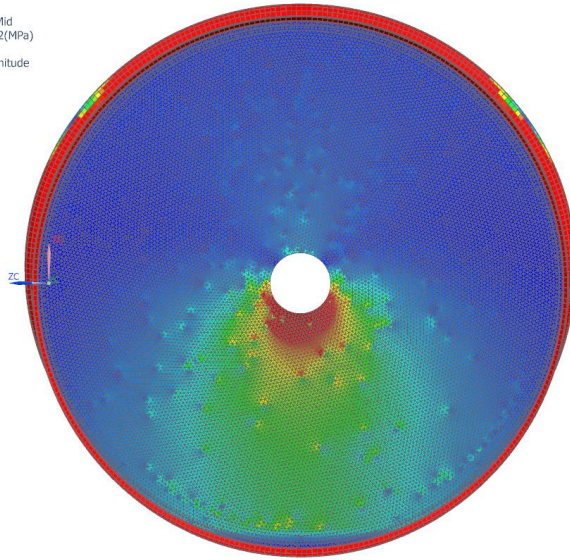
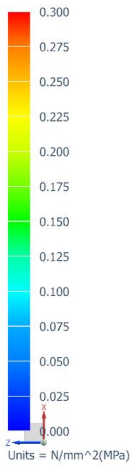


rimv2fix_sim2 : Static Center Result
Subcase = Static Loads 1, Static Step 1
Ply Stress - Elemental, Max Shear, Ply 3 Mid
Min : 0.00, Max : 19.22, Units = N/mm^2(MPa)
Coord sys : Native
Deformation : Displacement - Nodal Magnitude



DiabH35:

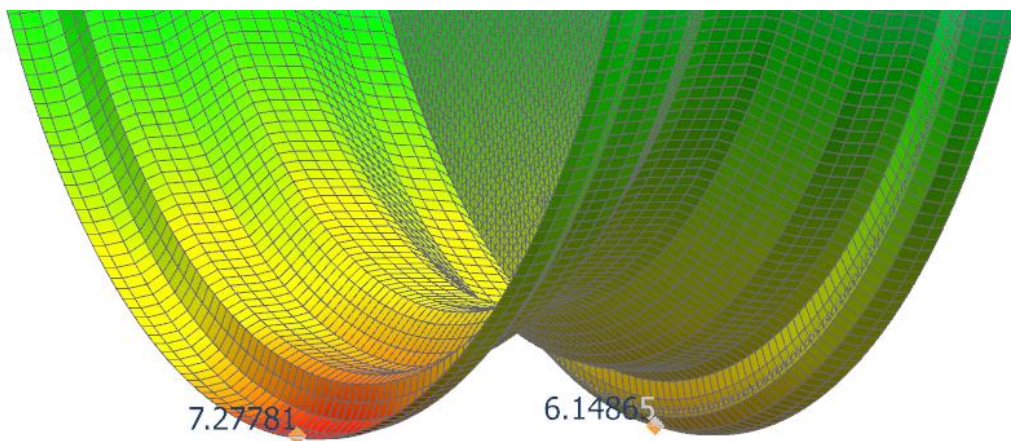
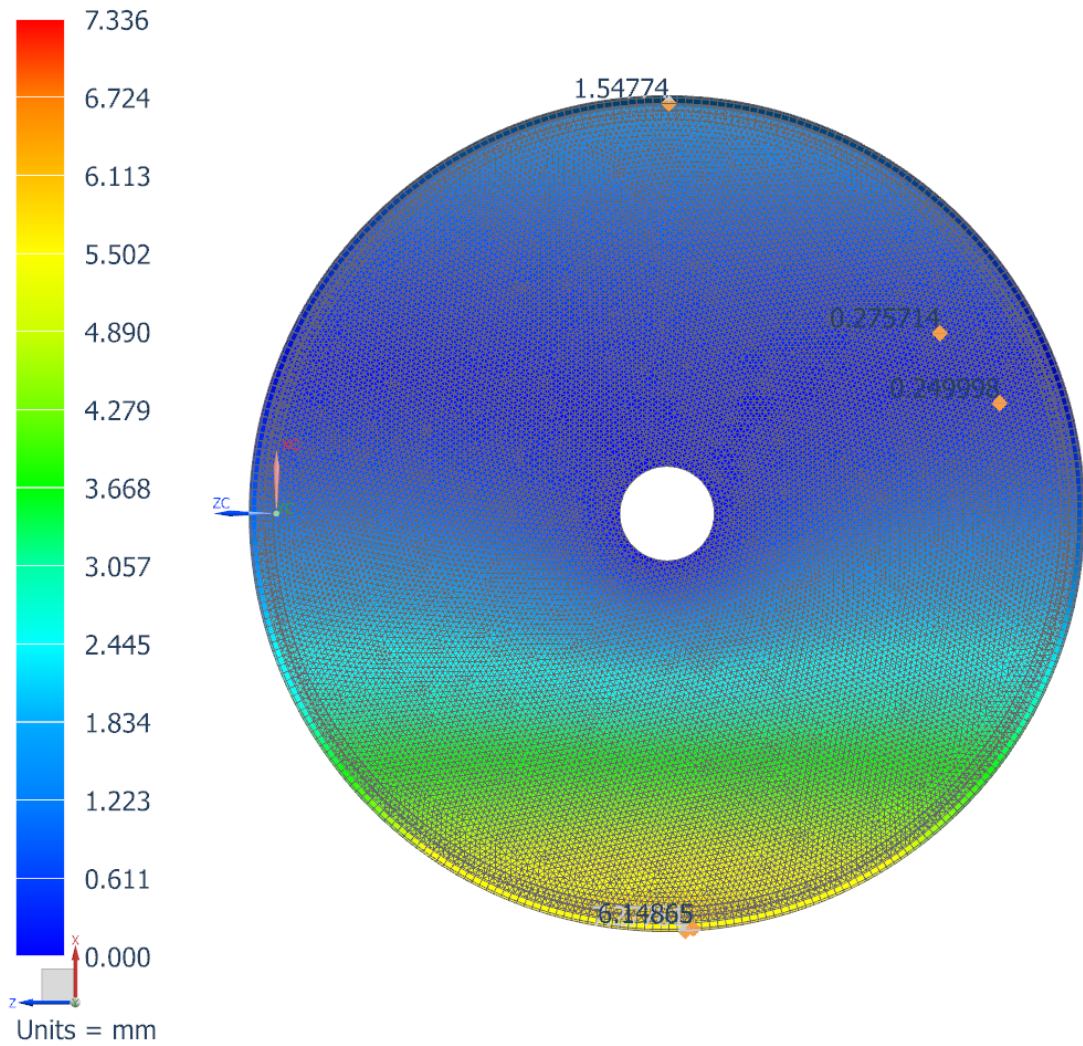
rmmvzrnx_simz : static center kesur
Subcase - Static Loads 1, Static Step 1
Ply Stress - Elemental, Max Shear, Ply 3 Mid
Min : 0.00, Max : 19.54, Units = N/mm^2(MPa)
Coord sys : Native
Deformation : Displacement - Nodal Magnitude



Med kjerne:

Deformations

rimv2fix_sim2 : Static Center Result
Subcase - Static Loads 1, Static Step 1
Displacement - Nodal, Magnitude
Min : 0.000, Max : 7.336, Units = mm
Coord sys : Native



Settings for easypreg:
 (The layout added to the 2D mesh as PCOMPG:)

The screenshot shows the 'Laminator Modeller' software interface. The window title is 'Laminator Modeller'. The interface is divided into several panels:

- Solver Properties:**
 - Physical Property Table: Name: CarbonFiber, Label: 2
 - Properties: Nonstructural Mass: 0 kg/mm², Damping coefficient: 0, Stress or Strain Output Request, Laminite Options: None, Output Format: PCOMPG
- Laminite Properties:**
 - Stacking Recipe: Regular
 - Reference Plane Location: Middle
 - Reference Temperature: 20 C
 - Ply Failure Theory: Tsai-Wu
 - Interlaminar Failure Theory: Transverse Shear
 - Interlaminar Allowables: Use Laminite Allowables
 - Shear Stress for Bonding: 64 N/mm²(MPa)
- Validation:** Contains icons for validation and help.
- Optimization:** Currently empty.
- Ply Layup / Ply Sketcher:**
 - Tools: Paste, Undo, Redo, Erase, Copy, Paste, Print, Help, (45/90)
 - Paste Repetition: 1
 - Reverse Plies and Glob:
 - Table:

Id	Composition	Thickness	Angle	Description	Solid Property
1	xpregxc110(210)	0.13	0	outer	Layered
2	xpregxc110(210)	0.278	0		Layered
3	xpregxc110(210)	0.278	0		Layered
4	xpregxc110(210)	0.278	0		Layered
5	xpregxc110(210)	0.278	45	45deg	Layered
6	xpregxc110(210)	0.278	0		Layered
7	xpregxc110(210)	0.278	0		Layered
8	xpregxc110(210)	0.278	0		Layered
 - Global ply id: 8 Ply Material Thickness: 0.278 mm
 - Material: xpregxc110(210) Angle: 0 deg
 - Description:

Buttons: OK, Cancel

Orthotropic Material

Property View

All Properties

Name - Description

wpregxc110(210)

Label 2

Description

Categorization

Properties

Mass Density (RHO) 1600 kg/m³

Mechanical

Strength

Durability

Thermal/Electrical

Creep

Viscoelasticity

Viscoplasticity

Damage

Miscellaneous

Young's Modulus (Ei)

Young's Modulus (E1)	Young's Modulus (E2)	Young's Modulus (E3)
55100 N/mm ² (N)	55100 N/mm ² (N)	7000 N/mm ² (N)

Major Poisson's Ratio

Poisson's Ratio (NUij)

Poisson's Ratio (NU12)	Poisson's Ratio (NU23)	Poisson's Ratio (NU13)
0.28*(7/120)	0.35	0.35

Shear Modulus (Gij)

Shear Modulus (G12)	Shear Modulus (G13)	Shear Modulus (G23)
4000 N/mm ² (N)	4000 N/mm ² (N)	4000 N/mm ² (N)

Structural Damping Coefficient (GE)

Stress-Strain Related Properties

Stress-Strain Input Data Type: Engineering Stress-Strain

Stress-Strain (H): N/mm²(MPa)

Type of Nonlinearity (TYPE): PLASTIC

Yield Function Criterion (YF): von Mises

Hardening Rule (HR): Isotropic

Initial Yield Point (LIMIT1): N/mm²(MPa)

Initial Friction Angle (LIMIT2): deg

Thermal Mechanical

Mechanical Power to Heat Ratio: 0

Card Name MAT3/MAT8/MAT11

Close

Mechanical

Strength

Durability

Thermal/Electrical

Creep

Viscoelasticity

Viscoplasticity

Damage

Miscellaneous

Strength

Yield - 1	Yield - 2	Yield - 12
N/mm ² (N)	N/mm ² (N)	N/mm ² (N)

Ultimate Tensile - 1	Ultimate Tensile - 2	Ultimate Tensile - 12
N/mm ² (N)	N/mm ² (N)	N/mm ² (N)

Tsai Wu Coefficient

Tsai-Wu Interaction Coefficient (F12): -0.5 mm⁴/N²

Stress Limits

Tension (ST1)	Tension (ST2)	Tension (ST3)
521 N/mm ² (N)	521 N/mm ² (N)	30 N/mm ² (N)

Compression (SC1)	Compression (SC2)	Compression (SC3)
483 N/mm ² (N)	483 N/mm ² (N)	150 N/mm ² (N)

Shear (SS12)	Shear (SS13)	Shear (SS23)
50 N/mm ² (N)	64 N/mm ² (N)	64 N/mm ² (N)

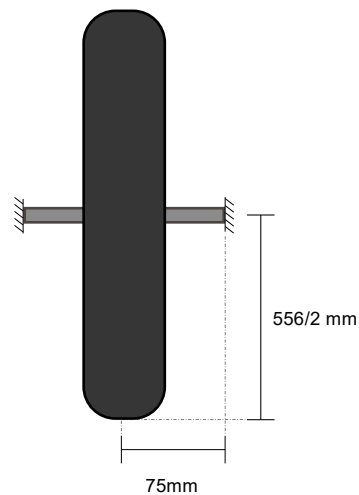
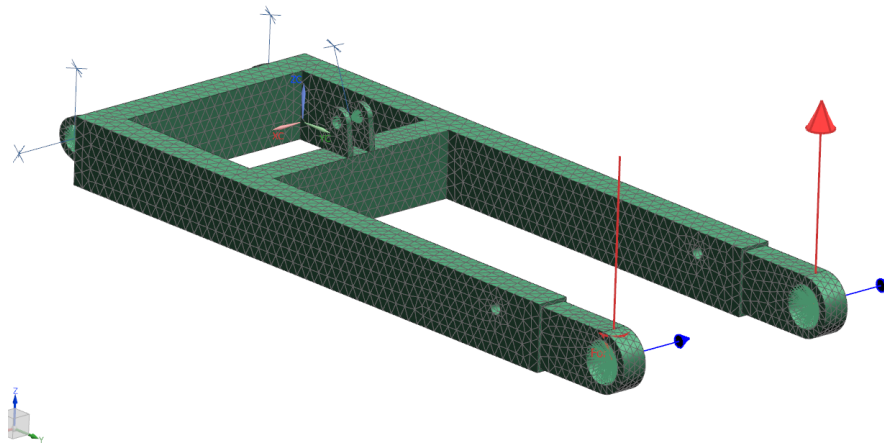
Strain Limits

Appendix D: Rotary vs stationary axle

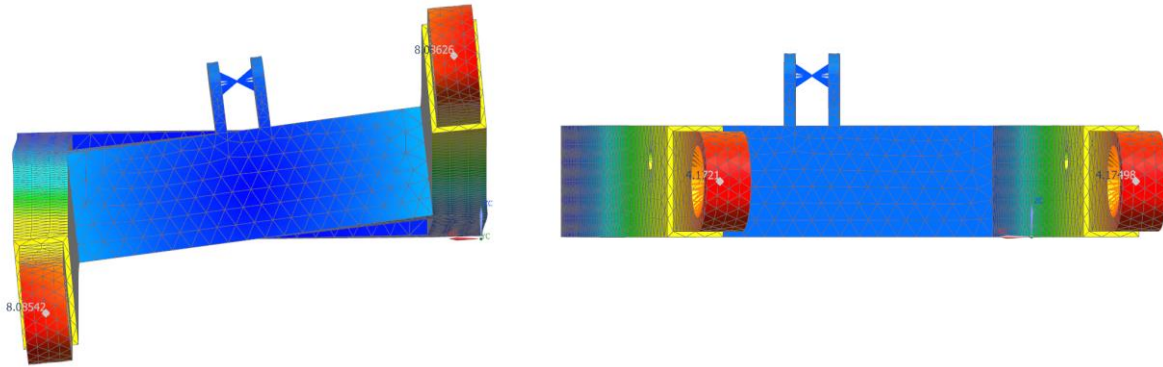
To find the effect of a rotary vs stationary axle one of the earlier powertrain CAD concepts with 2mm thick walls were analyze. The following constraints were set for the powertrain: No translation in any of the two wall mounts (locked translation) and no translation relative to the direction of where the suspension goes in (simply supported constraint).

Rotating Axle

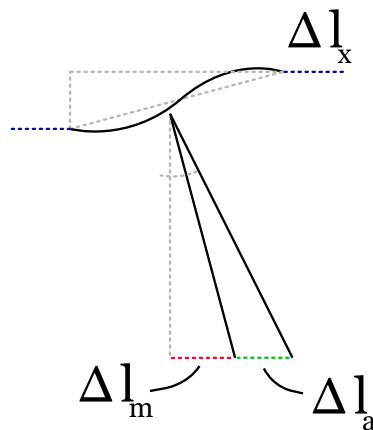
The simulation for rotating axle with play were conducted by assuming a solid aluminum axle of length 150mm and diameter in thickness. To say anything about the forces to the frame the force of 500N were added to each side of the powertrain with the assumption that the axles length direction didn't add any extra stiffness due to the symmetrical forces and design. The result became that forces from momentum ($\Sigma M = 0$) in the middle of the wheel axle were distributed as following: $F_m = F_{cornering} * r_{wheel}/2 * 75mm = 927N$ should be working upwards and downwards (red arrows) and that forces from ($\Sigma F_x = 0$) were equally distributed as $F_x = F_{cornering}/2 = 250N$.



The result for the stiffness of the frame in CAD were as following:



By assuming small deformations + superposition the total deformation can be described by the following geometry:



From the simulation the $\Delta l_m = 8.05mm * 2/150mm * 556mm/2 = 29.8mm$ and $\Delta l_x = 4.1mm$.

To find the Δl_a caused by bending in the axle a beam calculator from were used combined with the following data for aluminum: $E = 70GPa$. And $I = \frac{\pi r^4}{4} = 2485mm^4$ giving the following results displayed underneath. By using the angular deflection and still assuming small deformations the displacement due to the axle bending became $\Delta l_a = \tan(\theta_{max}) * r = 2.8mm$

INPUT PARAMETERS

Parameter	Symbol	Value	Unit
Moment *	M	139	N*m
Beam Length	L	150	mm
Distance a	a	75	
Distance x	x	75	
Modulus of Elasticity	E	70	GPa
Distance from neutral axis to extreme fibers	c	7.5	mm
Second moment of area**	I	2585	mm ⁴

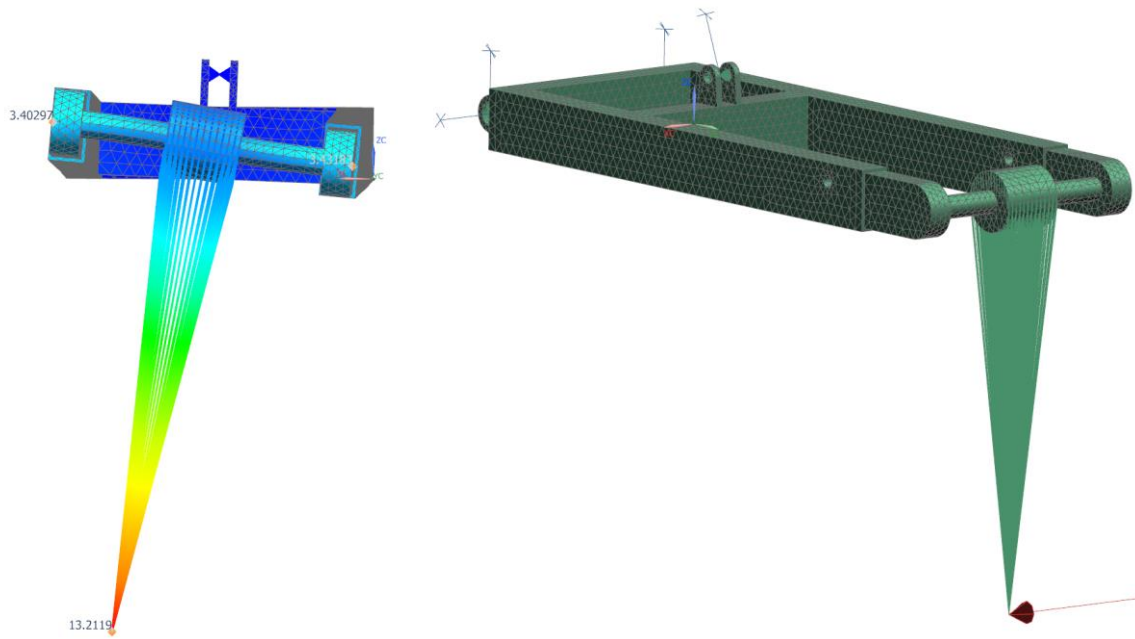
RESULTS			
Parameter	Symbol	Value	Unit
Reaction Force 1	R ₁	-208.3	lbf
Reaction Force 2	R ₂	208.3	
Transverse Shear Force @ distance x	V _x	-208.3	
Maximum Transverse Shear Force	V _{max}	-208.3	
Moment @ distance x	M _x	-615.1	lbf*in
Maximum Moment	M _{max}	-615.1	
Slope 1	θ ₁	0.005	radian
Slope 2	θ ₂	0.005	
Slope @ distance x	θ _x	-0.010	
Maximum Slope	θ _{max}	-0.010	
Deflection @ distance x	y _x	0.000	inch
Maximum Deflection	y _{max}	-0.005	
Bending Stress @ distance x	σ _x	201.6	MPa
Maximum Bending Stress	σ _{max}	201.6	

Calculated with <https://www.amesweb.info/StructuralBeamDeflection/SimpleBeamIntermediateMoment.aspx>

The total deformation of the free axle at 15mm became: $\Delta l_{tot} = \Delta l_a + \Delta l_m + \Delta l_x = 37\text{mm}$

Fixed Axle

For calculating the stiffness of a fixed axle the same 15mm axle were added to the design and simulated as following with a simplified hub:

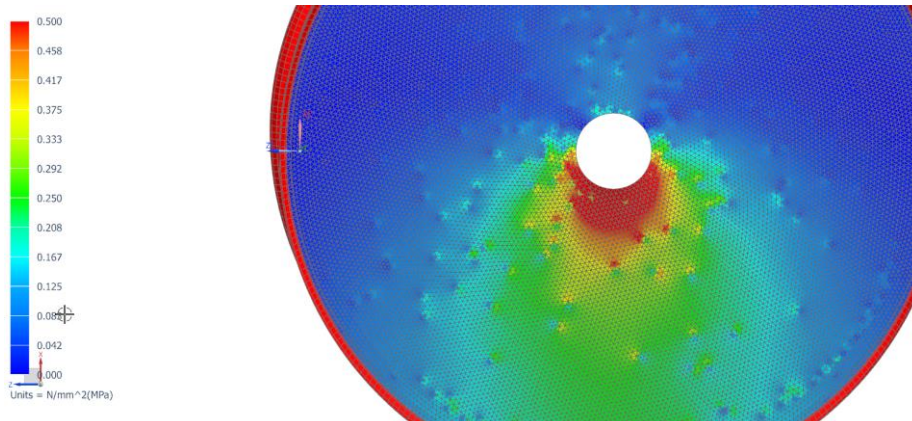


With this simulation no manual calculations had to be done to find the total deformation of 13.21 mm.

With the following structure the overall stiffness is **2.8x** stiffer for the design with the axle mounted rigidly.

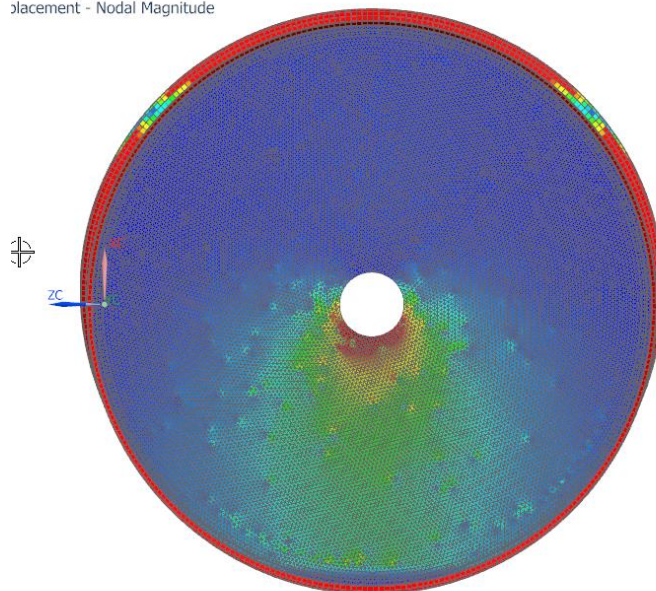
Appendix E: FEA of The Carbon Fiber Rim

Carbon fiber rim:



Core as is first proto

40.12, Units = N/mm²(MPa)
Placement - Nodal Magnitude

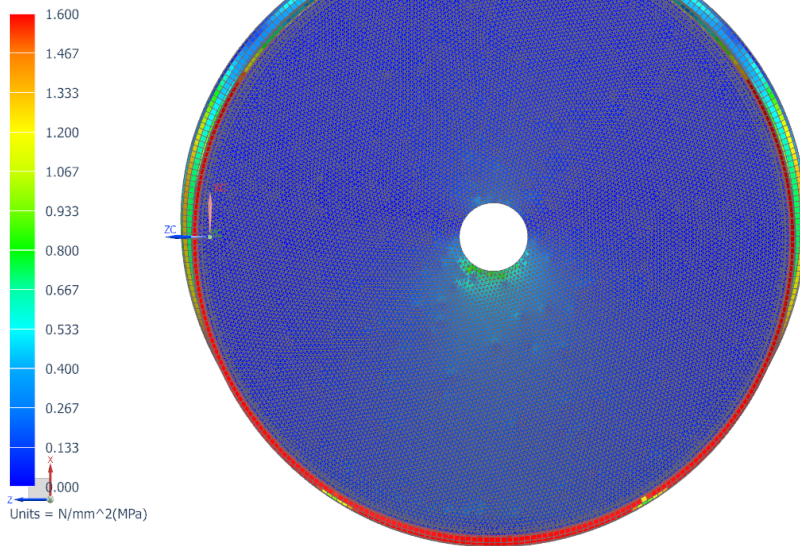


Fire lag – bedre men ikke perfekt

DiabH100:

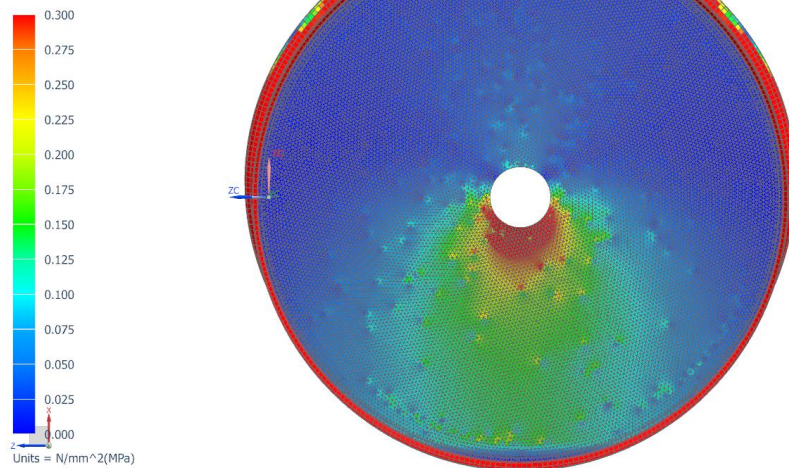
2 plies, 1.6MPa Shear

rimv2fix_sim2 : Static Center Result
Subcase - Static Loads 1, Static Step 1
Ply Stress - Elemental, Max Shear, Ply 3 Mid
Min : 0.00, Max : 19.22, Units = N/mm²(MPa)
Coord sys : Native
Deformation : Displacement - Nodal Magnitude



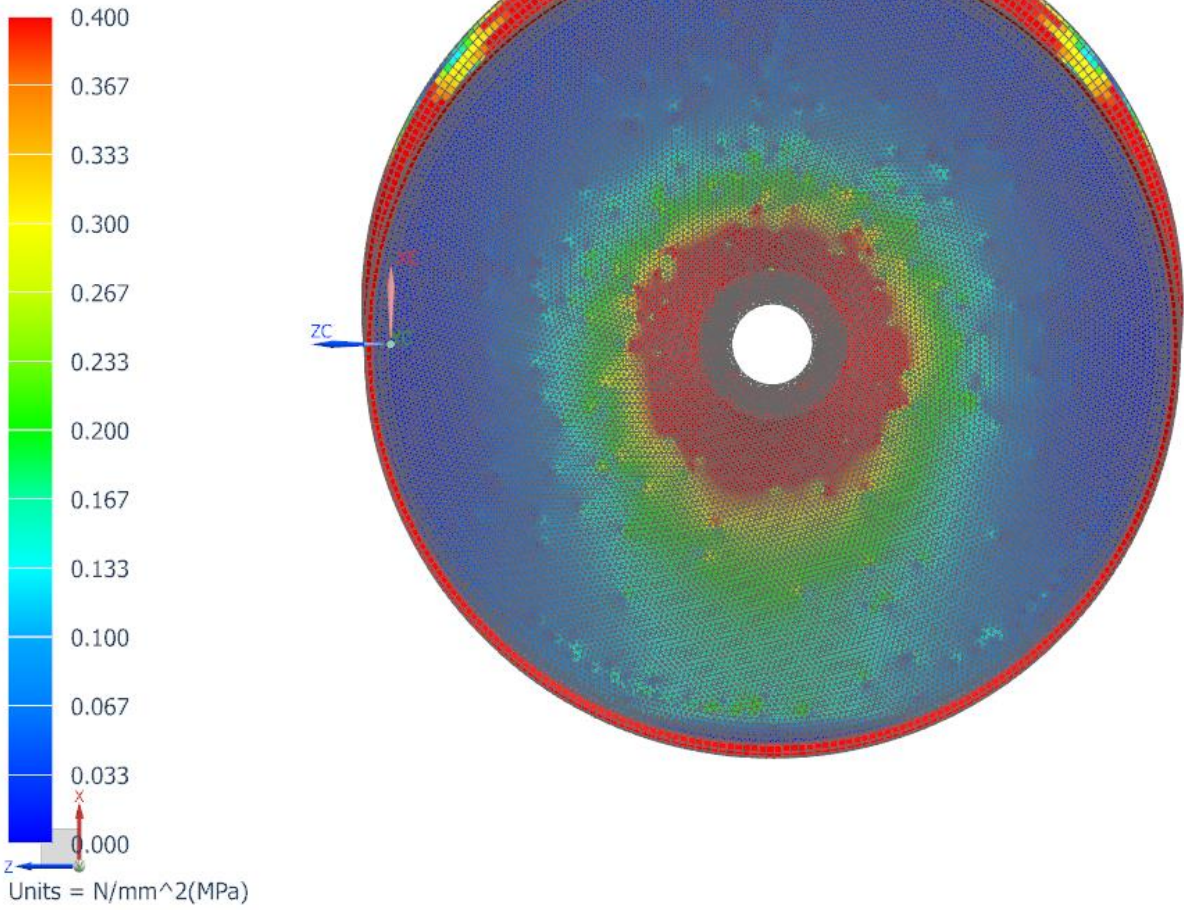
DiabH35:

rimv2rx_sim2 : Static Center Result
Subcase - Static Loads 1, Static Step 1
Ply Stress - Elemental, Max Shear, Ply 3 Mid
Min : 0.00, Max : 19.54, Units = N/mm²(MPa)
Coord sys : Native
Deformation : Displacement - Nodal Magnitude

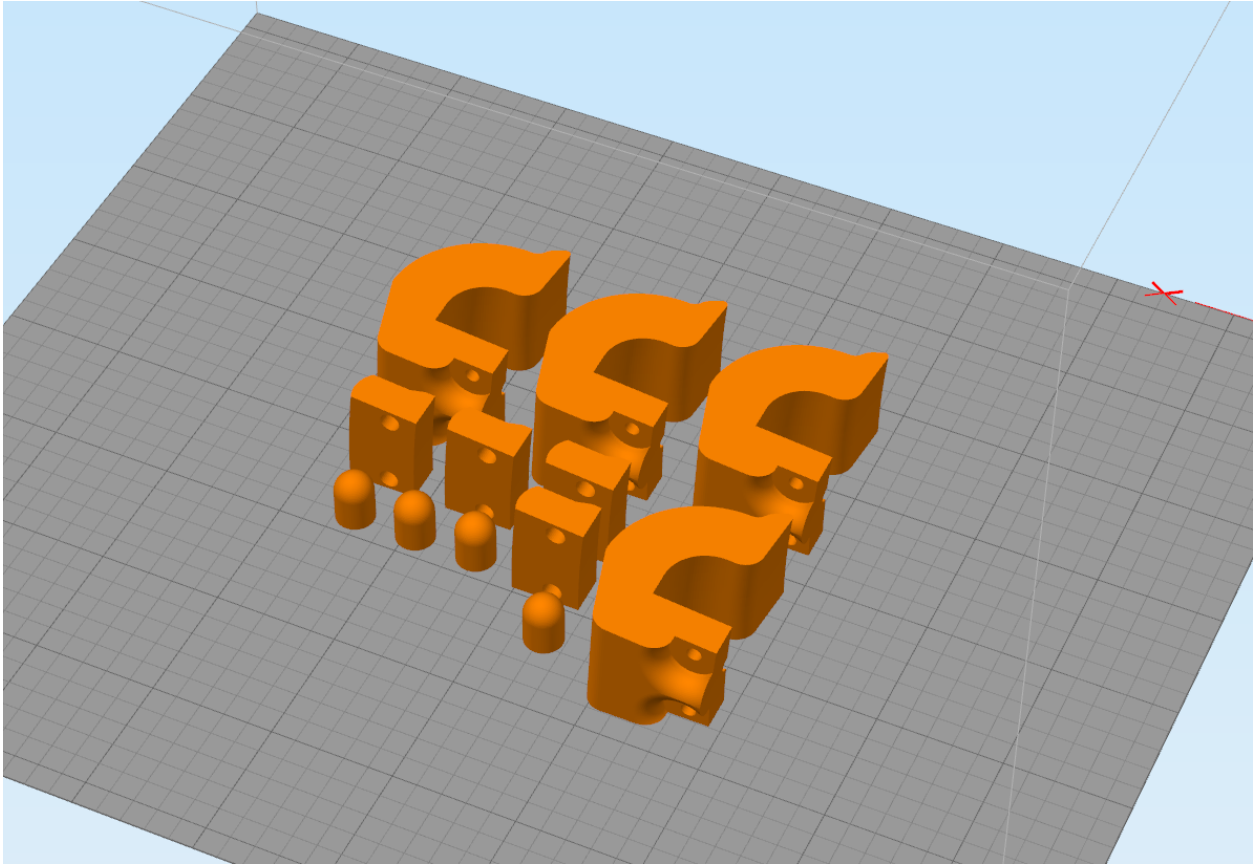


Med kjerne:

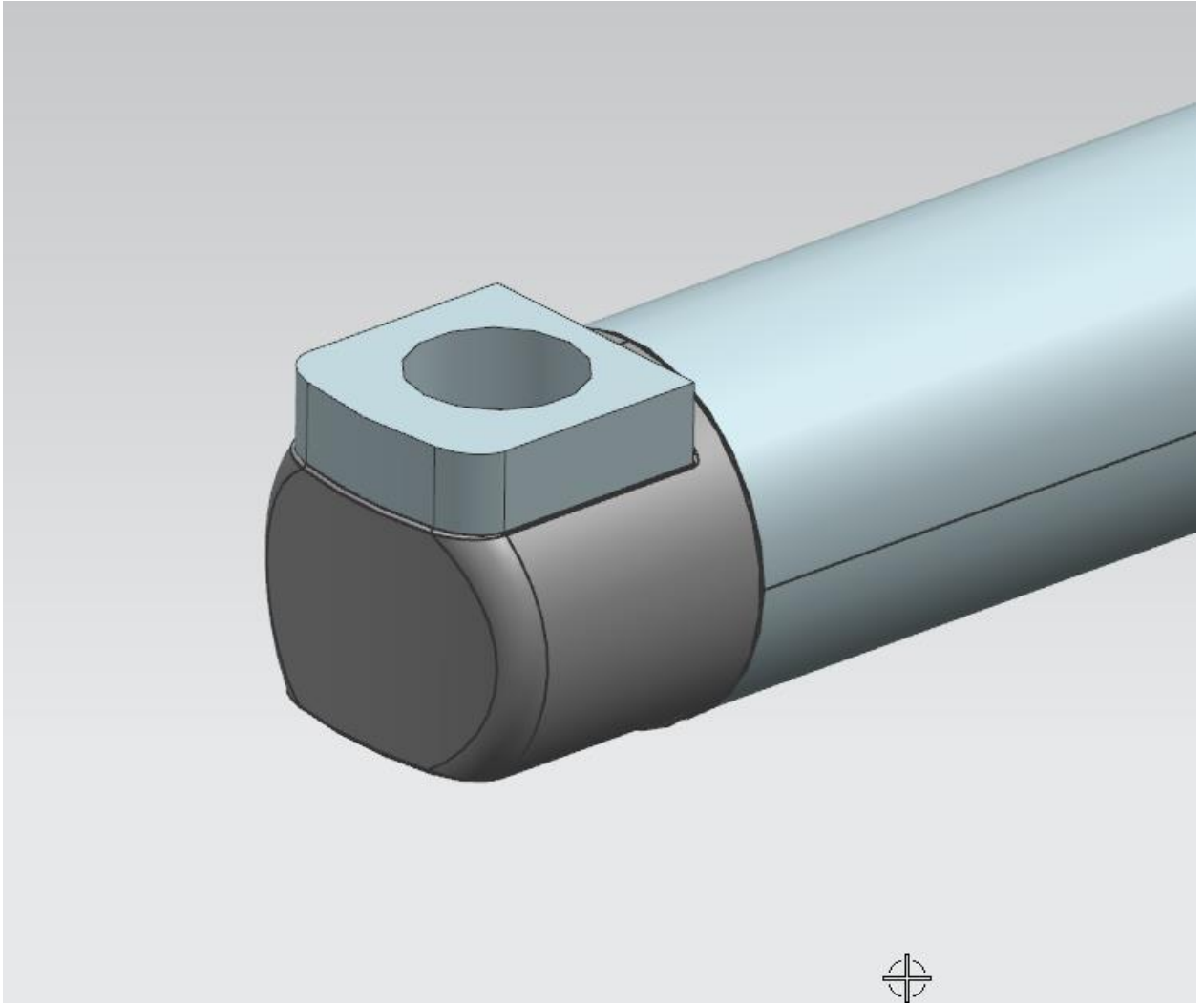
rimv2fix_sim2 : Static Center Result
Subcase - Static Loads 1, Static Step 1
Ply Stress - Elemental, Max Shear, Ply 3 Mid
Min : 0.00, Max : 19.59, Units = N/mm²(MPa)
Coord sys : Native
Deformation : Displacement - Nodal Magnitude

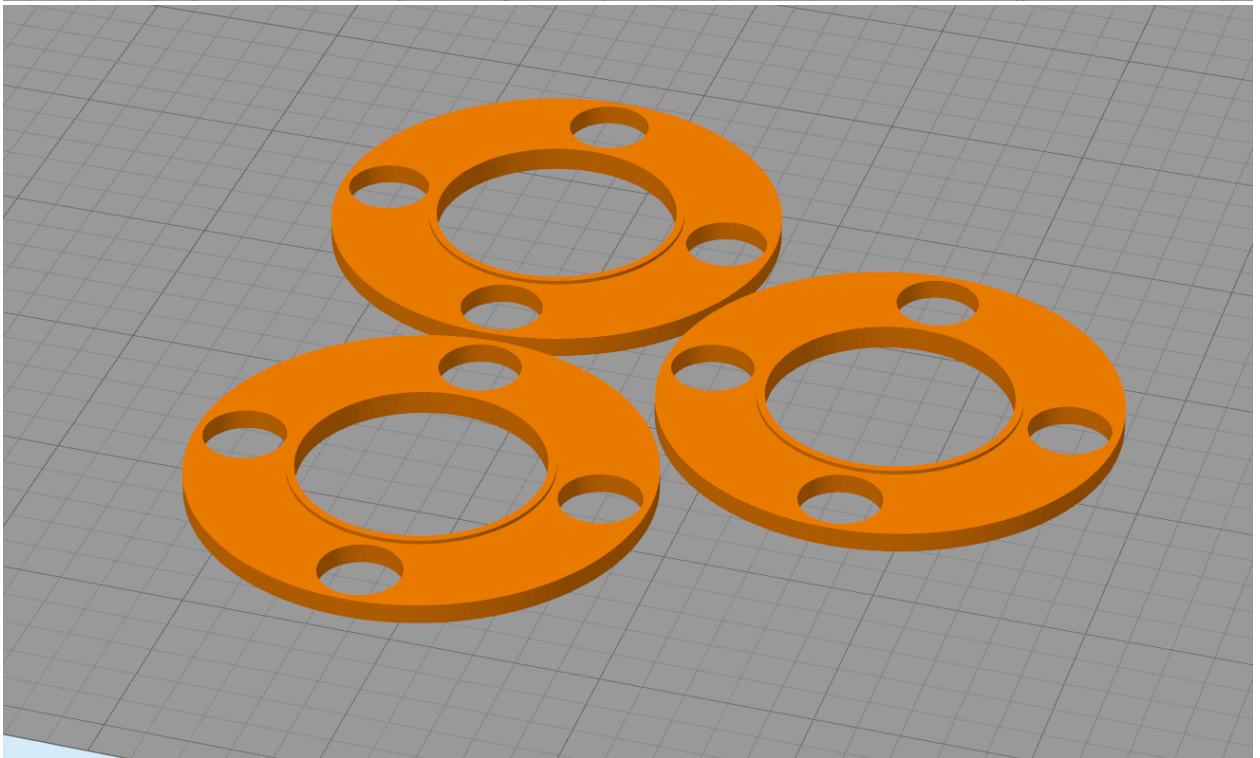
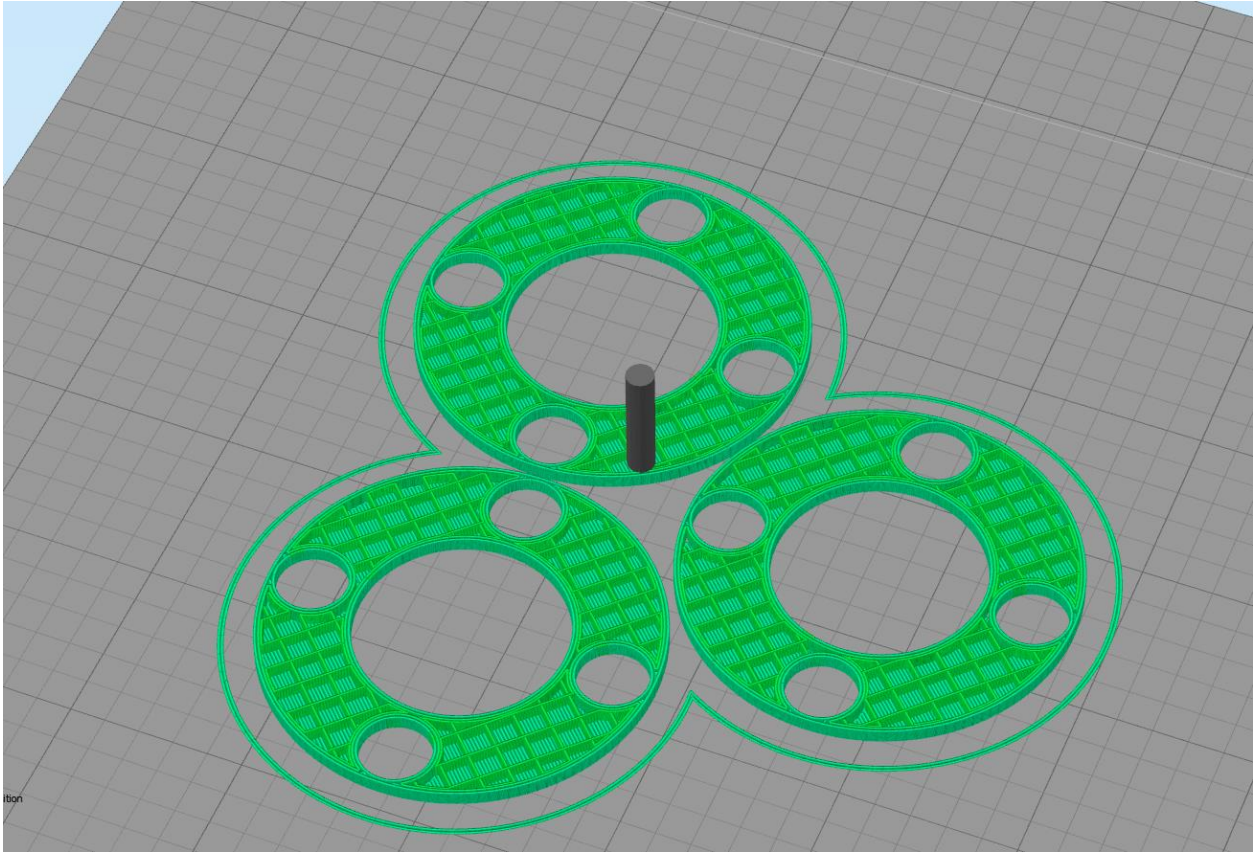


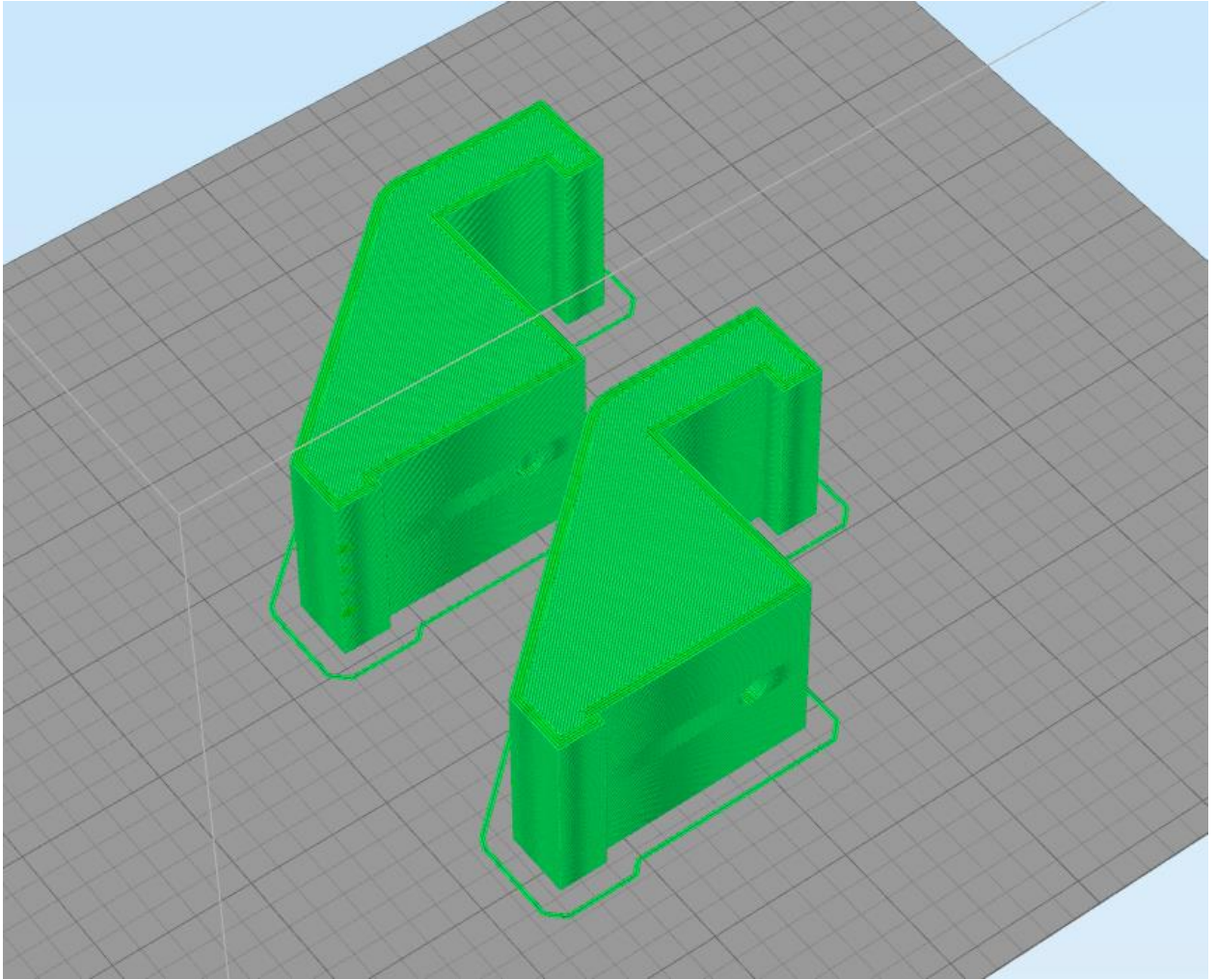
Centering tool



Actuator mount



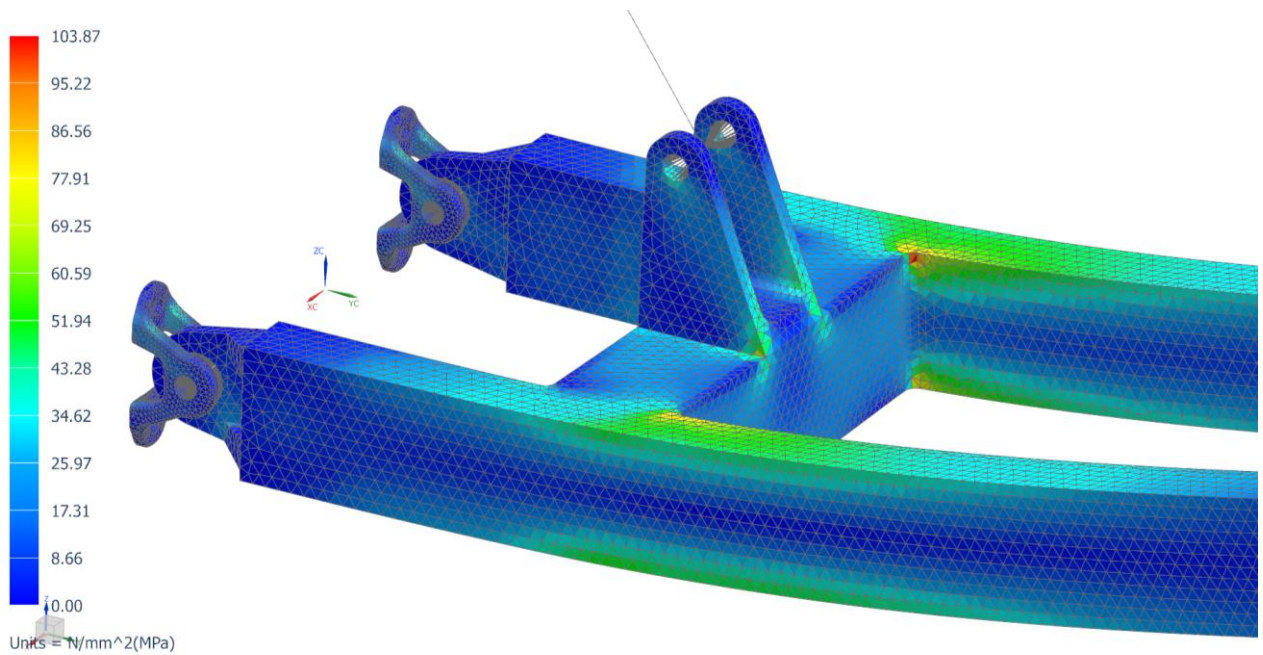
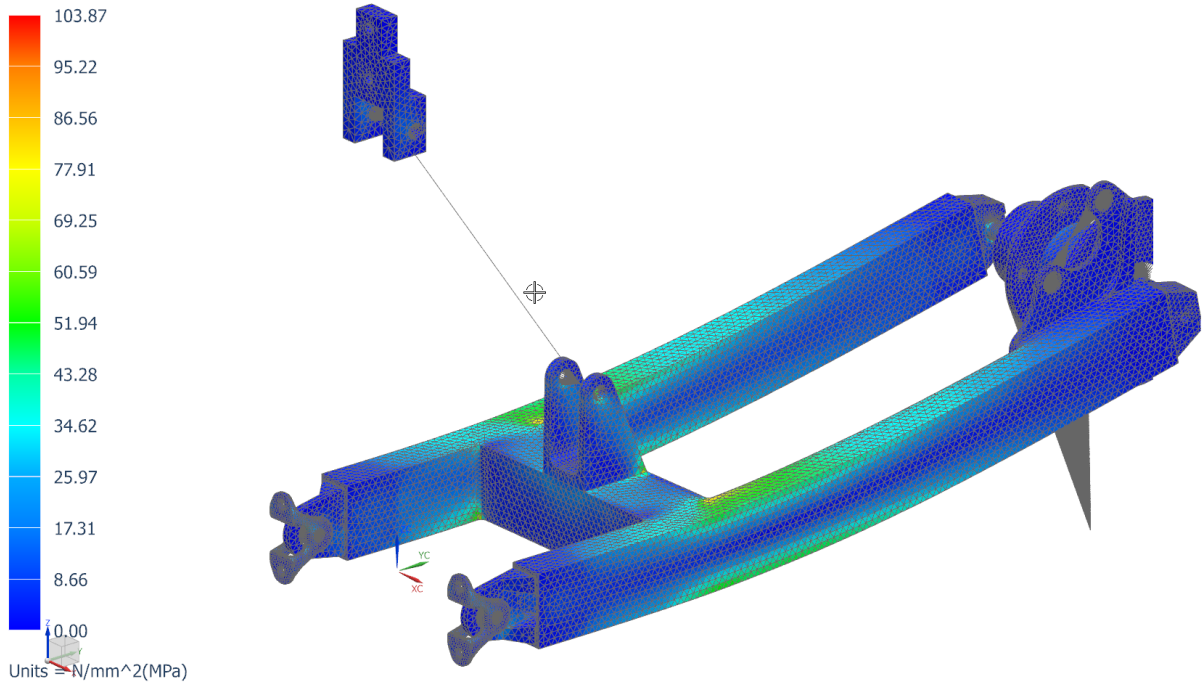


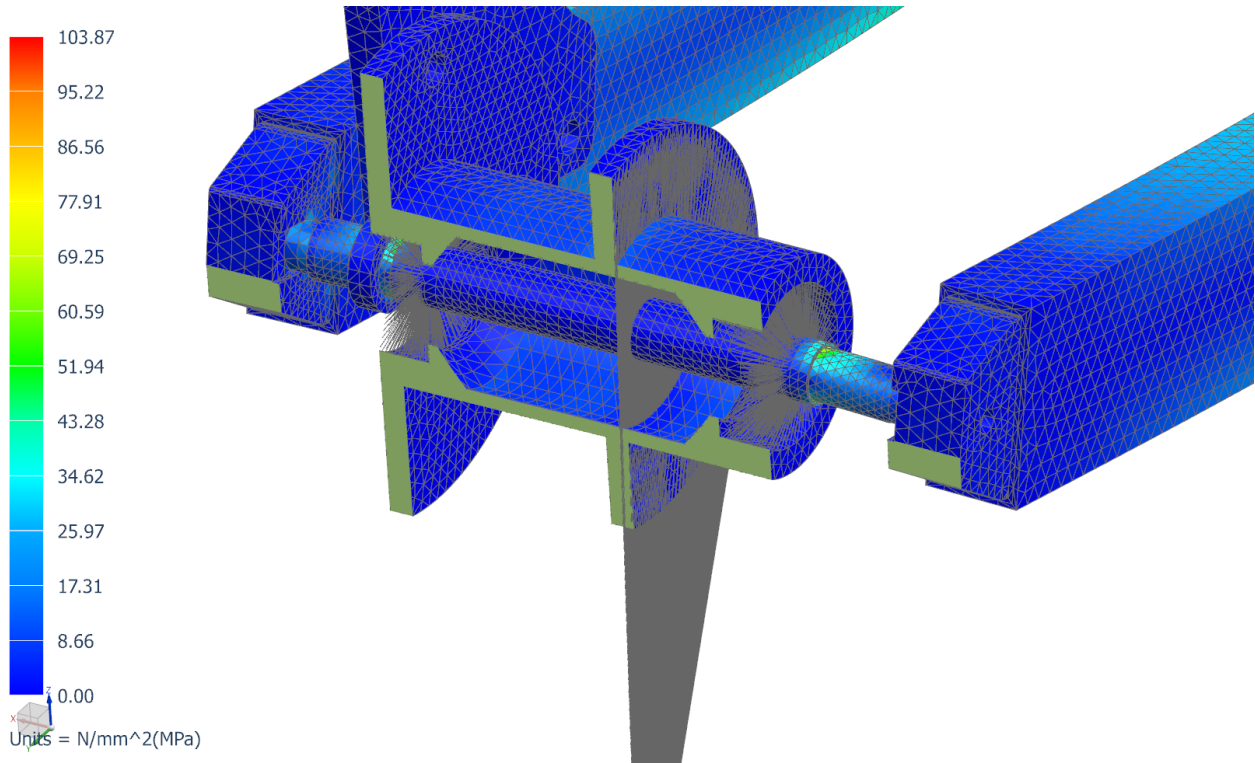


Appendix F: FEA of the Powertrain Design

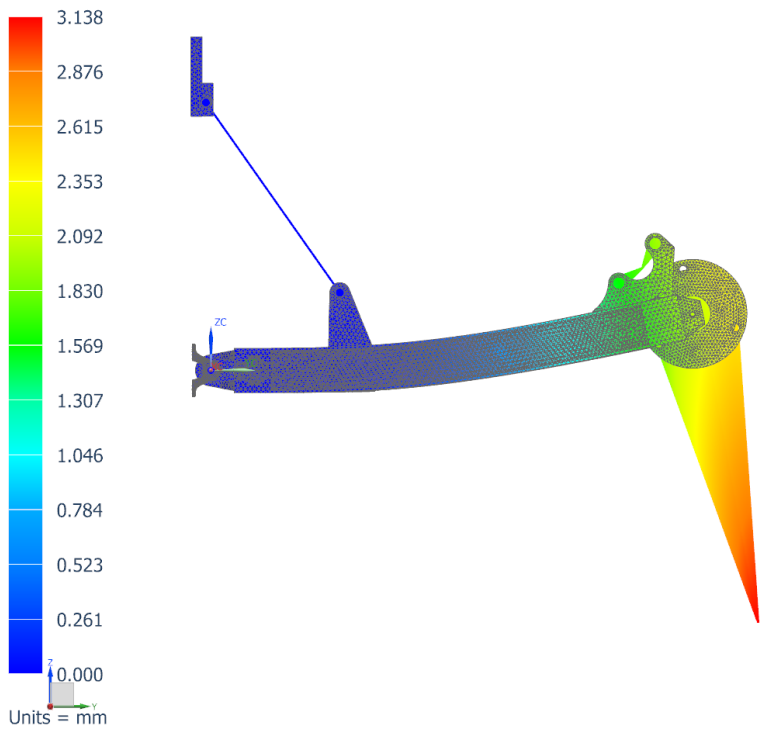
Bump force:

assam_Powertrain_v4_sim1 : Linear Result
Bump, Static Step 1
Stress - Elemental, Von-Mises
Min : 0.00, Max : 103.87, Units = N/mm²(MPa)
Deformation : Displacement - Nodal Magnitude

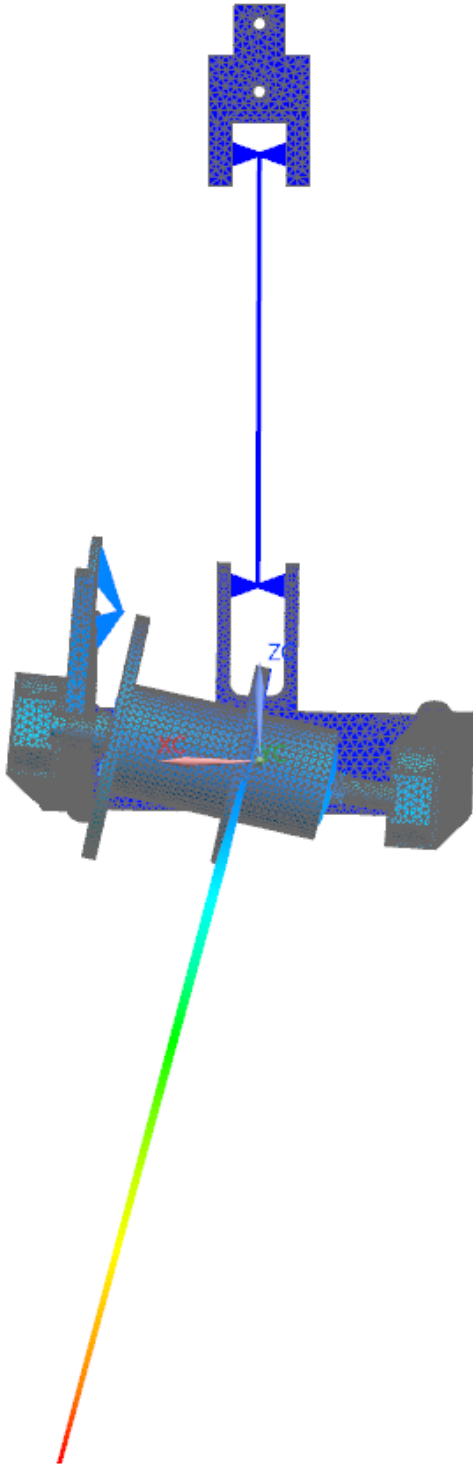
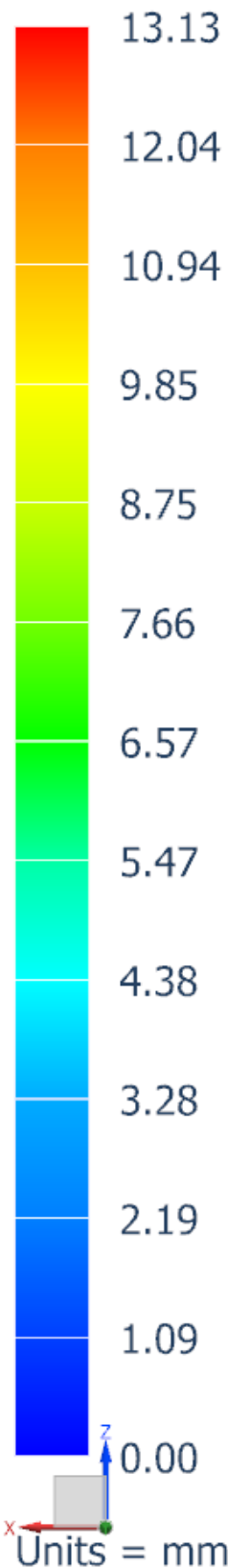




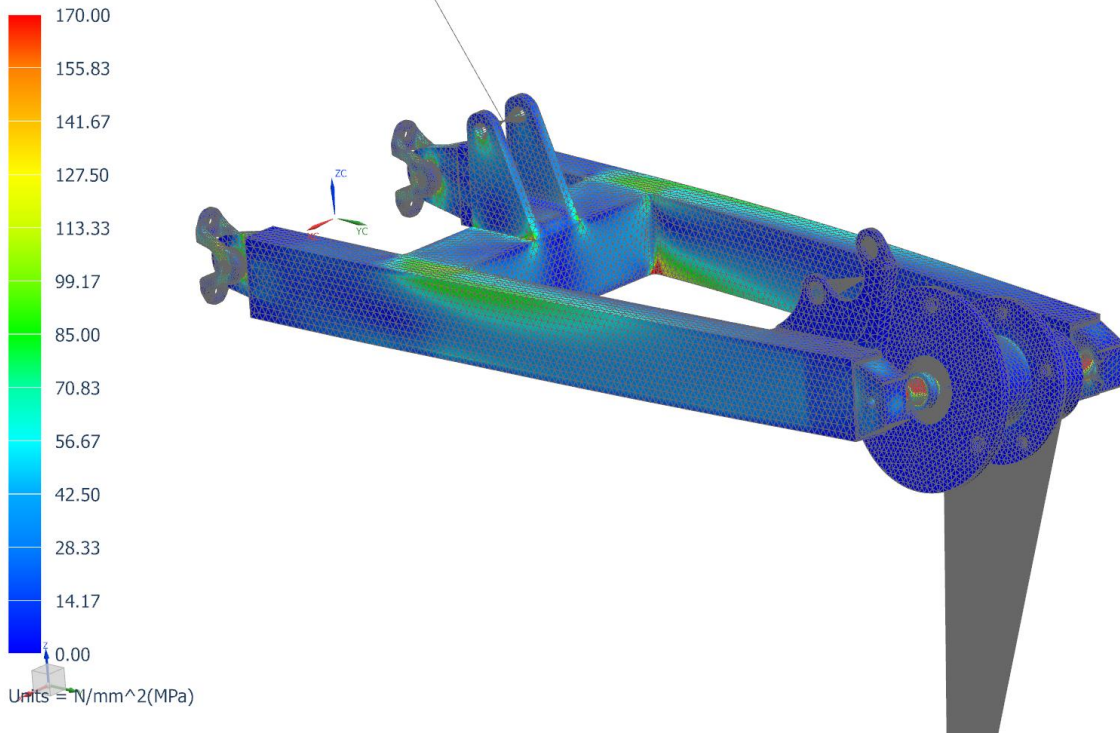
assam_Powertrain_v4_sim1 : Linear Result
Bump, Static Step 1
Displacement - Nodal, Magnitude
Min : 0.000, Max : 3.138, Units = mm
Deformation : Displacement - Nodal Magnitude



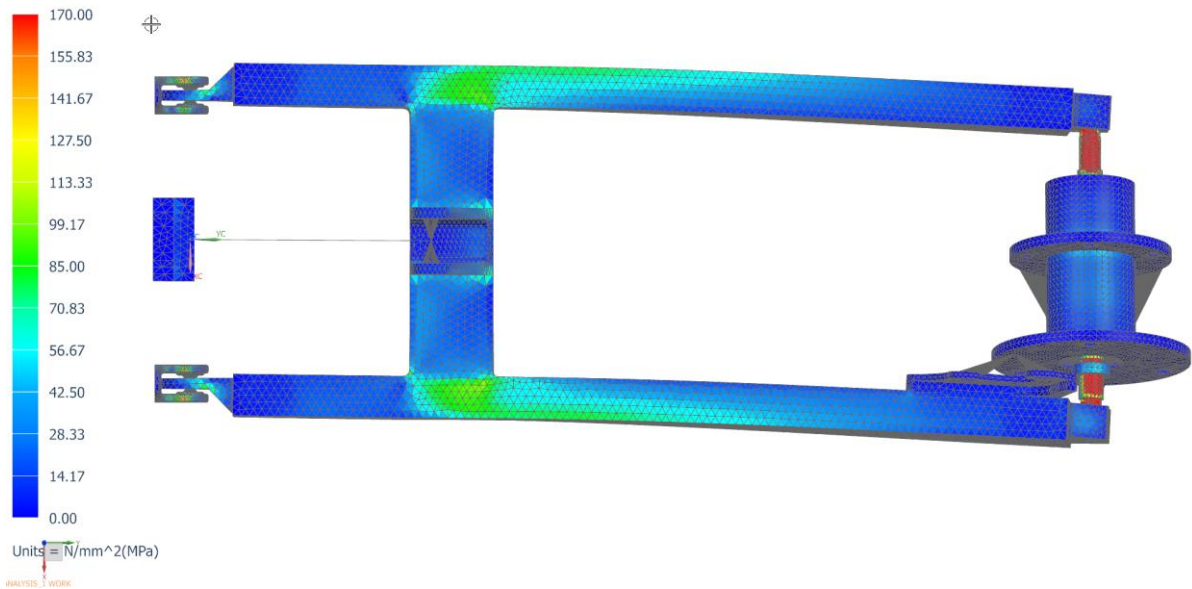
Cornering force:



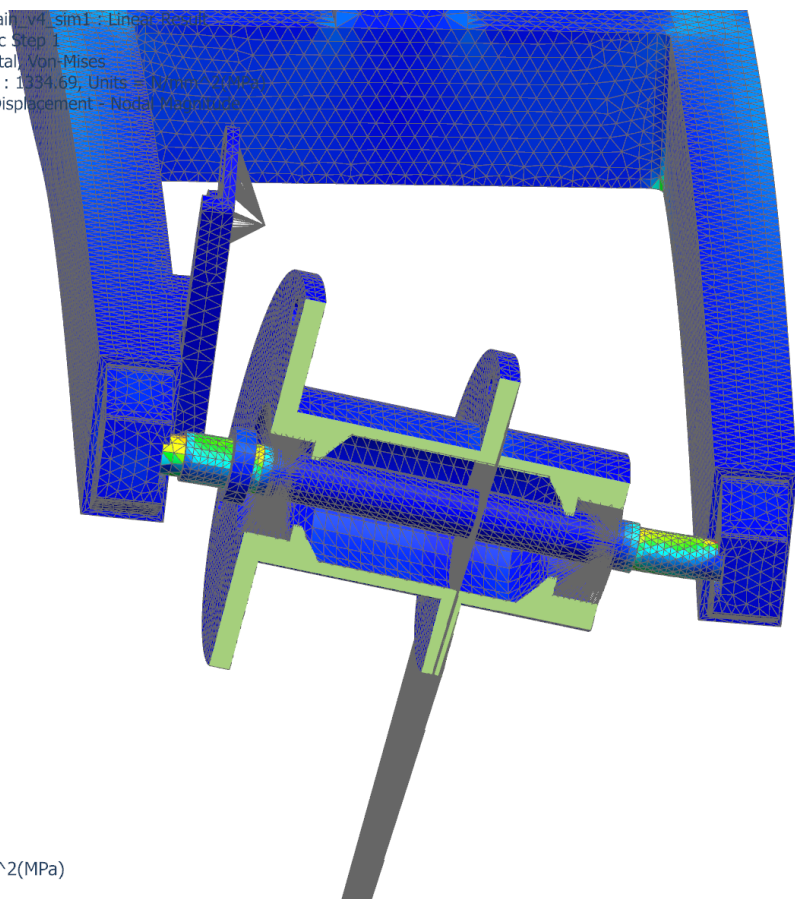
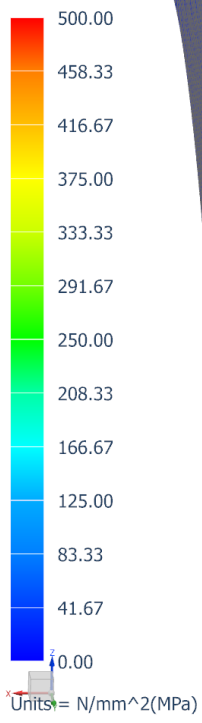
assam_Powertrain_v4_sim1 : Linear Result
Cornering, Static Step 1
Stress - Element-Nodal, Unaveraged, Von-Mises
Min : 0.00, Max : 3192.27, Units = N/mm²(MPa)
Deformation : Displacement - Nodal Magnitude



assam_Powertrain_v4_sim1 : Linear Result
Cornering, Static Step 1
Stress - Elemental, Von-Mises
Min : 0.00, Max : 1334.69, Units = N/mm²(MPa)
Deformation : Displacement - Nodal Magnitude

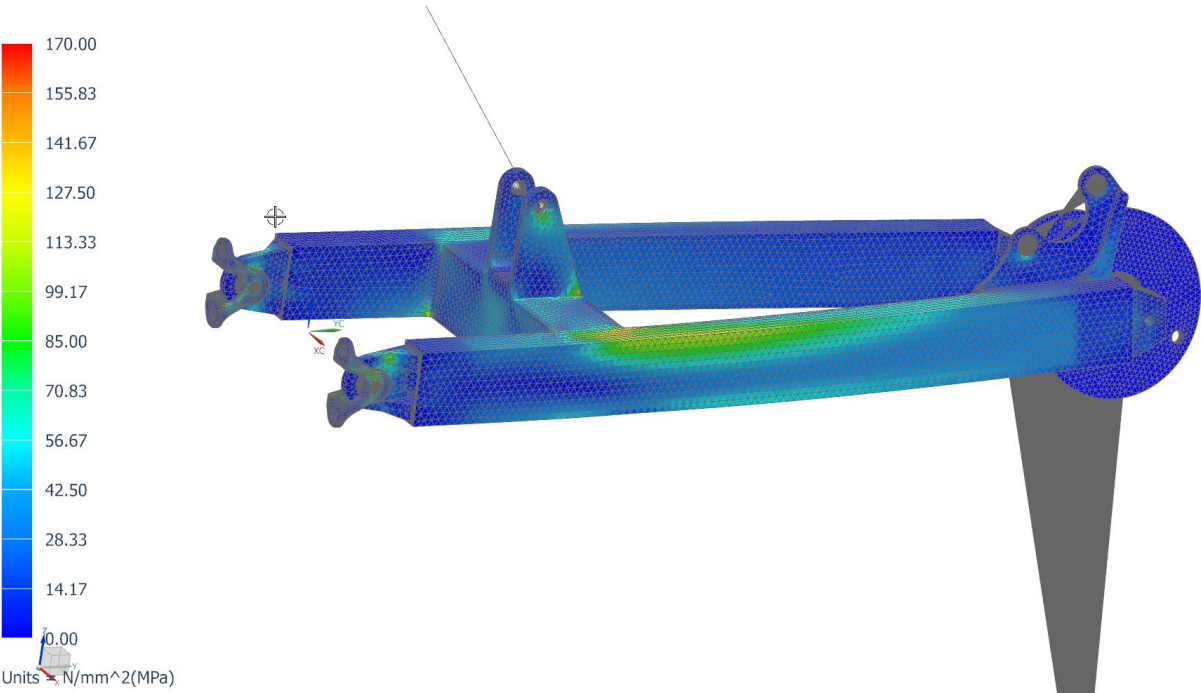
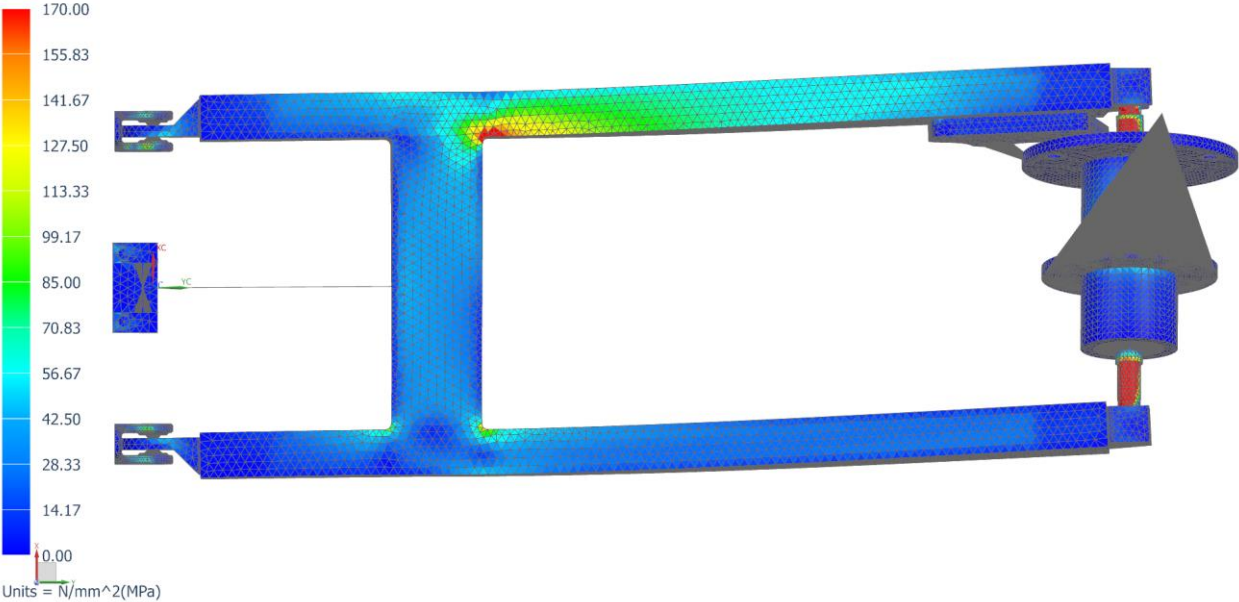


assam_Powertrain_v4_sim1 : Linear Result
Cornering, Static Step 1
Stress - Elemental, Von-Mises
Min : 0.00, Max : 1334.69, Units = N/mm^2(MPa)
Deformation : Displacement - Nodal Magnitude



Worst Case, all loads cases at once:

assam_Powertrain_v4_sim1 : Linear Result
Worst case, Static Step 1
Stress - Elemental, Von-Mises
Min : 0.00, Max : 1257.41, Units = N/mm²(MPa)
Deformation : Displacement - Nodal Magnitude



Appendix G: Gears

$$\sigma = W_t P / FY, \text{ where}$$

W_t = tangential tooth load

P = diametral pitch

F = face width of tooth

σ = bending stress in gear tooth

Y = Lewis form factor

Table 18-1 Form Factor, y

Number of Teeth	Form Factor		
	14.5°	20° Standard Tooth	20° Stub Tooth
12	0.355	0.415	0.496
14	0.399	0.468	0.540
16	0.430	0.503	0.578
18	0.458	0.522	0.603
20	0.480	0.544	0.628
22	0.496	0.559	0.648
24	0.509	0.572	0.664
26	0.522	0.588	0.678
28	0.535	0.597	0.688
30	0.540	0.606	0.698
34	0.553	0.628	0.714
38	0.565	0.651	0.729
40	0.569	0.657	0.733
50	0.588	0.694	0.757
60	0.604	0.713	0.774
75	0.613	0.735	0.792
100	0.622	0.757	0.808
150	0.635	0.779	0.830
300	0.650	0.801	0.855
Rack	0.660	0.823	0.881

Steel - Steel				Steel - Plastic			
RE50 - 48V @ 10A / (RE50 36V @14.5A)				RE50 - 48V @ 10A / (RE50 36V @14.5A)			
N teeth	15			N teeth	15		
MOD	1			MOD	1.5		
d_p	15 mm			d_p	22.5 mm		
A	10 A			A	10 A		
τ/A	0.094 Nm/A			τ/A	0.094 Nm/A		
Torque	0.94 Nm			Torque	0.94 Nm		
W_t	125.33333 N			W_t	83.555556 N		
W_{rad}	42.845682 N			W_{rad}	28.563788 N		
P	25.4			P	16.933333		
F	10 mm			F	20 mm		
Y	0.522			Y	0.522		
Max gear ratio	25			Max gear ratio	16.666667		
$\sigma_{driving}$	609.85951 Mpa			$\sigma_{driving}$	135.52434 Mpa		
σ_{driven}^*	386.81247 MPa			c_{driven}^*	85.958328 MPa		

*Assuming Y for driven (big internal and external) gears as close to rack, since huge amount of teeth

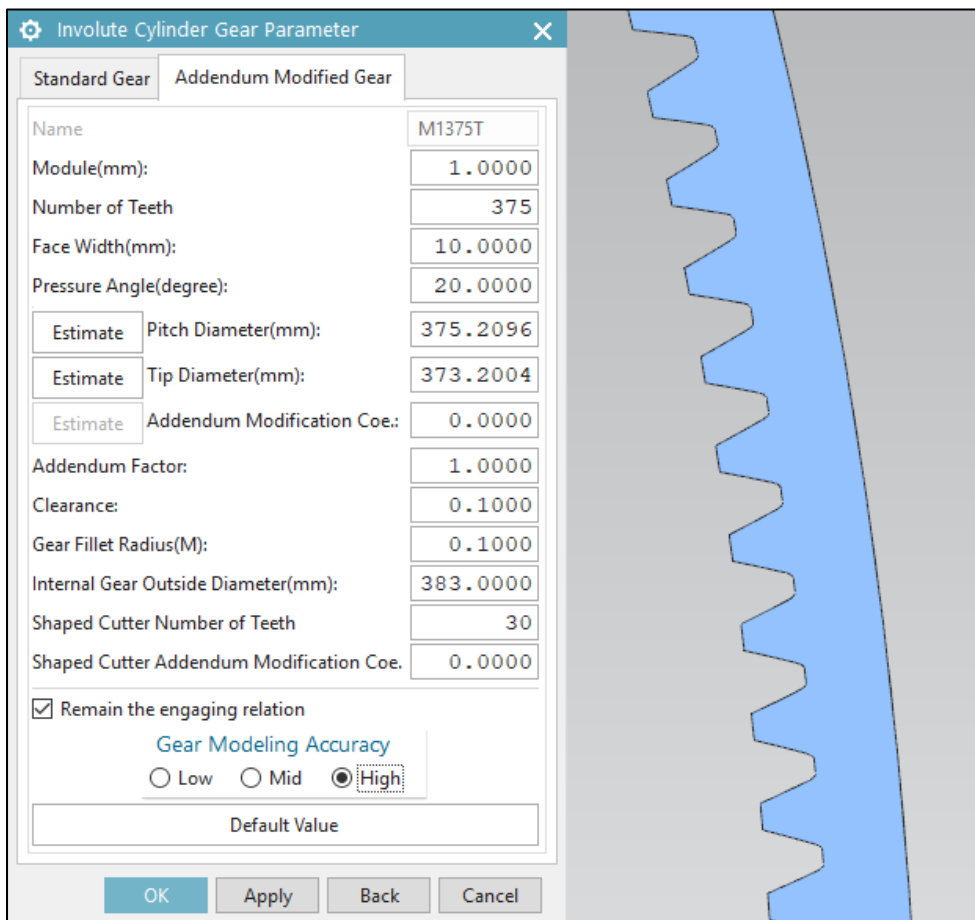
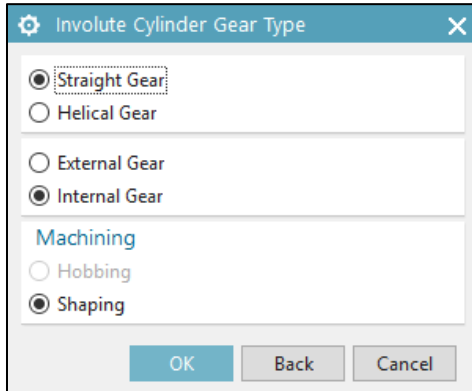
Steel - Steel			Steel - Plastic		
RE50 - 48V @ 10A / (RE50 36V @14.5A)			RE50 - 48V @ 10A / (RE50 36V @14.5A)		
N teeth	20		N teeth	15	
MOD	1		MOD	1	
d_p	20 mm		d_p	15 mm	
A	10 A		A	10 A	
τ/A	0.094 Nm/A		τ/A	0.094 Nm/A	
Torque	0.94 Nm		Torque	0.94 Nm	
W_t	94 N		W_t	125.33333 N	
W_rad	32.134262 N		W_rad	42.845682 N	
P	25.4		P	25.4	
F	10 mm		F	45 mm	
Y	0.522		Y	0.522	
Max gear ratio	18.75		Max gear ratio	25	
$\sigma_{driving}$	457.39464 Mpa		$\sigma_{driving}$	135.52434 Mpa	
σ_{driven}^*	290.10936 MPa		σ_{driven}^*	85.958328 MPa	
*Assuming Y for driven (big internal and external) gears as close to rack, since huge amount of teeth					
Steel - Steel					
RE50 - 48V @ 10A / (RE50 36V @14.5A)					
N teeth	18				
MOD	0.8				
d_p	14.4 mm				
A	10 A				
τ/A	0.094 Nm/A				
Torque	0.94 Nm				
W_t	130.55556 N				
W_rad	44.630919 N				
P	31.75				
F	15 mm				
Y	0.522				
Max gear ratio	26.041667				
$\sigma_{driving}$	529.39194 Mpa				
σ_{driven}^*	335.77472 MPa				
*Assuming Y for driven (big internal and external) gears as close to rack, since huge amount of teeth					

Gear production with GC toolkit in Siemens NX

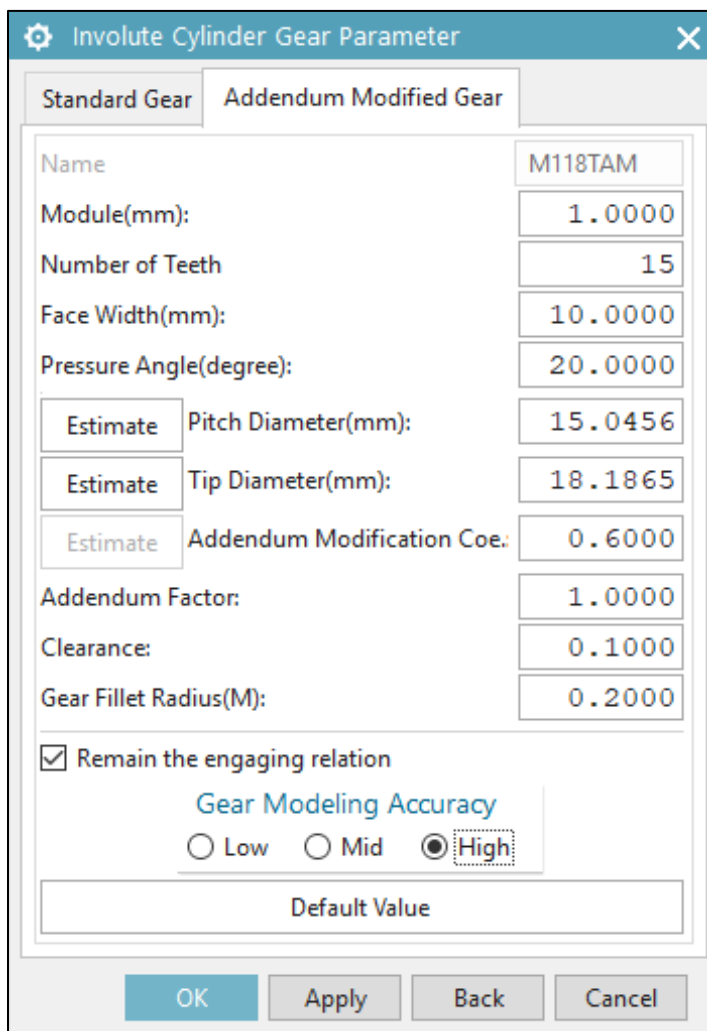
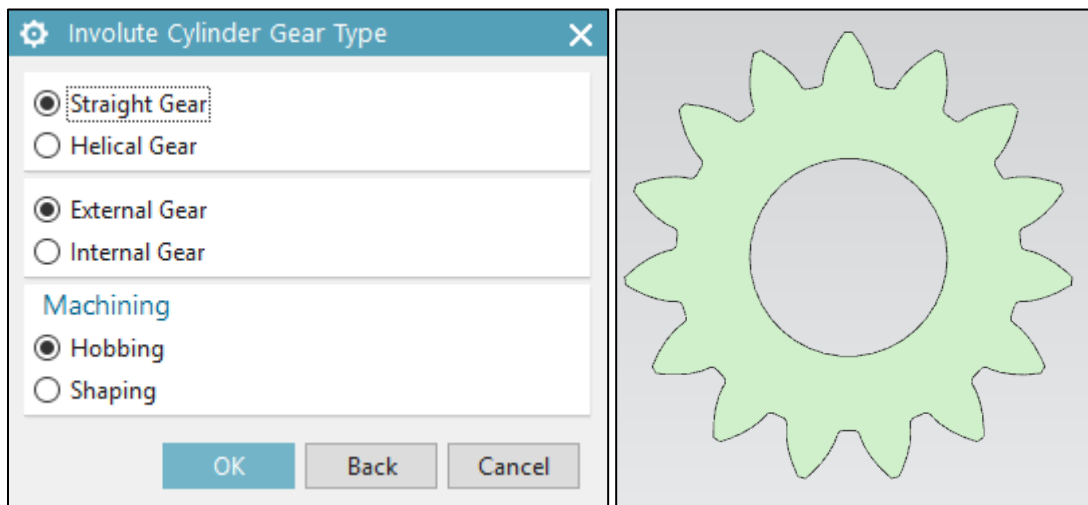
How to change registry entities into Chinese Siemens NX to add GC toolkit for gear modelling (one of few software alternatives capable of drawing such big involute gears):

<https://www.youtube.com/watch?v=yFvgOyAobNg>

Settings for 375 teeth internal module 1 spur gear:



Settings for the 15 teeth addendum modified gear



Appendix H: Old Rims Calculations

The image displays a 3D CAD model of a multi-spoke wheel rim. A coordinate system is centered at the hub, with axes labeled XC (red), YC (green), and ZC (blue). The ZC axis points towards the center of the rim, while XC and YC are tangential to the rim's circumference.

Below the model is a 'Weight Management' dialog box with the following settings:

- Calculation:** Work Part
- Selected Components:** (empty)
- Give Error Information
- Use Spreadsheet
- Accuracy Parameter:** 0.9999
- Definition:** Set Reference Set
- Current:** MODEL
- Set Component Group:** (empty)
- Current:** All Components
- Assert Values:** Work Part
- Work Part:** Selected Components
- Set and Clear Weight Limits:** (empty)

At the bottom of the dialog are 'OK', 'Back', and 'Cancel' buttons.

To the right is an 'Information' window showing the following data:

Information Units: kg - mm

Work part properties:

Weight data was calculated

Accuracy used	=	0.999900000
Density	=	0.000002810
Area	=	461242.265493490
Volume	=	861524.161980330
Mass	=	2.420882895

Center of Mass

Xcbar	=	-0.000001615
Ycbar	=	-0.018806136
Zcbar	=	-12.075284545

First Moments

Mxc	=	-0.000003910
Myc	=	-0.045527454
Mzc	=	-29.232849808

Moments of Inertia (Work)

Ixxw	=	36802.783684626
Iyyw	=	36811.449623139
Izzw	=	69606.618011514

Moments of Inertia (Centroidal)

Ixx	=	36449.787848948
Iyy	=	36458.454643657
Izz	=	69606.617155319

Moments of Inertia (Spherical)

I	=	71257.429823962
---	---	-----------------

Products of Inertia (Work)

Pyzw	=	-0.386693248
Pxzw	=	-0.000298486
Pxyw	=	0.003722843

Products of Inertia (Centroidal)

Pyz	=	-0.936450210
Pxz	=	-0.000345695
Pxy	=	0.003722770

Principal Moments of Inertia

Ixxp	=	69606.617181774
Iyyp	=	36458.454618801
Izzp	=	36449.787847349

Radii of Gyration (Work)

Rgxw	=	123.297265126
Rgyw	=	123.311780654
Rgzw	=	169.565843889

Radii of Gyration (Centroidal)

Rgx	=	122.704534297
Rgy	=	122.719121375
Rgz	=	169.565842847

Radii of Gyration (Spherical)

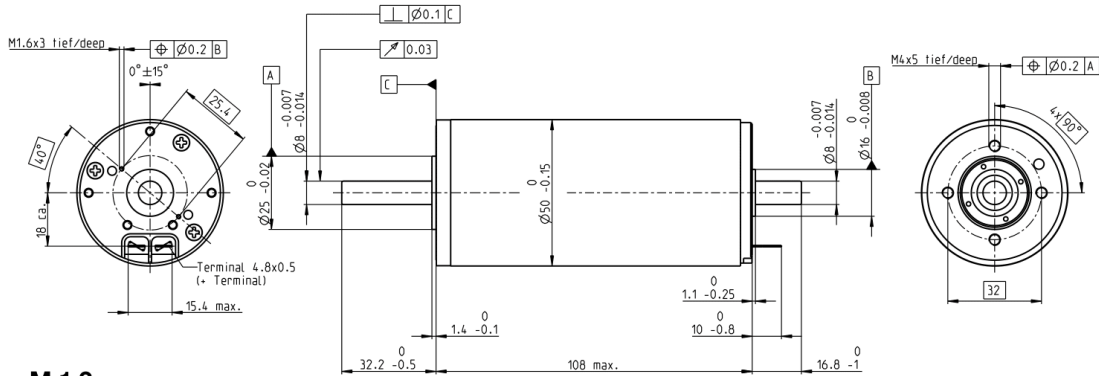
R	=	171.564799053
---	---	---------------



Measured weight:2.57 kg

Appendix I: Maxon RE50/65, Datasheet

RE 50 Ø50 mm, Graphite Brushes, 200 Watt



M 1:2

- Stock program
- Standard program
- Special program (on request)

Part Numbers

370354	370355	370356	370357
389089	389090	389091	389092

Industrial Version IP54*

Motor Data					
Values at nominal voltage					
1 Nominal voltage	V	24	36	48	70
2 No load speed	rpm	5950	5680	4900	2760
3 No load current	mA	236	147	88.4	27.4
4 Nominal speed	rpm	5680	5420	4620	2470
5 Nominal torque (max. continuous torque)	mNm	405	418	420	452
6 Nominal current (max. continuous current)	A	10.8	7.07	4.58	1.89
7 Stall torque	mNm	8920	8920	7370	4340
8 Stall current	A	232	148	78.9	17.9
9 Max. efficiency	%	94	94	94	92
Characteristics					
10 Terminal resistance	Ω	0.103	0.244	0.608	3.9
11 Terminal inductance	mH	0.072	0.177	0.423	2.83
12 Torque constant	mNm/A	38.5	60.4	93.4	242
13 Speed constant	rpm/V	248	158	102	39.5
14 Speed / torque gradient	rpm/mNm	0.668	0.638	0.666	0.638
15 Mechanical time constant	ms	3.75	3.74	3.78	3.74
16 Rotor inertia	gcm ²	536	560	542	560

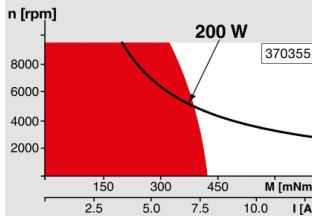
Specifications

Thermal data	
17 Thermal resistance housing-ambient	3.8 K/W
18 Thermal resistance winding-housing	1.2 K/W
19 Thermal time constant winding	71.7 s
20 Thermal time constant motor	1370 s
21 Ambient temperature	-30...+100°C
22 Max. winding temperature	+125°C
Mechanical data (preloaded ball bearings)	
23 Max. speed	9500 rpm
24 Axial play at axial load < 11.5 N	0 mm
	> 11.5 N
	0.1 mm
25 Radial play preloaded	30 N
26 Max. axial load (dynamic)	150 N
27 Max. force for press fits (static) (static, shaft supported)	6000 N
28 Max. radial load, 15 mm from flange	110 N
Other specifications	
29 Number of pole pairs	1
30 Number of commutator segments	15
31 Weight of motor	1100 g

Values listed in the table are nominal. Explanation of the figures on page 64.

* Industrial version with radial shaft seal ring (resulting in increased no load current). IP54 protection only if mounted on brush side, in compliance with maxon modular system.

Operating Range

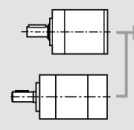


Comments

- Continuous operation**
In observation of above listed thermal resistance (lines 17 and 18) the maximum permissible winding temperature will be reached during continuous operation at 25°C ambient. = Thermal limit.
- Short term operation**
The motor may be briefly overloaded (recurring).
- Assigned power rating**

maxon Modular System

Planetary Gearhead
Ø52 mm
4 - 30 Nm
Page 350
Planetary Gearhead
Ø62 mm
8 - 50 Nm
Page 352



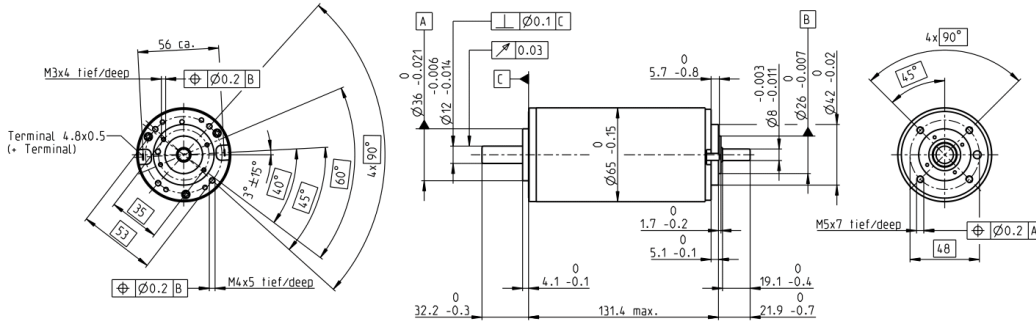
Recommended Electronics:

Notes	Page 30
ESCON Mod. 50/5	427
ESCON 50/5	428
ESCON 70/10	428
EPOS2 50/5	435
EPOS2 70/10	435
EPOS4 Module/CB 50/5	442
EPOS4 Module 50/8	443
EPOS4 Comp. 50/8 CAN	443
EPOS4 Module 50/15	444
EPOS4 Comp. 50/15 CAN	444
MAXPOS 50/5	447

Overview on page 28-36

Encoder HEDS 5540
500 CPT,
3 channels
Page 414
Encoder HEDL 5540
500 CPT,
3 channels
Page 416
Industrial Version IP54*
Encoder HEDL 9140
Page 420
Brake AB 44
Page 462
End cap
Page 463

RE 65 Ø65 mm, Graphite Brushes, 250 Watt



M 1:4

- Stock program
- Standard program
- Special program (on request)

Part Numbers

353294	353295	353296	353297	353298	353299	353300	353301
388984	388985	388986	388987	388988	388989	388990	388991

Industrial Version IP54*

Motor Data		Industrial Version IP54*							
Values at nominal voltage									
1 Nominal voltage	V	18	24	36	48	60	70	70	70
2 No load speed	rpm	3520	4090	3970	3670	3680	3440	3190	2690
3 No load current	mA	755	697	437	289	231	179	160	125
4 Nominal speed	rpm	3250	3810	3700	3420	3450	3220	2960	2470
5 Nominal torque (max. continuous torque)	mNm	427	501	751	800	813	832	839	888
6 Nominal current (max. continuous current)	A	10	10	9.32	6.8	5.53	4.51	4.21	3.74
7 Stall torque	mNm	13600	15700	17400	16100	16200	15100	13700	12200
8 Stall current	A	295	292	207	131	106	78.6	66.1	49.7
9 Max. efficiency	%	81	83	87	88	89	89	89	89
Characteristics									
10 Terminal resistance	Ω	0.0609	0.0821	0.174	0.365	0.568	0.891	1.06	1.41
11 Terminal inductance	mH	0.023	0.031	0.076	0.161	0.251	0.393	0.458	0.644
12 Torque constant	mNm/A	46	53.7	84.4	123	153	192	207	245
13 Speed constant	rpm/V	208	178	113	77.8	62.3	49.8	46.1	38.9
14 Speed / torque gradient	rpm/mNm	0.275	0.272	0.234	0.231	0.231	0.231	0.236	0.223
15 Mechanical time constant	ms	3.98	3.68	3.38	3.25	3.19	3.16	3.16	3.13
16 Rotor inertia	gcm ²	1380	1290	1380	1340	1320	1310	1280	1340

Specifications

Thermal data	
17 Thermal resistance housing-ambient	1.3 K/W
18 Thermal resistance winding-housing	1.85 K/W
19 Thermal time constant winding	123 s
20 Thermal time constant motor	1060 s
21 Ambient temperature	-30...+100°C
22 Max. winding temperature	+125°C

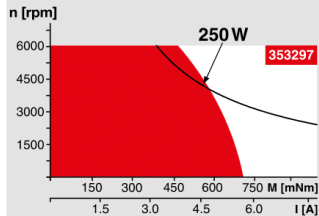
Mechanical data (preloaded ball bearings)	
23 Max. speed	5500 rpm
24 Axial play at axial load < 25 N	0 mm
24 Axial play at axial load > 25 N	0.1 mm
25 Radial play	70 N
26 Max. axial load (dynamic)	420 N
27 Max. force for press fits (static) (static, shaft supported)	12000 N
28 Max. radial load, 15 mm from flange	350 N

Other specifications	
29 Number of pole pairs	2
30 Number of commutator segments	26
31 Weight of motor	2100 g

Values listed in the table are nominal. Explanation of the figures on page 64.

* Industrial version with radial shaft seal ring (resulting in increased no load current). IP54 protection only if mounted on brush side, in compliance with maxon modular system.

Operating Range



Comments

- Continuous operation**
In observation of above listed thermal resistance (lines 17 and 18) the maximum permissible winding temperature will be reached during continuous operation at 25°C ambient. = Thermal limit.
- Short term operation**
The motor may be briefly overloaded (recurring).
- Assigned power rating**

maxon Modular System

Overview on page 28-36

Planetary Gearhead Ø81 mm 20 - 120 Nm Page 353		Encoder HEDS 5540 500 CPT, 3 channels Page 414
Recommended Electronics: Notes Page 30 ESCON Mod. 50/5 427 ESCON 50/5 428 ESCON 70/10 428 EPOS2 50/5 435 EPOS2 70/10 435 EPOS4 Module 50/8 443 EPOS4 Comp. 50/8 CAN 443 EPOS4 Module 50/15 444 EPOS4 Comp. 50/15 CAN 444 MAXPOS 50/5 447		Encoder HEDL 5540 500 CPT, 3 channels Page 416
		Industrial Version IP54* Encoder HEDL 9140 Page 420 Brake AB 44 Page 462 End cap Page 463

Appendix J: Analyze of SEM Telemetry Data

```
%gpsData.m
%author: Sivert Rød Hatletveit
%This function plots GPS data from Shells telemetry system

s= 1;          %starting measurement
e=1391;       %last measurement to consider

lat= zeros (1,1391);
lon= zeros (1,1391);
step=0;

for i = 1:1391
    lat_buf= tim_15.gps_latitude(i);
    lat(i) = str2num(lat_buf{1}(5:end-1));
    lon_buf= tim_15.gps_longitude(i);
    lon(i) = str2num(lon_buf{1}(6:end-1));
    if (tim_15Distance(i)*1000 >= step)
        text(lon(i),lat(i), sprintf('%dm',step))
        step=100+step;
    end
end
geoshow(lat,lon)
```

```
%analyzeOneLap.m
%author: Sivert Rød Hatletveit
%This function plots GPS data from Shells telemetry system

file=a4fix;

lapToAnalyze=8;

lap=1;

lapStart(1)= 1;

for d=2:height(file)
    lapOld=lap;
    lap=file.Lap(d);
    if lapOld ~= lap
        lapStart(lap)= d;
    end
end
lapStart(lap+1)= height(file);

x=(file.Time(lapStart(lapToAnalyze):lapStart(lapToAnalyze+1)) -
file.Time(lapStart(lapToAnalyze)))*3600;
yDistance=file.GPSDistancem(lapStart(lapToAnalyze):lapStart(lapToAnalyze+1)) -
file.GPSDistancem(lapStart(lapToAnalyze)) ;
yNetJoule= file.jm_netJoule(lapStart(lapToAnalyze):lapStart(lapToAnalyze+1)) -
file.jm_netJoule(lapStart(lapToAnalyze));
ySpeed=file.GPSSpeedms(lapStart(lapToAnalyze):lapStart(lapToAnalyze+1));

ylabels{1}='Distance [m]';
ylabels{2}='Energy [kJ]';
ylabels{3}='Speed [m/s]';

[ax,hlines] = plotyyy(x,yDistance,x,yNetJoule/1E3,x,ySpeed,ylabels);
```

Appendix K: Modeling and Simulation of the Car on the Track

Author: Johannes Nadler

Modelling and Simulation of the Car on the Track

Building a model of the car driving on the track and analysing it by running simulations can give worthwhile insights in how the car performs. It may be a base on finding a good driving strategy that results in lowest energy consumption. It helps to find a suitable gearing so that the motor performs most efficiently. It can be used to estimate the heat generated in the motors or the controllers. It may also be used to get an idea of how important low mass is or how important a low air drag coefficient is. The effect of hills on the track on the energy consumption can also be analysed if the height profile of the track is known.

Building the model of the car

The model of the car includes the mechanical part with all relevant forces acting on the car and the electrical description of the motors.

One of the forces acting on the car is the air drag

$$F_{air} = \frac{1}{2} \rho \cdot c_d \cdot A \cdot v^2 = C_c \cdot v^2$$

where ρ stands for the air density, c_d the drag coefficient and A the frontal area.

The rolling resistance is assumed to be a constant force and is calculated as

$$F_{roll} = \mu_r \cdot M_c \cdot g = N_c$$

where μ_r is the rolling friction coefficient, M_c is the car mass and g is the gravity.

Hill climb forces have not yet been implemented in the model.

Newton's second law states

$$F_m - F_{air} - F_{roll} = M_{c+I} \cdot \dot{v}$$

with F_m being the driving forces of the motors and M_{c+I} the mass of the car plus the equivalent mass of inertias.

The model of an electric motor has already been discussed in the document Behaviour of DC Machines under Electronics/All Parts/Motors.

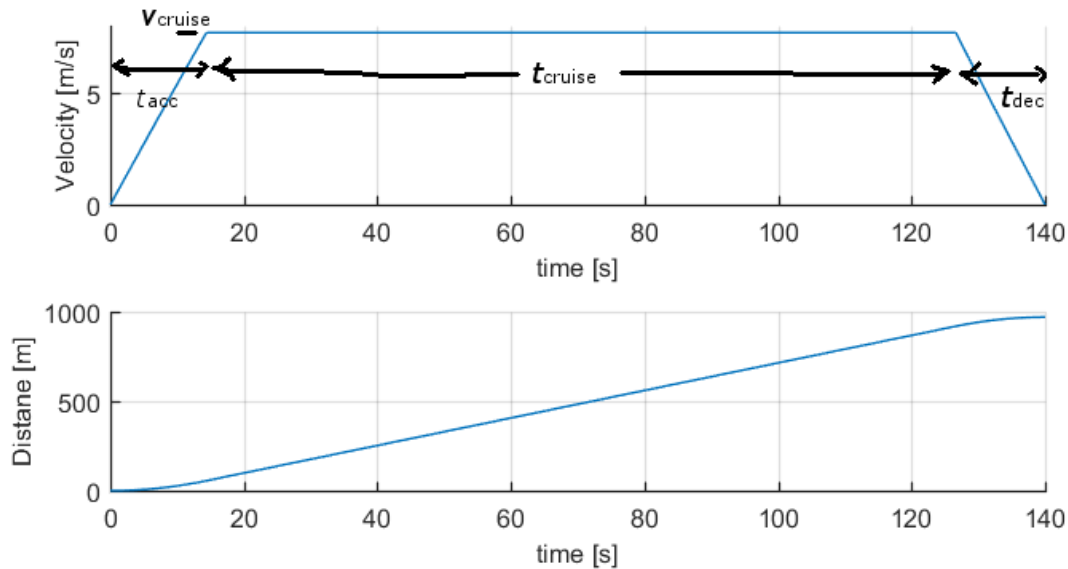
There are transformations between the linear velocity of the car and the angular velocity of the motors depending on wheel diameter and gear ratio. The same counts for the driving force F_m and the electric torque of one motor T_E where friction torque of the motor and transmission efficiency have been taken into account. See the simulink model CarModelJohannes.slx for more details.

The simulink model was built so that a driving force F_m is applied. The origin of it, which is motor torque, is calculated backwards. This makes running the simulation easier and no speed or torque control needs to be implemented.

Calculating accelerating, cruising and decelerating time intervals

The aim in this section is to derive the steps of calculating the time length of acceleration, cruising and deceleration. These values will then be passed over to the simulink model. To keep things

simple, it is assumed that there are three phases during each lap. For a time interval of t_{acc} , the motors will output a constant torque to accelerate the car up to cruising speed v_{cruise} . After that, the car keeps constant speed for a time interval of t_{cruise} . The last phase consist of the deceleration by applying a constant negative torque on the motors for a time length of t_{dec} . The figure below shows an example of the speed and the distance travelled of the car during one lap.



A lap is 970 m long. Because we need to finish 15 laps within 35 minutes, every lap takes 140 s. The car has to come to a full stop at the end of the lap.

The time intervals are calculated by solving differential equations to get the speed functions of the car with respect to time.

As given in the previous section, Newton's second law of motion applied on the car gives

$$F_m - C_c \cdot v^2 - N_c = M \cdot \dot{v} = M \cdot \frac{dv}{dt}$$

This differential equation can be solved by separation.

$$\int \frac{1}{\frac{F_m - N_c}{M} - \frac{C_c}{M} \cdot v^2} dv = \int dt = t + C_0$$

By introducing the variables $A = \frac{F_m - N_c}{M}$ and $B = -\frac{C_c}{M}$ the solution of the left integral is given in the book of formulas. Depending on the value of $A \cdot B$ it is

$$\text{i) } \int \frac{1}{A+B \cdot v^2} dv = \frac{-2}{\sqrt{-4AB}} \operatorname{artanh} \frac{2B \cdot v}{\sqrt{-4AB}} \quad \text{for } A \cdot B < 0 \text{ (Acceleration)}$$

$$\text{ii) } \int \frac{1}{A+B \cdot v^2} dv = \frac{2}{\sqrt{4AB}} \arctan \frac{2B \cdot v}{\sqrt{4AB}} \quad \text{for } A \cdot B > 0 \text{ (Deceleration)}$$

Let's consider case i) for acceleration.

$$\frac{-2}{\sqrt{-4AB}} \operatorname{artanh} \frac{2B \cdot v}{\sqrt{-4AB}} = t + C_0$$

The integral constant C_0 is found by setting in the condition for $t = 0$, which is $v(t = 0) = 0$. This leads to $C_0 = 0$. Rearranging the equation for speed gives the function we want:

$$v_{acc}(t) = \frac{\sqrt{-AB}}{-B} \cdot \tanh(\sqrt{-BA} \cdot t)$$

Integration brings us to the distance travelled since the begin of acceleration.

$$x_{acc}(t) = -\frac{1}{B} \ln(\cosh(\sqrt{-AB} \cdot t_{acc}))$$

Let's have a look at the deceleration (case ii).

$$\frac{2}{\sqrt{4AB}} \arctan \frac{2B \cdot v}{\sqrt{4AB}} = t + C_0$$

In this case, the speed at beginning of deceleration is not zero, but equal to the cruising speed $v_{dec}(t = 0) = v_{cruise}$. The integral constant is therefore

$$C_0 = -\frac{\operatorname{atan}(v_{cruise} \sqrt{B/A})}{\sqrt{AB}}$$

This yields

$$v_{dec}(t) = \frac{\sqrt{AB}}{B} \tan(\sqrt{AB} \cdot (t + C_0)).$$

Integration yields

$$x_{dec}(t) = -\frac{1}{B} \ln(\cos(\sqrt{AB} \cdot (t + C_0))) + C_1$$

The constant C_1 equals the distance travelled just before deceleration. It can be set to zero. Total distance will later be calculated by summation of the distances during acceleration, cruising and deceleration.

$$C_1 = \frac{1}{B} \ln(\cos(\sqrt{AB} \cdot C_0)) \text{ for } x_{dec}(t = 0) = 0$$

As now all necessary functions have been derived, a set of equations can be arranged to calculate t_{acc} , t_{dec} and t_{cruise} .

$$x_{acc} + y_{cruise} t_{cruise} + x_{dec} = x_{lap}$$

$$v_{cruise} = v_{acc}(t_{acc})$$

$$t_{cruise} = t_{lap} - t_{acc} - t_{dec}$$

As this set of equations is hard to solve analytically, the script AccelerationAnalysis.m solves it numerically.

Simulation results

The following parameters were used exemplarily to show the results of a simulation.

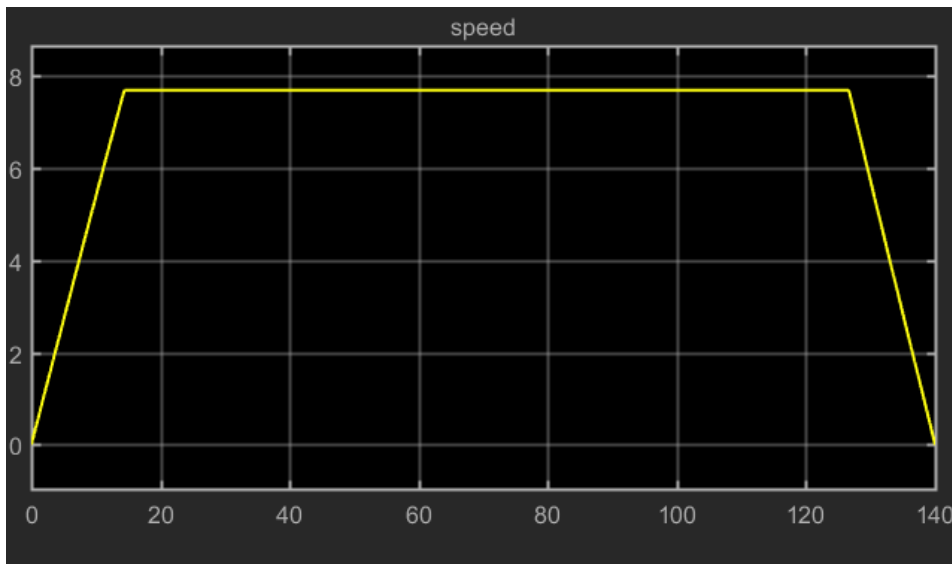
car mass including inertia = 170 kg

$c_d = 0.138$ (air drag coefficient)

$A_{\text{front}} = 0.882 \text{ m}^2$

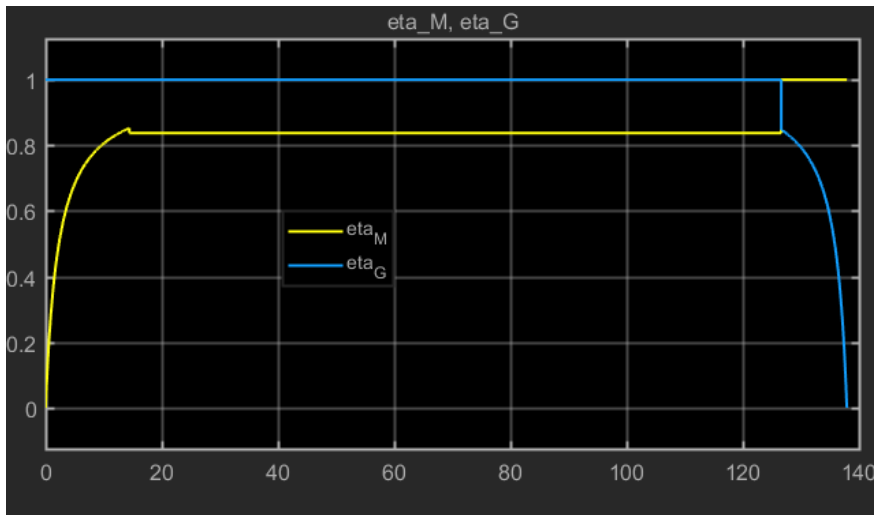
$\mu = 0.0013$ (rolling resistance coefficient)

One lap takes exactly 140 s and is 970 m long. For simplicity, the track is completely flat.



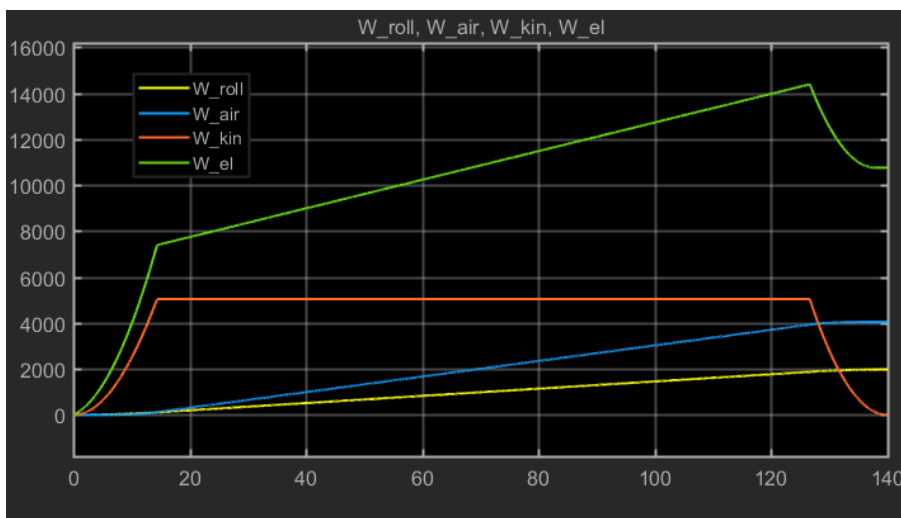
The motor applies constant torque during acceleration and deceleration. Because the corresponding force driving the car forward is much greater than the rolling and air drag forces, the Speed increases about linearly. Speed is kept constant during the cruising phase. Regenerative braking is used in the end to get some of the kinetic energy back into the battery. Fast acceleration and deceleration is preferred when it comes to decrease air drag because the cruising speed will be lower (most drag work arises during cruising at higher speed). However, fast acc and dec requires the motor to run under high load. DC motors typically have worse efficiency at high load.

The following graph shows efficiency of the motor.



Yellow represents motor efficiency. In the end of the lap, we are doing regenerative braking and the blue line represents the efficiency of it. Motors have low efficiency at low speeds. It is better to run them at higher speeds. That is why we are thinking of implementing a two-gear-transmission instead of the fixed one gear, that we have right now. The average efficiency during acceleration and deceleration is about 70%. During cruising it is higher than 80% and can be even higher if cruise control is used (motor is disengaged and engaged periodically).

The next graph shows the different kinds of works during one lap.



W_{roll} is rolling work, W_{air} is air drag work, W_{kin} is kinetic work and W_{el} is the electric input work that comes from the battery. The time derivative of these graphs would be power. W_{el} at $t = 140s$ is the total energy used which is drained from the battery. In this example, it is 10760 J. Rolling resistance is about 2000 J, air drag is about double, 4000 J.

Dissipative and conservative energy

Here is a rough calculation of how to estimate the energy needed for one lap. We will see that conservative energy like kinetic or potential energy has a different impact on energy consumption than dissipative energy.

If we had a motor and a drive train with 100% efficiency, the energy needed to drive one lap would be 6000 J, because that is the energy which is dissipated due to rolling resistance and air drag. The inefficiency of the motor makes this number go much higher though.

Let us assume an average motor efficiency of 85% during cruising. Most of the air and rolling resistance happens during cruising. Thus, the electric work to overcome these resistances is

$$E_{\text{roll_air}} = (W_{\text{roll}} + W_{\text{air}}) / 0,85 = 6000 * 1,17 = 7020 \text{ J}$$

This is still far away from the 10760 J that the simulation calculates. This is because of the motor losses during accelerating and decelerating. Lets assume an average motor efficiency of 70% during acc and dec. The kinetic energy to get up to cruising speed is 5045 J. The electric work needed to accelerate the car from the start is therefore

$$E_{\text{acc}} = E_{\text{kin}} / 0,7 = 5045 \text{ J} * 1,43 = 7214 \text{ J}.$$

Adding this to $E_{\text{roll_air}}$ gives us 14234 J. This would be the energy we need if we had no regenerative braking. But we have, so lets calculate how much energy we get back. I assume 70% efficiency for braking as well. We get the following energy back:

$$E_{\text{dec}} = -E_{\text{kin}} * 0,7 = -5045 \text{ J} * 0,7 = -3531 \text{ J}$$

We can summarise E_{acc} und E_{dec} to

$$E_{\text{acc/dec}} = E_{\text{kin}} * (1 - 0,7 * 0,7) / 0,7 = E_{\text{kin}} * 0,73 = 3682 \text{ J}$$

This means that the battery is drained by 7020 J because of drag and 3682 J because of kinetic energy. The sum of this is 10702 J, which is close to the 10760 J of the simulation.

What we see is that we actually need electric energy to speed up and slow down, but the amount of electric energy needed is just 73% of E_{kin} , while the energy needed to overcome the dissipative work is 143% of it.

Energy consumption of hill climbing

Similar considerations can be made for having hills on the track. The potential energy of climbing a hill is simply calculated as

$$E_{\text{pot}} = m * g * h$$

Going up a hill will consume around

$$E_{\text{up}} = E_{\text{pot}} / 0,7 = E_{\text{pot}} * 1,43$$

if an efficiency of 70% is assumed during the conversion of electrical energy to potential. When going down a hill, the energy regained depends on the steepness of the hill and the driving strategy. Ideally, the hill decline is just slightly so that drag and rolling forces equal the slope force and the car keeps steady speed. This way, the motors can be disengaged and all of the potential energy is used directly to overcome drag. This hill would 'cost' only $E_{\text{pot}} * 0,43$ of electric energy.

If the hill has a steep decline, there are different strategies. One could simply roll down the hill without motors engaged. This will speed up the car. All the potential energy is used directly to overcome drag and increased kinetic energy. If the car speeds up very fast, higher drag will occur. Another strategy would be to regenerate by braking down and keep steady speed. The upside of this

strategy is that drag will be lower. However, not all the potential energy can be turned back into the batteries because of limited efficiency during regen.

I guess that the best solution is to disengage the motors when rolling down a hill even if the speed is slightly increasing. The weight of the car will probably make sure that the speed does not increase by much and the hills during the race in London are not steep enough. Further simulations will follow!

Is the simulation realistic?

The simulation for one lap calculated one lap to consume 10760 J of electrical energy. This equals a specific consumption of $0,97 \text{ km}/(10760/60/60)\text{Wh} = 324 \text{ km/kWh}$. The best team 2017 (Urban concept, battery electric) won by consuming 186 km/kWh. It is highly improbable that our car will perform this well.

The simulation is very optimistic because of the following reasons:

- The track is assumed to be flat. But it is not. The potential energy to go up a small hill that is just 2 m high is $E_{\text{pot}} = m \cdot g \cdot h = (170 \cdot 9,81 \cdot 2) \text{ J} = 3335 \text{ J}$. If we roll down the hill and use regain all the potential energy, we would need around $3335 \text{ J} \cdot 0,43 = 1434 \text{ J}$.
- Air drag parameters were calculated on the computer and are probably higher in reality. During cornering, it will be higher.
- Rolling resistance was only estimated roughly $\mu = 0.0013$. I think no one knows how much it is in reality. Rolling resistance also increases during cornering.
- Motors get hot. This will increase copper resistance and the efficiency will get worse.
- Cruising at constant speed may not be possible because of corners and traffic. This means that we will reach higher peak velocities during a lap which increases air drag.
- Transmission efficiency of 95% is also just a rough guess
- Losses in the battery, wiring, motor controller were not taken into account
- all auxiliary components like dashboard, lights etc... need power and the new rules of the Shell Eco Marathon say that this power will be measured as well and contributes to the total energy needed

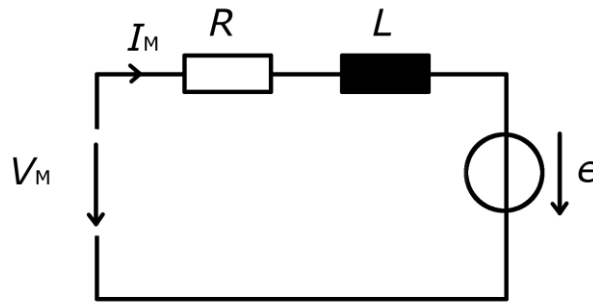
...

Appendix L: Behavior of DC Machines

Author: Johannes Nadler

The aim of this document is to present a simple model for a brushed DC motor and to derive various properties like current flow, power and voltage. The efficiency shall be illustrated in a contour plot with speed on the x-axis and output torque (or current) on the y-axis. The MATLAB script *MotorEfficiency.m* plots the results of the equations derived in this document.

The electrical equivalent circuit of a brushed DC motor is shown below.



Since we are only interested in the steady-state behavior of the motor, the inductance can be neglected. This circuit yields the equation

$$V_M = R \cdot I_M + e.$$

By multiplying this equation with motor current, the power equation of the circuit is obtained.

$$P_{el} = V_M \cdot I_M = R \cdot I_M^2 + e \cdot I_M \quad (1)$$

The back-EMF voltage e increases proportional to speed, i.e. $k_\omega e = \omega$, where k_ω is the motor speed constant in rad/(Vs) and ω is the angular velocity of the motor in rad/s.

A DC motor develops an electromagnetic torque T_E according to $T_E = k_T \cdot I_M$, where k_T is the motor torque constant in Nm/A. Both motor constants are connected to each other $k_T \cdot k_\omega = 1$.

The electromagnetic torque equals the sum of the output torque and a constant friction torque T_f .

$$T_E = T + T_f$$

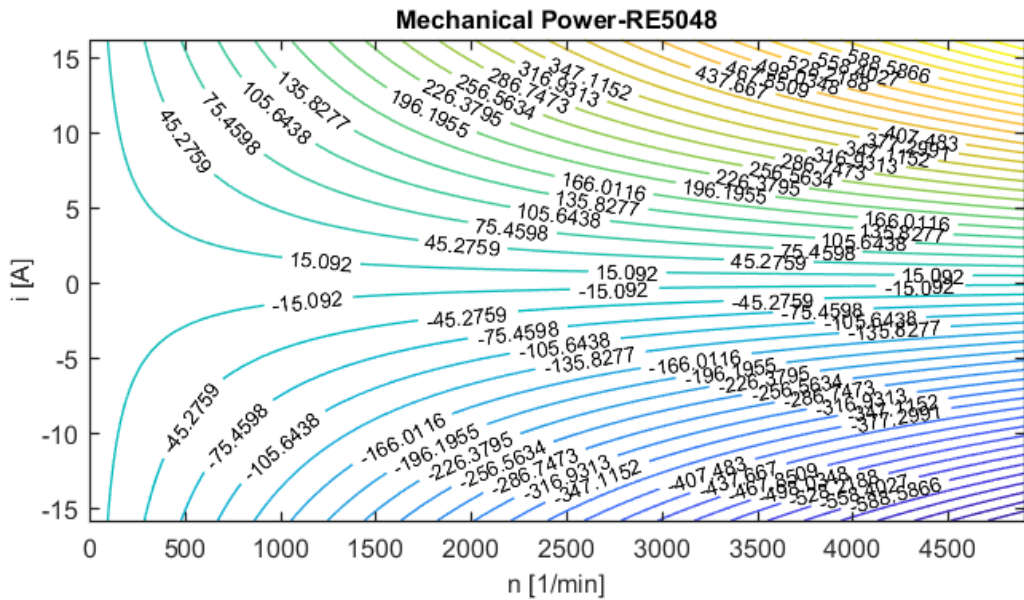
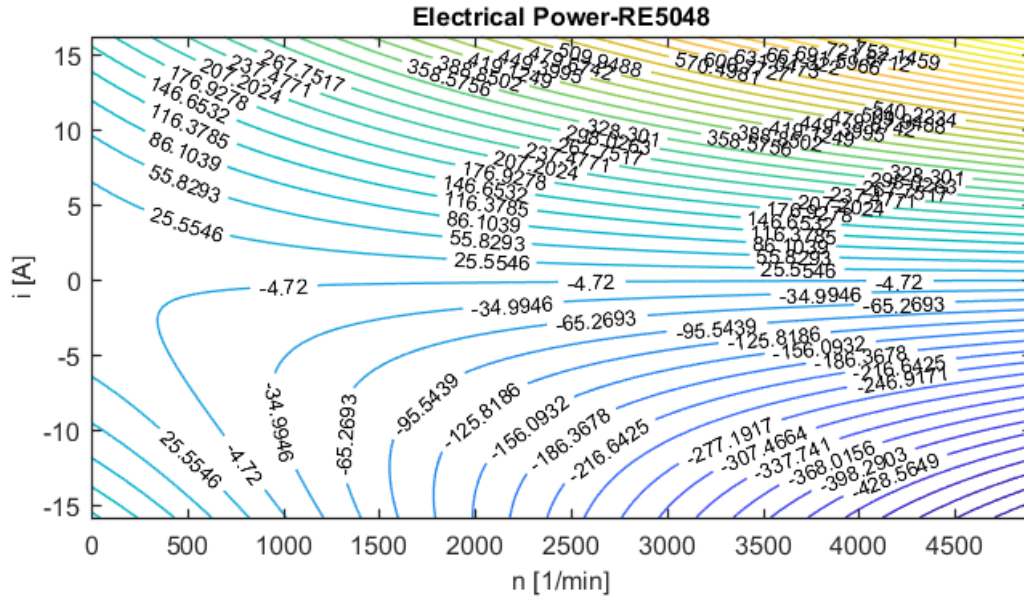
These two constitutive laws can be inserted in (1) to describe the electrical input power in terms of T and ω .

$$P_{el} = R \cdot k_\omega^2 (T + T_f)^2 + \omega \cdot (T + T_f) \quad (2)$$

The mechanical output power equals

$$P_{mech} = T \cdot \omega \quad (3)$$

The MATLAB script *MotorEfficiency.m* plots the electrical power P_{el} and mechanical output power P_{mech} shown below.



The efficiency during motor operation can now be derived in terms of T and ω using (2) and (3).

$$\eta_M = \frac{P_{mech}}{P_{el}} = \frac{T \cdot \omega}{R \cdot k_{\omega}^2 (T + T_f)^2 + \omega \cdot (T + T_f)} \quad (4)$$

The efficiency during operation as a generator is defined as the reciprocal value, i.e.

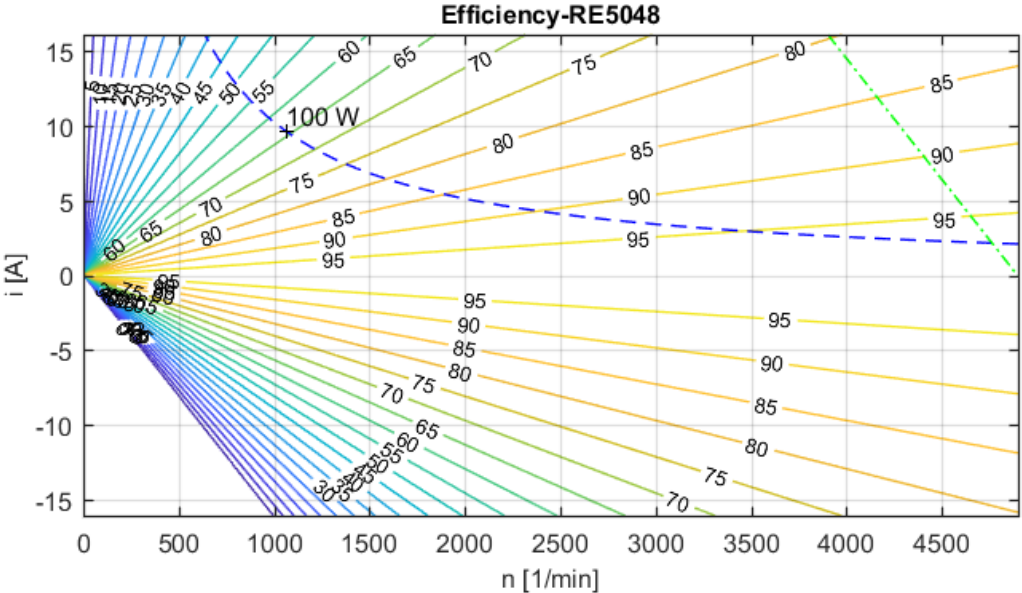
$$\eta_G = \frac{P_{el}}{P_{mech}} = \frac{R \cdot k_{\omega}^2 (T + T_f)^2 + \omega \cdot (T + T_f)}{T \cdot \omega} \quad (5)$$

When generating electric power, a reverse current $I_M < 0$ must flow while still applying positive voltage V_M . To meet these conditions, V_M must lie between zero and e .

The efficiency equation allows easier interpretation if the friction torque is neglected (5).

$$\eta_M = \frac{P_{mech}}{P_{el}} = \frac{T \cdot \omega}{R \cdot k_{\omega}^2 T^2 + \omega \cdot T} = \frac{1}{R \cdot k_{\omega}^2 \frac{T}{\omega} + 1} \quad (5)$$

Equation (5) leads to the conclusion, that the efficiency of the motor increases with speed and decreases with torque. MATLAB is used to get an efficiency plot using equation (4) and (5) without friction ($T_f = 0$). The RE50 motor rated for 48V serves as an example. The first quadrant shows motor efficiency, the second quadrant displays generator efficiency.



In this graph, the torque on the y-axis has been substituted for motor current.

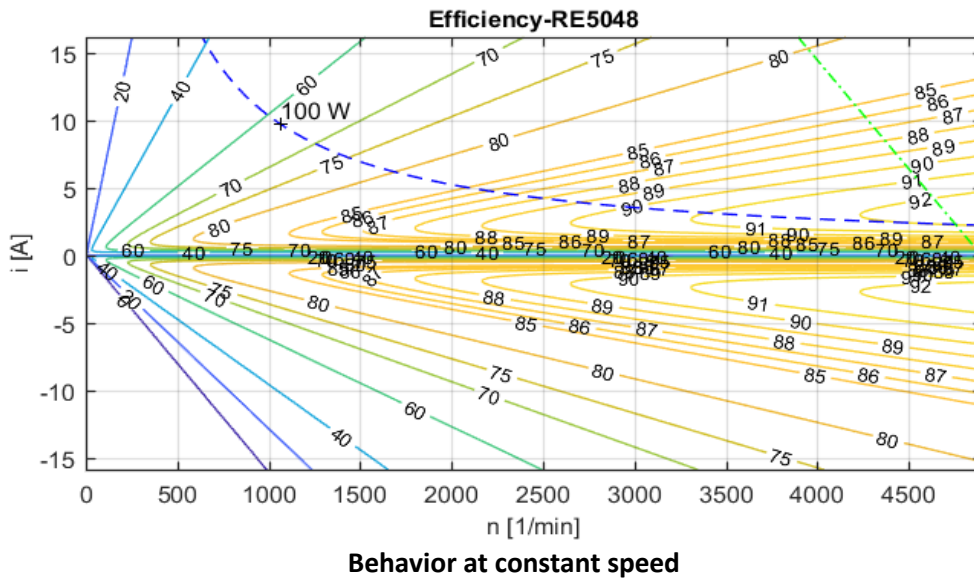
$$I_M = (T + T_f) \cdot k_\omega$$

This graph shows that efficiency goes up to 100% if no torque (or current) is applied and decreases as the load increases. Higher speed increases efficiency. The green line indicates the operation of the motor if 48 V are applied. Operation above this line is only possible if the battery voltage is higher than this. In generator mode, the efficiency drops to zero if zero voltage is applied to the motor. Negative voltage may be applied, but this will make the machine operate as a motor in reverse, as both I_M and V_M are negative.

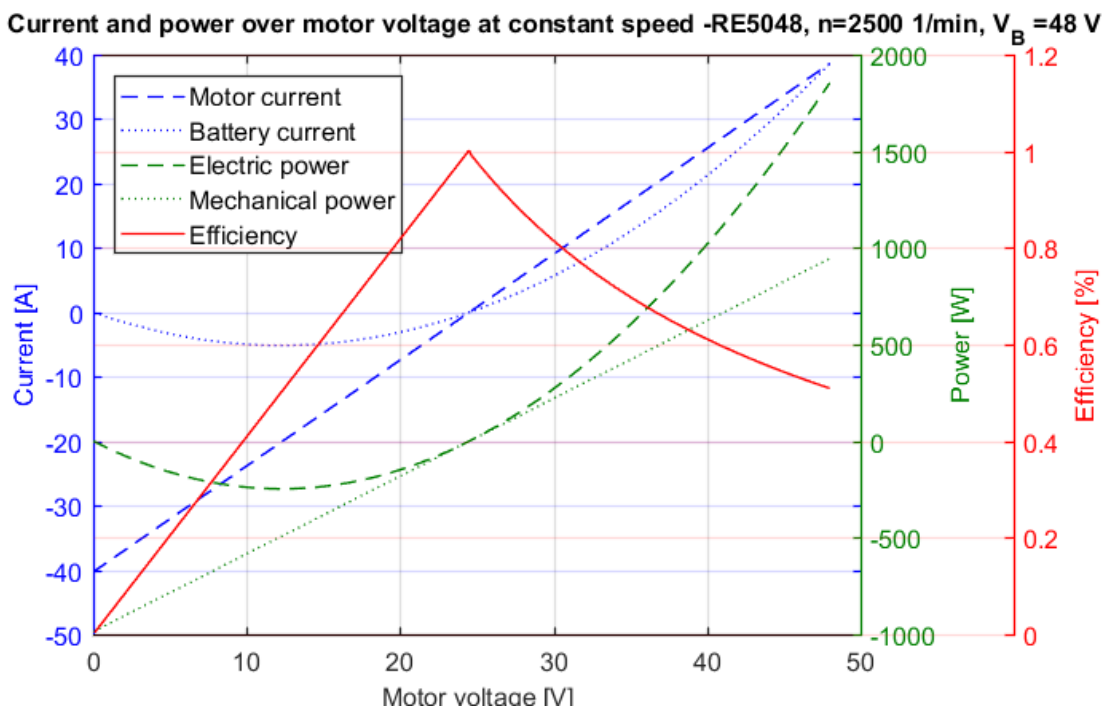
The efficiency map changes, when friction torque is introduced. Friction torque can be estimated by knowing the no-load current of the machine.

$$T_f \approx I_0 \cdot k_T$$

A constant friction torque results in a friction loss $P_f = T_f \cdot \omega$, which decreases efficiency at low loads. At higher loads, the friction loss is small compared to the output power and has less effect on efficiency.



The behavior of the motor at a constant speed shall be further discussed in this section. The graph below illustrates this behavior and shows applied motor voltage on the x-axis. The RE50 is used and spins at 2500 rpm. The battery voltage is set to 48V. Friction losses are neglected.



A constant speed generates a constant back-EMF e . If the applied motor voltage is higher than this, a positive current will flow, which increases linearly with motor voltage according to $I_M = (V_M - e)/R$. This produces a positive torque so that the machine operates as a motor. The mechanical power increases linearly according to $P_{mech} = e \cdot I_M$.

The battery current equals $I_B = I_M \frac{V_M}{V_B}$ and is a second order polynomial function of V_M after I_M has been substituted for $I_M = (V_M - e)/R$. The electrical power has the same shape as I_B because of $P_{el} = V_B \cdot I_B$. The electrical power which is gained in generating mode has its peak value at $V_M = e/2$. Efficiency drops linearly as motor voltage is decreased (and motor current increases).

Appendix M: Motor Efficiency Maxon RE50/RE65

```

%% motorEfficiency.m
Author: Johannes Nadler
t = -1.5:.005:1.5; % Torque range in [Nm]. Both positive and negative values allowed
rpm = 0:5:4900; % Speed range in [1/min]. Only positive values allowed
Motor = 'RE5048'; % Type of motor to analyse
V_B = 48; % Battery Voltage [V]
%% Motor constants

switch(Motor)
case 'RE5048'
    k_n = 102; % Speed constant [rpm/V]
    k_T = 0.0934; % Torque constant [Nm/A]
    R = 0.608;
    I_0 = 0.119; % No load current; used for calculating friction torque
case 'RE5070'
    k_n = 39.5; % Speed constant [rpm/V]
    k_T = 0.242; % Torque constant [Nm/A]
    R = 3.9;
    I_0 = 0.0274; % No load current; used for calculating friction torque
case 'RE5036'
    k_n = 158; % Speed constant [rpm/V]
    k_T = 0.0604; % Torque constant [Nm/A]
    R = .244;
    I_0 = 0.195; % No load current; used for calculating friction torque
case 'RE6548'
    k_n = 77.8; % Speed constant [rpm/V]
    k_T = 0.123; % Torque constant [Nm/A]
    R = .365;
    I_0 = 0.289; % No load current; used for calculating friction torque
End

%% Calculations
w = rpm*2*pi/60;
[T,W] = meshgrid(t,w);
k_w = k_n/60*2*pi; % convert k_n to k_w[rad/s/V]
T_f = I_0*k_T; % Friction torque [Nm], which is assumed to be constant over speed
P_m = W.*T; % Mechanical output power [W]
I = (T+T_f)/k_T; % Motor current [A]
P_e = R*I.*I+W*k_T.*I; % Electrical power [W]

% Motor efficiency
eta_M = P_m./P_e;

% Generator efficiency
eta_G = P_e./P_m;
q1 = P_e > 0; % First quadrant
q2 = P_e < 0; % Second quadrant
eta = eta_M.*q1 + eta_G.*q2; % Efficiency map uses motor eff. for first quadrant
and generator eff. for second quadrant

% Draw mechanical power contour plot
figure();
contour(W*60/2/pi,I,P_m,50, 'ShowText','on');
title(strcat('Mechanical Power- ', Motor));
xlabel('n [1/min]');
ylabel('i [A]');
% Draw electrical power contour plot
figure();
contour(W*60/2/pi,I,P_e,50, 'ShowText','on');
title(strcat('Electrical Power- ', Motor));
xlabel('n [1/min]');
ylabel('i [A]');
% Draw efficiency plot
figure();
levels=[0:0.2:0.6...

```

```

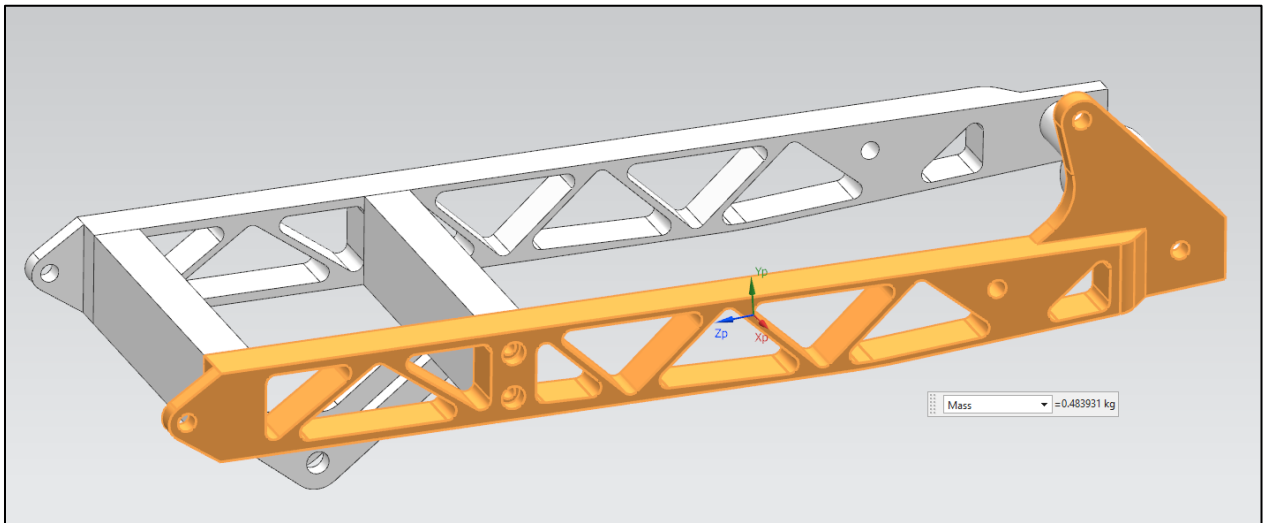
0.7:0.05:0.85...
0.86:0.01:0.95]*100; % Efficiency contour lines to draw
contour(W*60/2/pi,I,eta*100,levels, 'ShowText','on');
hold on;
[C,h] = contour(W*60/2/pi,I,P_m,[100,100], '--b', 'LineWidth', 1, 'ShowText','off'); %
Constant power curve
hcl = clabel(C);
set(hcl(2), 'String', '100 W', 'FontSize',12);
T_line = k_T/R*(V_B-w/k_w)-T_f; % Tw-line for constant motor voltage = V_B
I_line = (T_line+T_f)/k_T;
plot(W*60/2/pi, I_line, '-.g', 'LineWidth', 1);
ylim([I(1) I(end)]);
title(strcat('Efficiency- ', Motor));
xlabel('n [1/min]');
ylabel('i [A]');
grid on;
%% Motor and battery current over motor voltage
% Neglecting friction losses
n = 2500; % Motor speed [1/min]

w = n*pi/30;
e = w/k_w;
v_M = 0:0.1:V_B;
i_M = (v_M-e)/R;
i_B = v_M.*i_M/V_B;
P_m = w*i_M*k_T;
P_e = V_B*i_B;
eta_M = P_m./P_e;
eta_G = P_e./P_m;
q1 = i_M>0;
q2 = i_M<0;
eta = eta_M.*q1 + eta_G.*q2;

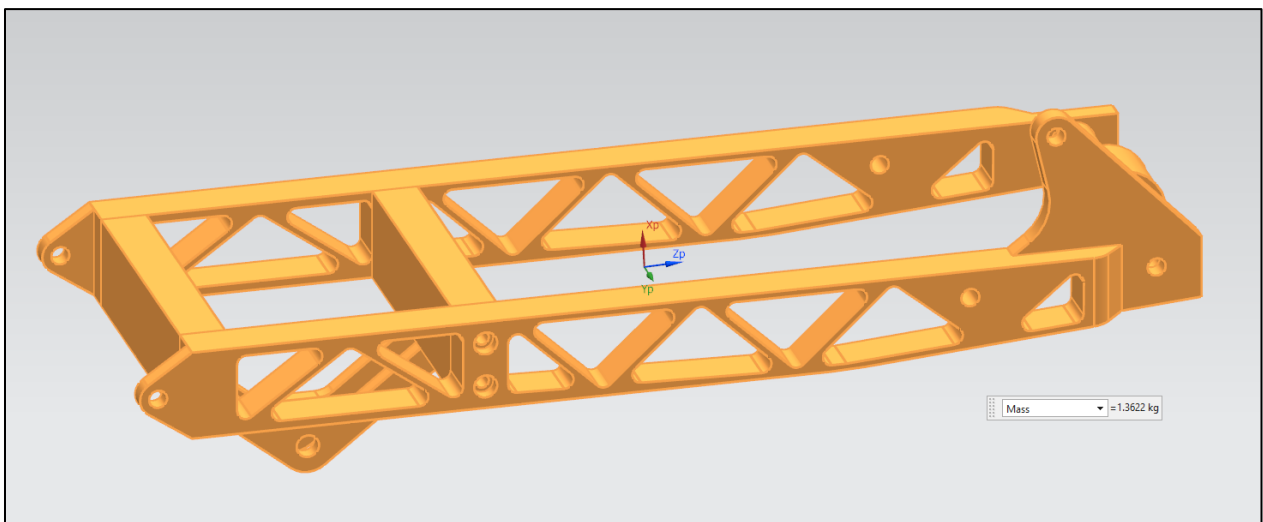
ylabels = {'Current [A]', 'Power [W]', 'Efficiency [%]'};
[ax,hlines] = multiplotyyy({v_M,i_M,v_M,i_B},{v_M,P_e, v_M, P_m},{v_M, eta},ylabels);
legend(cat(1,hlines{:}), 'Motor current', 'Battery current', 'Electric
power', 'Mechanical power', 'Efficiency', 'Location', 'northwest')
grid on;
header = strcat('Current and power over motor voltage at constant speed - ',Motor,',
n=', num2str(n), ' 1/min, V_B = ',num2str(V_B), ' V');
title(header);

```

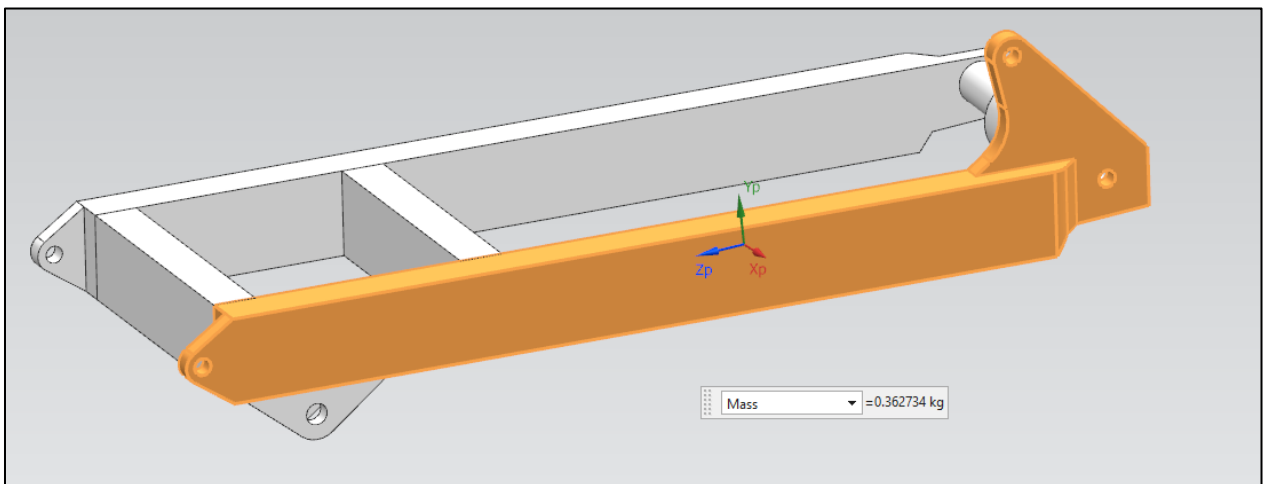
Appendix N: Topology optimized design vs square tubes
Topology inspired arms in the swing arm designed for one sided milling



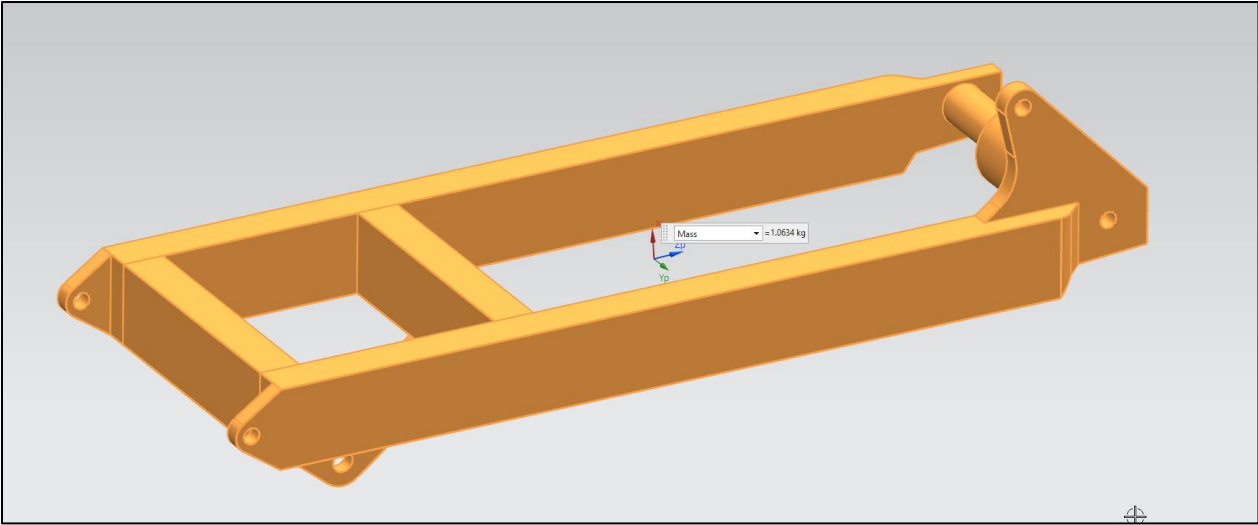
Weight of the arm with brake mount: 0.484kg



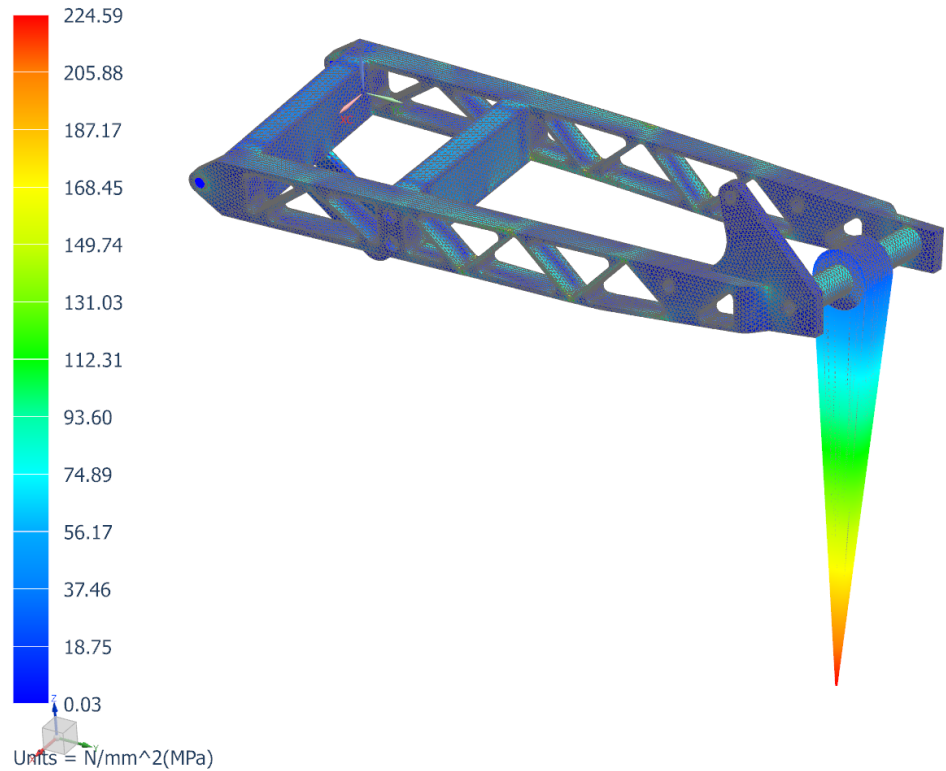
Total assembly weight: 1.36kg



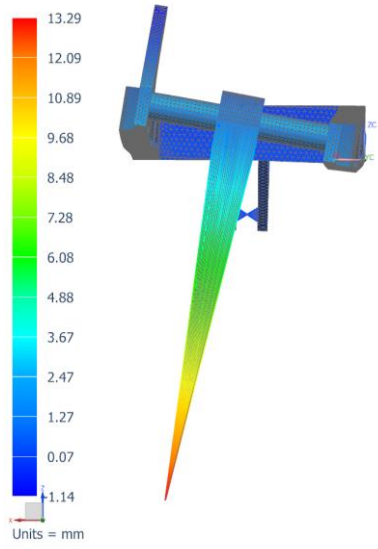
Weight of the arm with brake mount: 0.362kg



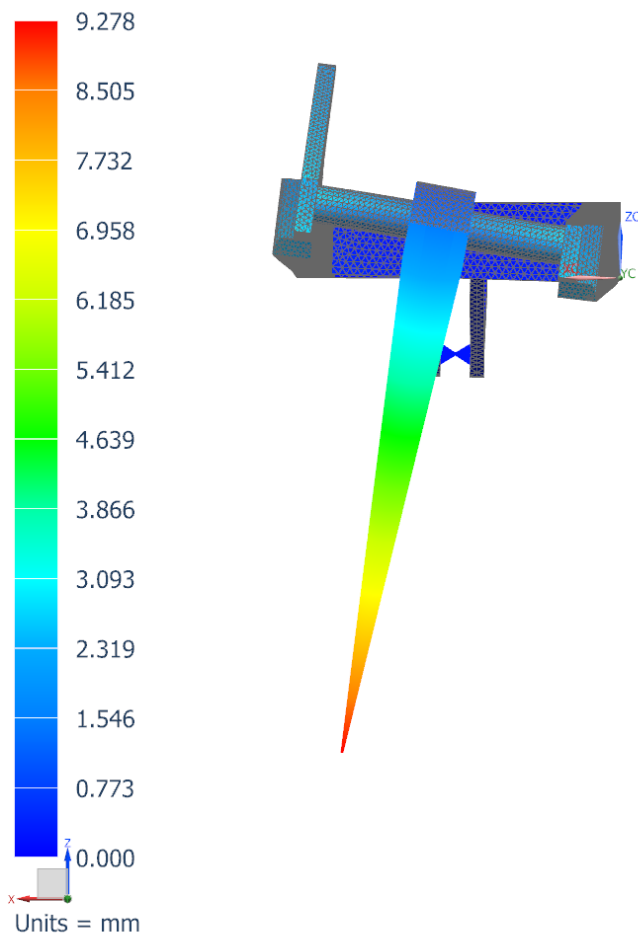
Total assembly weight: 1.06kg



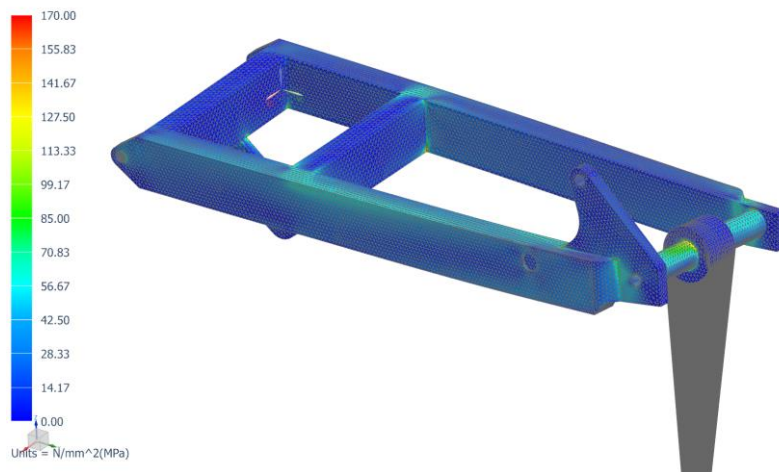
Material assumption: 7075-t6 aluminum, ca 500Mpa strength. Strong enough



Displacement: 13.29mm



Displacement: 9.278mm



Maximum forces in frame: Ca. half of the yield strength of 170Mpa. ("6060-T6 Aluminum", www.makeitfrom.com/material-properties/6060-T6-Aluminum, retrieved 2018-07-31.)

Appendix O: Datasheet for Actuonix P16



P16 Actual Size

Applications

- Robotics
- Consumer appliances
- Toys
- RC vehicles
- Industrial Automation
- Automotive

Miniature Linear Motion Series · P16

Actuonix Motion Devices unique line of Miniature Linear Actuators enables a new generation of motion-enabled product designs, with capabilities that have never before been combined in a device of this size. These linear actuators are a superior alternative to designing your own push/pull mechanisms.

The P16 actuators are complete, self-contained linear motion devices with position feedback for sophisticated position control capabilities, or end of stroke limit switches for simple two position automation. Several gear ratios are available to give you varied speed/force configurations.

The parallel design makes the P16 significantly shorter than the same stroke length L16, but the most attractive feature of this model is its high cycle life. Premium components in this model include: large sealed stainless steel bearings, planetary gearbox, stainless steel lead screw, and glass re-enforced nylon housing.

P16 Specifications

Gearing Option	22:1	64:1	256:1	
Peak Power Point	40N @26mm/s	80N @9mm/s	250N @2.5mm/s	
Peak Efficiency Point	25N @34mm/s	40N @14mm/s	150N @3.4mm/s	
Max Speed (no load)	46mm/s	18mm/s	4.8mm/s	
Max Force Lifted	50N	90N	300N	
Back Drive Force	75N	200N	>500N	
Stroke Option	50mm	100mm	150mm	200mm
Mass	95g	110g	125g	140g
Repeatability (-P & LAC)	0.3mm	0.4mm	0.6mm	0.8mm
Max Side Load	20N	15N	10N	4N
Closed Length hole to hole	97mm	147mm	197mm	247mm
Feedback Potentiometer	6kΩ±50%	11kΩ±50%	20kΩ±50%	23kΩ±50%
Feedback Linearity	Less than 2.00%			
Input Voltage	0-15 VDC. Rated at 12VDC.			
Stall Current	1000mA @ 12V			
Operating Temperature	-10°C to +50°C			
Audible Noise	62 dB @ 45cm			
Ingress Protection	IP-54			
Mechanical Backlash	0.3mm			
Limit Switches (-S)	Max. Current Leakage: 8uA			
Maximum Static Force	500N			
Maximum Duty Cycle	20%			

Basis of Operation

The P16 is designed to push or pull a load axially along its full stroke length. The speed of travel is determined by the load applied (See the Load Curves). Actuator speed can be reduced by lowering the drive voltage. When power is removed the actuator will hold its position, unless the applied load exceeds the back drive force. Repeated stalling or stalling for more than a few seconds will shorten the life of the actuator significantly. Actuators should be tested in each specific application to determine their effective life under those loading conditions and environment.

All data on this sheet is provided for information purposes only and is subject to change. Purchase and use of Actuonix Actuators is subject to our terms and conditions as posted here: <http://www.Actuonix.com/terms.asp>

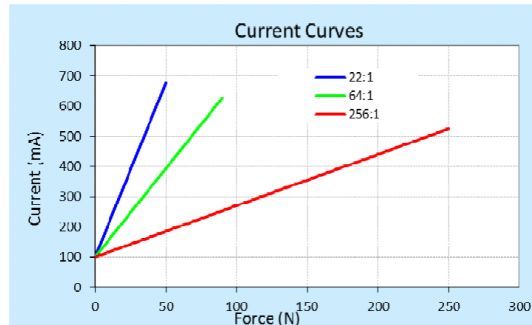
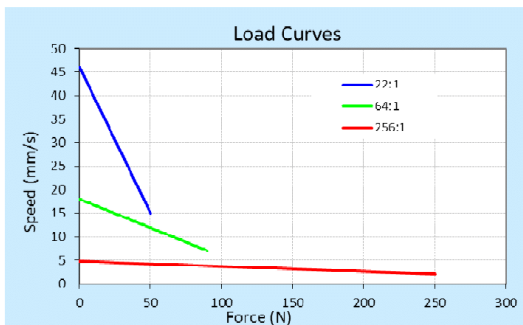


Actuonix Motion Devices Inc
580 Starling Lane
Victoria, BC, V9E 2A9
Canada

1 (206) 347-9684 phone
1 (888) 225-9198 toll-free
1 (206) 347-9684 fax

sales@actuonix.com
www.actuonix.com

Rev B Sept 2016



Model Selection

The P16 has 3 configuration choices: Stroke, Gear Ratio and Controller. P16 options are identified according to the following model numbering scheme:

P16-SS-GG-VV-C

Feature	Options
SS: Stroke	50, 100, 150, 200 (mm)
GG: Gear reduction ratio (refer to load curves above)	22, 64, 256 :1 (lower ratios are faster but push less force, and vice versa)
VV: Voltage	12 Volts DC
C: Controller	P Potentiometer Feedback S Limit Switches

P16 Controller Options

Option S – End of Stroke Limit Switches

WIRING: (see last page for pin numbering)
 1 - Red – Motor V+ (12V)
 2 - Black – Motor V- (Ground)

–S actuators are ideal for manually controlled applications and simple two position automated mechanisms. The –S actuators have limit switches that will turn off power to the motor when the actuator reaches within 0.5mm of the end of stroke. Internal diodes allow the actuator to reverse away from the limit switch. The limit switches cannot be moved once the actuator is manufactured. While voltage is applied to the motor power pins, (1 & 2) the actuator extends. Reverse the polarity and the actuator retracts. This can be accomplished manually with a DPDT switch or relay, or using an H-Bridge. The –S model cannot be used with the LAC control board.

Ordering

Small quantity orders can be placed directly online at www.Actuonix.com. Purchase orders, volume quotes, and custom order requests can be sent to sales@Actuonix.com. MOQ for custom strokes, cables or connectors is typically 500pcs. Each actuator ships with two mounting brackets and #8-32 mounting hardware. The cable length is approximately 300mm and connector is a 0.1" pitch female socket connector. The thread in the end of the round aluminum shaft is M8x1.25.

Option P – Potentiometer Position Feedback

WIRING: (see last page for pin numbering)
 1 - Orange – Feedback Potentiometer negative reference rail
 2 - Purple – Feedback Potentiometer wiper
 3 - Red – Motor V+ (12V)
 4 - Black – Motor V- (Ground)
 5 - Yellow – Feedback Potentiometer positive reference rail

–P actuators are suited to automatically controlled positioning systems, but they can also be driven manually. The –P actuators have no built in controller, but do provide an analog position feedback signal that can be input to an external closed loop controller. While voltage is applied to the motor power pins, (3 & 4) the actuator extends. Reverse the polarity and the actuator retracts. This can be accomplished manually with a DPDT switch or relay, or using an H-Bridge circuit. Position of the actuator stroke can be monitored by providing any stable low and high reference voltage on pins 1 & 5, then reading the position signal on pin 2. The voltage on pin 2 will vary linearly between the two reference voltages in proportion to the position of the actuator stroke.

The P16 –P actuator can be used as a linear servo by connecting the actuator to an external controller such as the LAC board offered by Actuonix. This control board reads the position signal from the P16, compares it with your input control signal then commands the actuator to move via an on-board H-bridge circuit. The LAC allows any one of the following control inputs: Analog 0-3.3V or 4-20mA, or Digital 0-5V PWM, 1-2ms Standard RC, or USB. The RC input effectively transforms your P16 into a linear servo, which is a direct replacement for any common hobby servo used in RC toys and robotics. Refer to the LAC datasheet for more details.

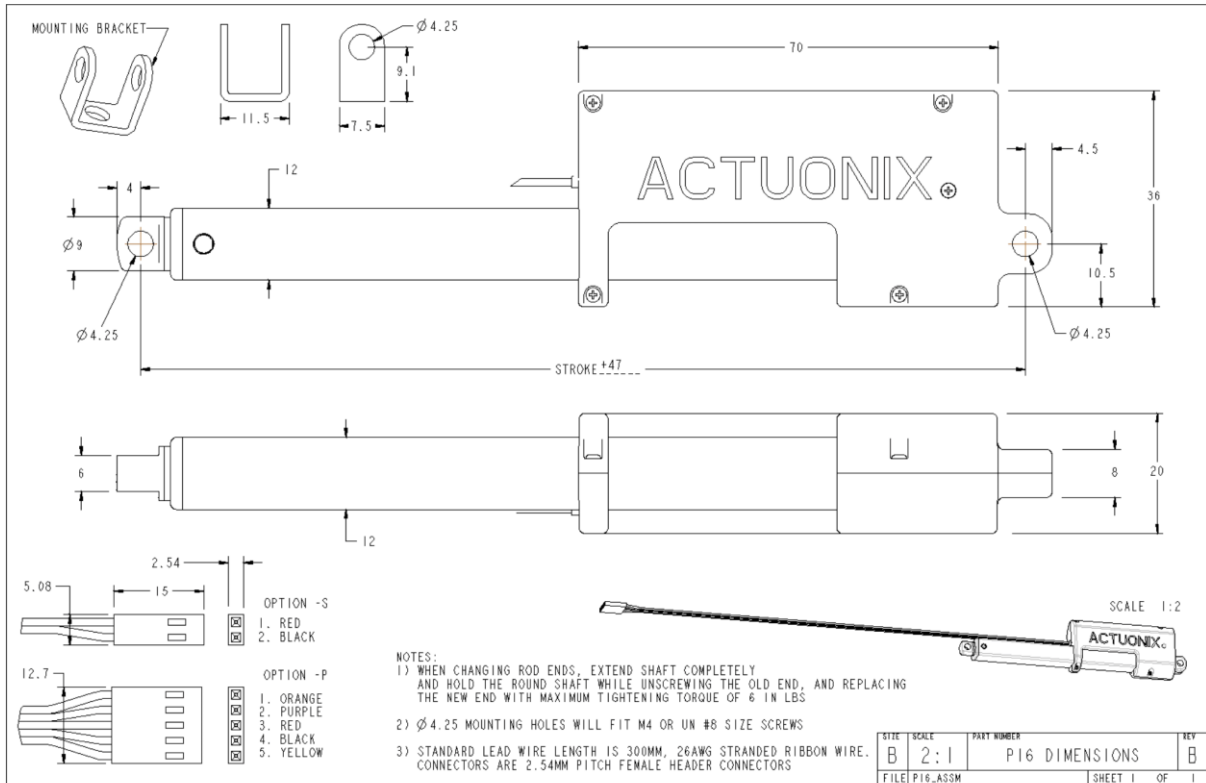
Copyright 2016 © Actuonix Motion Devices Inc.



Actuonix Motion Devices Inc
 580 Starling Lane
 Victoria, BC, V9E 2A9
 Canada

1 (206) 347-9684 phone
 1 (888) 225-9198 toll-free
 1 (206) 347-9684 fax

sales@actuonix.com
www.actuonix.com



Copyright 2016 © Actuonix Motion Devices Inc.



Actuonix Motion Devices Inc
 580 Starling Lane
 Victoria, BC, V9E 2A9
 Canada

1 (206) 347-9684 phone
 1 (888) 225-9198 toll-free
 1 (206) 347-9684 fax

sales@actuonix.com
www.actuonix.com

All data on this sheet is provided for information purposes only and is subject to change. Purchase and use of Actuonix Actuators is subject to our terms and conditions as posted here: <http://www.Actuonix.com/terms.asp>

AVERAGE PHYSICAL PROPERTIES - IMPERIAL UNITS

Table shows average values for the nominal densities and minimum values within the brackets for the minimum density.

Property	Unit	H 35	H 45	H 60	H 80	H 100	H 130	H 160	H 200	H 250
Nominal Density ¹⁾ ISO 845	lb/ft ³	2.4	3.0	3.8	5.0	6.3	8.1	10.0	12.5	15.6
Compressive Strength ²⁾ ASTM D 1621	psi	65 (44)	87 (72)	130 (102)	203 (167)	290 (239)	435 (348)	493 (406)	783 (653)	1,044 (885)
Compressive Modulus ²⁾ ASTM D 1621	psi	5,800 (4,206)	7,250 (6,525)	10,150 (8,700)	13,050 (11,600)	19,575 (16,675)	24,650 (21,030)	29,000 (25,382)	44,965 (38,435)	58,015 (50,763)
Tensile Strength ²⁾ ASTM D 1623	psi	145 (116)	203 (160)	261 (218)	363 (319)	508 (362)	696 (508)	783 (581)	1,030 (914)	1,334 (1,160)
Tensile Modulus ²⁾ ASTM D 1623	psi	7,105 (5,366)	7,975 (6,525)	10,875 (8,265)	13,775 (12,325)	18,850 (15,225)	25,375 (19,575)	29,730 (23,206)	36,250 (30,450)	46,400 (37,710)
Shear Strength ASTM C 273	psi	58 (44)	81 (67)	110 (91)	167 (138)	232 (203)	319 (276)	377 (319)	508 (464)	653 (566)
Shear Modulus ASTM C 273	psi	1,740 (1,305)	2,175 (1,740)	2,900 (2,320)	3,915 (3,335)	5,075 (4,060)	7,250 (5,800)	10,590 (7,252)	10,590 (9,427)	14,070 (11,748)
Shear Strain ASTM C 273	%	9 (4)	12 (8)	20 (10)	30 (15)	40 (25)	40 (30)	40 (30)	45 (35)	45 (35)
1) Typical density variation +/- 10%.										
2) Perpendicular to the plane. All values measured at +73.4°F.										

Continuous operating temperature is -325°F to +160°F (-200°C to +70°C). The foam can be used in sandwich structures, for outdoor exposure, with external skin temperatures up to +185°F (+85°C). For optimal design of applications used in high operating temperatures in combination with continuous load, please contact DIAB Technical Services for detailed design instructions. Normally Divinycell H can be processed at up to +194°F (+90°C) with minor dimensional changes. Maximum processing temperature is dependent on time, pressure and process conditions. Therefore users are advised to contact DIAB Technical Services to confirm that Divinycell H is compatible with their particular processing parameters.

Coefficient of linear expansion: approx. $22.2 \times 10^{-6}/^{\circ}\text{F}$ ($40 \times 10^{-6}/^{\circ}\text{C}$)

MICHELIN TIRES AND RIMS CHARACTERISTICS Urban Concept

— TECHNICAL SPECIFICATIONS —

Maximum pressure:	5 bars (500 kPa)
Max pressure for storage:	1 bar (100 kPa)
Load capacity:	100 kg
Speed limit:	70 km/h
Recommended rim size:	3.00 B16 - 3.50 B16
Electrical resistance:	> 5 E+12 Ω

— TIRE IDENTIFICATION (SIDEWALL MARKINGS) —

MAXIMUM PRESSURE 500 kPa (73 PSI)
PRESSURE FOR STORAGE 100 kPa (15 PSI)

NOT FOR USE ON PUBLIC ROAD
USE ON TRACK ONLY

Manufacturing week/year : WW12

FOR COMPETITION PURPOSE ONLY

Only tires with above markings, manufactured in 2012, are certified conform to this datasheet.

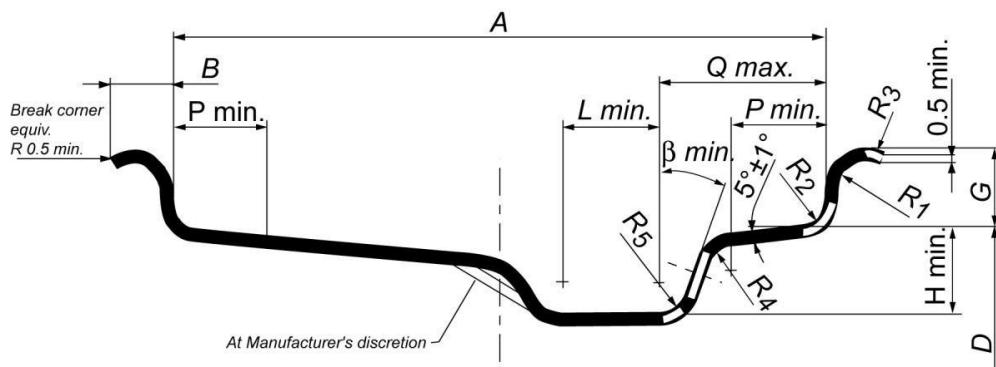
— TIRE DIMENSIONS —

TIRE SIZE DIMENSION	Section width mm	Overall Diameter mm
95/80 R16	95	558

Theoretical dimensions depending on pressure and rim

— RIM DIMENSIONS —

RIM Contour	DIMENSIONS (mm)												
	A		B		G	P	H	L	Q	R1	R2	ββ	D
		min	max	±0,6	min.	min.	min.	max.	min.	max.	min.		
3.00 B	76	±1	10	13	14,1	13	15	16	28	7,5	4,5	10°	405,6
3.50 B	89	±1	10	13	14,1	15	15	19	34	7,5	4,5	13°	405,6



Appendix R: Risk Assessment



Detailed Risk Report

ID	25945	Status	Date
Risk Area	Risikovurdering: Helse, miljø og sikkerhet (HMS)	Created	09.01.2018
Created by	Sivert Rød Hatletveit	Assessment started	09.01.2018
Responsible	Sivert Rød Hatletveit	Actions decided	
		Closed	

Risk Assessment:

Work Related to Master Thesis 2018 (Development of A Inertia Motor Generator Dynamometer and Work on a Vehicle For a Milage Race)

Valid from-to date:

12/9/2017 - 7/31/2018

Location:

MTP, NTNU, Trondheim

Goal / purpose

This is a risk assessment to map out the potential incidents and dangers and their consequences associated with the work for my premaster's project and master project. The project will involve working in the workshop and use of batteries with low classified as low voltage.

Background

This risk assessment is being carried out as standard procedure in preparation of experimental work at NTNU.

Description and limitations

The risk assessment concerns the author and other potential users in immediate proximity to work being carried out by author. Work will only be carried out within the confines of the Realization Lab (148) at Richard Birkelands vei 2B.

Activities included are use of workshop tools, including hand tools and machines covered with the MTP HSE course. In addition a safety course was given by the workshop leader on how to use the composite lab.

Prerequisites, assumptions and simplifications

I assume that the machines used are regularly maintenance and function as they should. And that other users of the workshop follow the HSE guidelines from NTNU's HME training course. I further assume that the knowledge HSE certification courses is sufficient to reduce the risks associated with operation of heavy machinery and tools.

Attachments

[Ingen registreringer]

References

[Ingen registreringer]

OK.
7/8-18 / *[Signature]*

Norges teknisk-naturvitenskapelige universitet (NTNU)

Unntatt offentlighet jf. Offentlighetsloven § 14

Print date:

06.08.2018

Printed by:

Sivert Rød Hatletveit

Page:

1/10



Summary, result and final evaluation

The summary presents an overview of hazards and incidents, in addition to risk result for each consequence area.

Hazard: Electric power tools

Incident: Large Cut Damage

Consequence area: Helse Risk before actions: Risiko after actions:

Hazard: Electric components

Incident: Fire

Consequence area: Materielle verdier
Omdømme Risk before actions: Risiko after actions:
Risk before actions: Risiko after actions:

Incident: Electric shock

Consequence area: Helse Risk before actions: Risiko after actions:

Hazard: Damage due to rotating parts in dynamometer

Incident: Large cut damage

Consequence area: Helse
Omdømme Risk before actions: Risiko after actions:
Risk before actions: Risiko after actions:

Final evaluation

Even by following guidelines there's always a risk of damage. Therefore working with care and asking personel in the realization lab should be done.



Organizational units and people involved

A risk assessment may apply to one or more organizational units, and involve several people. These are listed below.

Organizational units which this risk assessment applies to

- Institutt for maskinteknikk og produksjon

Participants

[Ingen registreringer]

Readers

[Ingen registreringer]

Others involved/stakeholders

[Ingen registreringer]

The following accept criteria have been decided for the risk area Risikovurdering: Helse, miljø og sikkerhet (HMS):

Helse



Materielle verdier



Omdømme



Ytre miljø





Overview of existing relevant measures which have been taken into account

The table below presents existing measures which have been taken into account when assessing the likelihood and consequence of relevant incidents.

Hazard	Incident	Measures taken into account
Electric power tools	Large Cut Damage	Retningslinjer for adgang til og arbeid i laboratorier ved MTP
	Large Cut Damage	HSE Certification course
Electric components	Fire	Retningslinjer for adgang til og arbeid i laboratorier ved MTP
	Fire	Limit to low voltage
	Electric shock	Retningslinjer for adgang til og arbeid i laboratorier ved MTP
	Electric shock	Limit to low voltage
Damage due to rotating parts in dynamometer	Electric shock	HSE Certification course
	Large cut damage	Retningslinjer for adgang til og arbeid i laboratorier ved MTP
	Large cut damage	HSE Certification course

Existing relevant measures with descriptions:

Retningslinjer for adgang til og arbeid i laboratorier ved MTP

Follow the regulations for safe use of the realization lab

Limit to low voltage

[Ingen registreringer]

HSE Certification course

[Ingen registreringer]

Courses for machines / labs needed

Mechatronics, composite lab and wooden CNC-machine



Risk analysis with evaluation of likelihood and consequence

This part of the report presents detailed documentation of hazards, incidents and causes which have been evaluated. A summary of hazards and associated incidents is listed at the beginning.

The following hazards and incidents has been evaluated in this risk assessment:

- **Electric power tools**
 - Large Cut Damage
- **Electric components**
 - Fire
 - Electric shock
- **Damage due to rotating parts in dynamometer**
 - Large cut damage



Detailed view of hazards and incidents:

Hazard: Electric power tools

Use of electric machinery at the realization lab

Incident: Large Cut Damage

Cause: Burning damage

Cause: Not following regulations

Description:

HSE regulations should be followed

Likelihood of the incident (common to all consequence areas): **Unlikely (1)**

Kommentar:

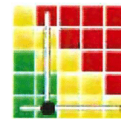
By following guidelines and rules set by the workshop guidelines it shouldn't be a huge risk for incidents

Consequence area: Helse

Assessed consequence: **Medium (2)**

Comment: Some of the machines are powerful and incidents can happen

Risk:





Hazard: Electric components

Incident: Fire

Likelihood of the incident (common to all consequence areas): **Unlikely (1)**

Kommentar:

[Ingen registreringer]

Consequence area: Materielle verdier

Assessed consequence: **Medium (2)**

Comment: [Ingen registreringer]

Risk:

**Consequence area: Omdømme**

Assessed consequence: **Medium (2)**

Comment: [Ingen registreringer]

Risk:

**Incident: Electric shock**

Shock caused by electricity

Cause: Touching

Likelihood of the incident (common to all consequence areas): **Less likely (2)**

Kommentar:

Covering parts and taking care gives low risk

Consequence area: Helse

Assessed consequence: **Small (1)**

Comment: Only low voltages (less than 50V DC)

Risk:





Hazard: Damage due to rotating parts in dynamometer

Covering moving parts or keeping distance just in case

Incident: Large cut damage

Cause: Not following HSE guidelines

Description:

Unnecessary risks and oversteps of HSE should't be done. Consolidation with the room responsible if in doubt.

Cause: (no title)

Likelihood of the incident (common to all consequence areas): **Unlikely (1)**

Kommentar:

HSE regulations are written.

Consequence area: Helse

Assessed consequence: **Medium (2)**

Comment: [Ingen registreringer]

Risk:



Consequence area: Omdømme

Assessed consequence: **Medium (2)**

Comment: [Ingen registreringer]

Risk:





Overview of risk mitigating actions which have been decided:

Below is an overview of risk mitigating actions, which are intended to contribute towards minimizing the likelihood and/or consequence of incidents:

Overview of risk mitigating actions which have been decided, with description:

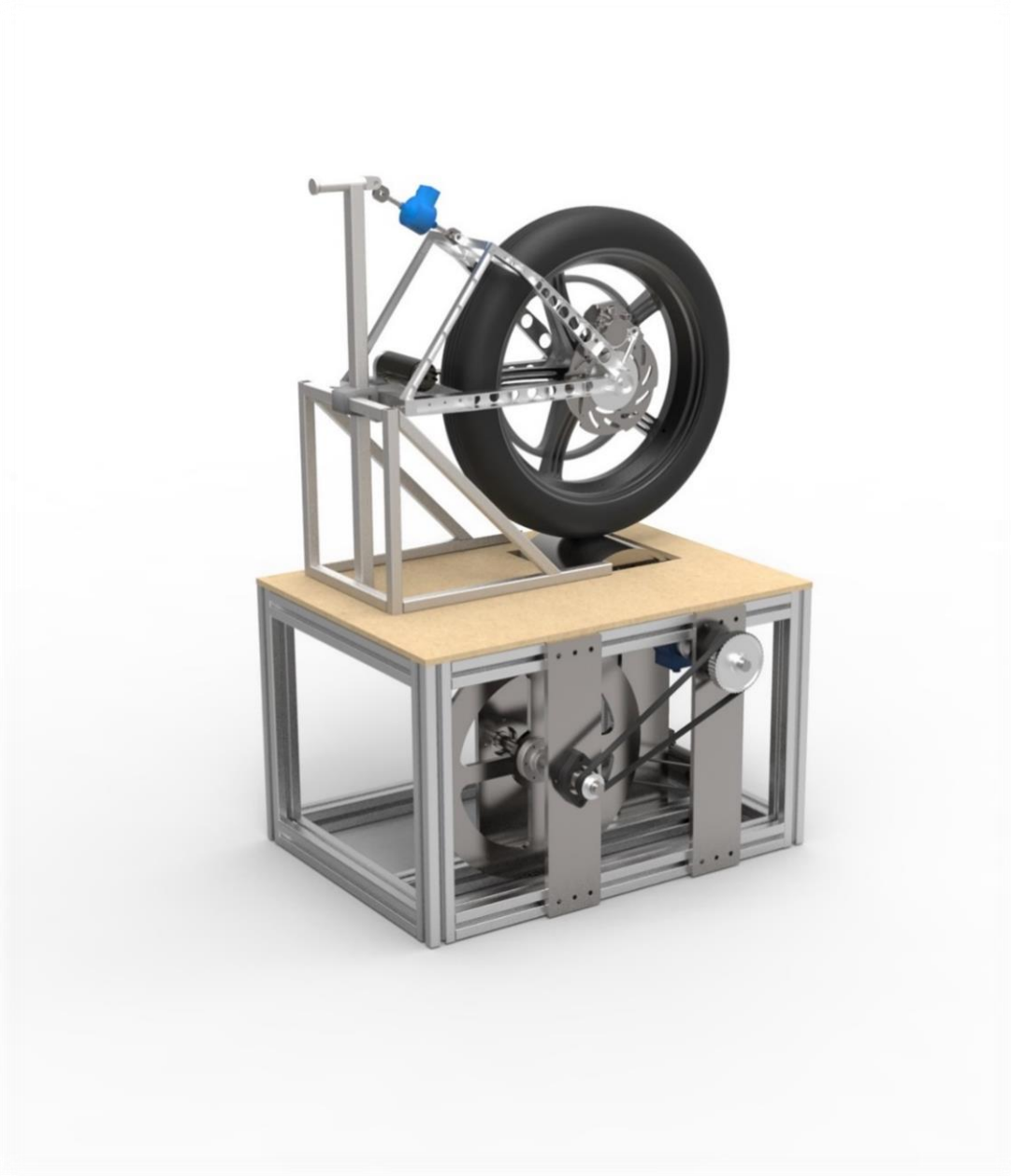


Detailed view of assessed risk for each hazard/incident before and after mitigating actions

Appendix S: Pre-Master Thesis

Specialization project:

DEVELOPMENT OF A MOTOR/GENERATOR INERTIA DYNAMOMETER FOR OPTIMIZATION AND RISK MITIGATION OF DNV GL FUEL FIGHTERS POWERTRAIN



Author: Sivert Rød Hatletveit

Submission date: 10.1.2018

Supervisor: Knut Einar Aasland

Norwegian University of Science and Technology,
Faculty of Engineering Science and Technology,
Department of Mechanical and Industrial Engineering

 **NTNU**
Kunnskap for en bedre verden

Summary

This project report describes the development of a test bench for verifying performance and reliability of the powertrain of a Shell Eco-Marathon vehicle.

The main goal of during the development have been to simulate the inertia of the vehicle and the forces acting on a car while driving and to act as a load so that verification that the cars powertrains work as it should. Secondary goals have been to enable measurements of the vehicles efficiency and to work as a tool developing of future powertrains.

The result is a test bench that could be classified as a Motor/Generator Inertia Dynamometer. It is controlled via Simulink and are collecting readings of speed, torque and motor/generator current at a rate of 100 samples per second.

It is in the current setup used in combination with one of two identical and decoupled powertrains for the car and tuned to mimic half of the total vehicle mass by using a flywheel. The motor/generator is simulating half the aerodynamic drag force, the rolling resistance and the bearing losses.

Initial test also show that it has potential for measuring the efficiency of driving a simulated track and for mapping out efficiency of the vehicle at different speeds and propulsion torques. However, some more work is needed before this is doable.

Sammendrag

Denne prosjektrapporten beskriver utviklingen av en testbenk for å verifisere ytelse og pålitelighet for drivlinjen på en bil laget for deltagelse i Shell Eco-Marthon.

Hovedmålet i utviklingsprosessen har vært å simulere en bilens treget og kreftene som virker på bilen under kjøring. Tilleggs mål har vært å gjøre det mulig å måle bilens effektivitet og støtte utvikling av fremtidige drivlinjer.

Resultatet er en testbenk som kan klassifiseres som en «Motor/Generator Inertia Dynamometer». Den er kontrollerbar via Simulink og henter data om blant annet hastighet, moment og strøm som går i motor/generator.

I det foreløpige oppsettet brukes den til å simulere en av to identiske, frakoblede drivlinjer og etterligner halve bilens tregthet ved bruk av et svinghjul. Motoren simulerer halvparten av bilens luftmotstand, rullemotstand og kulelagertap.

Foreløpige tester viser at den har potensiale to å måle effektivitet ved å simulere banekjøring og ved å måle effektivitet over ulike hastigheter og moment. For å få til dette må det noe mer arbeid til.

Table of Contents

1	Introduction	2
2	Risk management	4
3	Physics.....	5
3.1	Forces acting on the car	5
3.1.1	Rolling resistance (FR)	5
3.1.2	Aerodynamic drag (FD).....	6
3.1.3	Inertia Forces(FI)	7
3.1.4	Gravity (FG).....	7
3.1.5	Bearing losses (FB).....	7
3.1.6	Speed dependent net forces calculated.....	8
3.2	Physics for the test bench (Inertia Dynamometer)	9
3.3	Estimate for energy consumption.....	11
3.3.1	Is regenerative braking beneficial?	12
3.3.2	Verification of the different phases.....	13
4	Development	14
4.1	Requirements.....	14
4.2	Modular design	14
4.3	The main frame	15
4.4	Rapid production of the plates	16
4.5	The Roller	17
4.6	Powertrain mounting frame	18
4.7	Simulating the inertia forces	21
4.8	The Electronics.....	24
4.8.1	Components used for variable braking/accelerating	24
4.8.2	Data acquisition.....	25
4.8.3	Control Center - Simulink	25
5	Results and Discussion	26
5.1	The effect of a not slightly oval tire	26
5.2	Iterative tuning of the test bench	27
5.3	Torque Transducer testing.....	30
6	Conclusion and Further work.....	31
7	Sources.....	33

1 Introduction



FIGURE 1-A DNV GL FUEL FIGHTER 4 AND THE 2017 TEAM DURING SHELL ECO MARATHON 2017 IN LONDON

Shell Eco Marathon(SEM) is a competition that challenges students to design, build and compete with the energy-efficient vehicles. The race is about driving with least amount of energy for a given track within a given maximum time. The competition has been arranged annually as a student competition since 1985, where NTNU is participating for the 11.th time. The 2018 competition is going to be arranged from 3-5. July in London once again, but with a much flatter track than in 2017.

There are two different classes in SEM called Prototype and Urban concept. The prototype class is all about the ultimate efficiency were the best cars are aerodynamic “capsules” where the driver is lying down while driving. The Urban Concept is more about making a small energy-efficient car meant as a future urban concept. This class has some dimensional rules like height and width and the cars also need to have wipers, light and space for a brief case. It’s also required to make a complete stop after each lap in this class.

In addition, each class has three different energy categories: Battery electric, hydrogen and internal combustion engines. Each team are allowed only to have one car per class and category. In 2018 the team are only going to compete in urban concept with an improved version of the car DNV GL Fuel Fighter 4.

This car was also first used the race in the 2017 competition and was built in one year. Unfortunately, due to too little time to test it and make the car reliable the car didn’t manage to get any valid attempts during the race. The two first runs because of mechanical parts loosened and in the latest attempt the motor controller shorted and destroyed the drivelines clutch because of too much current giving a higher torque than the clutch was rated for.

For the team two years before that it didn’t go as planned either with a lot of problems with the powertrain. By reading the reports from previous years one thing becomes clear: Too little time for physical testing of the car is always an issue both for reliable mechanics and electronics of the car. And

the powertrain is usually a problem in various ways. Examples of problems with the powertrain from later years is:

- Not enough torque from the motor from stand still (2016)
- Motor Controller failure under load (2017)
- Change in bearings during the race due to optimistic gearing (2017)
- Belts slipping (2015, 2016)

Testing under real conditions is complex with the need of a drivable car, transportation to a track, and a lot of manpower. As the powertrain statistically has been one of the most troublesome parts and one of the hardest parts to test and measure under controlled environments, a strategy to test the powertrain more rapidly would benefit the development of the car.

SCOPE

The goal for the work described in this paper was to develop a test bench for the DNV GL Fuel Fighter 4's powertrain, where the primary goal has been to make a system that mimics real world driving condition as much as possible so that stress testing of motors, motor controller and the transmission is easily achievable. In this way the powertrain could be tested in more controlled environments with the possibility to visually see how the mechanics is behaving and the motor controller could be analyzed for example with an oscilloscope or heat camera to find problems in the design.

Secondary goals are to be able to measure the systems efficiency with the same test bench and use the results for planning the driving strategy together. By adding everything in one solution it could be hard to get accurate enough results as the system would act as a black box where changing parameter could lead change other parameters.

Finally, enabling using the test bench as a support for designing future powertrains and verifying that the new designs are efficient and reliable is a goal. Hopefully the developed test bench could be great asset to verify and mitigate risk for the coming years of the project.

To simulate the car, the test bench's final design have a mounting frame for the powertrain with the ability to apply the same mass as the cars weight on that wheel down to a dynamo roller. The roller is connected to a flywheel which mimics the mass of the car and a motor/generator for simulating the other net forces working on the car. It also has a torque transducer connected to the axle and a speed sensor and software for controlling it.

2 Risk management

Most projects have a certain uncertainty which leads to a risk of something going wrong or things not working as planned. Especially for a project like building a one of a kind car for competing these uncertainties are inevitable. By trying to push the limits of what's possible mechanical safety factors are kept low and components that are more efficient, but less reliable and proven chosen/ designed. To deal with this the understanding of risk and how to reduce it is crucial.

To estimate the probability of a risk happening two components should be measured: the undesirable consequence if the event if it occurs and the likelihood that the event occurs. (Walden et al., 2015) There is no other way to eliminate risk could occur than to set the technical goals very low by using only failsafe parts which isn't a choice to make a car that are supposed to be among the most efficient cars in its competition. However – reducing the probability of something happening by making a good risk management plan is needed.

One easy way to reduce the consequence for our car to fail at the race is to design the car in such a way that it could be fixed during competition. This could be done by for example bringing spare parts, tools like lathes, glue and 3D printers for making better dimensioned parts and avoid risks that could potentially have horrible outcomes, like for example to small safety factors on the brakes.

Likelihood could be expressed as a probability for an undesirable event happening. Therefore, mapping out and reducing the probability of an event could be a good way to allow risks with high consequences without having to have a high probability. It's not always easy to map out the likelihood for components to fail before using them.

Therefore, testing as a strategy in the product development to reduce likelihood before accepting a solution could clearly give results. For illustrating this problem looking at the Vee model(Figure 2-B) commonly used as in systems engineering (Walden et al., 2015) could be done. The Verification, integration and validation phases must be done in order to verify that the needs of the product is met.

This usually leads to a incremental and iterative development where problems are fixed by going back as shown with the horizontal arrows and change the requirements, design and specifications to meet the needs and there by an accept with a acceptable risk.

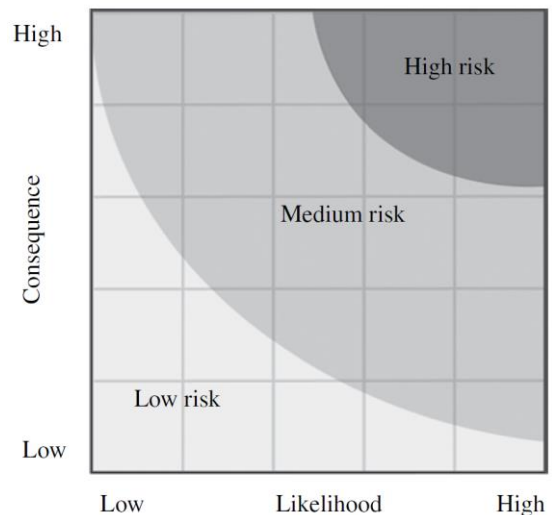


FIGURE 2-A RISK LEVEL DEPENDS ON BOTH LIKELIHOOD AND CONSEQUENCE (WALDEN ET AL., 2015)

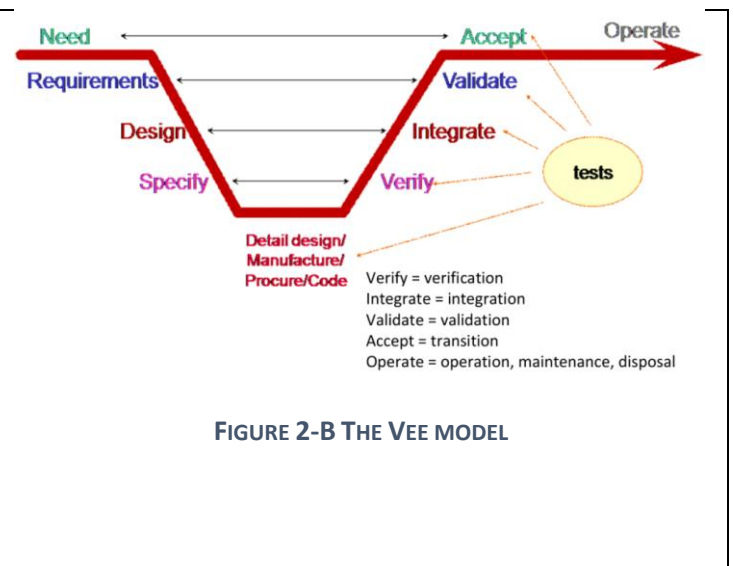


FIGURE 2-B THE VEE MODEL

3 Physics

3.1 Forces acting on the car

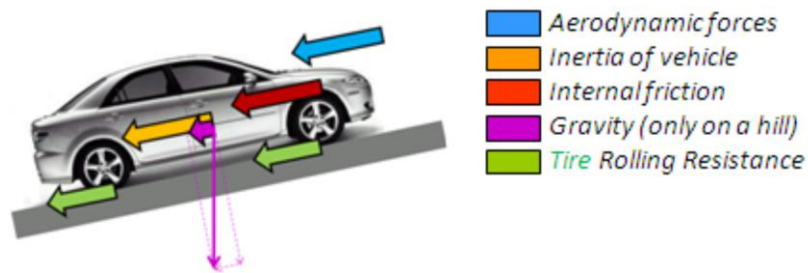


FIGURE 3-A FORCES ON A CAR (MICHELIN, 2017)

It's important to know the forces acting on our car to know how much the test bench should brake the driveline at different speeds and simulated elevations.

The total forces working on the car could be simplified to (Ward et al., 2015):

$$\sum F = F_R + F_D + F_G + F_I + F_P + F_B \tag{3.1}$$

Where:

- F_R Rolling resistance
- F_D Aerodynamic drag
- F_G Gravity forces in slopes
- F_I Inertia forces
- F_P Forces from powertrain (battery to road)
- F_B Bearing losses

3.1.1 Rolling resistance (F_R)

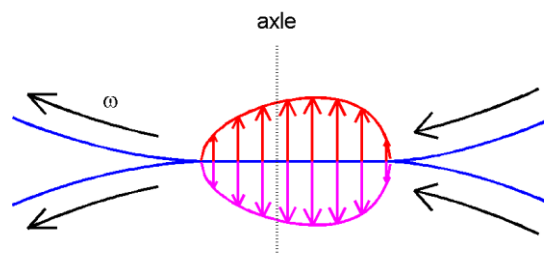


FIGURE 3-B DIFFERENT PRESSURE IN DIFFERENT AREAS IN THE WHEEL SOURCE: WIKIPEDIA.COM

Rolling resistance is mainly caused by hysteresis in the rubber where the tire deflects and doesn't recover its energy totally. This viscoelastic behavior causes a different pressure (Figure 3-B) distribution on each side of the vertical line of the wheel. This pressure distribution causes a backward working momentum which brakes the car.

The usual formula for calculating the rolling resistance force is $F_r = C_{rr} * N$ (Michelin, 2017), where N is the normal force $N = m * g$ and C_{rr} is a unitless coefficient for the tire. This means that the retarding force could be considered constant at different speeds. However, the force is usually increasing caused by acceleration since the rubber is deforming more therefore breaking more because of rubbers viscoelastic behavior.

The rolling coefficient is usually measured by a the “force -torque” method (Figure 3-C) where a tire is rolling at a roller while the normal force is simulated by applying a force towards the center of the roller and a motor with torque readings read the torque required to maintain a constant speed. (MTS Systems, 2017)



FIGURE 3-C ROLLING RESISTANCE TEST MACHINE (MTS SYSTEMS, 2017)

Some regular numbers for the rolling coefficient is shown in Table 1 were our car have the most efficient wheel I could find data for. It’s more efficient than for example the lowest measured racing bike tire (Vittoria Corsa Speed) resistance according to bicyclerollingresistance.com

TABLE 1 ROLLING RESISTANCE FOR DIFFERENT TYPES OF TIRES

Schwalbe Marathon (Efficient e-bike tire)	0.00474
Michelin Energy Saver Plus (Efficient car tire)	0.08
Michelin Urban Concept Tire	0.0013
Vittoria Corsa Speed (High end racing bike tire)	0.00231

Data from (bicyclerollingresistance.com, 2017), (Bierman, 2017) and (Michelin, 2017)

3.1.2 Aerodynamic drag (F_D)

In regular cars the aerodynamic drag force is usually the most dominant force working in highway speeds. (Michelin, 2017) The formula for aerodynamic drag is:

$$F_D = \frac{1}{2} \rho_{air} C_D A v^2$$

Where ρ is air density, C_D is the drag coefficient, A is the frontal area of the car and v is the vehicle speed.

Most of the cars in the Shell Eco Marathon Urban Concept class is made to minimize the effect of the aerodynamic drag. To achieve a good aerodynamic form a minimization of frontal area combined with a drop like aerodynamic shape is wanted.

3.1.3 Inertia Forces(F_I)

Inertia is the resistance of a physical object to change it's state of motion. For our car there is three major inertia forces:

- Linear inertia from accelerating the mass of the car
- Rotational inertia from spinning up the wheels
- Cornering inertia from changing the cars direction

Since the cornering forces are acting perpendicular to the driving directions and the steering frictional isn't easily calculated or physically simulated the cornering forces aren't considered for making of the test bench. Linear and rotational inertia however are important to simulate what happens when the car accelerates. The formulas for linear and rotational inertia forces are:

$$\text{Linear inertia} \quad F = ma$$

$$\text{Rotational inertia} \quad \tau = I\alpha$$

Rewriting these two formulas give the total inertia force of the car:

$$F_I = \left(m + \frac{I_w}{r_w} \right) \dot{v}$$

Since the work from F_I are speed dependent they aren't a huge factor in low speeds where we need similar behavior. The "build up" of kinetic energy change speed through F_{la} and F_{ra} however are major forces at low speed with high acceleration.

It's worth noting that if a change in inertia also changes speed and that the energy added to change the speed (overcoming inertia) could be described as kinetic energy.

3.1.4 Gravity (F_G)

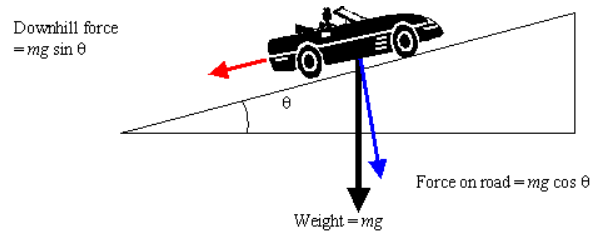


FIGURE 3-D GRAVITY FORCES (ANTONNINE EDUACTION, 2018)

When driving uphill/downhill gravity forces the car backwards. By decomposing the gravity force relative to cars angle θ as in Figure 3-D the gravity force opposing the cars motion can described as:

$$F_G = mg \sin \theta$$

Since a movement in the gravitational field also causes a change in the potential energy, driving uphill stores energy as potential energy given back when driving downhill to the same height as started.

3.1.5 Bearing losses (F_B)

According to SKF's paper "The SKF model for calculating the frictional moment" (SKF, 2017) the calculation of total frictional moment of a bearing is complicated as the result is depending on many factors. They state that the total bearing moment (M) is:

$$M = M_{rr} + M_{sl} + M_{seal} + M_{drag}$$

where:

- M_{rr} The rolling frictional moment, and includes effects of lubricant starvation and inlet shear heating
- M_{sl} The sliding frictional moment, and includes the effects of the quality of lubrication conditions
- M_{seal} The frictional moment from integral seals
Where bearings are fitted with contact seals, the frictional losses from the seals may exceed those generated in the bearing.
- M_{drag} The frictional moment from drag losses, churning, splashing, etc., in an oil bath

Some of these moments are quite hard to calculate and factors such as temperature, how much worn the bearings are and speed affect the resulting moment. Therefore, it's hard to calculate the correct losses due to bearing losses. However, tools like SKF's bearing calculator gives an indication of how big the losses are.

But, if done right the bearing losses should be much lower than for example the losses from the tire. The book *The World's Most Fuel Efficient Vehicle: Design and Development of Pac Car II* (Santin, 2007) states that if deep groove bearings or angular contact bearings are used the bearing losses should be at least 100 times lower than the rolling forces in a SEM prototype vehicle.

3.1.6 Speed dependent net forces calculated

TABLE 2 (CARLSEN AND OMA, 2017), (MICHELIN, 2017)

Calculated Drag Coefficient (C_d)	0.138
Frontal Area	$0.882m^2$
Rolling coefficient (C_{rr})	0.0013
Mass of Car	95 kg
Drivers Minimum Weight	70 kg
Total mass (m)	165 kg
Rotational Inertia of rim + tire (I_w)	0.204

To calculate net forces for our car the formulas above, SKF's bearing calculator and the cars characteristics given in Table 2 were used. By using assuming acceleration and height gradient is zero ($a = \theta = 0$) the results are (Figure 3-E The cars calculated net forces):

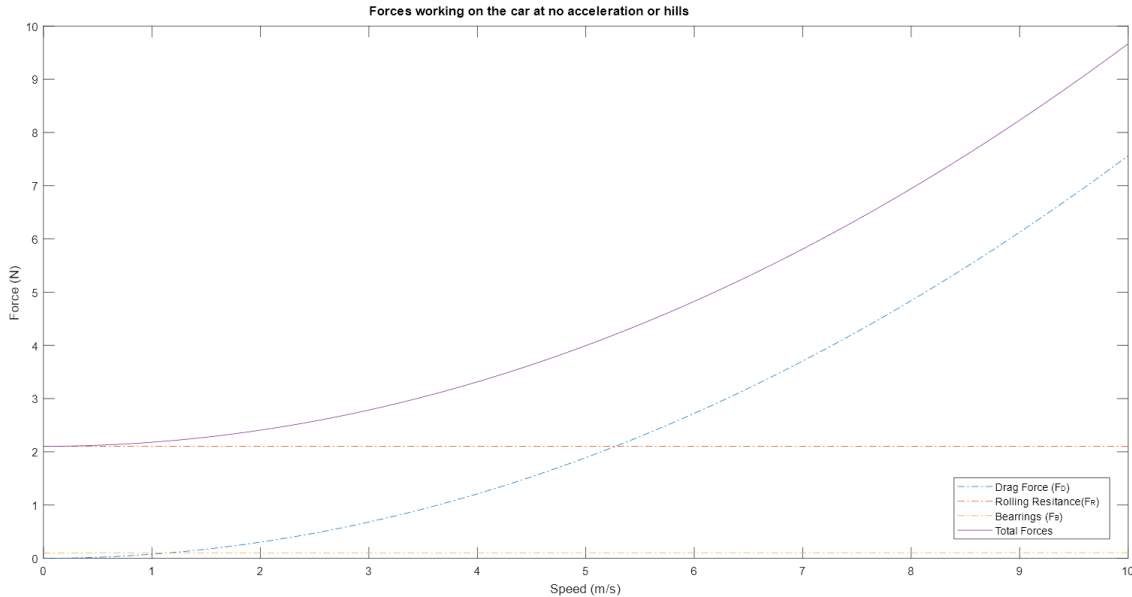


FIGURE 3-E THE CARS CALCULATED NET FORCES

3.2 Physics for the test bench (Inertia Dynamometer)

It's important to find a way to find a way to simulate the cars inertia if one want to have a realistic way to mimic accelerating on a test bench. According to work done by (Ward et al., 2015) on how to simulate this force a flywheel tuned with the correct rotational speed and inertia to get the same inertia as the car. To tune the parameters kinetic energy of the car

By assuming that a car drives straight flat forward without any losses (from rolling, drag, bearings etc.) it could be considered the work done by the powertrain is conserved as kinetic energy. This energy is caused by the change in inertia could be described as:

The formula for the kinetic energy of the car (E_{kb}) is:

$$E_{k_car} = \frac{1}{2}mv^2 + 4 * \frac{1}{2}I_h\omega_h^2$$

Where m is the mass of the car and driver combined and I_h is the inertia of each of the four wheels.

By trying to simulate this behavior on the test bench one must simulate the inertia to get the same behavior while acceleration.

The formula for storing this energy in a flywheel (F) is:

$$E_k = \frac{1}{2}I_f\omega_f^2$$

And by also considering inertia of a point mass being:

$$I = mr^2$$

It's easy to see that to increase inertia it's more efficient to double the radius of the flywheel than to add mass since mass is linear and distance from mass center is quadratic. Furthermore, it's more efficient to rotate a freewheel faster for the same reason.

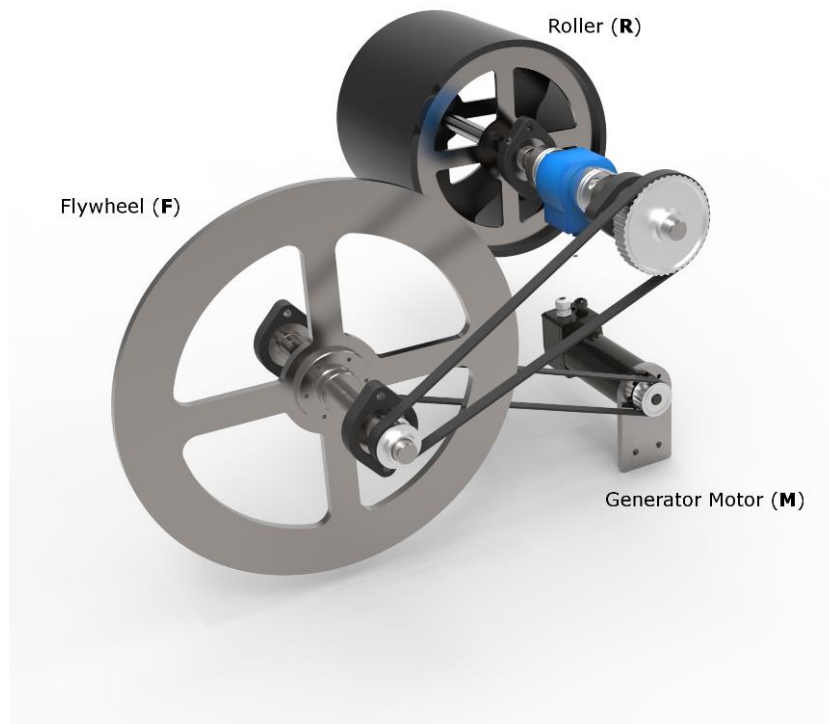


FIGURE 3-F THE TEST RIGS ROTATIONAL PARTS

By also introducing a roller (R) and a geared drive like in between each subsystem we get the energy storage:

$$E_{k_testbench} = \frac{1}{2} I_F \omega_F^2 + \frac{1}{2} I_R \omega_R^2$$

Where the angular speed of the roller equals the peripheral speed (speed of wheel/car) divided by the radius of the roller.

$$\omega_R = v/r_R$$

Since the roller is geared belt pulleys (n) in a belt driven system angular speed of the flywheel is bigger than the rollers angular speed:

$$\omega_F = \frac{n_R}{n_F} * \omega_R$$

Since the powertrain of the car is equal on both sides with no coupling and a separate motor one could simulate half the car and remove the inertia of the back wheel as this is spinning and therefore not needed, giving the energy formulas for simulating cars mass:

$$\frac{1}{4} m v^2 + \frac{1}{2} I_H \omega_H^2 = \frac{1}{2} I_F \omega_F^2 + \frac{1}{2} I_R \omega_R^2$$

Where the formula can be simplified, and by cancelling speed could be canceled:

$$\frac{1}{2} m + \frac{I_H}{r_H^2} = I_R/r_R^2 + \frac{n_R}{n_F} \frac{I_F}{r_R^2}$$

From here it's easy to tweak the parameters to fit the cars mass which is what's needed in combination with a way to simulate the other losses which all are speed dependent or depending on the hills angle.

By using the flywheel, considering a way to simulate the rest forces working on acting the car is needed which is usually done in a few different ways according to the Wikipedia article ("Dynamometer," 2017):

- Eddy current or electromagnetic brake (absorption only)
- Magnetic powder brake (absorption only)
- Hysteresis brake (absorption only)
- Electric motor/generator (absorb or drive)
- Fan brake (absorption only)
- Hydraulic brake (absorption only)
- Force lubricated, oil shear friction brake (absorption only)
- Water brake (absorption only)
- Compound dyno (usually an absorption dyno in tandem with an electric/motoring dyno)

With a goal to simulate the track and thereby gravity forces caused downhill driving the test bench must supply energy (drive) if this force makes the cars net force moving forward. As this were the case for the 2017 track this left only one possibility: adding a motor/generator and herby making a inertia based drive. If needed in order to brake enough a compound based generator should also be considered by adding a absorption type brake.

3.3 Estimate for energy consumption

Length per lap	970 meters
Total change in elevation	2 meters
Laps to complete	15
Max time	35 minutes
Competition Rules	<ul style="list-style-type: none">• Must come to a complete stop each lap• Not allowed with more than a 1000Wh battery

Estimating the power consumption per lap is a hard task where you need know a lot data for the car to get accurate numbers. Some of these numbers were calculated by the previous team and given by manufacturers, while other need to be measured to calculate them.

As we were given the track profile and the track almost flat with only two meters change in elevation from lowest to highest point the effects of hill climbing haven't been assumed neglectable. Another aspect that hasn't been dealt with the cornering losses, as these are time consuming and hard to calculate. As we don't know how sharp turns we need to take it's also been assumed that the car is able to drive at full speed during the whole track, the case was for last year's track. With these simplifications, the main forces working on acting on the car could be considered:

- Rolling resistance (FR)
- Aerodynamic drag (FD)
- Inertia Forces(FI)

- Bearing losses (FB)

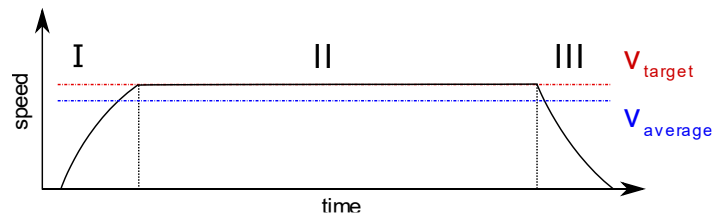


FIGURE 3-G SEPARATING INTO THE THREE PHASES PER LAP: ACCELERATION(I), CONSTANT SPEED(II) AND DEACCELERATING(III)

By knowing that driving slow and finishing just in time is better for saving power as this minimize the total work overcoming the drag force on could say that keeping constant speed (phase II) for most of the race. This makes it beneficial to divide driving into three phases as listed Figure 3-G.

3.3.1 Is regenerative braking beneficial?

Regenerative braking wasn't a priority last year for multiple reasons:

- Harder to make a motor controller supporting two quadrant operations
- A regular clutch must be made (not one-way clutch bearing as current powertrain) Power loss when car is moving with motor connected and belts moving
- Time limits and limited time for testing made the

As the track have changed from 1659 meters to 970 meters and the track this year is flatter so natural braking would take longer time an estimate on whether regenerative braking would be beneficial would give a benefit was needed.

To calculate a "best case" scenario in terms of reaching a speed v_{target} close to $v_{average}$ the efficiency of the cars powertrain is assumed $\eta_{driveline} = 100\%$ and acceleration is assumed to happen suddenly. It's also assumed that braking is happening suddenly, which could be worse than naturally slowing down. The η_{Regen} determines how much of the energy could be converted back to energy in the battery. Our current car doesn't support regenerative braking and therefore have a $\eta_{Regen} = 0\%$

$$v_{target} \approx v_{average} = \frac{15 * 970m}{35min * 60s/min} = 6.93m/s$$

$$W_{lap} = W_{phase 1} + W_{phase 2} + W_{phase 3}$$

$$F_{tot}(v_{average}) = 9.365N$$

	$\eta_{regen} = 0\%$	$\eta_{regen} = 100\%$
$W_{phase 1} = \eta_{driveline} * \frac{1}{2}mv_{average}^2,$	3960.4J	3960.4J
$W_{phase 2} = F_{tot,v_{average}} \cdot l_{track}$	9084.1J	9084.1J
$W_{phase 3} = -\eta_{regen} * \frac{1}{2}mv_{average}^2$	0	-3960.4J
W_{lap}	13 044. 5J (267.7 km/kwh)	9084. 1J (384.4km/kwh)

By using this simple model regenerative braking would give us about 30% lower energy use per lap. If we are only able to half or less of this energy back, it would still be beneficial to include regen if it's done in a good way.

3.3.2 Verification of the different phases

An inertia based motor/generator dynamometer could be used to verify that the behaves as it should under load the test in many ways.

ACCELERATION

The fact that the inertia is tuned to mimic the cars inertia the test bench for the acceleration phase which have caused problems the two last years could easily be simulated Figure 3-G. The same goes for the deaccelerating phase if regenerative braking is going to be tested.

DRIVING

By also simulating the cars forces at the current speed and a set any driving conditions could be tested. Lastly the track data (elevation per position) combined with measurement of makes it possible to simulate the track.

QUASI-STATIC (CONSTANT SPEED)

By going one step back and not trying to simulate the forces due to change in inertia but rather constant speed efficiency calculations get easier.

By measuring the electrical energy drawn from the battery and the mechanical energy one gets the efficiency of the power conversion:

$$\eta = \frac{P_{OUT}}{P_{IN}} = \frac{\tau\omega}{UI} = \frac{Fv}{UI}$$

This is a very powerful tool and commonly used in dynamometers being able to keep constant speed. An example for this used for measuring a DC motor at different speeds and torques is shown in system is in shown in Figure 3-H. Calculations of a more efficient acceleration efficient acceleration and a pulse and glide strategy where ideal torque is applied to accelerate to a certain speed and motor then disconnected till a lower speed limit repeats the process.

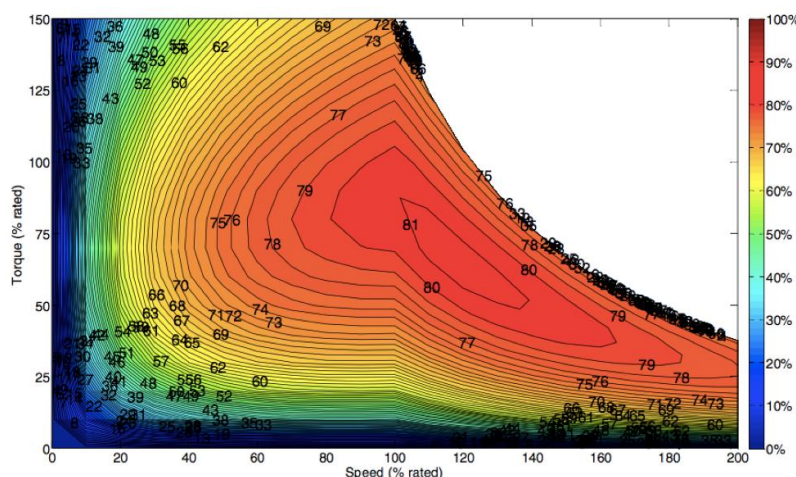


FIGURE 3-H ISO-EFFICIENCY PLOT, MEASURED BY A DYNAMOMETER WITH A TORQUE TRANSDUCER (POON ET AL., 2015)

4 Development

4.1 Requirements

To develop the test bench, the requirements/priorities of the system were made in collaboration with the person in charge of motor controller development and by separating needs from musts. As top priority for the test bench is to support development of motor controller, powertrain and to stress test the whole powertrain an incremental approach for the building were enabling more functionality after knowing that the rig was able to do its job was chosen. A main goal was to get a modular frame ready as early as possible testing of both the test bench and powertrain.

MUST

- Apply variable braking of the powertrain
- Simulate inertia of the car
- Show speed
- Be available for use early in the project as a support to motor controller development
- Modular, to enable adding "Should" to the test bench
- Be ready for testing as fast as possible

SHOULD

- Measure accurately
- Correct load relative to car
- Correct weight
- Enable physical simulation of track
- Measure torque
- Reusable – possible to use with a different car or configuration
- Be able to simulate two drivelines or car

4.2 Modular design

To design the system a CAD model was made in NX, where the initial concept with a roller and a flywheel connected with belts was fitted into a square frame to some initial dimensions. As we had a HBM T22 20Nm torque transducer, this was also added in the CAD. The reason for adding it before the belts is that it's hard to calculate power loss in the belts and because the torque meter was able to measure quite high torques.

15mm wide synchronous belts of type Gates HTD 5M were chosen for a few reasons:

- Efficient and strong, up to 99% efficient and up to 10kW power according to(Gates Corp., 2018)
- Easy to do modular design with as a change in belt length is enough to make the center distance
- These belts have been used many of the previous cars with success and therefore we already had some belts and pulleys

In collaboration with the realization lab at MTP and Trondheim Staal a strategy for making the main parts were made. Since the goal was to get the parts ready as fast as possible laser cutting with steel of all circular and square plates were chosen together with use of the modular Bosch Rexroth system and timing belts that allow easy re-gearing of the system.

For braking/applying force a motor was added in the CAD concept. In case we wouldn't be able to control the torque in a good way with a motor the possibility to add a Eddy current brake to the

flywheel or a Prony brake was held open by the square design combined with possibility to add longer axles.

A over dimensioned 20 mm high precision steel rod with only +/- 0.01 mm dimensional error was chosen for all rotating axes. This made it more flexible to change parts and easier to get bearings since it only had to be one dimension without the need to machine the rod. Another bonus was that the connectors for the torque meter was easier to mount since their mounting couplings were also 20mm in diameter.

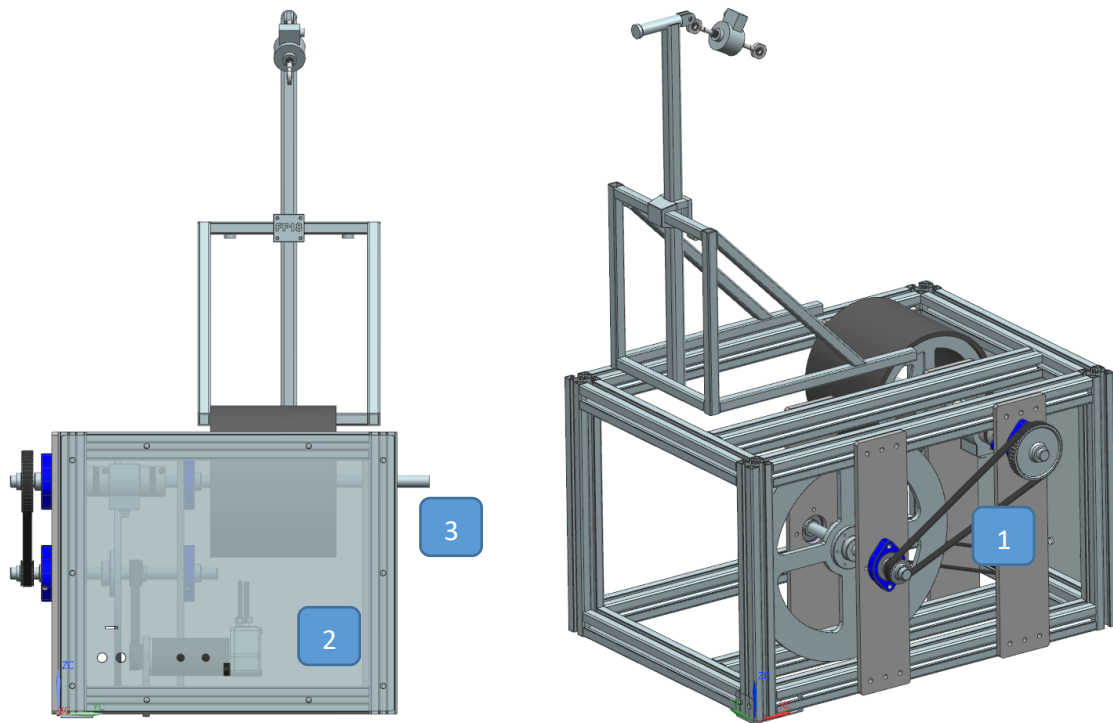


FIGURE 4-A THE FINAL CAD MODEL

The finalized CAD file after a few iterations could be seen in Figure 4-A The final CAD model with a few remarks:

1. Belt length calculations is simple by using NXs curve length function
2. Modeling side walls is easier with a cad in the correct dimension
3. The axle from the test rig was longer on purpose for possibility to add a second roller for simulating the whole car or to test different designs for belts etc.

4.3 The main frame

To keep the system as modular as possible aluminum profiles from the Bosch Rexroth in a large dimension (45x45 mm) were chosen. The benefits of these profiles are that they have a slot in each side wall with possibility to mount things with specially made nuts (t-nuts) and screws. There is also a lot of other parts that could be fitted. These rails also simplify the use of plates connected to the system as it's easy to mount them on the rails by adding screw holes where needed. The choice of a relatively huge dimension was done to ensure a stiff system.



FIGURE 4-B THE ALUMINUM PROFILES ENABLES A MODULE BASED DESIGN

The lengths of the profiles were measured in NX and a workshop at NTNU specifying on making racks with these profiles cut the profiles to the correct length.

4.4 Rapid production of the plates

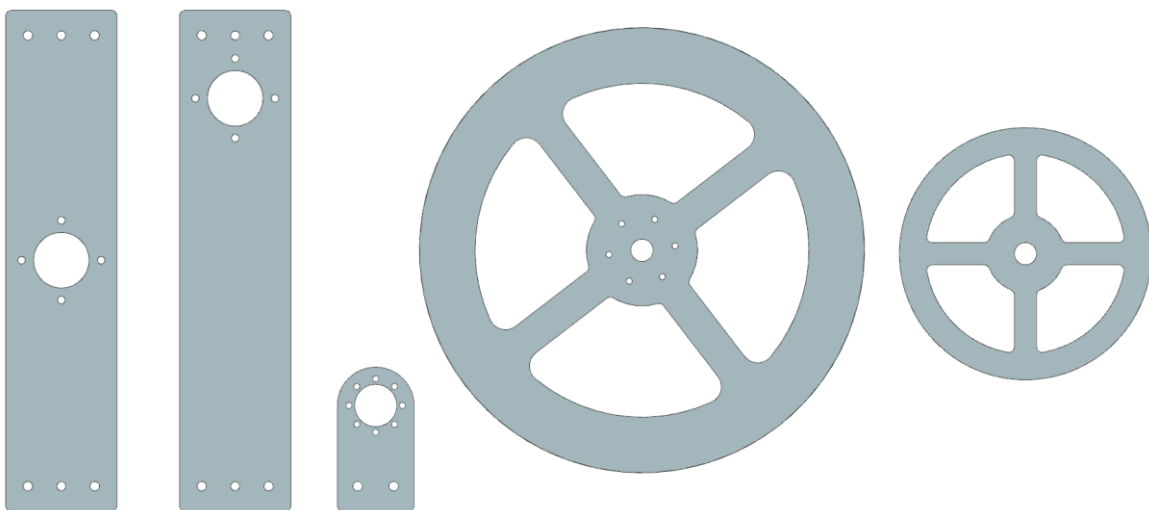


FIGURE 4-C THE PLATES FROM FOR THE TEST BENCH. FROM LEFT TO RIGHT: FLYWHEEL WALL (x2), ROLLER/TORQUE TRANSDUCER WALL (x3), MOTOR MOUNT FOR MAXON EC60 (x1), FLYWHEEL (x2) AND ROLLER WALL (x2)

To get the plates in the CAD drawings (Figure 4-C) realized a production method had to be chosen. Two alternatives were considered, CNC milling the plates or Laser cutting them. For CNC-milling the plates a lot of manual work had to be done, which is a time-consuming task. However, the precision from CNC-milling is higher than for laser cutting and a CNC mill enables a 2.5D or 3D design. Laser cutting is much faster as it doesn't require any setups other than placing the plate in the Laser Cutter and all parts would then be cut in one operation in a matter of minutes. Since the amount of work of making 10 different pieces with 5 different designs by milling would be time demanding and still require some lathing to get the circles of the flywheel correct, and since Trondheim Staal offered to sponsor the plate making laser cutting were chosen.

According to Trondheim Staal there was a few things to take into consideration to get good results:

- Laser cutting in general isn't very precise. Their machine had a +/- 0.2 mm accuracy
- Threading holes made by laser cutting isn't a good idea as the walls get locally hardened because of the heat
- Plates tends to bend after cutting caused by different internal stresses in the plate.

To keep the material cost and weight down the SSAB Laser S355MC plus steel plates made for laser cutting with a thickness of 5mm were chosen. These plates are made by hot rolling steel with low internal stresses are kept to a minimum and would therefore not bend that much caused by a different geometry. They are also cheap, relatively strong with a yield strength of minimum 355 MPa and were in stock at Trondheim Staal.

To handle the loss in precision bearing housings (NSK LFTC20) were chosen to be screwed into the roller/torque transducer wall and the flywheel plate instead of press fitting bearings into the holes which couldn't be made with the required tolerance for bearings. For this design to work the holes that holds the bearing housings was only engraved with crosses to show where to drill the holes which needed threads to hold the housing in place.

Lastly the inner and outer circle of the flywheel and the roller was with 2mm extra material which were then were removed in the lathe to get a good fit to the axles and to the walls of the roller. The reason for doing it this way was to remove any possibility of the center of the rotating parts and the axle being misaligned so that vibrations in the system would occur.



FIGURE 4-D THE PLATES READY FOR ASSEMBLY WITH THE MAIN FRAME IN THE BACKGROUND

4.5 The Roller

The roller acts as a simplification of the road. Ideally, this roller should be as big as possible to get a almost flat track to drive, like the ISO approved roller bench in Figure 3-C but several reasons the roller was chosen to be smaller:

- Lathe in the workshops at NTNU doesn't handle to big tubes
- SINTEF gave us a 250mm dimension steel oil tube with 10mm walls used in fatigue testing (not the fractured part of the tube)
- Lower diameter means higher rotational speed for the roller axle which means less need for high gearing ratio to get a fast spinning flywheel

To produce the roller the tube was first mounted on the lathe and rounded on the inside. Then the roller walls made by Trondheim Staal was lathed to fit the tube and the axle tightly. Then the axle and tube were spot welded to make sure the roller became rigid. This ensured that the center of the tube and axle was in the same rotational axis. Finally, the outer wall was rounded.

Unfortunately the tube we got had really bad tolerances needed to be cut 2-3 mm on the inside and outside make it round, not oval. The lathe wasn't big enough for the tool post and crossslide to get under the tube either. Therefore the production of lathe had to be run in reverse with the tool running with a long arm. This caused some vibrations in the tool and made the outer surface of the roller a bit rougher than planned.



FIGURE 4-E THE ROLLER WELDED AND IN THE LATHE

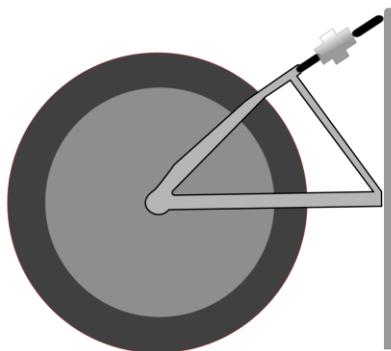
4.6 Powertrain mounting frame

To mount the powertrain to the test bench a frame for mounting was needed. The requirements for this frame was as following:

- Apply force / weight to hold the power train on the roller – preferably easy to adjust weight
- Be flexible enough to accept a small variation in the wheels geometry
- Hold the powertrain safely in its mounting points
- Know downforce from wheel to roller
- Mountable to the rails in the Rexroth system

A few different solutions were considered to satisfying the requirements:

Alternative 1



Mount drivetrain like it's mounted in the car but with a load cell to measure downward force and a screw mechanism to apply weight through the loadcell

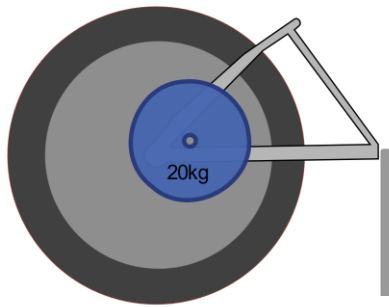
PROS

- Easy to apply different loads

CONS

- Tire not perfectly round – will cause a difference in load because of the stiffness of the system
- Need to add a loadcell and read it

Alternative 2



Weight in combination with the two bottom mounts on the drivetrain mounted to the rig.

PROS

- Doesn't need to compensate for wheel being oval
- Could physically see how much weight that has been applied

CONS

- Need to add a weight holder close to the wheel axle
- Need a lot of mass to simulate the cars pressure to the
- Could cause damage to the driveline – not simulated for holding weights

To know how much weight was needed for the car an assumption that each wheel of the car holds the same weight was taken. Based on this assumption the normal force working on the wheel would be:

$$N = \frac{70kg + 95kg}{4} * 9.81 = 420N$$

As mounting almost 45 kg of weight on the fragile driveline with very thin aluminum walls as in alternative 1 could be risky and bulky alternative 2 was chosen. In order to know how much weight the driveline needed to be pushed down with some calculations had to be done. For simplifying the calculations and loading the driveline as it's designed to be loaded the angle θ was chosen to be tangential to the rotation point B. As both N and F_A is tangential on the rotation point the factor between them is:

$$F_A = \frac{r_N}{r_A} * N = 1.42 * N$$

For making the frame in square tubes of S235 steel in 20mm with 2mm wall thickness for the frame and 25mm with 3mm wall thickness for the load cell holder was chosen and the frame drawn in NX.

The S 235 quality was assumed a good choice. Reasons for this was:

- Weight not critical
- Easy to work with and to weld
- In stock at the Realization Lab
- S235 is a quite ductile alloy compared to higher strength steel (Hechler et al., 2015) meaning It would most likely bend rather than snap (brittle failure) if too much force is used for holding the powertrain to the roller (Figure 4-G)

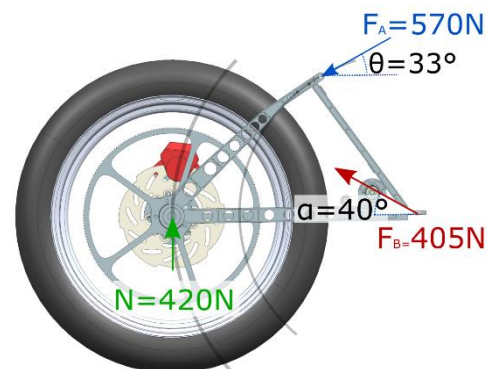


FIGURE 4-F FORCES

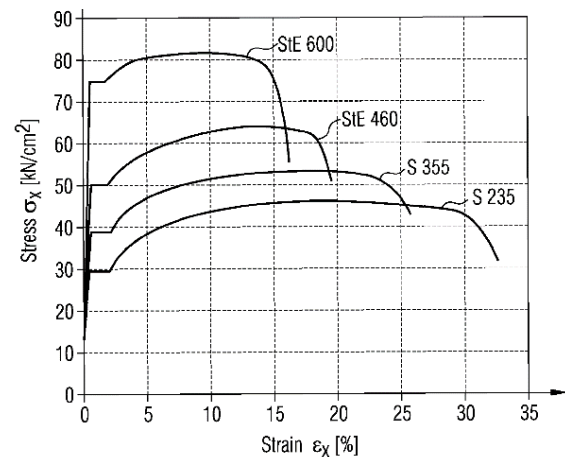


FIGURE 4-G DIFFERENT STEEL ALLOYS (HECHLER ET AL., 2015)

Since flexibility and safety was most important a finite element analysis (FEA) of the system was done in Siemens NX 11. The mesh chosen was TETRA10 with two elements in the thickness and a fine mesh. A fine mesh with tetraeder elements aren't the most computational efficient way to calculate thin walls, but should give just as good results if done right with a small enough mesh size (Wang et al., 2004). In

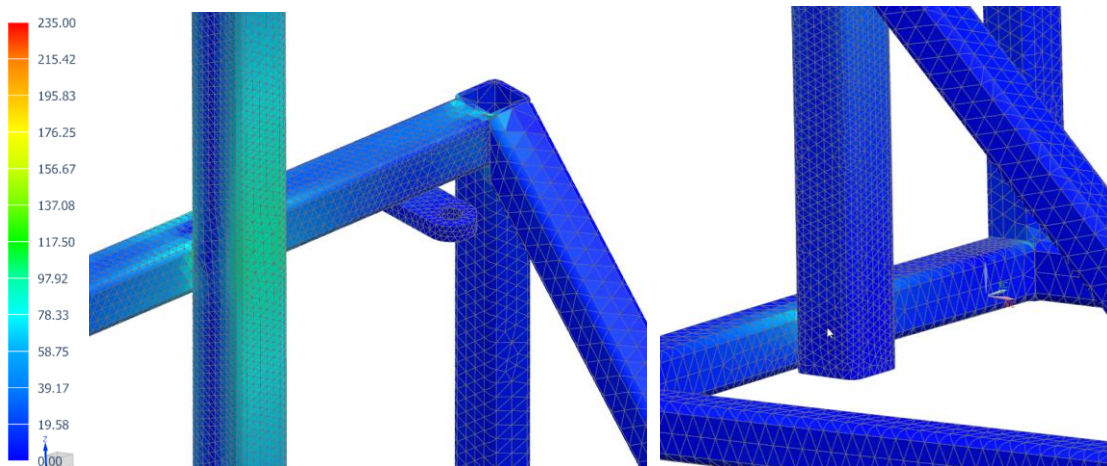


FIGURE 4-H FEA RESULTS - MAXIMUM VON MISES STRESS (MPA)

total it saves a lot of time using TETRA 10, because it's easier to mesh on a complicated geometry.

The two goals from was to make sure that the frame would hold the load and that the frame wouldn't be too stiff to accept a small ovalities in the tire. By looking at the results one could see that the maximum load on the load cell holding tube is 93 MPa and that the small 20mm tubes making the rest of the frame is only loaded to about 80 MPa. This gives a yield safety factor of 2.5 wich gives a bit of room in case we want to test higher loads.

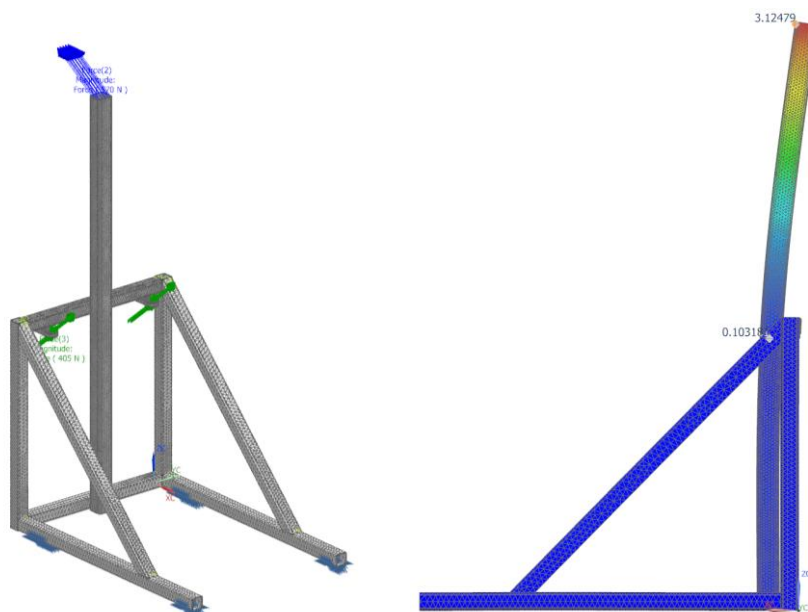


FIGURE 4-I THE FINITE ELEMENT MODEL AND ITS RESULTS

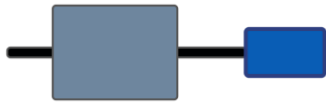
Maximum displacement happens where the load cell will be fastened and is 3.12 for the load case. By assuming small deformations, one could also linearize the displacement and know how much a difference in radius of the wheel will add in force to the measurement in the load cell:

$$F_{loadcell}/\Delta r_{wheel} = \frac{420N}{3.12mm \cdot 1.41} = 95.5N/mm \quad (4.1)$$

4.7 Simulating the inertia forces

To simulate the inertia forces of the car and the energy from accelerating the cars mass a few different choices were considered:

1. MOTOR/GENERATOR TO SIMULATE MASS ACCELERATION



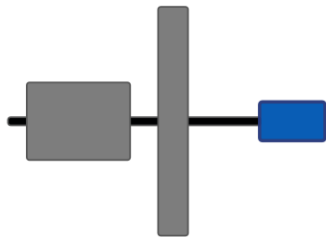
Pros:

- Simple system
- Lightweight

Cons:

- Accurate control needed
- Control of motors in low speed was a problem for last team
- Manufacturability
- Withstand rotational forces
- Weight
- Enough inertia
- Scalability – change mass of the car

2. FLYWHEEL ON ROLLER AXLE



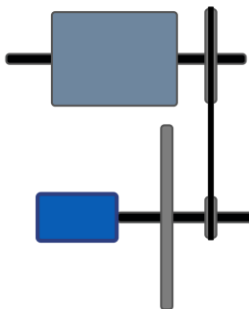
Pros:

- Simulates weight if flywheel mass is tuned correctly
- Simple, mechanical design

Cons:

- Need a lot of inertia due to low rotation speed

3. FLYWHEEL ON SEPARATED GEARED AXLE FROM ROLLER



Pros:

- Simulates weight if flywheel mass is tuned correctly
- Utilizes gearing and higher rotational speed to get more energy stored in the same inertia mass

Cons:

- More complex, need belts, chain or gears

Since option 1 needs really good motor control algorithm and accurate real time acceleration and no good sources on how to make one was found, to add actual inertia was the only option left.

By assuming that gearing from the roller was 3.3:1 and keeping the wish of producing the geometry of the freewheel as described in sub chapter 4.4 the flywheel would have needed to be $3.3^2 \approx 11$ times thicker than as of now (10 mm) in option 2 resulting in a weight of $5.9 * 11 = 65$ kg Option 3 were therefore selected.

A final element model for the rotational moment was conducted to verify that high rotational speeds the geometry were ok (Figure 4-J). The results showed that 5000 RPM made a maximum Von Mises stress of 135MPa, giving a safety factor of more than 2 for at this rotational speed. This means that a speed of 85 km/h should have this safety factor with the current gearing which were considered

satisfying. Appendix C shows Excel calculations for tuning the inertia in addition to inertia and mass calculations of the freewheel.

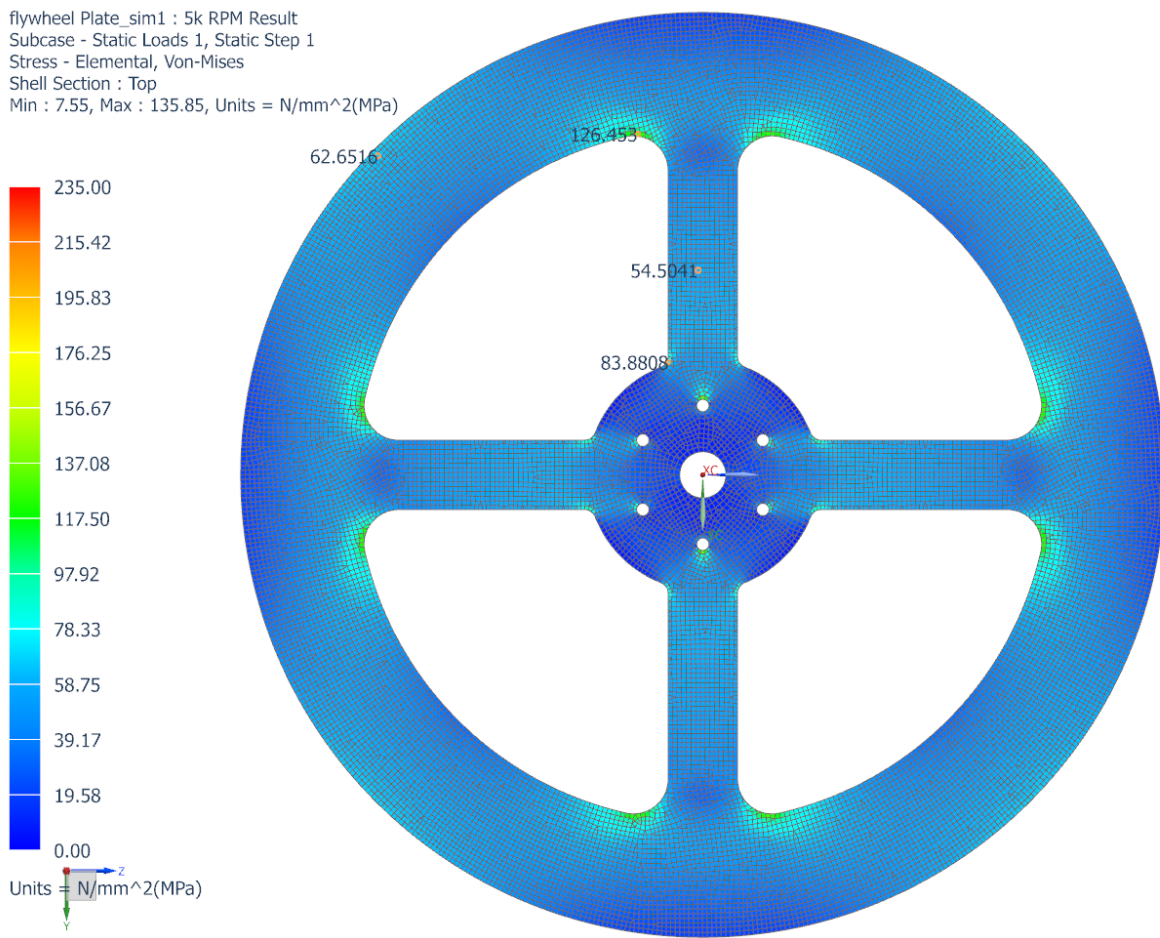


FIGURE 4-J FINITE ELEMENT MODEL OF THE FREEWHEEL

4.8 The Electronics

Variable braking and speed readings were considered a “must” in the design requirements and torque and simulating the track with the test bench was considered as “should”. To solve these requirements a strategy for controlling variable braking/accelerating of data acquisition had to be made. Since the team already had quite a few components, reuse of some of the parts were added early in the concept phase. The final flow chart of the components could be seen in Figure 4-K followed by a description of the subsystems.

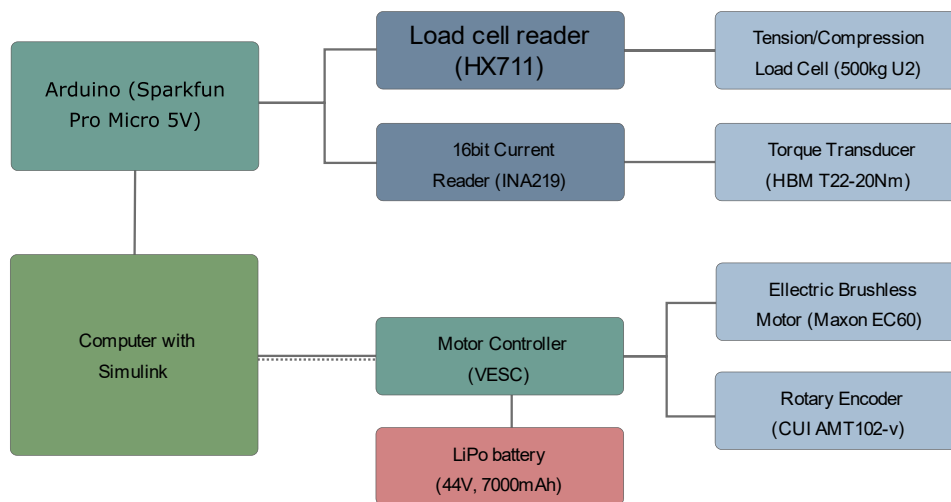


FIGURE 4-K FLOW CHART OF THE ELECTRONICS

4.8.1 Components used for variable braking/accelerating

MOTOR CONTROLLER - VESC

This motor controller is an open source project by Benjamin Vedder initially meant for skateboards (Vedder, 2015). It supports four quadrant operation of brushless DC (BLDC) motors which means it could both brake and accelerate the test rig. It also supports advanced field oriented control which reduces torque ripple compared to simpler control algorithms for BLDC motors (Cravotta, 2011)

Possibility to set a motor current target (PID controlled) makes it ideal for fine adjusting the test bench brake characteristics. Since motor current (I) and output torque (M) is (almost) proportional calculations of how much torque the motor delivers is easy by using the formula sheet given by Maxon (Maxon Motor, 2014):

$$M = k_m \cdot I$$

With a real time, plugin library that communicates via USB with Simulink a lot of parameters could be set and read while, enabling easy use of real time simulations with Simulink.

MOTOR/GENERATOR – MAXON EC60

A Maxon EC60 BLDC motor has been used for propulsion of many of the older DNV GL Fuel Fighter cars and we still had two lying around unused. As this motor is highly efficient, has a higher power rating than the one on the existing powertrain (400 watts vs a Maxon RE50 200 watts) and low torque ripple (Maxon Motor, 2014) it was considered strong enough and used.

SPEED ENCODER – AMT 102-V

At the beginning the test bench was run sensor less with the VESC supports by reading speed analyzing the back-EMF of the motor. However, as this gave choppy control and bad speed estimates

at low speed, a Rotary encoder was added. The choice fell on a AMT 102-V optical rotary encoder with 2048 readings per revolution as Benjamin Vedder had a video tutorial explaining how to implement it to the VESC (Vedder, Benjamin, 2016). In addition to giving smooth control at slow speeds it also gave a about 20 000 incremental reading points with the test bench gearing, meaning that a forward motion of the powertrain could be detected in less than 0.1 mm steps.

4.8.2 Data acquisition

SENSORS

A **HBM T22 Torque Transducer** rated to 20Nm with a maximum error of 0.5% in the readings were used for torque readings. Unfortunately, this only have a speed read out needed to calculate the power, but as this is the most expensive component in the test rig and we already had one switching it was no option.

For measuring how much force the powertrain would be held down with a old **U2 type tension/compression load cell** rated at 500 kg. As this was more than 25 years old (from *Western Germany*) no datasheet were found. Therefore, it was verified to read the correct value by calibrating it by weighing items with known weights.

ELECTRONICS

To read the sensor data a **Sparkfun Pro Micro 5V** was used. This micro controller board supports programming through the Arduino software which were preferred by the author as a fast way to read sensor data.

To get enough precision on the sensor readings a **Sparkfun HX711** 24 bit load cell amplifier break out board and a **Adafruit INA219** 16 bit current reading break out board were chosen. These in combination with the Arduino libraries for supplied by the manufactures made it easy to make a code to send data through the Arduinos USB (APPENDIX E).

4.8.3 Control Center - Simulink

To make it convenient to control the system a control center was made where setting control mode of the motor/generator is possible. Visual indicators for sensor readings the results can also be seen on the screen in addition to being sampled 100 times per second from the Arduino board and the VESC. A screenshot from the Simulink Dashboard is shown in Figure 4-M. The rest of Simulink Model is shown in Appendix E and the Arduino Code in Appendix F.

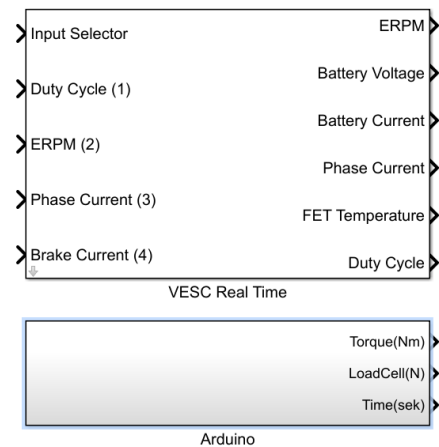


FIGURE 4-L INPUTS AND OUTPUTS IN SIMULINK

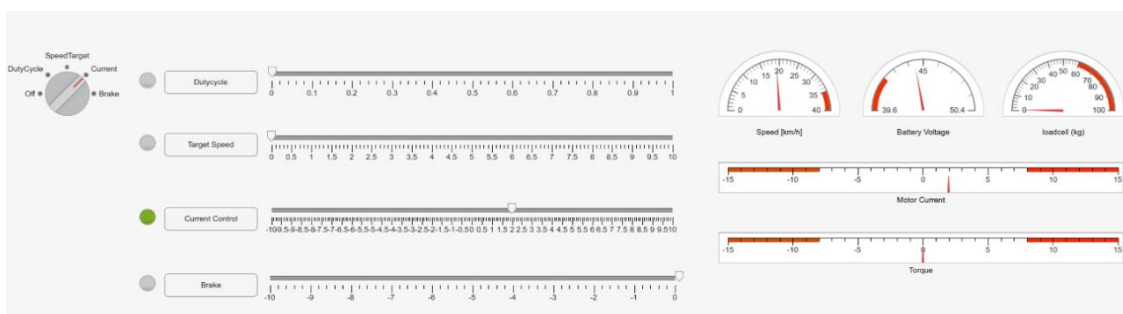


FIGURE 4-M DASHBOARD FOR CONTROLLING THE TEST RIG

5 Results and Discussion

5.1 The effect of a not slightly oval tire



FIGURE 5-A USING DIAL INDICATOR TO MEASURE DISPLACEMENT

One noticeable problem with the test bench was that the wheels radius wasn't constant which caused the test bench's loadcell holder to move quite a lot during testing of the powertrain. To verify that the FEA calculations done to make the load cell holders displacement calculations were correct and to assure that the load wasn't too high to make any plastic deformation measurements had to be taken.

The actual displacement of the wheel center was measured by using a dial indicator in the center between the rotation point where the power train is fastened and the wheel axle since it was hard to place the dial indicator closer to the wheel center. By doing it this way the formula for change in radius (center position) could be measured as:

$$\Delta r_{wheel} = (measurement_{max} - measurement_{min}) * 2$$

To calculate the displacement of the wheel center the structure was assumed much stiffer than the spring square rod. This assumption was based on no visible bending happening to the powertrains aluminum frame while a clearly visible displacement happened in the load holder.

Then the test bench was set for constant speed by using the test benches motor/generator and sending a constant speed 1 m/s command from the Simulink Control center to the VESC. After a stabilization of speed the following readings were analyzed in MATLAB:

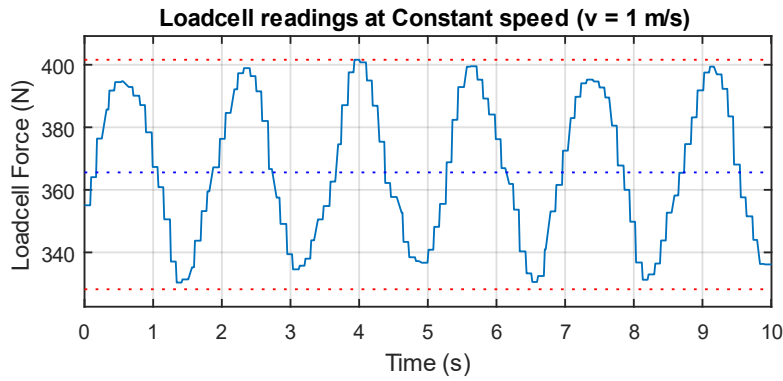


FIGURE 5-B SENSOR DATA FROM LOAD CELL

To verify that the numbers from the FEA were about the same as in the real setup the measured displacement Δr_{wheel} were calculated and used with Equation (4.1):

$$F_{loadcell}/\Delta r_{wheel} = \frac{420N}{3.12mm \cdot 1.41} = 95.5N/mm$$

$$\Delta r_{wheel} = 0.45mm * 2 = 0.90mm$$

$$\Delta F_{loadcell} = \Delta F_{loadcell}/\Delta r_{wheel} = 95.5N/mm * 0.9mm = 86.0N$$

By analyzing the graph (Figure 5-B) the actual numbers change in force is:

$$\Delta F_{loadcell} = F_{max} - F_{min} = 74.4N$$

Which is 86% of to the calculated value. The fact that the real value is lower than the calculated value for displacement is good.

This means that the amplitude is $F = 420N \pm 74.4N/1.41 * 2 = 420N \pm 26.4N$

5.2 Iterative tuning of the test bench

Since there is a lot of different losses which are braking the test rig like bearing losses in motor (Maxon Motor, 2014), the axle bearings, efficiency calculations for the test bench were conducted. The strategy used was to accelerate the test rig by using the Simulink control to a peripheral speed of about 7 m/s or more and then turn the test rigs motor/generator off. To be able to integrate the speed/time curve were made continuously by using a fifth-degree polynomial regression of fifth degree, which made a quite good approximation with no noticeable systematic error. (See APPENDIX A)

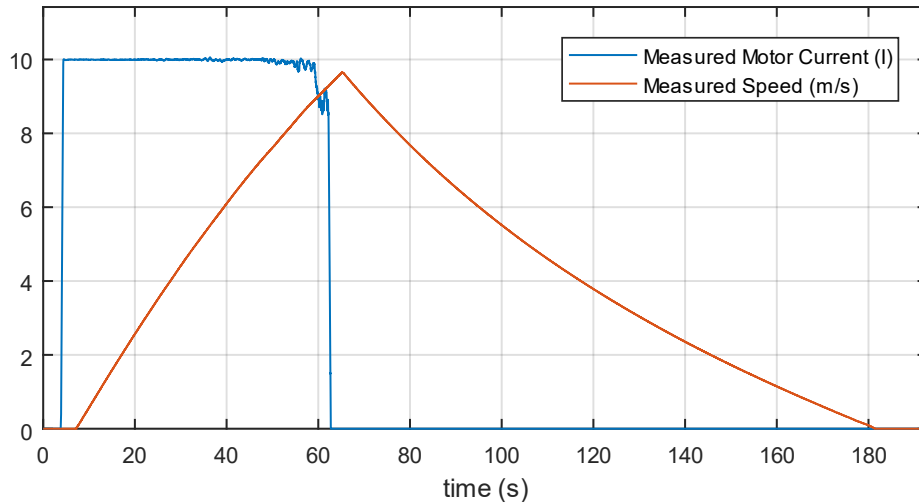


FIGURE 5-C SPEED ACCELERATING THE TEST RIG WITH 10A MOTOR CURRENT IN 60 SECONDS, THEN FROM CA 70 SECONDS TO 180 SECONDS MEASURING SPEED CHANGE CAUSED BY LOSSES IN THE TEST RIG

Then the kinetic energy of the rig for each time step were found by using MATLAB (See: Appendix A) and the power loss breaking Inertia for the test bench. Finally, by combining $F=P/v$, $P =dW/dt$ and looking at the slow down period.

This analysis was used for five iterations where the goal was to reduce the losses of the test bench by changing parts so that braking of the car happens as close as possible to how half the cars forces would brake a inertia of one wheel on the car + half the inertia of car and driver (target in Figure 5-D). The results of the five iterations (i1,i2..i5) can be seen in Figure 5-D followed by comments of whats been changed per iteration.

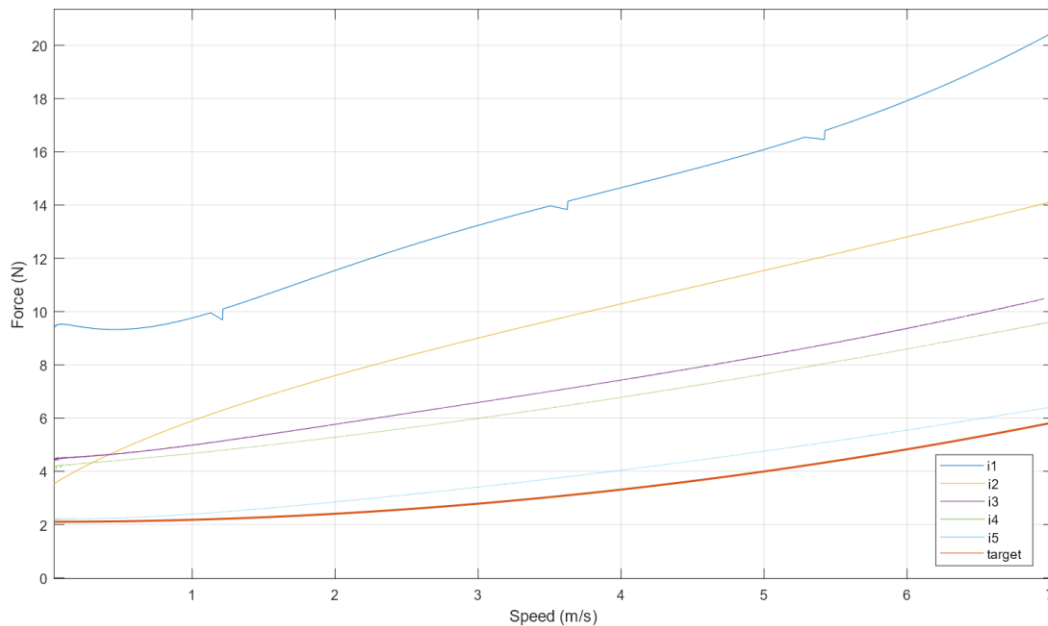


FIGURE 5-D FIVE ITERATIONS FOR REACHING A “CLOSE TO CAR PERFORMANCE”

ITERATION 1 (i1):

First attempt where Simulink didn't read the time smoothly, seen as chops in the graph, fixed for the rest of the iterations. The test rig's motor failed shortly after. Since we had two motors of the same sort a new one was installed and a goal to reduce the difference between the target and i1 was a goal since calculating $P_{1@7m/s} = F \cdot v = 140$ watt of losses for keeping 7m/s equivalent speed were considered a bit risky for the motor, where it had to add a lot of power to compensate for the difference between target and even more if one wanted to test regen at that speed.

ITERATION 2 (i2):

With a new motor the test rig got better results, but still were over the target. The company Abra Kulelager A/S which specializes on bearings gave us a theory for the huge braking moment of the bearings: By being optimized for surviving harsh environments over efficiency, the sealings frictional moment (M_{RR}) could be braking a lot. two options were then considered.

1. Removing the seals and run without them
2. Replacing the bearings with SKF's ultra efficient E2 series

Option 2 was chosen as Abra Kulelager A/S kindly sponsored the project with the efficient bearings and removing the sealings also causes the grease not to stay in place, meaning increased maintenance.

ITERATION 3 (i3):

Bearings did the trick at high speeds, with about 40% improved efficiency at 7m/s. Next up was fixing a poorly aligned mount for the bearings which felt inefficient as it felt hard to rotate, possibly because of the rotation centers not being totally aligned to each other. To fix this a new bearing mount was made.



FIGURE 5-E OLD VS NEW BEARING HOUSING

ITERATION 4 (i4):

The change of bearings caused a small overall effect and in addition made the torque transducer less since the new design ensured a better mounting. By finally cutting the braking force to the half compared to i1 thus requiring only under 70 watts to keep the test rig spinning at 7m/s the strategy of using the motor for fine adjustments were made. By knowing that motor current and torque is linear and the torque constant(Nm/A) a strategy to setting the VESC at 1.0A constant current to compensate for the difference between the results from i4 and the target.

ITERATION 5 (i5):

The 1A current did the trick and got the compensated the braking force all over the line with the lower speeds almost spot on and at 7 m/s about 15% of the over the real value.

DISCUSSION

After the final iteration done the test bench performed very similar to the car model. However, since sending constant current doesn't do the trick a more accurate function should be done. Possibly one that can calculate the difference between the target and the actual readings at all speed and then calculate the torque needed to be applied to motor at the given speed.

It's also worth noticing that the calculated car model for the car and the actual forces isn't necessary the same due for example a different aerodynamic drag and the tires not being new. Therefore, analyzing real time car data versus the model could also be useful.

5.3 Torque Transducer testing

To verify that the test bench can be used to test efficiency an experiment where accelerating the test bench to 4 m/s by using the VESCs constant speed were conducted. When the speed reached the target of 5.5 Amps at ca. $t = 80s$, giving ca 75 watts of driving power.

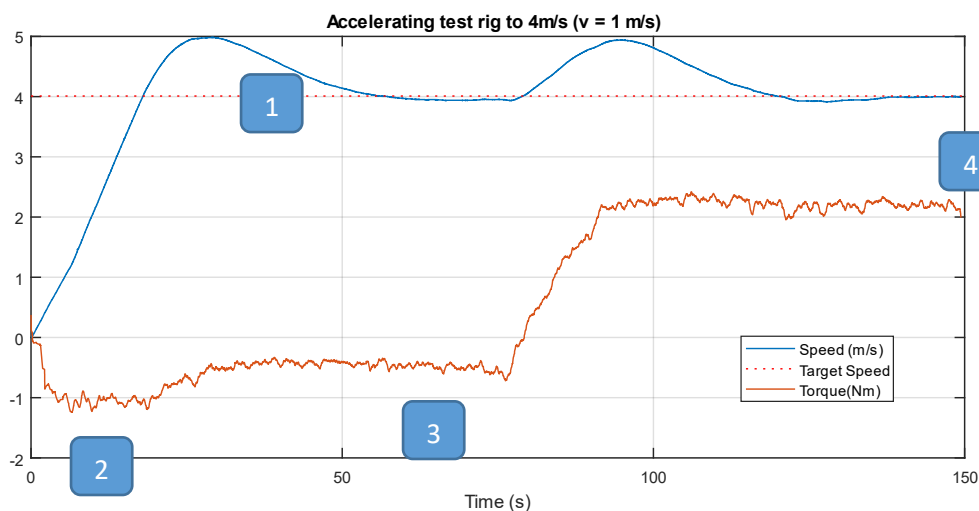


FIGURE 5-F SPEED AND TORQUE READING

A few things to notice from the readings (Figure 5-F):

1. The VESCs ability to keep constant speed isn't very well tuned. This is resulting in a overshoot of about 20% when trying to accelerate to 4 m/s with the test bench and ca half a minute from overshooting to it gets down to its target speed. This could most likely be improved by changing the VESCs PID settings, but isn't tried yet.
2. In the acceleration phase the accelerating of the roller and wheel is causing an inertia torque in the test bench's motor
3. In steady state there is still some negative torque, caused by the powertrains rolling losses (mainly rolling resistance) and by the bearings in the test rig
4. The power calculations can be done by looking at the system as quasi-static. Calculating the power by $P = F \cdot v$ one gets the total P_{OUT} . By subtracting the rolling losses at constant 4 m/s (point 3) from the reading one also gets the efficiency at a given torque and speed. By doing this for different values, possibly by implementing functionality for Simulink to do an automatically sweep where 1Amp, 2Amp ... n Amp etc. are sent in to the motor at 1m/s, 2m/s... n m/s. For this to work implementation of Simulink control of the motor controller for the car also needs implementation.

6 Conclusion and Further work

The goals for the test bench were described as following in the introduction, in prioritized order:

1. Mimic real driving
2. Measure efficiency
3. Support further work with developing a new powertrain

With comments on how close the test bench is these goals and further work on those:

MIMIC REAL DRIVING (1)

The iterative approach for building the test bench with prioritizing the “musts” design requirements before “should” made it possible to use the test bench as an inertia load supporting the motor controller already in October. This made testing of the teams’ new motor controller with an inertia load possible. What we didn’t know at that time was that the test bench was braking a lot due to the torque losses, meaning than more braking than needed to simulating driving was done.

By using the iterative method to get the test bench tuned the calculated values the last iteration showed that the rig was quite close to real car performance. Hopefully the planned implementation of a variable motor current discussed in chapter 5.2 will at different speed will give an even more accurate model.

The calculations on a slightly oval tire were also showed to be quite correct to the real data giving $420N \pm 26.4N$ variance between maximum and minimum readings. With a more oval tire than first thought the design of the load cell holder to act as a spring showed useful. Some further work on the problem could be done and two suggestions are to either trying to align the tire better to the rim or to make a load arm with different geometry or using a smaller square tube with higher yield strength to compensate for being structurally weaker.

MEASURE EFFICENCY (2)

The torque transducer test showed great potential in combination with the VESCs keep speed function. As this was the first test most of the problems would likely be easy fixable and could be considered as further work.

In addition, the motor controller need to be able to send data to Simulink to measure the efficiency. This is being worked on by other team members and a new design is soon ready for testing, giving the possibility to fully automate a testing sequence in Simulink with. If we will succeed with this, we will be able to plan a driving strategy with power efficiency map. As long as the potential errors on the

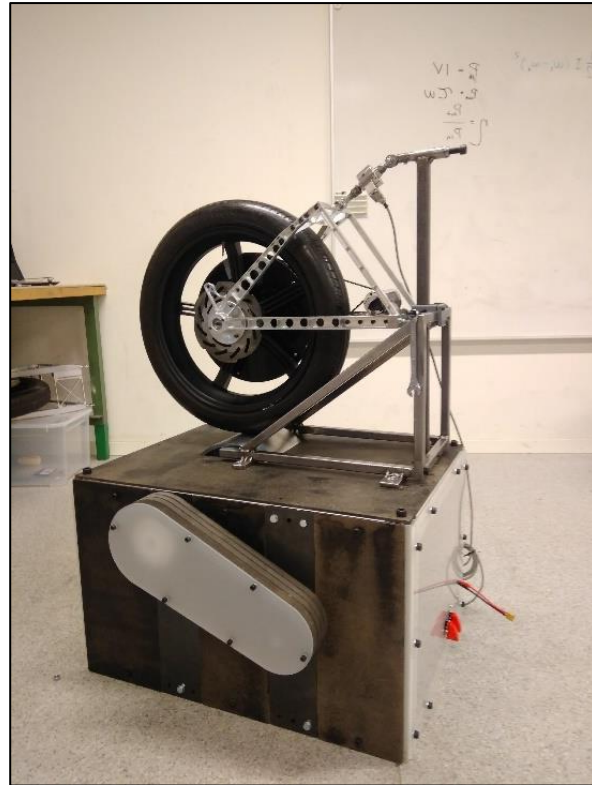


**FIGURE 6-A THE FINAL PRODUCT
WITH THE CURRENT POWERTRAIN MOUNTED**

readings are the same or proportional, we will still know where the best efficiency lies which will enable a pulse and glide strategy. Time will show if it works. But the potential is huge.

Lastly a comment on accuracy is needed here: If the test bench performs the same at all times or need calibration after each use isn't tested yet. And, since the bearings

and grease will heat up a bit during driving an investigation on this effect is needed. After trying to do readings

SUPPORT FURTHER WORK WITH DEVELOPING A NEW POWERTRAIN (3)

The authors further work for the master thesis will most likely involve development of a new powertrain with the use of the test bench for verification of reliability and efficiency.

The timing belts in the current powertrain is supposed to be efficient, but the frictional loss of the one-way bearing used to keep the belts and motor stationary while not accelerating is still there. And worse: the bearing makes regen impossible and a choice between regen and major losses of not using one must be considered. With a much shorter track for the 2018 competition regeneration to brake at each lap shows potential.

Therefore, verification on a new design is in the planning. The goal with the new powertrain is to consider the effects of adding a second gear and the possibility to disconnect the motor with a linear actuator. The test of such a system will first be done by utilizing the test bench's modularity. To illustrate this concept, look in Figure 6-B and Figure 6-C.

Lastly remembering that risk is more than no matter how good the test bench is simulating, it's not the same thing. Therefore, is always a risk of something not thought of. Therefore, the test bench should only be considered a tool for mitigating risk and not a way to eliminate it.

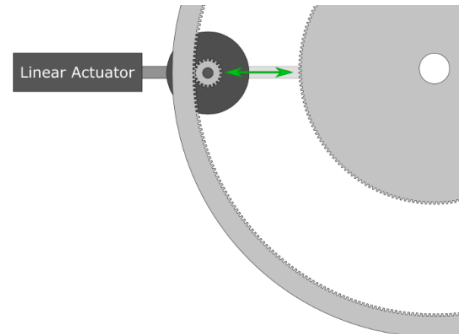


FIGURE 6-B LINEAR ACTUATOR CONCEPT WITH TWO GEARS



FIGURE 6-C 3D PRINTED PROTOTYPE FOR A MINIATURE VERSION OF THE CONCEPT

7 Sources

- Antonine Eduaction, 2018. Mechanics Tutorial 1 [WWW Document]. URL https://www.antonine-education.co.uk/Pages/Physics_2/Mechanics/MEC_01/Mechanics_1.htm (accessed 1.9.18).
- bicyclerollingresistance.com, 2017. Rolling Resistance Tests [WWW Document]. URL <https://www.bicyclerollingresistance.com/default.aspx> (accessed 12.2.17).
- Bierman, J., 2017. Schwalbe Marathon Almotion Rolling Resistance Review [WWW Document]. URL <https://www.bicyclerollingresistance.com/tour-reviews/schwalbe-marathon-almotion-2016> (accessed 12.2.17).
- Cravotta, N., 2011. Increasing Motor Performance with Field-Oriented Control [WWW Document]. URL <https://www.digikey.it/en/articles/techzone/2011/oct/increasing-motor-performance-with-field-oriented-control> (accessed 1.9.18).
- Dynamometer, 2017. . Wikipedia.
- Gates Corp., 2018. PowerGrip® HTD® [WWW Document]. URL http://ww2.gates.com/europe/brochure.cfm?brochure=12782&location_id=19467 (accessed 1.7.18).
- Hechler, O., Axmann, G., Donnay, B., 2015. The right choice of steel – according to the Eurocode, in: Economical Bridge Solutions Based on Innovative Composite Dowels and Integrated Abutments. Springer Vieweg, Wiesbaden, pp. 21–43. https://doi.org/10.1007/978-3-658-06417-4_2
- Maxon Motor, 2014. Maxon DC motor and maxon EC motor: Key information [WWW Document]. URL https://www.maxonmotor.com/medias/sys_master/root/8815460712478/DC-EC-Key-Information-14-EN-42-50.pdf?attachment=true (accessed 1.8.18).
- Michelin, 2017. Performance - Ultimate energy tire | Michelin The tire digest [WWW Document]. URL <http://thetiredigest.michelin.com/michelin-ultimate-energy-tire> (accessed 11.30.17).
- MTS Systems, 2017. Tire Rolling Resistance Measurement System [WWW Document]. URL https://www.mts.com/cs/groups/public/documents/library/dev_002230.pdf (accessed 12.2.17).
- Poon, K.K., Chen, Z., Huang, K., 2015. Computer Aided Measurement and Analysis of Equal Efficiency Characteristics of Electrical Machines [WWW Document]. URL https://www.eleceng.adelaide.edu.au/students/wiki/projects/index.php/Projects:2015s1-61_Computer_Aided_Measurement_and_Analysis_of_Equal_Efficiency_Characteristics_of_Electrical_Machines (accessed 1.10.18).

- Santin, J.J., 2007. The World's Most Fuel Efficient Vehicle: Design and Development of Pac Car II. vdf Hochschulverlag AG.
- SKF, 2017. The SKF model for calculating the frictional moment_tcm_12-299767.pdf [WWW Document]. URL http://www.skf.com/binary/101-299767/The%20SKF%20model%20for%20calculating%20the%20frictional%20moment_tcm_12-299767.pdf (accessed 12.5.17).
- Vedder, B., 2015. VESC – Open Source ESC | Benjamin's robotics.
- Vedder, Benjamin, 2016. VESC FOC Encoder position control.
- Walden, D., Roedler, G., Forseberg, K.J., Hamelin, R.D., Shortell, T.M., 2015. INCOSE Systems Engineering Handbook: A Guide for System Life Cycle Processes and Activities, 4.th Edition. ed. John Wiley & Sons, Inc., San Diego, CA.
- Wang, E., Nelson, T., Rauch, R., 2004. Back to elements-tetrahedra vs. hexahedra, in: Proceedings of the 2004 International ANSYS Conference. ANSYS Pennsylvania.
- Ward, T., Sheng, O., Hanapi, S., Sainan, K., 2015. Design and Testing of Inertia Dynamometer for Prototype Fuel Cell Electric Vehicle. Journal of Engineering and Applied Sciences 10, 7416–7422.